CHARACTERISING *DAPHNIA MAGNA* AS A MODEL FOR AGEING RESEARCH

by

JULIA KATE CONSTANTINOU

A thesis submitted to

The University of Birmingham

for the degree of

DOCTOR OF PHILOSOPHY

School of Biosciences

College of Life and Environmental Sciences

University of Birmingham

September 2020

UNIVERSITYOF
BIRMINGHAM

University of Birmingham Research Archive

e-theses repository

Abstract

Daphnia species are gaining interest as a model for ageing research due to characteristics such as easy generation of large clonal populations and short lifespan. Most interestingly, genetically identical female and male *Daphnia* have evolved different average lifespans, providing a unique opportunity for investigating sex differences in longevity to provide insight into the underlying mechanisms of ageing and regulation of lifespan. Data presented here begins to delineate these mechanisms. Significant differences between sexes in markers such as lifespan, growth rate, heart rate and swimming speed in addition to lipid peroxidation product accumulation, thiol content decline and age-dependent decline in DNA damage repair efficiency are reported. Furthermore, lipids play a significant role in regulation of health and disease. Here, dynamic changes in lipid composition as a function of age and sex are presented such as statistically significant age-related changes in triglycerides, diglycerides, phosphatidylcholine, phosphatidylethanolamine, ceramide and sphingomyelin lipid groups. Most interestingly, the rate and direction of change can differ between sexes, which could partly be the cause and/or the consequence of the different average lifespans between them. Transcriptome data also revealed rate and directional differences between sexes with age. Finally, evolutionary theories of ageing focus on genetic inheritance, but many observations suggest non-genetic inheritance also influences ageing phenotype. Here, findings show maternal age-effect on offspring. Importantly, the maternal age-effects can in part be recovered if subsequent generations are produced from younger mothers. Overall, this thesis supports that investigating sex differences in longevity in the clonal organism *Daphnia* under

controlled laboratory conditions can provide insight into principal mechanisms of ageing and lifespan regulation.

Data presented in Chapter 3 and Chapter 4 have been published in first author papers (Constantinou et al., 2019) and (Constantinou et al., 2020). The co-authors can confirm that the paper was written by the first author. Thus the wording used in the publications also presented in this thesis submitted by Julia Constantinou are also entirely written by her.

J. Constantinou

Julia Constantinou (first author)

L. Mirbahai

Dr Leda Mirbahai (senior author)

Acknowledgements

Table of Contents

List of Figures

List of Tables

List of Abbreviations

AD	Alzheimer's disease
Cer	Ceramides
Che	Cholesterol ester
CL	Cardiolipin
CR	Caloric restriction
CtBP1	C-terminal binding protein 1
CVD	Cardiovascular disease
DG	Diglycerides
dHJ	double-Holliday junction
DSBs	Double strand breaks
EEAA	Extrinsic epigenetic ageing
FRTA	Free Radical Theory of Ageing
GSH	Glutathione
GSSG	Glutathionine disulphide
HDL	High-density lipoprotein
IEAA	Intrinsic epigenetic ageing
JH	Juvenile hormone
LCA	Lithocholic bile acid
LCAT	Lecithin:cholesterol acyltransferase
MF	(E,E) Methyl Farnesoate
PA	Phosphatidic acid
PARP	poly (ADP-ribose) polymerase
PC	Phosphatidylcholines
PD	Parkinson's disease
PE	Phosphatidylethanolamine
PG	Phosphatidylglycerol
PR	Prenol lipids
PS	Phosphatidylserine
ROS	Reactive Oxygen Species
SASP	senescence-associated secretory phenotype
SDSA	Synthesis-dependent strand annealing
SM	Sphingomyelin
SPH	Senescent parent hypothesis
T2D	Type 2 Diabetes
TG	Triglycerides

CHAPTER 1:

General Introduction

Ageing

Ageing is broadly defined as the gradual time-dependent decline of physiological functions. It is widely known that increased age is associated with higher susceptibility to disease and illness with frailty being a common description for elderly people, the cause of which has been attributed to many factors. Lifespan and rate of healthy ageing has been investigated in many organisms which has led to identification of nine hallmarks of ageing summarised in Figure 1.1 (Lopez-Otin et al., 2013). Changes observed with age are not consistent for all individuals and are influenced by multiple factors including the environment (WHO, 2015).
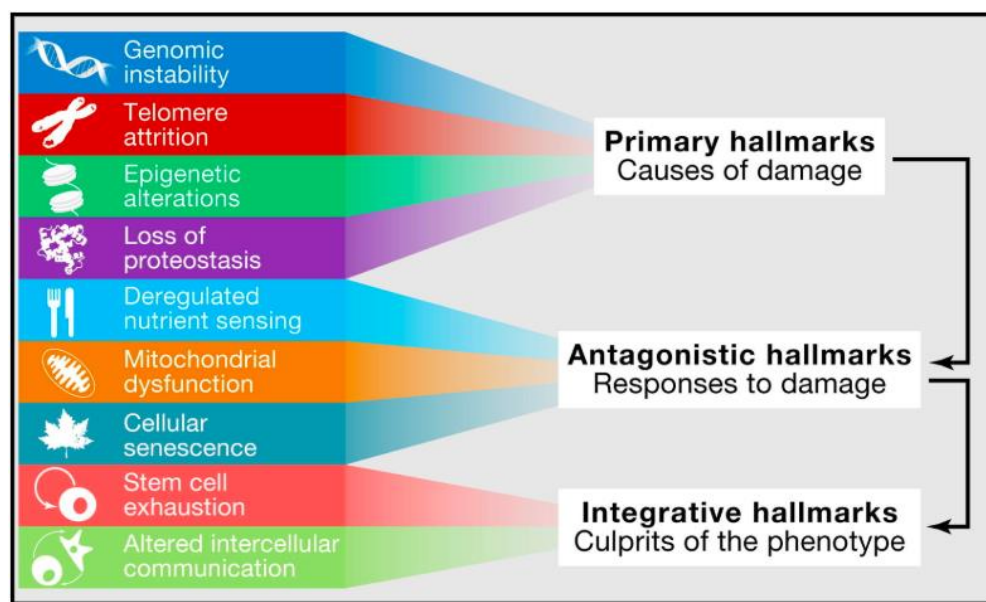
Figure 1.1. The nine hallmarks of ageing. Originally described by Lopez-Otin et al. (2013), this figure has been adapted by Amin (2018) and copied here. The nine hallmarks of ageing can be categorised in to three groups: primary, antagonistic and integrative hallmarks. Primary hallmarks are those considered to be the primary cause of damage. Antagonistic hallmarks are the responses to the damage which initially can mitigate the damage but can be problematic when chronic. Finally, integrative hallmarks are the phenotypic result of primary and antagonistic hallmarks which present the functional decline associated with ageing.

1.1 Ageing and disease risk

Molecular and physiological changes happen through-out ageing. These molecular and physiological changes associated with ageing can subsequently increase the risk of development of certain diseases. By age 60, the major burdens of disability and death rise from age-related losses in hearing, sight and mobility, and diseases, such as cardiovascular (heart) diseases, cancers and arthritis, see Figure 1.2 (WHO, 2015).
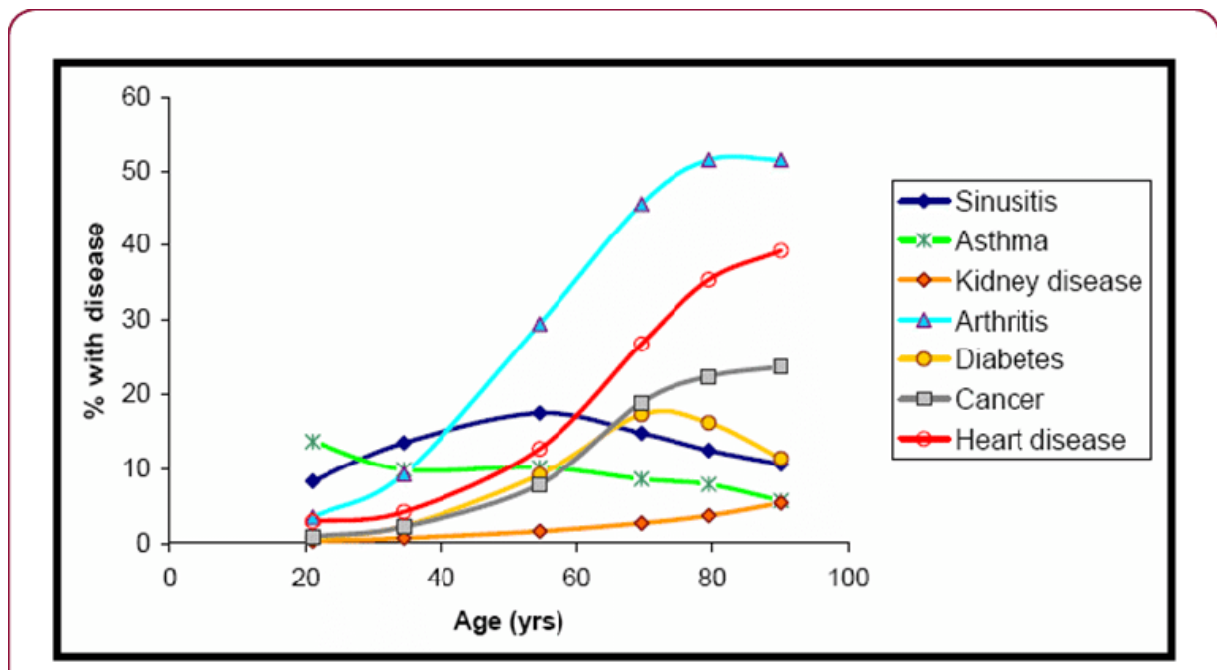
Figure 1.2: Disease incidence for common age-related diseases. Figure copied from van Ginneken (2017). Arthritis, heart disease and cancer show a clear increase in prevalence with age as evidenced by an increasing percentage of the population living with these diseases in older age.

1.2 Why study ageing?

Ageing is a process that affects every living person and in mid-2019, 12.4 million people aged over 65 were recorded in the UK, totalling 18.5% of the population of which 2.5% were aged 85 years and over (OFNS, 2020). The proportion of the

population aged over 85 years is projected to double by 2039 (OFNS, 2020). As lifespan has increased, the number of years an individual exists free from age-associated disease has not increased by the same measure. The ever-growing older population suffering from age-related disease, some of which are highlighted in Section 1.1, places a heavy burden on the National Health Service (NHS) and other medical facilities in addition to social burdens, such as care and mental well-being of family members (see Figure 1.3).
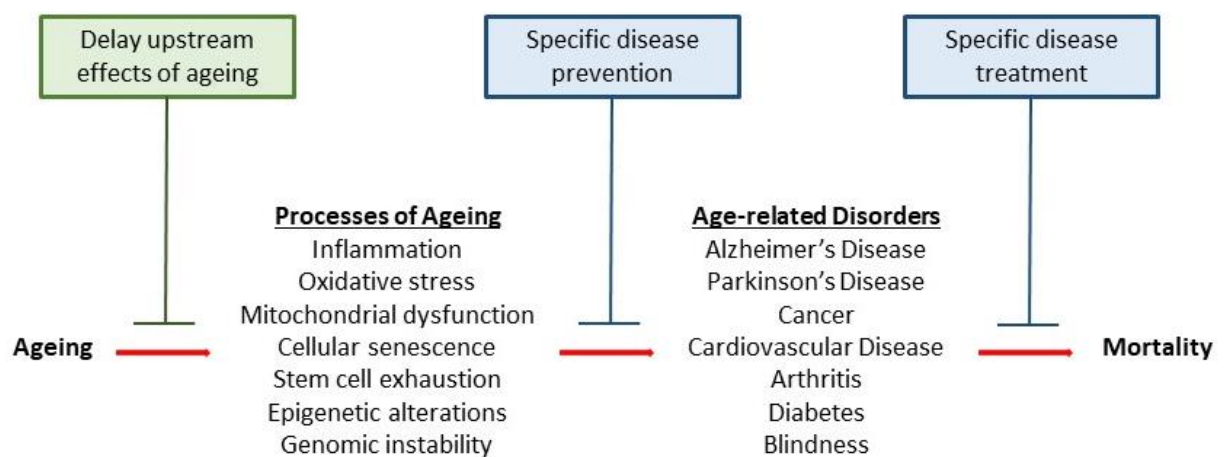
Figure 1.3: Age-related illnesses. Figure modified from Seals and Melov (2014). Ageing is linked to the progression of many diseases which are specially and separately investigated by numerous research organisations and charities for preventative and reactive measures. By targeting ageing and delaying upstream effects, it is possible to target all age-associated diseases at once and to do so mechanisms controlling the ageing process must be elucidated.

Health-span describes both the length of healthy life and the fraction of total lifespan spent free of disease (Campisi et al., 2019). Health cannot be extended indefinitely and it will inevitably decline, however, the aim of ageing research is to maximise health-span by maintaining physical and cognitive abilities for as long as possible,

compressing ill health in to a shorter time frame as possible, see Figure 1.4 (Hewitt, 2017).
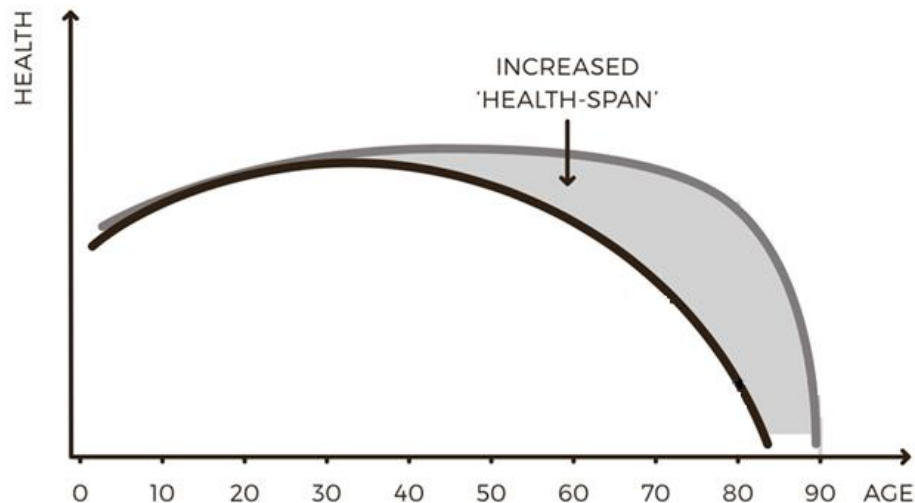
Figure 1.4: Increased health-span. Image modified from Hewitt (2017). The aim of ageing research is not to further extend lifespan but to increase the number of years an individual lives in good health, maintaining physical and cognitive ability for longer portions of life.

To increase health-span we must promote healthy ageing. Healthy ageing is defined as '*the process of developing and maintaining the functional ability that enables well-being in older age* ' (WHO, 2015). To do so, the ageing process must be fully understood and therefore it is imperative that research is undertaken to elucidate ageing mechanisms for the final aim of increasing health-span and reducing social and economic complications promoted by an ageing population (WHO, 2015).

1.3 Molecular basis of ageing

The last 30 years has seen an emergence of research aiming to characterise the biological basis of human longevity with a target to elucidate the relationship between biological and environmental factors influencing health-span and lifespan. As

previously shown in Figure 1.1, nine hallmarks of ageing have been identified by Lopez-Otin et al. (2013) using the following key attributes;

i) The hallmark must manifest during normal ageing

ii) Experimental magnification should speed up normal ageing

iii) Experimental amelioration should slow down normal ageing

1.3.1 Biological basis of Ageing

The nine hallmarks set out by Lopez-Otin et al. (2013) are briefly outlined below and comprise genomic instability, telomere attrition, loss of proteostasis, deregulated nutrient sensing, mitochondrial dysfunction, cellular senescence, stem cell exhaustion, altered intracellular communication and epigenetic alterations.

Genomic Instability

Briefly, genomic instability arises from extrinsic means such as physical, chemical, and biological damage as well as intrinsic means such as DNA replication aberrations and reactive oxygen species (Lopez-Otin et al., 2013). Majority of the induced damages can be repaired by the cell. However, if the cell is overwhelmed by the amount of damage, for example due to damage to the repair machinery, it can lead to genome instability, which is seen at steady rate or accelerated rate during normal ageing and premature ageing, respectively (Lopez-Otin et al., 2013).

Genomic instability and accumulated DNA damage are observed in aged cells and tissues above the level detected in healthy young cells. Following DNA damage, poly (ADP-ribose) polymerases (PARPs) are activated and are key in the cellular response to DNA damage (Fakouri et al., 2019). Where DNA damage takes the form of DNA double strand breaks, the preferred form of repair is through homologous

recombination which is facilitated by RAD51 (Delabaere et al., 2017). Across normal ageing and age-related disorders, an increase in PARP1 activation has been reported (Fakouri et al., 2019) in addition to reduced efficiency of RAD51 (Delabaere et al., 2017). These are common features in Alzheimer's disease, many DNA repair deficiency diseases and in premature ageing disorders (Fakouri et al., 2019). A theory for this observation is that cells with higher metabolic rate, such as brain and heart, are more susceptible to DNA repair defects due to higher levels of endogenous oxidative stress and reactive oxygen species. As a result, these higher metabolic cells rely more heavily on DNA damage response compared to cells with lower metabolic rates. Therefore in the absence of efficient DNA damage response and repair, the cell function will decline more rapidly with age (Fakouri et al., 2019). It is possible the increased incidence of neurodegenerative and cardiovascular disorders with age are linked to the genomic instability which may more rapidly impact tissues such as brain and heart (Fakouri et al., 2019).

Telomere Attrition

Telomere attrition describes the cumulative loss of telomeres, the protective sequences located at the end of chromosomes (Lopez-Otin et al., 2013). Loss of telomeres is observed during normal mammalian ageing as DNA replication is unable to copy the entire length therefore the repetitive DNA sequences located in the telomeres become shortened with each cell division. Increased telomerase activity can promote healthy ageing in mice whilst telomere dysfunction can promote early on-set of ageing (Lopez-Otin et al., 2013).

Telomere length is deemed a biological clock as once shortened to critical length, the cell can no longer proliferate and consequently enters senescence or undergoes

programmed cell death (Davinelli and De Vivo, 2019). This limiting factor can be observed through those with shorter telomeres often having shorter lifespan. Furthermore, lifestyle factors known to have a negative impact on lifespan such as smoking, stress and high body mass index correlate to faster telomere attrition which is linked to the oxidative stress caused by these factors (Davinelli and De Vivo, 2019).

Proteostasis

Another described hallmark of ageing is loss of proteostasis characterised by the accumulation of unfolded, misfolded or aggregated proteins (Lopez-Otin et al., 2013). An array of systems work in combination to either restore normal protein structure or to remove and degrade the abnormal element to prevent accumulation over time. However, multiple studies have confirmed that these systems fall out of regulation with age and that accumulation of aberrant proteins leads to loss of proteostasis which can in turn lead to age-related illnesses such as Alzheimer's disease and cataracts (Lopez-Otin et al., 2013).

Studies in *C. elegans* have revealed extensive protein remodelling and protein abundance changes during ageing (Hipp et al., 2019). Of all quantified proteins, one third were found to increase or decrease by two-fold at the end of the first week of adulthood (Hipp et al., 2019). Interestingly, in long-lived *daf-2* mutant worms the protein remodelling was reduced suggesting that the ability to maintain the proteostasis network is correlated with longevity (Hipp et al., 2019). Daf-2 is homologous to the Insulin-like growth factor 1 receptor (IGF-1R) found in humans and conserved across many taxa, discussed in more detail in section 1.4. Briefly, in 1993, Kenyon et al showed that mutations in the *daf-2* gene could extend *C. elegans* lifespan by up to 2.3-fold and increase resistance to temperature change. This created a model for

investigating difference between short and long-lived worms for elucidating molecular mechanisms underpinning ageing, including the role of proteostasis as described above.

Deregulated Nutrient Sensing

Deregulated nutrient sensing has been observed with age in many species ranging from yeast to mammals. The conserved nutrient sensing pathway known as the insulin and IGF-1 signalling (IIS) pathway (or simply IIS pathway) has been linked to longevity (Longo et al., 2005). The pathway includes IGF-1 and has downstream targets such as FOXO family, mTOR and AKT. Mutations in many of these targets have influenced longevity in some manner confirming this pathway is essential for regulation of both lifespan and health-span (Lopez-Otin et al., 2013). In support of nutrient sensing as an important role in ageing, dietary restriction has been shown to increase lifespan and/or health-span in species including *C. elgans*, *Drosophila melanogaster, Mus musculus* and non-human primates (Lopez-Otin et al., 2013). Deregulated nutrient sensing and specifically the IIS pathway will be considered in more detail in section 1.4.

Mitochondrial dysfunction

A fifth hallmark described is mitochondrial dysfunction. This arose from the reactive oxygen theory of ageing whereby reactive oxygen species (ROS), a natural by-product created by the inefficiency of the mitochondrial respiratory chain, would cause damage to the cell and propagate further ROS production which could accumulate overtime and cause cellular dysfunction (Lopez-Otin et al., 2013). However, it was noted that in yeast and *C. elegans* increased ROS could be used to promote lifespan whilst in mice there was no influence on ageing. Given these observations, it is suggested that ROS at low levels acts as a signalling system to promote survival (Lopez-Otin et al., 2013).

The concept of mitohormesis suggests low levels of ROS improve systemic defence mechanisms by inducing adaptive responses, such as mitochondrial biogenesis and oxidative metabolism (Ristow and Schmeisser, 2014). When levels of ROS surpass a threshold it becomes detrimental and damaging to the cell (Lopez-Otin et al., 2013).

Cellular Senescence

Cellular senescence is the stable arrest of the cell cycle with the main function of protecting damaged cells from replicating and inciting their removal. The number of cells in stable arrest increases with age which may be due to an inefficient turnover system whereby cells entering senescence are not effectively removed and the progenitors required to establish cell replacement are not mobilised, exhausting a tissues regenerative capacity in older organisms (Lopez-Otin et al., 2013). Furthermore, senescent cells secrete pro-inflammatory molecules that can cause damage to the cellular environment. If senescent cells are not efficiently removed these pro-inflammatory secretions can result in chronic tissue inflammation and other age-related conditions (Lopez-Otin et al., 2013).

The senescence-associated secretory phenotype (SASP) is a distinct secretome profile released by senescent cells which acts as a communicative mechanism to promote tissue regeneration by stimulating nearby progenitor cells (de Magalhães and Passos, 2018). If exposed to SASP for long enough, senescence is induced in young adjacent cells which can lead to tissue dysfunction. Senescent cells also show mitochondrial dysfunction and increased production of ROS which has been shown to induce DNA damage in nearby proliferating cells. The disruption to tissue microenvironment from SASP may interfere with tissue homeostasis and function.

Furthermore, use of mutant mice showed removal of senescent cells delayed onset of age-associated disorders in older age (de Magalhães and Passos, 2018).

Stem cell exhaustion

Stem cell exhaustion is caused by a culmination of age-related damages such as telomere shortening, DNA damage and cellular senescence (Lopez-Otin et al., 2013). Stem cells are rare cells that remain dormant in stem cell niches with retained capacity to differentiate into the cell type of the organ in which they are situated until required to repair and restore damaged tissues (Lopez-Otin et al., 2013, Ermolaeva et al., 2018). Adult stem cells are the longest living proliferative cells in multicellular organisms and so are inherently more likely to be exposed to these age-related damages (Ermolaeva et al., 2018). Interestingly, stem cell proliferation becomes deficient over time, which is a key contributor to tissue and organismal ageing. However, the process can occur over a shorter time period if stem cell proliferation occurs in excess. Aggravated stem cell proliferation in *Drosophila melanogaster* resulted in stem cell exhaustion and premature ageing (Lopez-Otin et al., 2013).

The role of stem cells to maintain capacity to differentiate in order to repair damaged tissue means they contribute to the regeneration and homeostasis of almost all tissues throughout lifespan (Ermolaeva et al., 2018). Therefore, stem cell exhaustion and decreased stem cell capacity will result in detriment to the tissue/organ within which they reside and ultimately lead to tissue degeneration (Ermolaeva et al., 2018).

Altered intracellular communication

The eighth described hallmark of ageing is altered intracellular communication. This arises in many forms and can be due to inefficient secretion of signalling molecules or

the reduced ability to receive and respond to signals accordingly (Lopez-Otin et al., 2013). Such disarray can lead to immune deficiency where pathogens or damaged cells are not recognised as detrimental and are thus not removed efficiently. It can also lead to chronic tissue inflammation and increased susceptibility to illness and disease (Lopez-Otin et al., 2013).

Epigenetics

The final hallmark of ageing is epigenetic modification. Epigenetic modifications have been shown to influence longevity and variations in life expectancy with epigenetic drift now identified as a primary hallmark of ageing (Lopez-Otin et al., 2013). The epigenome is comprised of a multitude of epigenetic modifications, some of which have been linked to ageing, see Figure 1.5 (D'Aquila et al., 2013, Pal and Tyler, 2016).
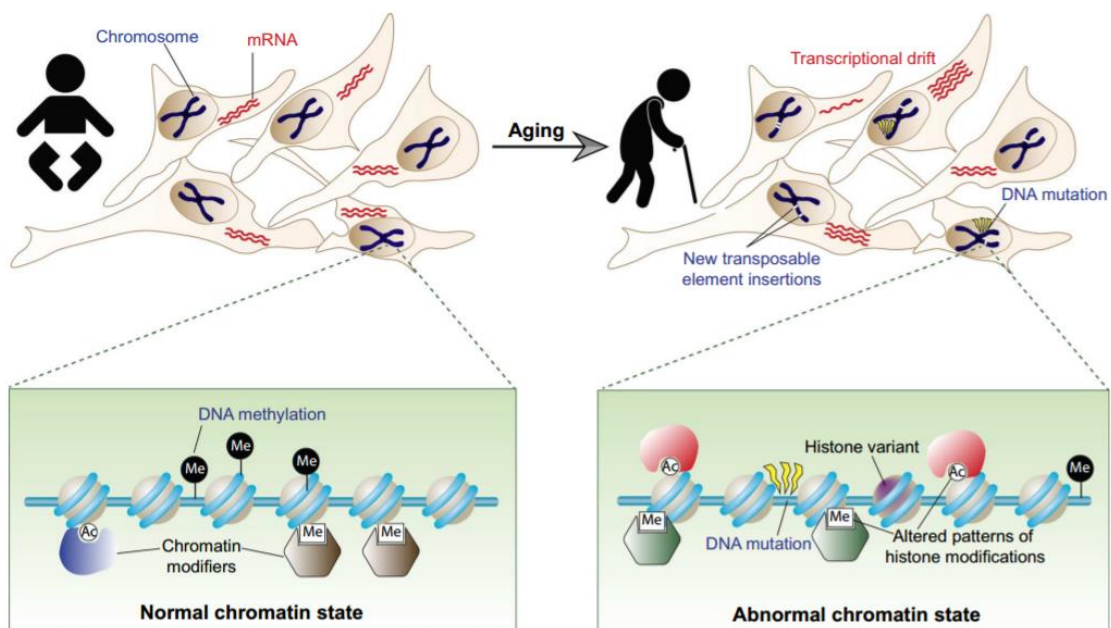
Figure 1.5: Schematic of epigenetic modifications during ageing. Similar patterns of gene expression are observed in cells of the same cell type which is a result of homogenous epigenetic information contained with-in each cell type. Throughout ageing epigenetic marks are modified sporadically by both exogenous and endogenous factors resulting in changed epigenetic profiles within cell types. Abnormal

chromatin state can be caused by incorporation of histone variants and changed DNA methylation and/or histone modification profiles leading to recruitment of different chromatin modifiers. Abnormal chromatin state includes altered transcriptional patterns and drift within the population and leads to new transposable elements being inserted into the genome and genomic instability, including DNA mutations (Pal and Tyler, 2016).

It has been established in model organisms that the genomic landscape of DNA methylation is altered throughout life, known as epigenetic drift, which can create a memory of received signals (Teschendorff et al., 2013). Epigenetic drift encompasses both hypo- and hyper-methylation and pertains to a gradual shift of the epigenome away from the baseline as opposed to an abrupt or programmed change and can be caused by environmental factors or spontaneous stochastic errors in the process of DNA methylation transmission (Pal and Tyler, 2016). Many early studies focussed on the hyper-methylation of promotor CpG islands linked to cancer susceptibility and progression. Methylation levels of approximately 70-80% of promoter CpG islands has been shown to increase in various cancers with age (Issa, 2014). Genome-wide studies in ageing cells and tissues, in addition to longitudinal studies, have provided further support to the phenomena of epigenetic drift. These studies have demonstrated that age-associated hyper-methylation occurs preferentially in the promoter regions of key developmental genes, many of which encode tumour suppressors and transcription factors involved in differentiation in embryonic stem cells. These changes can subsequently alter plasticity of ageing stem cells, causing stem cell exhaustion and defects that may result in cancer (Teschendorff et al., 2013, Issa, 2014).

Many studies have sought to identify links between chronological age, race/ethnicity and sex on mortality rates and disease susceptibility, however the relationship between biological age and these factors is less widely studied. In recent years' the 'epigenetic

clock' has been developed as an attractive biomarker of ageing. The epigenetic clock is based on the DNA methylation profile of 353 CpGs and has to some success been used to determine the biological age of human cell types including CD4+ T cells and neurons, tissues, and organs such as blood, brain, breast, kidney, liver and lung, with an accurate translation to chronological age (Horvath, 2013, Horvath et al., 2016). Horvath et al (2016) successfully used the epigenetic clock to demonstrate differences between racial/ethnic groups. This epigenetic approach to understanding biological ageing combines environmental and genetic factors to further understand epidemiological paradoxes and race/ethnicity and sex differences (Horvath et al., 2016).

1.4 Sex Differences in Ageing

It has long been observed in the human population that females live longer than males on average, noted at least as far back as the 1750's (Kalben, 2000). Historically it was considered that male lifespan was shorter due to tendencies towards higher risk-taking activities. However, research into molecular biology of ageing has revealed a much more complex picture with multiple biological factors playing a part in determining and influencing sex difference in ageing rate (Kalben, 2000, Austad and Fischer, 2016).

The molecular basis for sex differences in mammalian ageing initially focussed on hormone differences, the asymmetric inheritance of mitochondria and sex chromosomes (Austad and Fischer, 2016). The X chromosome and compensation theory proposed that males have a shorter lifespan due to having only a single X-chromosome. The idea behind this was that in females where there may be a deleterious allele on one X-chromosome, this would be balanced out by the other X-

chromosome, a compensation mechanism not available to males with only a single X-chromosome (Tower, 2006). The asymmetric inheritance of mitochondria theory suggests that due to maternal inheritance of mitochondria, lifespan-shortening mutations in mitochondria continue in males but are less frequent in females due to natural selection preferentially selecting those that increase female survival (Tower, 2006). However, this does not explain where similar sex differences are observed in models where sex is not genetically controlled.

Shorter lifespan of males compared to females has also been linked to earlier onset of senescence in males (Clutton-Brock and Isvaran, 2007). The current reasoning behind this early onset is that competition for sexual partners results in trade-offs for competitive success and thus selection pressure weighs more heavily on males compared to females. Consequently, there is a weaker selection for longer lifespan in males (Clutton-Brock and Isvaran, 2007).

With DNA methylation showing such an influential role in ageing process (see Section 1.3.1, sub-section Epigenetics, above), it is also resonable to expect and investigate the contribution of DNA methylation changes in some of the differences observed in ageing rate between sexes.. For exmple, a recently performed epigenome-wide association study found there to be sex-related differences in age-associated trajectories of DNA methylation, and that largely these were present on the X-chromosome (McCartney et al., 2019). Notably, many of these differences were located within genes previously linked to sexually dimorphic traits, such as prostate cancer and body mass index (McCartney et al., 2019).

Research into molecular baisis of sex-based differences in againg rate and process is still in its early stages. Considering the complexity of the ageing process alone, it is clear there is much more to be revealed before it is possible to fullly understand why and how lifespan and healthspan differs between the sexess (Austad and Fischer, 2016).

1.5 Current models used for research into the ageing process and key findings

To achieve the goal of increasing health-span in humans, it is fundamental that we understand the ageing process and mechanisms behind chronic diseases. Model organisms are widely used to investigate ageing for a multitude of reasons, such as relatively short lifespan, ease of maintenance, conserved genes sets between the model organisms used and humans. Commonly used model organisms are the yeast *Saccharomyces cerevisiae* (*S. cerevisiae*), the worm *Caenorhabditis elegans* (*C. elegans*)*,* the fruit fly *Drosophila melanogaster* (*D. melanogaster*) and the mouse *Mus musculus* (*M. musculus*)*.* A summary of key findings in these commonly used models can be found in Table 1.1.

Table 1.1: Key findings identified in commonly used models of ageing research

Species	Key Finding	Areas of research	Reference
S. cerevisiae	- Calorie restriction can increase lifespan. - Identification and manipulation of the insulin/IGF-1 signaling pathway has confirmed the importance of insulin signalling in longevity. - Measuring cell senescence to identify the genes that are essential for telomerase recruitment and assembly. - Functional peroxisomes may be important to preserve genome integrity specifically in old cells. - Metabolomic, transcriptomic and proteomic changes can be mapped to develop a holistic description of the cellular phenotype during ageing.	Lifespan extension DNA damage Omics studies Genetic manipulations to understand molecular basis for lifespan / health-span	(Liu et al., 2019) (Leupold et al., 2019) (Novarina et al., 2020)
C. elegans	- Temperature and food can be used to influence lifespan. - Mutations on genetic locus *age-1* can alter lifespan. - A heavy trade off between lifespan and health-span/fertility exists in long lived *daf-2* (IIS receptor) mutants. - Both *daf-2* and *age-1* can be suppressed by mutations in *daf-16* (FOXO transcription factor). - Mitochondria, signal transduction, stress response, protein translation, gene expression and metabolism can modulate lifespan.	Lifespan extension DNA damage Omics studies Genetic manipulations to understand molecular basis for lifespan / health-span	Tissenbaum (2015) (Garsin et al., 2003) (Benedetto et al., 2019)

	• Research in *C. elegans* has helped identify evolutionary conserved pathways crucial for longevity. • Bacterial resistance and longevity are inherently modulated by insulin signalling pathway. • Severe thermal stress resistance positively correlates with lifespan, severe oxidative stress resistance does not. Thus temperature-sensitive protein-handling processes play a role in *C. elegan* ageing.		
D. melaongaster	• FOXO is a central regulator of lifespan • The role of *p53* homologue found in flies is the control of apoptosis during development, the role as a tumour suppressor in vertebrates is an evolutionary advancement. • Lifespan modification can be achieved through insulin, TOR, GCN2 and AMPK signalling. • A healthy gut microbiome and muscle function are important for healthy ageing in flies. • Late-reproducing flies have almost double the lifespan of early-reproducing flies, these differences are heritable and thus support the hypothesis that genes determine lifespan.	Genetic manipulations to understand molecular basis for lifespan / health-span	Tissenbaum (2015) Aranda-Anzaldo and Dent (2007) (Piper and Partridge, 2018) (Campisi et al., 2019)
M. musculus	• Caloric restriction can extend lifespan. • Sirtuins regulate lifespan, delay ageing and can mediate reduced oxidative damage under caloric restriction to prevent age-related hearing loss. • The core circadian clock machinery, BMAL1 and CLOCK, directly regulates expression of NAMPT in the	Lifespan extension Genetic manipulations to understand molecular basis for lifespan/health-span	(Campisi et al., 2019)

		NAD+ salvage pathway in mice. The progressive loss of circadian behavioural patterns and diminished circadian gene expression is a common characteristic of ageing. Circadian clocks modulate various biological processes, and thus disruption is linked with age-related pathologies.		

*Note: this is not an exhaustive list but represents the diverse and useful nature of model research in understanding the biology of ageing.

S. cerevisiae are a widely used model organism due to commonalities at the genetic level to higher organisms. The short lifespan makes yeast a useful model for ageing and it has been shown that caloric restriction can extend lifespan in yeast which has also been observed in other models (Anderson et al., 2003). Furthermore, genomic methods have been developed which allow interrogation of an organisms' entire genetic make-up which has identified cell signalling pathways that influence lifespan and cell replication in yeast (AFAR, 2011). Although useful, yeast cannot provide an understanding of the complexity of ageing across multiple organ systems and thus is limited for ageing research (AFAR, 2011).

C. elegans has a short lifespan of 20-days making it a useful model for ageing. Amongst the 400 genes described to control longevity in *C. elegans* are encoded proteins that embody the role of insulin (AFAR, 2011). These proteins direct reproduction and longevity. Research into clock genes has also yielded effect on longevity and metabolism whereby increased lifespan is associated with stress resistance from bacterial infections, high temperature, radiation and oxidative damage (Lakowski and Hekimi, 1996, AFAR, 2011). Additionally, caloric restriction has been shown to extend lifespan of *C. elegans* (Tissenbaum, 2015).

Lifespan of *D. melanogaster* has been manipulated in various ways. One such way is by promoting mutations in the Indy gene that result in double the average lifespan without a trade-off with fertility of physical activity (Rogina et al., 2000). The Indy gene produces a protein similar to a human protein involved in energy production. This correlation to human biology means *D. melanogaster* has potential to yield useful results for understanding the ageing process in humans, however given the rise in

interest of epigenetics in ageing, the sexual reproduction of these flies may result in genetic differences where a clonal population would be better suited (AFAR, 2011).

Mice and rats are often used for research as they are genetically more closely related to humans than alternative models such as yeast and worms. Their small size and short-lifespan in comparison to other mammals also makes them more useful for ageing research than longer-lived species (AFAR, 2011). Caloric restriction and gene mutations have been shown to extend lifespan by up to 50% by interfering with hormones or increasing stress tolerance (Heilbronn and Ravussin, 2003, Masoro, 2005). With the readily available mouse genome and tools to model human genetic disease in mice it makes rodents an alluring model for ageing research, however rodents are limited by their longer lifespan in comparison to other available models (AFAR, 2011).
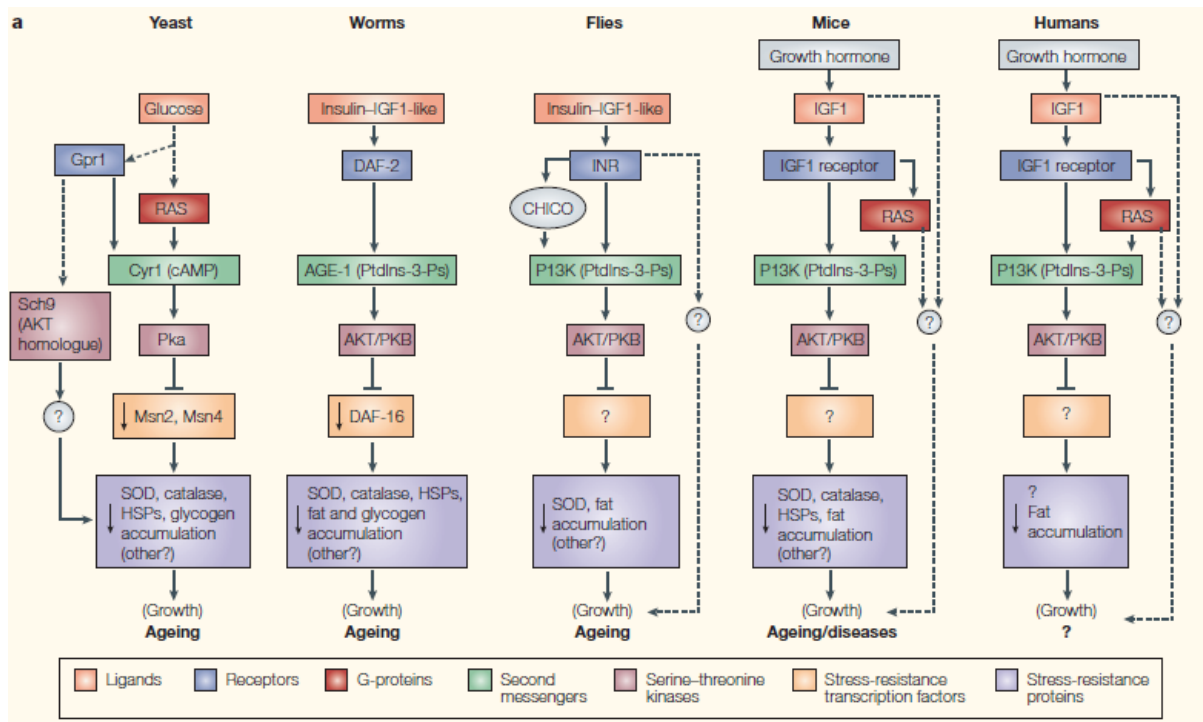
Figure 1.6: Conserved longevity pathways. Figure copied from Longo et al. (2005). Corresponding genes involved in longevity across model organisms are shown. These

pathways are conserved in model species making it possible to undertake ageing research using yeast, worms, flies and mice that are applicable to humans (Longo et al., 2005).

From use of these models, two major discoveries unfolded. The first was that conserved across these models was insulin-like growth factor 1 receptor (IGF-IR) pathway, as shown in figure 1.6 (Longo et al., 2005). This highly conserved pathway was shown to regulate ageing. Mutations in the IGF-IR counterpart in *C. elegans* titled *daf-2* and other downstream genes such at PI3K and AKT resulted in more than a 2-fold extension of lifespan and were effectively shown to delay the onset of ageing (Kenyon, 2010). Similar results have been obtained in *S. cerevisiae, D. melanogaster* and mice (Barbieri et al., 2003).

The second major discovery was that the mechanistic target of rapamycin (mTOR) pathway appeared to regulate ageing, also shown in figure 1.6 (Longo et al., 2005). Inhibition of mTOR activity has been shown to extend lifespan in yeast, worms and flies and is suggested to influence mammalian ageing (Barbieri et al., 2003). An mTOR hypomorphic mouse model expressing mTOR at a level 25% of wild-type showed increased lifespan without impact on food intake, glucose homeostasis or metabolic rate (Barbieri et al., 2003). Furthermore, the hypomorphic mice exhibited fewer biomarkers of ageing in tissue and showed preservation in many organ systems (Wu et al., 2013). Such results suggest that the central mechanisms of ageing may be conserved from yeast to mammals (Barbieri et al., 2003, Wu et al., 2013).

1.6 Non-canonical models for ageing research

Canonical model organisms, as described above, have advanced our understanding of the ageing process significantly. However, ageing process is complex and significant number of research questions remain unanswered. It is widely accepted that using a

diverse panel of organisms can help identify conserved and unique pathways of ageing across the animal kingdom. Therefore, over the last decade, there has been an increased interest in using non-conical model organisms to address some of the key questions in the field of ageing with some of the used models and their findings listed in Table 1.2.

Table 1.2: Key findings identified in non-canonical models of ageing research

Species	Key Findings and Characteristics	Areas of research	Reference
Botryllus schlosserri (Golden Star Tunicate)	• Identified genomic events underlying the evolution of vertebrates and lymphoid-mediated immunity. As the closest living invertebrate relatives to vertebrates, this model provides scope to investigate loss of immune system function with age relevant to humans. • This model has a stem cell-mediated budding programme useful for investigating regeneration and stem cell biology.	Immunology Stem cell biology Evolutionary biology Regeneration	Murthy and Ram (2015)
Ciona intestinalis (sea squirt)	• The siphons and the brain are capable of complete regeneration. • Regeneration of the neural complex has aided describing the molecular basis for age-related neurodegenerative disease. • Regenerative capacity is dependent on stem cell potency and number. • The rate of regeneration declines with age until completely ceasing in old age.	Regeneration	Murthy and Ram (2015) (Jeffery, 2018)
Nothobranchius furzeri (Killifish)	• Gut microbiota plays a key role in modulating vertebrate lifespan. • The heart shows oxidative stress accumulation and increase in microRNAs (miRNAs) activity in the ageing heart. The research suggests that the u*p*-regulation of the miR-29 family may be an endogenous mechanism linked to	Gut microbiome Gene expression	(Smith et al., 2017) (Heid et al., 2017) (Zupkovitz et al., 2018a) (Zupkovitz et al., 2018b)

	age-dependent cardiac damage leading to hypertrophy and fibrosis. • Identified members of the Klotho gene family as modulators of the ageing process. • A lifespan study found that histone deacetylase 1 is significantly down-regulated in muscle, liver, and brain with age correlating with increased mRNA levels of the cyclin-dependent kinase inhibitor cdkn1a (p21), similar to that seen in mouse brain.		
Nasonia vitripennis (wasp) / *Apis mellifera* (bee)	• Useful for investigating relationship between fecundity and longevity as Queen bee is reproductive whilst worker bees are not. Queen bees often outlive worker bees. • The social relationship expressed by bee colonies is unique and can be used to explore the effect of social as well as intrinsic regulation on longevity. • DNA methylation in invertebrates is at its highest at exon 2 and is linked to gene expression regulation, a pattern also seen in vertebrates. It is suggested that vertebrates may have later developed high methylation at CpG sites in addition to exon 2 in association with gene expression regulation as a secondary mechanism. Using invertebrate models that have DNA methylation alongside vertebrate models will help understand the evolution of the regulation of ageing.	Social influence on longevity Fecundity and longevity relationship Evolution of DNA methylation as a regulator of lifespan	(Rueppell et al., 2016) (Eyer et al., 2017) (Kvist et al., 2018)
Oryzias latipes (Japanese Rice Fish)	• Sex differences show females have longer telomere length compared to males, and females have a longer lifespan.	Sex difference Telomere length	(Gopalakrishnan et al., 2013)

	• A natural, 'menopause'-like decline of plasma estrogen was observed in females during ageing.	Hormone regulation	
Brachionus manjavacas (Rotifer)	• Caloric restriction, small molecule inhibitors, and dietary supplements extend lifespan. • RNAi can be used to identify key genes involved in modulating the ageing response. • Used to investigate maternal age-effects with offspring of older mothers showing decreased lifespan, fecundity, and stress resistance compared to offspring of younger mothers. • Accumulation of DNA is observed in offspring of older mothers as evidenced by changes in offspring mitochondrial number and morphology. • Maternal caloric restriction increases offspring lifespan and fecundity without direct offspring exposure to caloric restriction.	Calorie restriction Genetic manipulation Maternal age effects	(Snell et al., 2015) (Gribble, 2018)

1.7 Sex difference and ageing in model organisms

As described in Section 1.5, *D. melanogaster* has played an important role in the elucidation of ageing mechanisms, including the discovery of conserved IIS pathway. Notably, sex differences in the response to mutations of the IIS pathway have also been observed in *D. melanogaster* (Magwere et al., 2004). Mutations in the insulin receptor (*InR*, Figure 1.6) have been shown to increase the lifespan in females by 85%, yet decrease male lifespan (Tatar et al., 2001). This is thought to be driven by the reduction in juvenile hormone caused by the mutation in *InR* (Tatar et al., 2001). Juvenile hormone plays a significant role in multiple developmental and physiological processes in *D. melanogaster* and is synthesised in the corpus allatum (Gruntenko et al., 2010). Ablation of the corpus allatum resulted in significant physiological effects yet no such impact was observed in males, suggesting the role of juvenile hormone is sexually dimorphic (Gruntenko et al., 2010).

Research using model organism *Telegryllus commodus*, a cricket, found significant differences between sexes in age-dependent reproductive performance trajectories when exposed to sex-specific diets (Maklakov et al., 2009). Female fecundity reached it's peak in early adulthood whilst male sexual advertisement increased throughout lifespan and only declined after maximum field lifespan. This suggested that sexual selection and sex-dependent mortality may be of equal importance in reproductive ageing (Maklakov et al., 2009).

A study in both female and male mice at juvenile, young adult and middle age found that diet-induced obesity had differing impacts on the sexes dependent on the age at onset (Salinero et al., 2018). For example, when onset occurs in juveniles there is a larger impact on male body weight and glucose tolerance compared to females, yet

this is reversed where onset occurs in middle age (Salinero et al., 2018). Another study in mice has found that ageing female brains have lower oxidant capacity and higher anti-oxidant capacity in comparison to males (Sobočanec et al., 2003).

The above studies are a small demonstration of the variety of differences shown between sexes with age across multiple organisms. They also highlight the potential held within these models to discover important underlying ageing mechanisms that may drive differences between sexes.

1.8 *Daphnia spp.* as a research model

Daphnia species

Daphnia spp. are small planktonic crustaceans of the order Cladocera, shown in Figure 1.7. *Daphnia spp.* are considered keystone species due to their role as efficient phytoplankton grazers and as an essential food supply for planktivorous fish (Saebelfeld et al., 2017, Kim et al., 2018).

Figure 1.7: Female *Daphnia magna*. Female aged 10 days from a culture maintained at the University of Birmingham.

Daphnia spp. has a long history of use in ecology, evolution and ecotoxicology studies due to ideal characteristics such as large reproductive broods, easy and cost-effective maintenance in laboratory settings and field manipulation (Colbourne et al., 2011, Saebelfeld et al., 2017). *Daphnia magna* (*D. magna*) has a history of use in ecotoxicology assays whilst *Daphnia pulex* (*D. pulex*) is a National Institute of Health, USA listed model for biochemical research (Colbourne et al., 2011). Given the long history of investigative use coupled with the release of the *D. pulex* and *D. magna* genomes, in recent years research undertaken in *Daphnia spp.* has expanded to include large-scale genomic and metabolomic studies (environmental and toxicological) as well as genetic and epigenetic studies (Schumpert et al., 2014, Schumpert et al., 2016, Saebelfeld et al., 2017, Kim et al., 2018).

Much epigenetic research has been undertaken in *Daphnia* model due to sex determination and sexual reproduction relying on epigenetic mechanisms in response to environmental stressors (Harris et al., 2012). Likewise, *Daphnia* are known for phenotypic plasticity and adapt quickly to environmental conditions thus epigenetic modifications in response to toxicants and heavy metals are widely studied (Stollewerk, 2010, Harris et al., 2012).

Daphnia for ageing research

One emerging area of interest is the use of *Daphnia spp.* as a model for ageing research. For a model organism to be deemed suitable for use in ageing research it ideally needs to meet certain criteria. Firstly, a short lifespan is ideal so that life-time studies and lifespan modifications can be completed in a timely manner. *D. magna* strain Bham 2 has a short maximum lifespan of 120 days (Constantinou et al., 2019). Furthermore, *Daphnia spp.* have naturally occurring ecotypes with diverse lifespans

ranging from a few days to several months, for example *D. pulex* and *D. pulicaria* have recorded lifespan of between 20-25 days and 65-70 days respectively, allowing comparative ageing studies (Ebert, 2005, Harris et al., 2012). *Daphnia* also have the unique capacity for continued cell renewal and proliferation throughout their life (Ebert, 2005, Ram and Costa II, 2018).

Ageing studies using *Daphnia* model have shown that age-related decline was linked to increased oxidative stress and oxidative damage represented by increased formation of lipid peroxides and decline in unsaturated fatty acids (Barata et al., 2005a). It is suggested that the selective loss of antioxidant enzymes and changed availability of unsaturated fatty acids impacted oxidative stress, membrane lipid peroxide and decreased survival by unbalancing antioxidant defences (Barata et al., 2005b). Oxidative damage is associated with the mitochondrial theory of ageing therefore results obtained by Barata et al. (2005b) show *Daphnia* have potential to elucidate ageing mechanisms. Furthermore, more recent research has utilised short and long lived *Daphnia spp.* to investigate heat shock response and telomerase activity and telomere shortening with age (Schumpert et al., 2014, Schumpert et al., 2015a, Schumpert et al., 2016). These investigations utilise the beneficial characteristics of *Daphnia* as an ageing model.

Given the increasing interest in the role of epigenetics in ageing, a clonal population is ideal for ageing research. *Daphnia* reproduce via cyclical parthenogenesis, see Figure 1.8. This form of reproduction can result in large broods of genetically identical sisters which removes background genetic differences. This is essential for epigenetic research as it becomes possible to isolate epigenetic influence on ageing from genetic factors. The possibility of monitoring epigenetic influence across large populations

gives strong statistical power to results observed and therefore makes *Daphnia* an ideal model for ageing (Ebert, 2005). Furthermore, the production of males under environmental stress or hormonal exposure results in the production of genetically identical female and male individuals which provides large populations of genetically identical individuals to investigate sex differences.
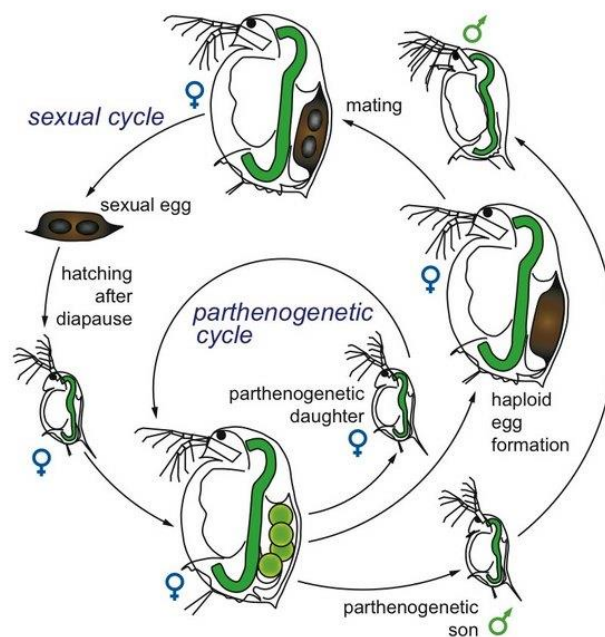
Figure 1.8: Life cycle of *Daphnia*. Under normal conditions, female *Daphnia* reproduce parthenogenetically and produce genetically identical daughters. Under stressful conditions males are produced and sexual reproduction results in formation of epphipia which can remain in diapause until optimal conditions return (Ebert, 2005).

1.6 Aims of the project

There is an increasing effort to enhance our understanding of the ageing process to combat the rise in age-associated diseases in a society where lifespan has increased in a disproportionate manner to health-span. As outlined in the general introduction, there are various avenues for research, including achieving a better understanding of

the role of epigenetic factors, including DNA methylation drift observed during ageing and promoting healthy ageing. The challenge is that majority of the short-lived organisms used currently for research into ageing process have no detectable DNA methylation. Ideally, there is a need for a model organism that is suitable for ageing research (e.g. short lifespan, availability of genome editing resources, easy to maintain in the laboratory setting), has a characterised epigenome, including methylome, and above all can generate a clonal population. The latter will allow investigation into the role of epigenetic factors in regulation of lifespan and health-span in the absence of genetic variation. *Daphnia magna* meets all the requirements outlined. Therefore, it can potentially serve as an ideal model organism for research into regulation of lifespan via DNA methylation. However, prior to that it is essential to characterise 'ageing' in *Daphnia*. To achieve that few key steps are required which outline the aims of this thesis:

1) To characterise biomarkers of ageing in female and male *Daphnia* and in doing so, to measure ageing rate and lifespan in both male and female *Daphnia*,

2) To characterise molecular changes that occur in female and male *Daphnia* during ageing. In this thesis, I focused on capturing the dynamic nature of lipids and gene expression throughout the lifespan of male and female *Daphnia magna*, and,

3) To investigate if there is an element of inheritance in ageing rate in *Daphnia* by investigating if the age of the mother at the time of reproduction has an impact on the fitness and health of the subsequent generations.

The data gathered and presented in this thesis will not only help to establish *Daphnia* as a suitable model organism for research into the ageing process, but will also help

to elucidate some of the sex differences observed during the ageing process at the molecular level. It is important to highlight that the data presented in this thesis also clearly demonstrated that genetically identical female and male *Daphnia* have different ageing rates and this further strengthens the need for investigating the role of non-genetic factors in regulation of lifespan and health-span. The research presented in this thesis will pave the way towards future research into using *Daphnia* for understating epigenetics of ageing.

CHAPTER 2:

Material and Methodologies

2.1 *Daphnia magna* stocks and maintenance

Cultures of *Daphnia magna* Bham 2 strain (originally obtained from the University of Reading (Heckmann et al., 2006)) have been maintained in the laboratory conditions at the *Daphnia* Facility, University of Birmingham, UK for over 10 years as previously described (Athanasio et al., 2016, Athanasio et al., 2018, Kilham et al., 1998). *D. magna* Bham 2 strain were maintained in photoperiodic lighting (16 h of light: 8 h of dark) and temperature of 20 ± 1 °C, in high hardness COMBO medium (HH COMBO). HH COMBO components are shown in Table 2.1.

Table 2.1: HH COMBO components

Number	Compound	Chemical Formula	Stock (g/L)	Notes	Volume added to 1L ddH$_2$O (ml)
1	<u>Calcium Chloride, Dihydrate</u>	CaCl$_2$ ·2H$_2$O	110.28		1
2	<u>Magnesium sulphate heptahydrate</u>	MgSO$_4$·7H$_2$O	113.5	Equal to 55.45 (if MgSO$_4$)	1
3	Potassium phosphate dibasic	K$_2$HPO$_4$	1.742		1
4	Sodium nitrate	NaNO$_3$	17		1
5	Sodium metasilicate nonahydrate (98% pure)	Na$_2$SiO$_3$ ·9H$_2$O	13.27		1
6	Boric acid	H$_3$BO$_3$	24	Requires heating to dissolve	1
8	<u>Sodium Bicarbonate</u>	NaHCO$_3$	63	Half strength stock	2

For each litre of HH COMBO, 1ml animal trace elements (ANIMATE), 1ml algal trace elements (ATE) and 0.5ml vitamins (VIM) were added. Details of ANIMATE, ATE and VIM are described in Tables 2.2, 2.3 and 2.4, respectively.

Table 2.2: Animal Trace Elements (ANIMATE) stored at 4°C;

Compound	Chemical Formula	Stock (g/100ml)	Volume to add to 1L stock (ml)	Final Concentration (mg/L)
Lithium chloride	LiCl	31	1	0.31
Rubidium chloride	RbCl	7	1	0.07
Strontium chloride Hexahydrate	$SrCl_2 \cdot 6H_2O$	15	1	0.15
Sodium bromide	NaBr	1.6	1	0.016
Potassium iodide	KI	0.33	1	0.0033

Table 2.3: Algae Trace Elements (ATE) stored at 4°C;

Compound	Chemical Formula	Stock (g/100ml)	Volume to add to 1L stock (ml)	Final Concentration (mg/L)
Iron Chloride hexahydrate	$FeCl_3.6H_2O$	50	1	1.0
Manganese Chloride tetrahydrate	$MnCl_2 \cdot 4H_2O$	18	1	0.18
Copper sulfate pentahydrate	$CuSO_4.5H_2O$	0.1	1	0.001
Zinc sulfate heptahydrate	$ZnSO_4.7H_2O$	2.2	1	0.022
Colbalt chloride Hexahydrate	$CoCl_2 \cdot 6H_2O$	1.0	1	0.01
Sodium molybdate	$NaMoO_4.H_2O$	2.2	1	0.022
Selenous acid	H_2SeO_3	0.16	1	0.0016
Sodium orthovanadate	Na_3Vo_4	0.18	1	0.0018

Table 2.4: VIM stored at 4°C;

Compound	Stock concentration	Volume added to 50ml ddH$_2$O
Biotin (*d*-biotin)	10 mg into 96 ml dH$_2$O	0.5ml
B12 (cyanocobalamin)	10 mg into 89 ml dH$_2$O	0.5ml
Thiamine Hydrochloride		0.01g

Media was changed three times a week and cultures maintained at a maximum of 1 adult/50ml of media at a minimum density of 5 individuals/250ml.

Animals were fed every other day with *Chlorella vulgaris* at a concentration of ≈27,550 cells of algae per individual *Daphnia*. *Chlorella vulgaris* is cultured in Bolds Basal Medium (BBM), detailed in Table 2.5.

Table 2.5: BBM components

Solution No.	Name	Formula	Weight (g)	Distilled water (ml)	Volume required for 1 L BBM (ml)
1	di-potassium hydrogen orthophosphate	K$_2$HPO$_4$	1.875	250	10
2	Potassium di-hydrogen orthophosphate	KH$_2$PO$_4$	4.375	250	10
3	Magnesium sulphate	MgSO$_4$.7H$_2$O	1.875	250	10
4	Sodium Nitrate	NaNO$_3$	6.250	250	10
5	Calcium chloride	CaCl$_2$.2H$_2$O	0.625	250	10
6	Sodium Chloride	NaCl	0.625	250	10
7	EDTA tetrasodium salt Potassium hydroxide	EDTA - Na$_4$ KOH	5.000 3.100	100	1
8	Ferrous sulphate	FeSO$_4$7H$_2$O H$_2$SO$_4$	0.498 0.1mL	100	1

	Sulphuric acid conc. (wt per mL = 1.84g)				
9	Boric acid	H_3BO_3	1.142	100	1
10	Zinc sulphate	$ZnSO_4.7H_2O$	0.353	25	0.1
11	Manganese chloride	$MnCl_2.4H_2O$	0.058	25	0.1
12	Cupric sulphate	$CuSO_4.5H_2O$	0.063	25	0.1
13	Cobaltous nitrate	$Co(NO_3)_2.6H_2O$	0.020	25	0.1
14	Sodium molybdate	$Na_2MoO_4.2H_2O$	0.048	25	0.1

The pH of BBM should be in the range of 6.7 ± 0.3 (6.4-7.0) and it is autoclaved prior to use. To harvest the algae, the algae grown in BBM is centrifuged at 3500 rpm for 15 minutes within a temperature range of 4-9°C. The pellet is re-suspended in Standard COMBO as detailed in Table 2.6, to a density of where a 1 in 10 dilution measures an absorbance of approximately 0.800 at a wavelength of 440nm using a 1cm cuvette. The algae stock was stored at 4°C and used within maximum of 1 week from date of preparation.

Table 2.6: Standard COMBO components

Compound	Chemical formula	Stock (g/L)	Notes
Calcium Chloride, Dihydrate	CaCl2 2H2O	36.76	
Magnesium Sulfate, Heptahydrate	MgSO4 7H2O	36.97	
Potassium phosphate dibasic	K2HPO4	8.71	
Sodium nitrate	NaNO3	85.01	
Sodium Bicarbonate	NaHCO3	12.60	
Sodium metasilicate nonahydrate (98% pure)	Na2SiO3 9H2O	13.27	
Boric acid	H3BO3	24.00	Requires heating to dissolve

2.2 Chemical-induction of genetically identical male *D. magna* BHAM 2

A stock solution of the crustacean reproductive hormone, (E,E) Methyl Farnesoate (MF; Tebu-Bio ltd, Peterborough, UK) was prepared by dissolving the chemical in dimethyl sulfoxide (80mM stock concentration). The stock was stored at -80°C until use. The stock was diluted 50-fold in DMSO to 1600μM then directly added to 50 mL of culture water (Final concentration: 400nM) containing sexually matured individual female *Daphnia* (age of maturity for *D.magna* Bham 2 strain: 9 days old). This concentration is sufficient to induce male *Daphnia* at 100% efficiency (Olmstead and Leblanc, 2002). Due to the instability of MF, media was changed daily to ensure consistent exposure. The first brood was discarded and male neonates were collected from 2nd – 5th broods. Female and male cultures were maintained separately.

2.3 Life history study

Life history studies were conducted for both female and male *D. magna* Bham 2 strain under normal culturing conditions. Survival and reproduction rate (only in females) were assessed for 50 individuals. Growth rate was calculated by measuring body length (L), body width (W) and tail length (T; n=25 individuals) as described previously (Martínez-Jerónimo, 2011, Athanasio et al., 2018) and shown in Figure 2.1. To measure growth rate, *Daphnia* (n= 25 individuals) were photographed at aged 1 day, 10 days then at 10 day intervals throughout their life using a stereomicroscope SMZ800 (Nikon, Japan) coupled to a digital camera DS-Fi2 (Nikon, Japan) and images were analysed using ImageJ software. Furthermore, heart rate (beats per minute; BPM) was measured for 25 individuals at 10 days intervals starting when the *Daphnia* were 10 days old until the end of their lifespan. To measure heart rate, video footages of the

Daphnia heart were captured using NIS-Elements F imaging software and Video Velocity software.
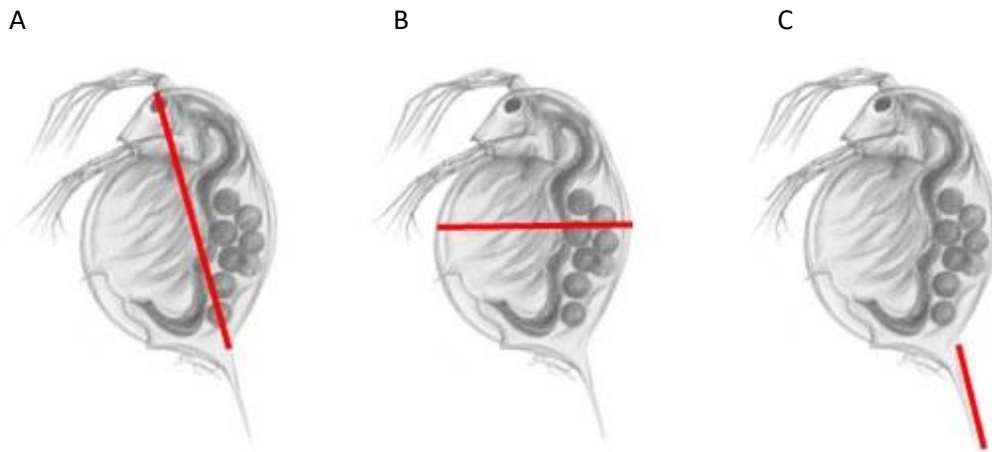
Figure 2.1: Body measurements taken using ImageJ software. Length, width and tail length were measured using ImageJ measuring tool. A) Length was taken from above the compound eye to the top of the tail spine. B) width was measured from opening of carapace to back of brood pouch. C) Tail spine was measured from top of the tail spine (point where body length measurement ended) to the bottom of the tail.

2.4 Measuring swimming speed for different age groups of *Daphnia magna* Bham 2 strain

The method described by Whitman and Miller (1982) with some modifications, was used to measure the time required for different age groups of female (10, 20, 40, 80 days old, n=5) and male (10, 20, 40 days old, n=5) *Daphnia* to travel a defined distance (s/cm). The method takes advantage of the phototactic behaviour of the *Daphnia* to guide them to swim a defined route and distance away from the light source. This was achieved by placing individual *D. magna* of appropriate ages in a stripette levelled and sealed with parafilm at one end and containing the culturing media HH COMBO. The sealed end of the stripette was fixed 4.5cm from the TransLight Illuminator light box

(Orsam 797-3453, 8kWh/1000h). The *Daphnia* were allowed to acclimatise to darkness for 10 minutes before being exposed to light. Time taken for each *Daphnia* to travel 10cm following exposure to light was recorded at 0.5x speed using Slo Mo Video mobile application, see Figure 2.2 for experimental set up.
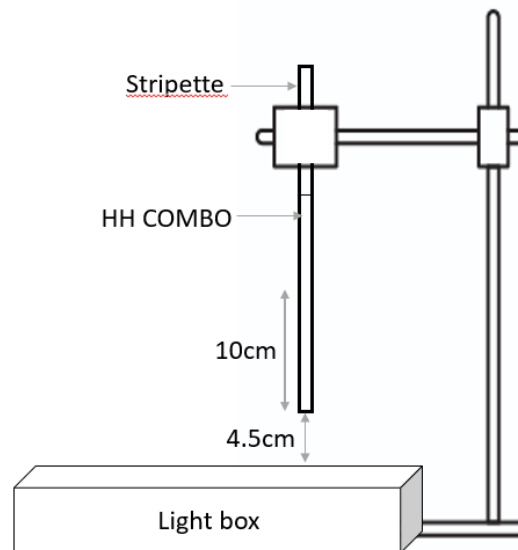
Figure 2.2: Swimming speed experiment set up. A single daphnid is placed in to the stripette and allowed to climatise to darkness for 10 minutes before turning the light box on and time taken to swim 10cm is recorded.

2.5 Comet Assay

Comet assay was performed to assess accumulation of DNA damage with age in female and male *Daphnia* according to the method developed by Pellegri et al (2014) for *Daphnia magna*. Due to variance in DNA damage across different tissue types, haemolymph was selected as the tissue for analysis. To avoid contamination of the haemolymph with non-haemolymph cell the method described by Auld et al (2010) was used to directly extract haemolymph from the heart of the *Daphnia*. This was achieved by piercing the haemocoel and allowing the heart to force haemolymph through the tear and directly into the collecting buffer, Phosphate Buffer Saline (PBS).

Haemolymph from 5 *Daphnia* were combined per replicate for each age group (n=3). The alkaline comet assay was completed following the methods in Pellegri et al (2014). The single haemolymph cells were suspended in low melting point agarose (1%) then spread on slides coated with high melting point agarose (1%) and covered with a coverslip and allowed to solidify at 4°C. After solidification a second layer of low melting point agarose was added and the plasma and the nuclear membranes were digested using a lysis buffer. DNA unwinding and electrophoresis (0.78V/cm, 300 mA) were performed in an alkaline buffer (1 mM Na2EDTA, 300 mM NaOH, pH > 13). After electrophoresis, each slide was neutralised with 2 ml of neutralisation buffer (0.4 M Tris–HCl, pH 7.5), fixed in 100 % ethanol at −20˚C, air dried and stored in closed microscope slide container before staining with 1:1000 dilution of SybrGold (ThermoFisher, S11494) and counting using a Zeiss Axiovert 10 microscope. Slides were scored counting 50 nuclei per sample using an automatic image analysis system (Comet Assay IV; Perceptive Instruments Limited, Haverhill, Suffolk, UK). Tail Intensity (TI, %) was selected as the representative DNA damage parameter as measured by Comet Assay IV software. TI(%) is defined as the ratio of total tail intensity to total intensity of the comet expressed as a percentage (Vojnovic et al., 2013). Comet tail is shown in Figure 2.3.
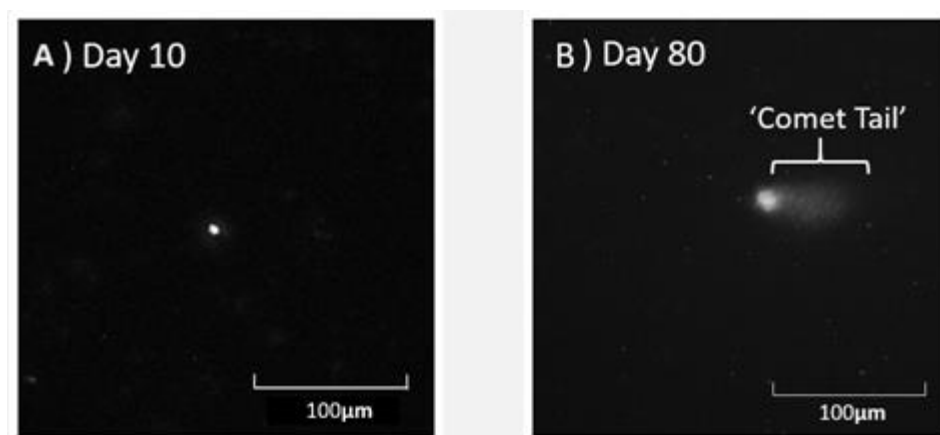
Figure 2.3: Examples of comets from female D. magna. At day 10 comets are tights and much of the intensity comes from the comet head with very little tail (A). Comet tail becomes much larger with older age and makes up a greater proportion of overall comet intensity (B).

2.6 Immunofluorescence microscopy

2.6.1. Experimental design

Two groups of samples were used for immunofluorescence microscopy: (I) Female and male *D.magna* Bham 2 strain cultured under normal laboratory conditions, representing natural ageing group, (II) Female and male *D.magna* Bham 2 strain treated with cisplatin for 6 hours (0.1µg/ml dissolved in culture media, Sigma, UK), representing the group with induced DNA damage. For both natural ageing (I) and induced damaged (II) groups the following female and male ages were used, respectively: 10, 20, 40 and 80 days old females (representing 10%, 20%, 40% and 80% of the lifespan of a female *D.magna* Bham 2 strain, respectively; n=3 with each replicate containing 7 individuals) and 10, 20 and 40 days old males (representing 20%, 40% and 80% of the lifespan of a male *D.magna* Bham 2 strain, respectively; n=3 with each replicate containing 7 individuals). In addition, for the induced damaged group (II) not only samples were collected immediately after 6 hours of cisplatin exposure (no recovery) but also samples were collected after 1.5, 3 and 6 hrs of recovery in clean media free of cisplatin. The later was used to assess the change in DNA damage levels and DNA repair efficiency with age.

2.6.2. Procedure

The immunolabelling technique described for *D. magna* by Gómez et al. (2016) was used. Haemolymph was extracted as explained earlier and immediately added to fixative (PBS, 5% formaldehyde, 0.05% triton-X-100). The fixed haemolymph cells

were transferred on to a poly-L-lysine coated slide and fixed in liquid nitrogen. Slides were washed 3 x 5 minutes in PBS followed by incubation with primary antibody RAD51 (1:50, Calbiochem PC130-100UL) overnight at 4˚C protected from light. Slides were washed 3 x 5 minutes in PBS before incubation with secondary antibody goat anti-rabbit (1:200, Abcam ab150078) at room temperature for 45 minutes protected from light. Slides were washed 2 x 5 minutes PBS and incubated with Hoechst (10µg/µl, Thermo Scientific 62249) for 10 minutes at room temperature protected from light. Slides were washed 3 x 5 minutes in PBS and mounted in sterile glycerol. Slides were imaged using a Nikon Eclipse E600 microscope equipped with epifluorescence optics, a motorized z-drive, and a Hamamatsu ORCA-ER C4742-95 digital camera controlled by NIS-Elements AR v4.13 software on. A minimum of 25 foci were counted per replicate using ImageJ software. Panel images were produced using Fiji software.

2.7 Western blot

To determine the specific immunoreactivity of anti-Rad51, Western Blot analysis of *Daphnia* haemolymph extracts was performed. *Daphnia* haemolymph was transferred into RIPA buffer according to previous Western Blot protocols for *Daphnia* (Schumpert et al., 2016). The blot was incubated with the primary antibody at a dilution of 1:1000, followed by incubation with HRP-conjugated goat anti-rabbit IgG (1:2000, Abcam ab150078). Visualization was performed using alkaline phosphatase detection system (BioRad).

2.8 Quantification of Protein Levels

Protein content was determined using the Coomassie Brilliant Blue G-250-based assay (Grintzalis et al., 2015). BSA was used to create a standard curve. Female and male samples were collected at 10 day intervals between ages 10–100 days for

females and 10–50 days for males (5 individuals per replicate, n=3). Eggs were removed from the female brood pouch. Samples were homogenised in 800µl deionised water using a Precellys 24 lysis and homogenisation machine (2 x 10s, 2500rpm). Bradford reagent was prepared as follows; Coomassie brilliant blue dissolved in 2M hydrochloric acid (60mg/100ml), 2M hydrochloric acid and deionised water (dH$_2$O) combined in a ratio of 1:1:3 respectively. Samples of each sample group were set up in a clear flat-bottomed 96-well plate; 3 x blank comprising 125µl dH$_2$O plus 125µl Bradford reagent and 4 x 25µl sample, 100µl dH$_2$O and 125µl Bradford reagent. The plate was incubated at room temperature for 10 minutes before absorbance was read on a spectrophotometer at wavelength 595nm. The resulting absorbance was converted to protein (µg/ml).

2.9 Quantification of the Lipid Peroxidation Product

Lipid peroxidation products free-malondialdehyde (FrMDA) and protein-bound malondialdehyde (PrMDA) were measured following the Thiobarbituric Acid Reactive Substances (TBARS) assay (Grintzalis et al., 2013). MDA was used to create a standard curve. The same samples used for protein quantification were combined with 25mg/ml thiobarbituric acid (TBA) dissolved in 0.2M sodium hydroxide and 1g/ml trichloroacetic acid (TCA) dissolved in 12M hydrochloric acid (HCl) in a 5:1 (sample: TBA-TCA-HCl) ratio. For reagent blanks dH$_2$O was used in place of the sample. Replicates were incubated for 20 minutes at 100˚C in a water bath with the lid of the microcentrifuge tube open. Following incubation 100% ethanol was added in a 1:1 ratio. Samples were vortexed and centrifuged to clear debris before transferring supernatant in to a black 96-well plate. Fluorescence was measured at Ex/Em 485/535nm. Results were normalised to protein level.

2.10 Quantification of Protein Thiols

Concentration of reduced thiols was determined using the 4',4'-dithiopyridine (DTP) assay (Grintzalis et al., 2014). A standard curve was produced using glutathionine. For samples, to a clear 96-well plate 150µl sample used for protein determination and TBARS assay was combined with 50µl 12M formamide and 50mM acetic acid (pH 4.5). For the sample, 50µl 0.75mM DTP in 12M formamide and 50mM acetic acid (pH4.5) was added but for sample blank only 12M formamide and 50mM acetic acid (pH4.5) was added. For reagent blank 200µl of 12M formamide and 50mM acetic acid (pH4.5) was combined with 50µl 0.75mM DTP in 12M formamide and 50mM acetic acid (pH4.5). Sample reagent blank comprised of only 250µl 12M formamide and 50mM acetic acid (pH4.5). Replicates were incubated at room temperature for 10 minutes before absorbance was measured at 325nm.

2.11 Ultra High-Performance Mass Spectromentry (UHPLC-MS) lipidomics

2.11.1 Sample collection for UHPLC-MS lipidomics

Samples were collected at regular intervals for female and male *D. magna*, as shown in Figure 2.4.
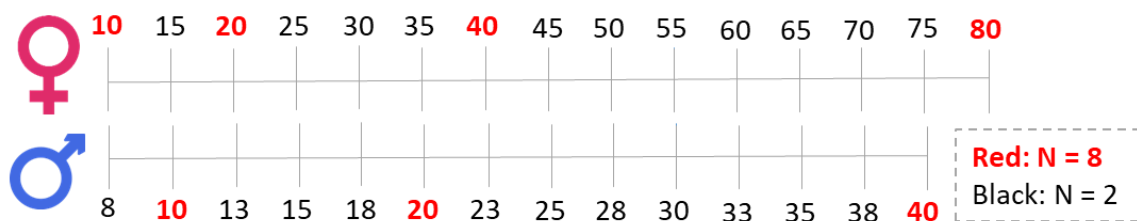
Figure 2.4: Sample collection details for female and male D. magna. Sample ages for females are shown at the top where the minimum sampled age is 10 days and the maximum sampled age is 80 days. Male sample ages are shown on the bottom and have a minimum sampled age of 8 days and maximum sample age of 40 days. Ages shown in red have a biological replicate number of 8, ages shown in black have a biological replicate number of 2.

When male *D. magna* had reached the sampling age, samples were collected at the same time of day for all sampling groups and were washed with deionised water. Excess fluid was removed using a Kimberley-clarke wipe before being flash frozen in liquid nitrogen. Female samples were collected using the same method, however, to ensure females were in a similar reproductive stage and no signal would be detected from neonates, individuals with empty brood pouches were collected within a 2 hour window of brood release.

2.11.2 Sample preparation UHPLC-MS lipidomics

To ensure the same amount of biomass was used for lipid extractions regardless of the age and size of the *Daphnia*, an initial experiment was conducted to measure the dry mass of male and female *Daphnia* at different ages and calibration curves were created (Figure 2.5 and Figure 2.6). This enabled the used of consistent biomass (equivalent to dry mass 4.37mg) for each lipid extraction for all sample groups, see Tables 2.7 and 2.8 (Đức et al., 2016).

$$y = 2E\text{-}05x + 6E\text{-}05$$

$y = 1E\text{-}06x + 0.0008$
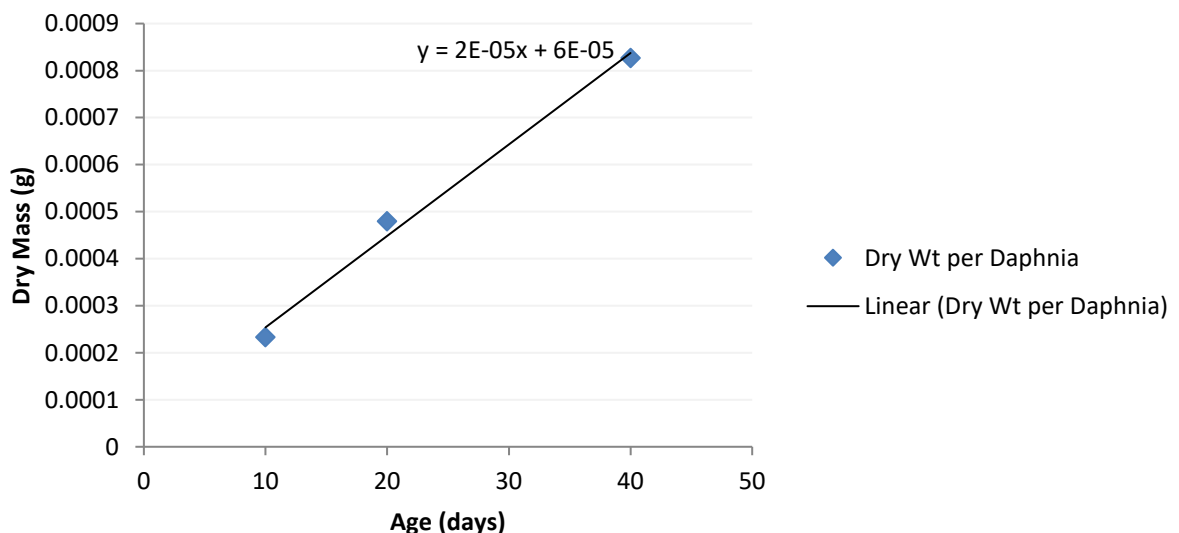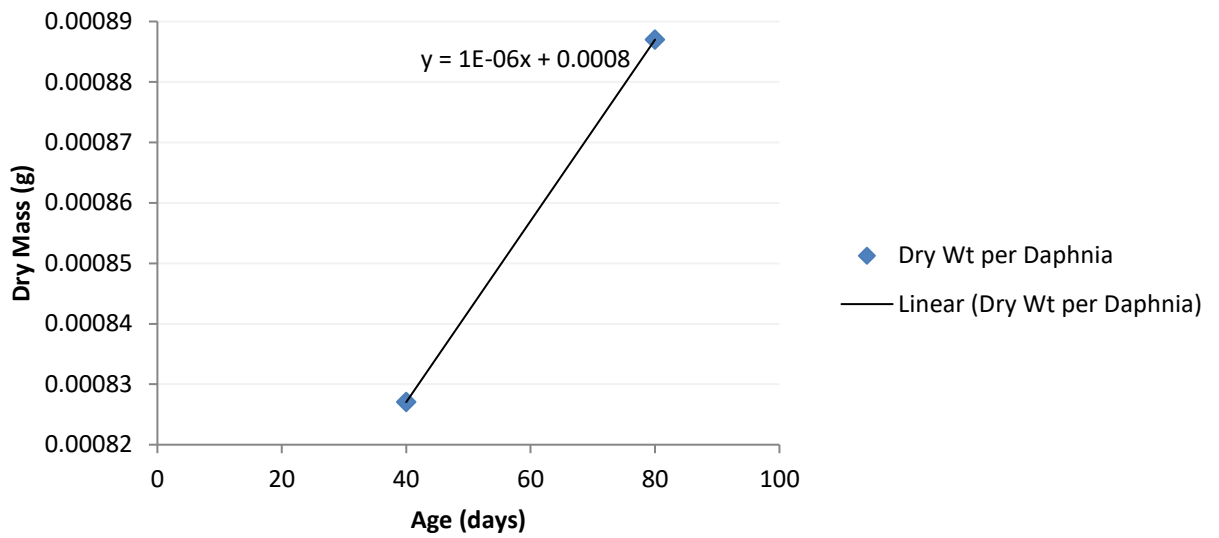
Figure 2.5: Dry mass of female D. magna. A) Dry mass of female *D. magna* from aged 10, 20 and 40 days with linear tend line. Equation of the line was used to predict dry mass of female animals for intermediate age groups between 10 and 40 days of age, see Table 2.7. B) Dry mass of female *D. magna* from aged 40 and 80 days with linear tend line. Equation of the line was used to predict dry mass of female animals for intermediate age groups between 40 and 80 days of age, see Table 2.7.

$y = 1E\text{-}05x + 7E\text{-}06$
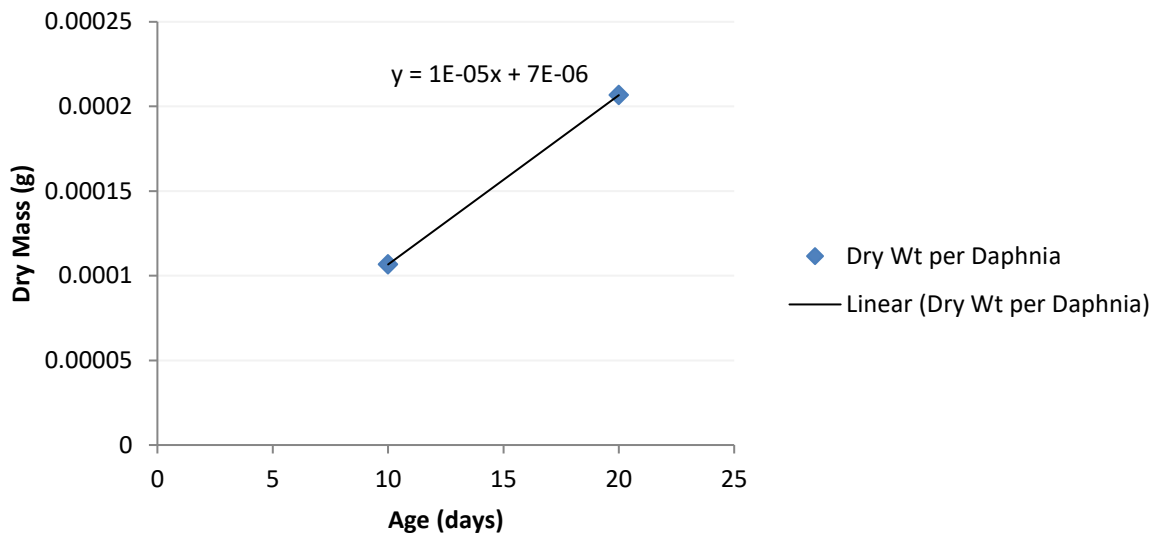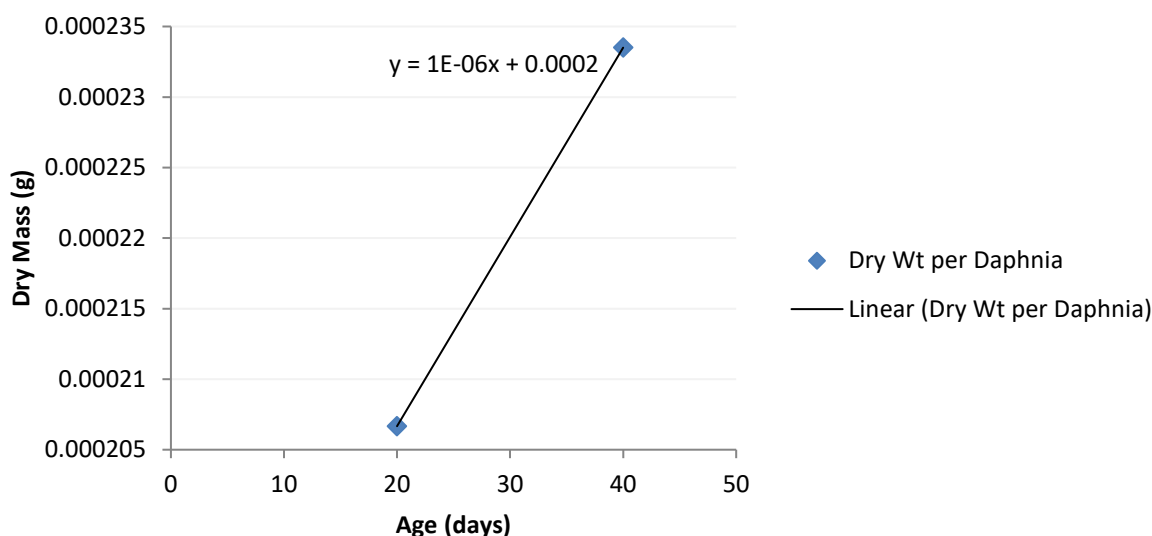
Figure 2.6: Dry mass of male D. magna. A) Dry mass of male *D. magna* from aged 10 and 20 days with linear tend line. Equation of the line was used to predict dry mass of male animals for intermediate age groups between 10 and 20 days of age, see Table 2.8. B) Dry mass of male *D. magna* from aged 20 and 40 days with linear tend line. Equation of the line was used to predict dry mass of male animals for intermediate age groups between 20 and 40 days of age, see Table 2.8.

Table 2.7: Number of female *D. magna* used for each intermediate age group per replicate based on actual and predicted weight

Predicted weights at intermediate ages				
Age	Predicted Weight (g)	No. daph required to approx. 5xFD80 sample		Animals required per rep	Total weight of replicate (g)
Using Supplementary Figure S1a				
15	0.00036	0.004435 / 0.00036	12.31944	12	0.00432
25	0.00056	0.004435 / 0.00056	7.919643	8	0.00448
30	0.00066	0.004435 / 0.00066	6.719697	7	0.00462
35	0.00076	0.004435 / 0.00076	5.835526	6	0.00456
Using Supplementary Figure S1b				
45	0.000845	0.004435 / 0.000845	5.248521	5	0.004225
50	0.00085	0.004435 / 0.00085	5.217647	5	0.00425
55	0.000855	0.004435 / 0.000855	5.187135	5	0.004275
60	0.00086	0.004435 / 0.00086	5.156977	5	0.0043
65	0.000865	0.004435 / 0.000865	5.127168	5	0.004325

| 70 | 0.00087 | 0.004435 / 0.00087 | 5.097701 | | 5 | 0.00435 |
| 75 | 0.000875 | 0.004435 / 0.000875 | 5.068571 | | 5 | 0.004375 |

Age in days	Dry Weight per single *Daphnia* (actual)
10	0.000233
20	0.000479
40	0.000827
80	0.000887

Table 2.8: Number of male *D. magna* used for each intermediate age group per replicate based on actual and predicted weight

Predicted weights at intermediate ages				
Age	Predicted Weight (g)	No. daph required to approx. 5xFD80 sample	Animals required per rep	Total weight of replicate (g)
Using Supplementary Figure S2a				
8	0.000087	0.004435 / 0.000087	50.97701	51	0.004437
13	0.000137	0.004435 / 0.000137	32.37226	32	0.004384
15	0.000157	0.004435 / 0.000157	28.24841	28	0.004396
18	0.000187	0.004435 / 0.000187	23.71658	24	0.004488
Using Supplementary Figure S2b				
23	0.000223	0.004435 / 0.000223	19.88789	20	0.00446
25	0.000225	0.004435 / 0.000225	19.71111	20	0.0045
28	0.000228	0.004435 / 0.000228	19.45175	19	0.004332
30	0.00023	0.004435 / 0.00023	19.28261	19	0.00437
33	0.000233	0.004435 / 0.000233	19.03433	19	0.004427
35	0.000235	0.004435 / 0.000235	18.87234	19	0.004465
38	0.000238	0.004435 / 0.000238	18.63445	19	0.004522

Age in days	Dry Weight per single *Daphnia* (actual)
10	0.000107
20	0.000207
40	0.000233

Lipid extractions were conducted using a biphasic approach as described by Wu et al. (2008) and Mirbahai et al. (2013). Samples were homogenised in 320µl ice-cold methanol (LC-MS grade reagent, JT Baker, 9822) and 128µl water (UHPLC-gradient grade, Merck, 1.15333.2500) using a Precellys 24 lysis and homogenisation machine

(2 x 10s, 6400rpm). Ice-cold chloroform (320µl, 98% purity, stabilised with amylenes; Merck, 1.02444.2500) was added to each vial and vortexed briefly. After adding water (160µl), samples were vortexed for 30s and kept on ice for 10 minutes. Samples were centrifuged for 10 minutes (4000rpm, 4˚C) then kept at room temperature for 5 minutes to allow separation of the phases. The non-polar (lipid) layer was transferred into a 1.8ml glass vial and dried using nitrogen steam for 15 minutes before being stored at -80˚C. Extract blanks were produced following the same protocol without *Daphnia* material.

2.11.3 Sample resuspension UHPLC-MS lipidomics

Ice-cold 1:1 acetonitrile: propan-2-ol (80µl; Fisher Chemicals: LC/MS grade A955-212, LC-MS grade A461-212) was added to the dried extracts and vortexed (30 s). Equal amount (15µl) was taken from each sample, pooled and vortexed to create the intra-study quality control (QC) sample. Samples were centrifuged (4˚C, 4000rpm, 10 minutes). Supernatant (55µl) was transferred to a low-volume HPLC vial (Thermo Fisher) and stored on ice. The QC sample was vortexed and centrifuged (4˚C, 4000rpm, 10 minutes) and divided into 23 aliquots of 50µl and loaded into low-volume HPLC vials. Vials were placed in an autosampler (7˚C).

2.11.4 UHPLC-MS/MS lipidomics

Lipidomics data were acquired using a Dionex UltiMate 3000 Rapid Separation LC system (Thermo Fisher Scientific, MA, USA) coupled with a heated electrospray Q Exactive mass spectrometer (Thermo Fisher Scientific, MA, USA). Extracts were analysed on a C30 column (Accucore 150 x 2.1mm, 1.7 µm; Thermo Fisher Scientific, MA, USA). Mobile phase A consisted of 10mM ammonium formate in 50% v/v acetonitrile (Fisher Chemicals, A955-212) with 0.1% formic acid and mobile phase B

consisted of 2mM ammonium formate in 10:88:2 v/v/v acetonitrile, isoproponyl (Fisher Chemicals, A461-212) and water (Merck, 1.15333.2500) with 0.02% formic acid. Gradient: t=0.0, 22% B; t=6.0, 60% B; t=14.0, 85% B; t=23.0, 100% B; t=26.0, 100% B; t=26.1, 22% B; t=30.0, 22% B. All changes were linear (curve = 5) and the flow rate was 0.40 mL/min. Column temperature was 45°C and injection volume was 5 µL. Data were acquired in both positive and negative ionisation UHPLC-MS/MS within the mass range of 200 - 1800 m/z at resolution 70,000 (full scan data; FWHM at m/z 200) and 35,000 (MS/MS data). The UHPLC-MS/MS scan cycle was as follows: full scan, 5xHCD MS/MS (top 5 most intense ions), repeat. An MS/MS exclusion list - created from an extract blank sample was used in the method. Stepped normalised collision energies of 25 and 30 were used, and dynamic exclusion was set to 8s. Ion source parameters were set as follows: sheath gas = 60 arbitrary units, aux gas = 20 arbitrary units, sweep gas = 1 arbitrary units, spray voltage = 3kV capillary temp. = 285°C, aux gas heater temp. = 370°C. Automatic gain targets of 1e6 (full scan MS) and 1e5 (MS/MS) were used.

2.12 RNA Sequencing

2.12.1 Sample collection for RNA-sequencing

Samples were collected using the same method and at the same age groups as detailed in section 2.11, however here 3 replicates for each age group were collected.

2.12.2 RNA Extraction

Samples were extracted using the Qiagen RNEasy Micro Kit following manufacturer instructions. Briefly, samples were homogenised in 350µl RLT buffer containing 1% β-mercaptoethanol, using ceramic beads in precelleys tubes and a precelleys 24 lysis homogenisation machine (Bertin Technologies) set to 6400rpm (2 x 10s with 20s

break). The homogenate was transferred to a 1.7ml clear microcentrifuge tube (Axygen; MCT-175-C) and centrifuged at 14,000rpm for 3 minutes at 28°C. The supernatant was carried forward to a fresh microcentrifuge tube and gently mixed with 350µl 70% ethanol (Fischerbrand, HPLC Grade; E/0665DF/17). The mixture was transferred on to the column and centrifuged for 30s at 10,000rpm at 28°C. The column was then washed with 350µl of RW1, centrifuged at 10,000rpm at 28°C. To each column, 80µl of RDD buffer with DNase 1 (7:1 ratio) was added directly to the column and maintained at room temperature for 15 minutes. Again, the column was washed in 350µl RW1 buffer by centrifuging for 30s at 10,000rpm, 28°C. The column was then washed with 50µl RPE buffer and centrifuged for 30s at 10,000rpm, 28°C followed by washing with 500µl 80% ethanol, centrifuged for 2 minutes at 10,000rpm, 28°C. The column was dried by centrifuging for 5 minutes at 14,000rpm, 28°C and the dried column was transferred in to a clean 1.5ml microcentrifuge tube. To elute the RNA, 40µl DEPC-treated water (Ambion; AM9915G) was added and incubated at room temperature for 1 minute. Samples were centrifuged for 1 minutes at 14,000rpm, 28°C. Samples were stored at -80°C until required and 5µl was taken forward for quantification.

2.12.3 RNA Quantification

RNA extractions were quantified using Nano-drop and Qubit. Using a nano-drop (ND8000, 8-Sample spectrophotometer), RNA content of 1µl undiluted sample was quantified. Additionally, purity of the RNA was also assessed by looking for protein and phenol contamination (260:280 ratio), and phenolate and organic compound contamination (260:230 ratio). Samples with a 260:280 and 260:230 ratio of >1.8 were carried forward.

Based on the nano-drop quantification, appropriate dilutions were prepared for quantification by Qubit which has an initial sample range of 250pg/ul to 100ng/ul and can quantitate from 5 – 100ng. Using 1µl of appropriately diluted sample added to 200µl of 1:200 Qubit™ High Sensitivity RNA buffer (Invitrogen; Q32855), RNA samples were quantified.

To determine quality of RNA, High Sensitivity RNA Screen Tape (Aglient Technologies; 5067-5579) were used. The initial sample range is 500-10,000pg/µl and so samples were diluted appropriately based on Qubit quantification. Samples were prepared by adding 1µl of appropriately diluted sample to 10µl sample buffer. Samples were heated to 72°C for 3 minutes and cooled for 2 minutes on ice. Samples were spun down and ran on the Aglient 2200 TapeStation System with Aglient 2200 TapeStation software.

2.12.4 RNA sequencing sample preparation

Samples were prepared in a 96-well plate for library preparation by combining the appropriate volume of each sample to equal 200ng RNA, plus the manufacturer recommended proportion of Spike-In RNA Variant Mixes E0, E1 and E2 (Lexogen, 025.03). Samples were made up to a total volume of 50µl by adding DEPC-treated water. The plate was sealed and stored at -20°C until library preparation commenced.

2.12.5 RNA Library Preparation and Sequencing

RNA libraries were prepared by the Environmental 'Omics Facility at the University of Birmingham. Briefly, samples were prepared by following the NEBNext® Ultra II Directional RNA Library Prep Kit for Illumina® E7765. This included the PolyA purification module (E7490). During library construction, the indexes NEBNext Multiplex Oligos for Illumina (96 Unique Dual Index Primer Pairs (E6440L). The

libraries were sequenced by BGI Europe (Copenhagen) using a Hi-Seq 4000 (Illumina). Each sample had 20x coverage using paired-end reads of 100 base pairs.

CHAPTER 3:

Biomarkers of ageing in *Daphnia magna* strain Bham2

This chapter has been published in (Constantinou et al., 2019)

3.1 Introduction

Ageing is the gradual decline in the normal physiological functions in a time-dependent manner, affecting all biological systems, such as molecular interactions, cellular function, tissue structure and systemic physiological homeostasis. A more detailed description of factors affecting ageing are reported in Chapter 1. The adverse effects of this decline partly manifests as an increased incidence of age-related diseases and illnesses such as cancer, cardiovascular diseases, Alzheimer's and type 2 diabetes (He and Jasper, 2014). With the world's older population (age 60 and over) continuing to grow, the socio-economic impact of an ageing population has led to significant emphases on understanding different aspects of the ageing process in the hope to promote "healthy ageing" (Valenzano Dario et al., 2017).

There are more than 350 theories about the mechanisms of age related changes (Vina et al., 2007) with conflicting and supportive evidence presented for each theory, including senescence theory of ageing (Weismann, 1882), Free Radical Theory of Ageing (FRTA) (Harman, 1956) and DNA damage theory of ageing (Gensler and Bernstein, 1981). Broadly the theories of ageing can be divided into two main categories of programmed ageing and ageing caused by the accumulation of damage (Sergiev et al., 2015). However, no one theory is sufficiently able to explain the process of ageing, and they often contradict one another. This demonstrates the complex nature of ageing and contribution of multiple mechanisms, as cause or as consequence, to the ageing process. For example, oxidative stress induced-damage to the cellular macromolecules has long been highlighted as a fundamental mechanism involved in most senescence-associated alterations (Praticò, 2002) and ageing process. The progressive and irreversible accumulation of oxidative damage can

contribute to impaired physiological function, increased incidence of disease and can potentially impact the ageing process (Chen et al., 2007).

During oxidative stress, an imbalance between the generation of reactive oxygen species (ROS) and their detoxification leads to various oxygen radicals to escape and damage a range of macromolecules, including mitochondrial and nuclear genomic DNA, lipids and proteins, leading to genome instability and protein/lipid peroxidation. It has been widely demonstrated that there is an age-associated increase in the steady-state concentrations of lipid peroxidation. Oxidised lipid products are linked to initiation and/or mediation of some of the aspects of the ageing process. Furthermore, it is accepted that lipid peroxidation propagates more lipid peroxidation, promoting further damage (Wanjala et al., 2017). The damaging effects of lipid peroxidation include altering cellular structural integrity, fluidity and permeability as well as loss of bio-membrane function and have been noted to generate potentially toxic products. These changes have been identified as key contributing factors to development of many age-related diseases including cancer, cardiovascular disease and Alzheimer's (Freitas and de Magalhaes, 2011, Niedernhofer et al., 2018).

The increase in macromolecules peroxidation and genome instability can be partly driven by depletion of antioxidant defence mechanisms, such as thiol-containing glutathione, as well as decline in the efficiency of the DNA damage repair machinery as a function of age, contributing to the ageing process and premature age-related syndromes (Delabaere et al., 2017). The antioxidant glutathione in its reduced form (GSH) is the most abundant non-protein thiol and acts as a substrate for glutathione peroxidase. The latter is the principal mechanism of hydrogen peroxide and lipid hyperoxide reduction and also plays a role in catalysing the reduction of hydrogen

peroxide by peroxiredoxins. The reaction of GSH with hydrogen peroxide results in the production of its disulphide form; glutathionine disulphide (GSSG) (Dickinson and Forman, 2002). During ageing, the levels of the antioxidant glutathione appear to decline in a number of tissues, thereby putting cells at increased risk of oxidative stress. The observed age-related decline is possibly partly due to increased oxidative load over time (Giustarini et al., 2006). Furthermore, reduced age-dependent repair capacity can contribute to the ageing process. In both ageing and premature ageing syndromes common characteristics include higher incidence of DNA double strand breaks (DSBs). The preferential repair mechanism for DSBs is homologous recombination (HR), whereby accurate repair of the break site is fulfilled using a homologous DNA sequence as a template which is able to correctly restore the lost information. Initiation of HR repair is facilitated by the Mre11-RAD50-Nbs1 complex in addition to the C-terminal binding protein 1 (CtBP1) interacting protein (CtIP). This complex drives 5'-3' sectioning, resulting in a 3' protruding single-stranded DNA. Following this, RAD51 is recruited to the site which drives recognition of homology and strand exchange between homologous templates. RAD51 binds to the single-stranded DNA and forms a joint molecule to the repair template resulting in the formation of a D-loop. Subsequently, RAD51 is removed and further processing of the break can take two paths; formation of a double-Holliday junction (dHJ) or synthesis-dependent strand annealing (SDSA). dHJ produces two Holliday junctions by extending the D-loop to result in either crossover or non-crossover products, whereas SDSA produces only a non-crossover product by separating the newly synthesised sequence from the template and re-ligating to the original break site. dHJ and SDSA are used predominantly for meiosis and mitosis respectively. It was found that in older flies high

levels of RAD51 were expressed for longer periods of time following DSB induction. It is believed this excessive RAD51 recruitment to the break site and inhibited dissociation of RAD51 blocks the progress of HR resulting in less effective repair of damaged sites (Delabaere et al., 2017).

In the past two decades, significant progress has been made in identifying and characterising the regulatory processes involved in the mechanisms of ageing. It is important to highlight that these advances would have been hindered without the use of model organisms. Majority of the molecular mechanisms underpinning ageing processes were characterised through the use of the yeast *Saccharomyces cerevisiae,* the nematode worm *Caenorhabditis elegans*, the fruit fly *Drosophila melanogaster*, and the house mouse *Mus musculus* (Evans et al., 2008, Valenzano Dario et al., 2017, Kapahi et al., 2017, Ziehm et al., 2017, de Magalhaes et al., 2017). However, the use of "canonical" model organisms in the field of ageing is not without limitations. For example, the unicellular nature of yeast prevents systematic ageing studies. Both adult nematode worms and flies are mostly composed of post-mitotic cells, limiting their use as a model for stem cell ageing studies (Tissenbaum and Guarente, 2002). Furthermore, their DNA methylation machinery is either absent or not comparable to humans, thus limiting their use for investigating the role of DNA methylation in the ageing process. While the maximum lifespan of mouse (more than 3 years) requires considerable time and resources for lifespan studies (Valenzano Dario et al., 2017). Therefore, use of other complementary organisms, such as the African turquoise killifish (*Nothobranchius furzeri*) (Valenzano et al., 2011, Valenzano et al., 2015, Harel and Brunet, 2015, Harel et al., 2015), the planarian flatworm (*Dugesia tigrina*) (Dasheiff and Dasheiff, 2002), the naked mole rat (*Heterocephalus glaber*) (Buffenstein, 2005,

Andziak et al., 2006, Buffenstein, 2008, Pérez et al., 2009, Edrey et al., 2011, Ruby et al., 2018), and the water flea (*Daphnia spp.*) (Barata et al., 2005a, Iampolskiĭ and Galimov, 2005, Pietrzak et al., 2010b, Dudycha and Hassel, 2013, Kim et al., 2013, Schumpert et al., 2014, Schumpert et al., 2015a, Schumpert et al., 2016, Hearn et al., 2018b, Hearn et al., 2018a), will greatly diversify the approach and understanding of different factors underpinning the ageing process and the potential translation for human application (Buffenstein et al., 2008).

Several unique characteristics makes *Daphnia* an attractive model organisms for research into ageing and regulation of lifespan, such as transparent body, short generation time, well-characterised methylome (Kvist et al., 2018), regenerative capabilities with continued cell renewal and proliferation throughout their lifespan, availability of naturally occurring ecotypes with diverse lifespans ranging from a few days to several months. The availability of naturally occurring closely related subtypes will enable interbreeding and producing viable offspring with diverse lifespans (Ebert, 2005, Benzie, 2005, Asselman et al., 2016, Ram and Costa II, 2018). Moreover, *Daphnia* reproduces via cyclic parthenogenesis, allowing the generation of large clonal populations and providing a unique setup for delineating genetic and epigenetic factors contributing to the ageing process as well as enabling investigation into the impact of different environmental conditions and treatments on lifespan and ageing rate. Additionally, a genetically static population allows for phenotypic characterisation of single gene knock outs for statistically relevant sample sizes. The latter is easily achievable due to the availability of various genetic manipulation tools such as CRISPR, TALEN and RNAi for *Daphnia* (Schumpert et al., 2016, Nakanishi et al., 2016, Kumagai et al., 2017). Furthermore, *Daphnia* shares the most genes in common with

humans among any other arthropod and other established invertebrate model organisms of ageing (Colbourne et al 2011). Most interestingly, genetically identical female and male *Daphnia* have evolved different average lifespans (Schwarzenberger et al., 2014), providing a unique opportunity for understanding the underlying mechanisms of ageing and regulation of lifespan.

Sex differences are commonly observed in many biological aspects with nearly all species exhibiting conditional differences in longevity except in humans where females are known to have a ubiquitous survival advantage over males. Investigating sex differences in longevity could provide insight into principal mechanisms of ageing and lifespan regulation. However, this area of research is extremely understudied and majority of the research on sex differences in longevity has been focused on observing wild animals in their natural environment in a bid to elucidate underlying differences in life history traits and behaviour of different sexes. Although the supporting evidence is weak, these observations have formed the foundation of multiple evolutionary hypotheses regarding the origin of sex differences in longevity, such as variable vulnerability to environmental risks (Williams George, 1957), sexual selection pressures (Promislow, 1992) and parental care regimes (Allman et al., 1998) in addition to more mechanistic drivers, such as asymmetric inheritance of sex chromosomes (Trivers, 1985) and mitochondria (Tower, 2006). Results obtained from observing animals in uncontrolled environments means reliability can be unclear especially when considering factors such as risk-taking behaviour which may result in a bias towards mortality in one sex compared to the other. Given this uncertainty the current understanding of sex difference is useful for insight into causes of ageing but leaves more to be determined for mechanistic differences for sex difference and

intrinsic rate of ageing (Austad and Fischer, 2016). Therefore conducting controlled experiments in model organisms that show considerable sex-dependent variation in the lifespan and ageing rate can greatly improve understanding of the ageing process. Given the cyclical parthenogenetic nature of *Daphnia* reproduction the resultant genetically identical female and male populations provide a useful platform for investigating sex differences in longevity. Male *Daphnia magna*, although genetically identical to their mothers and sisters (Hebert & Ward, 1972), under laboratory conditions have significantly shorter lifespan compared to female *Daphnia*. This can potentially be attributed to the differences in biological roles, energy expenditure (EE) and metabolism (Manini, 2010, Plaistow et al., 2015), strategies employed to maximize fitness, rates of damage to macromolecules and ageing between females and males (Pietrzak et al., 2010a). Therefore in this chapter the aim was to (I) provide evidence is support of establishing genetically identical female and male *Daphnia* as unique and valuable resources for research into mechanisms of ageing and (II) to delineate the mechanism involved in sex differences in lifespan. This was achieved by establishing and investigating several biomarkers of ageing and comparing the rates of DNA damage and DNA repair capacity in genetically identical female and male *Daphnia*. Furthermore, to identify life stages that the rate of ageing alters for males and females. The data clearly demonstrates decline in heart rate, movement, antioxidant protection and DNA repair capacity as well as increase in DNA damage and lipid peroxidation as a percentage of lifespan in both sexes. Most importantly, as shown in the results section, the rate of these changes is significantly different between the two genetically identical sexes, with males displaying approximately two folder higher rate of DNA damage accumulation. Overall, the data indicates that investigating sex differences in

longevity in the clonal organism *Daphnia* under controlled laboratory conditions can provide insight into principal mechanisms of ageing and lifespan regulation.

3.2 Overview of Experimental Design

Life history studies were performed for female and male *D. magna* as described in section 2.3 and swimming speed was determined as described in section 2.4. DNA damage was calculated by comet assay, as described in section 2.5 and DNA damage repair was interpreted from RAD51 presence, calculated as described in section 2.6. Data was analysed as described below. An overview of the experimental design for female daphnids are shown in Figure 3.1 and for males in Figure 3.2.
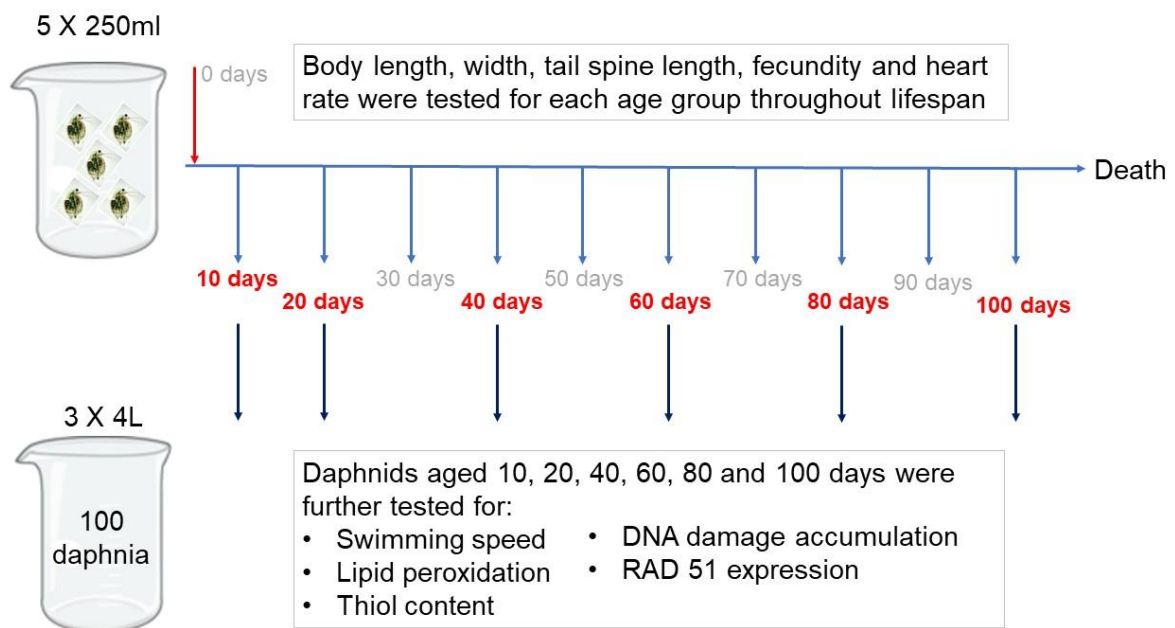
Figure 3.1: Experimental design for female *D. magna* biomarkers of ageing. At 10-day intervals body length, body width, tail spine length, fecundity and heart rate were measured throughout lifespan. From separate cultures, *D. magna* at ages 10, 20, 40, 80 and where possible 100 days were analysed for swimming speed, lipid peroxidation, thiol content, DNA damage and RAD51 accumulation. See Chapter 2 for details.
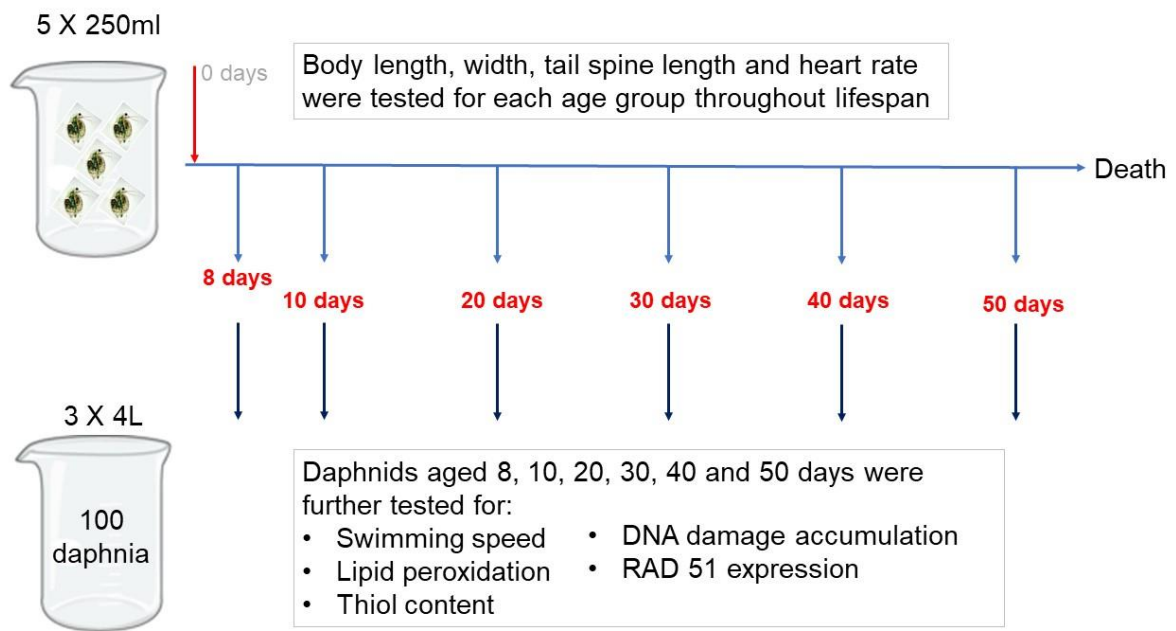
Figure 3.: Experimental design for male *D. magna* biomarkers of ageing. At 10-day intervals body length, body width, tail spine length, and heart rate were measured throughout lifespan. From separate cultures, *D. magna* at ages 8, 10, 20, 40 and where possible 50 days were analysed for swimming speed, lipid peroxidation, thiol content, DNA damage and RAD51 accumulation. See Chapter 2 for details.

Briefly, to determine lifespan of female *D. magna*, 10 cultures containing 5 individuals were maintained under normal conditions as described in section 2.3. Fecundity was determined by counting the number of neonates produced every other day. For male lifespan, 5 cultures containing 5 individuals were maintained. The volume of media and amount of algae were adjusted accordingly as the number of individuals was reduced across the duration of the lifespan study. The average lifespan and neonate production per culture was calculated followed by the average across the replicate cultures.

For life history studies, 5 cultures containing 5 daphnids were maintained under normal conditions as described in section 2.3. For the duration of their lifespan, the individuals from each culture were measured at 10-day intervals for body measurements as described above. The average body measurements per culture for each age were then

taken and an average across the 5 cultures calculated. Average heart rate was calculated in the same way. Throughout the lifespan study, where individual daphnids died, the volume of media and amount of algae per culture were reduced to maintain a consistent environment.

For the remaining biomarker experiments, three larger cultures were maintained, ensuring the 50ml media per daphnid and algae ratio was maintained. Comet analysis, immunofluorescence analysis and protein and thiol analysis were performed on multiple individuals across three replicates as described in sections 2.5-2.10. A single replicate (containing multiple individuals) was taken from each of the larger cultures and individual daphnids selected from throughout the 1L beaker so as not to select only those from a single area (e.g. not to select only those at the top of the beaker).

3.3 Data Analysis

3.3.1 Biomarkers of ageing data analysis

Data analysis was conducted as follows; statistical analysis was undertaken using IBM SPSS Statistics 25 software package and R (v3.4.3). Data was visualised using R (v3.4.3) and Microsoft Excel 2016. Normality was tested using Shapiro-wilk test. Survival analysis was performed using the R Survival package which stipulates the use of Kaplan-Meier estimate and log-rank test. Growth data was analysed using a linear regression model testing Log_{10} transformed age in days against measurement (mm) and as percent of lifespan using a one-way ANOVA with multiple pairwise comparison corrected by Bonferroni to accommodate for normality violation and multiple hypothesis testing. Fecundity was analysed using linear regression model testing Log_2 transformed age in days against cumulative neonate production. Average heart rate was analysed for both age in days and age as percent of lifespan using a linear

regression model and using a one-way ANOVA with multiple pairwise comparison corrected by Bonferroni. Swimming speed, lipid peroxidation product and thiol content and comet tail intensity were normalised to body size by dividing by average body length per age group and analysed using a linear regression model. RAD51 foci counts were analysed using one-way ANOVA with multiple pairwise comparison corrected by Bonferroni. The majority of reported molecular analysis compares females aged 20 days and 80 days and males at aged 10 days and 40 days to reflect 20% and 80% of lifespan respectively. This is because males are not sexually mature until aged 8 days therefore at 10% of lifespan (5 days) are juveniles.

3.4 Results

3.4.1 Genetically identical female and male *Daphnia magna* have significantly different lifespans

Life history studies were undertaken for female and male *D. magna* Bham2 strain under optimal conditions as described by Kilham *et al* (1998), monitoring survival, growth, tail length, age of sexual maturity and reproduction (female only). Survivorship patterns are significantly different between the genetically identical female and male *Daphnia* (Figure 3.3; log-rank test: p-value = 0.0002, X^2 = 56.2, df = 1). The medium lifespan of female *D. magna* Bham2 strain is twice as long as male *D. magna* Bham2 strain, with a medium lifespan of 83 days (95% CI: 77-91, n=50 individuals) and 41 days (95% CI: 38-45, n=50 individuals), respectively.

Although lifespan is significantly different between the sexes, as a percent of their lifespan, growth and tail loss occur at comparable times. Body length, width and tail length were monitored every 10 days from aged 1 day until death. As shown by Figure 3.4 and A2.F2 (Appendix 2A), body size is significantly different between sexes (*p*-

value = 2.2×10^{-16}) with females being approximately twice as large as males. However, body length and body width show a stabilisation of growth following 40% of lifespan in both female and male individuals (FA2.F1 and A2.F3, Appendix 2A). Tail loss occurs with age as identified in Figure 3.5. When tail loss is normalised to body size it becomes clear that tail length is proportional to body size across both sexes (Figure 3.6). Tail loss is significantly linked with age but as percent of lifespan has no significant difference between sexes (linear regression model: tail loss as percent of lifespan p-value = 4.20×10^{-5}, tail loss between sexes p-value = 0.94).

Daphnia spp. exists as females under non-stressed conditions and reproduce via cyclical parthenogenesis. *D. magna* strain Bham2 become sexually mature at aged 9 days when the first clutch appears in the brood pouch which are released as neonates at aged 11 days. Neonates were counted daily throughout life and cumulative neonate production was assessed (Figure 3.7). Fecundity declines with age (p-value = 2.22×10^{-16}) and begins to regress early in the female life cycle at approximately aged 20 days but notably reproduction continues throughout lifespan. In nature males are produced under stressed conditions to allow the production of resting eggs by sexual reproduction but in laboratory conditions can be induced by exposure to the juvenile hormone methyl farnesoate (MF). Bham2 males induced by MF were identified as sexually mature at aged 8 days by the development of hook-like first appendages used for clasping females during mating.
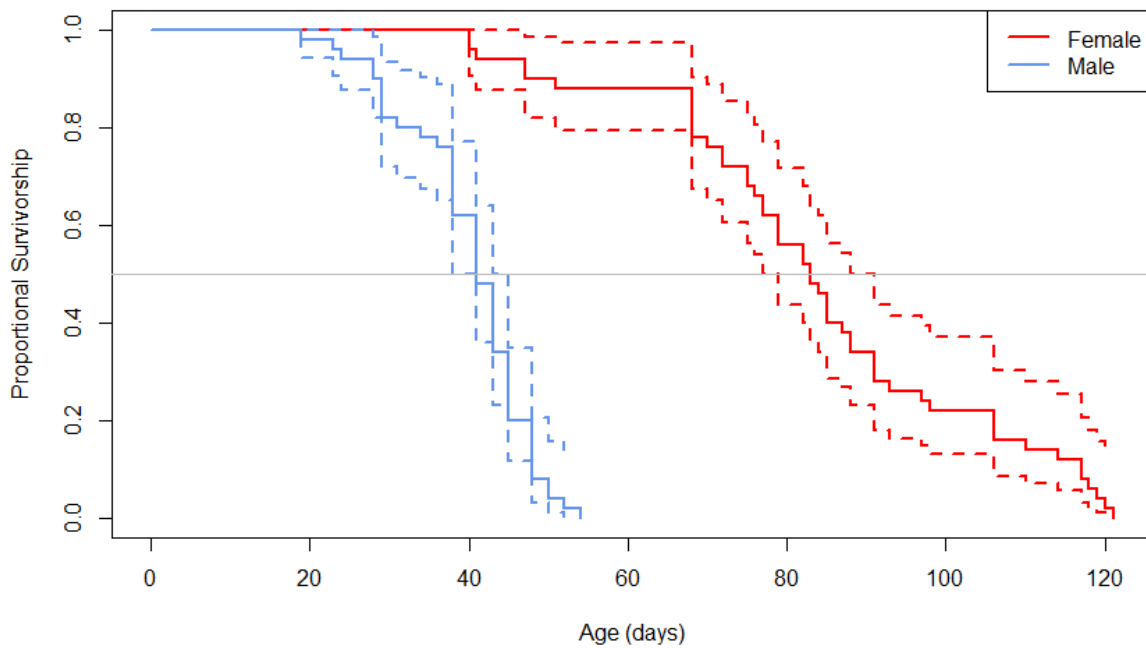
Figure 3.3 Proportional survivorship for female and male D. magna Bham2.
Kaplan-Meier survival curves for female (red, n=50) and male (blue, n=25) *D. magna*
Bham2 show significant difference in proportional survivorship (log-rank test *p*-value =
0.0002; 95% confidence intervals (CI) are shown for the survival curves with red and
blue dash-lines).
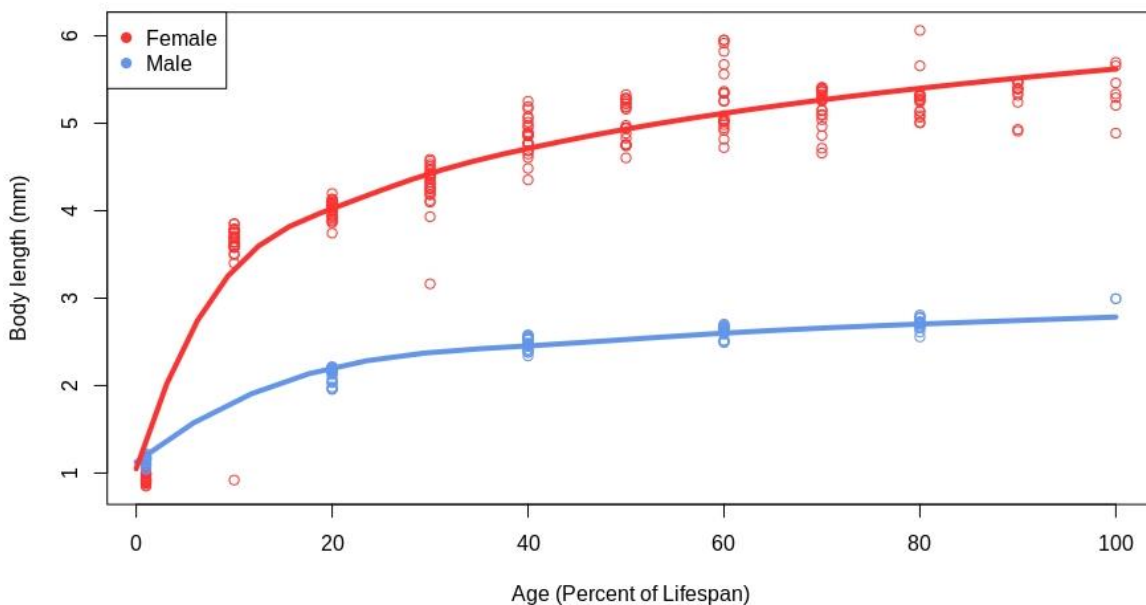
Figure 3.4 Body length for female and male D. magna Bham2 across lifespan.
Growth stabilises at approximately 40% of lifespan in both females (red, n=25) and
males (blue, n=25) *D. magna* Bham2, however females show an overall larger body

length compared to males (Log$_{10}$ linear regression model: significant female growth with age R^2 = 0.94, *p*-value = 2.22 x 10^{-16}; significant male growth with age R^2 = 0.98, *p*-value = 2.22 x 10^{-16}).

Figure 3.5 Lipid droplet accumulation and tail loss occurs with ageing D. magna Bham2. Representative images of young (10 days) and old (80 days) female D. magna Bham2 showing visible signs of ageing, including accumulation of lipid droplets, tails and antenna loss and build-up of algae and bacteria around the *Daphnia*.
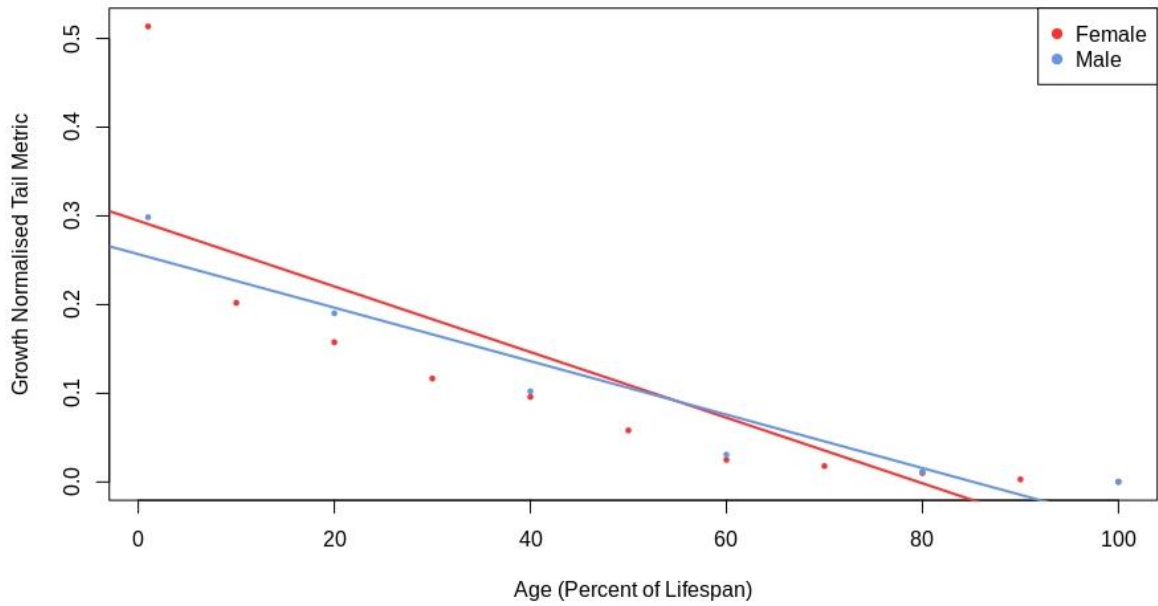
Figure 3.6 Tail loss with age in female and male *D. magna* Bham2. Tail loss occurs in proportion to body size at the same rate in both female (red, n=25) and male (blue, n=25) *D. magna* Bham2 as a percentage of lifespan (linear regression model: combined tail loss as percent of lifespan *p*-value = 4.20 x 10^{-5}, tail loss between sexes *p*-value = 0.94, female only R^2 = 0.66, *p*-value = 0.0023; males only R^2 = 0.90, *p*-value = 0.0042;).
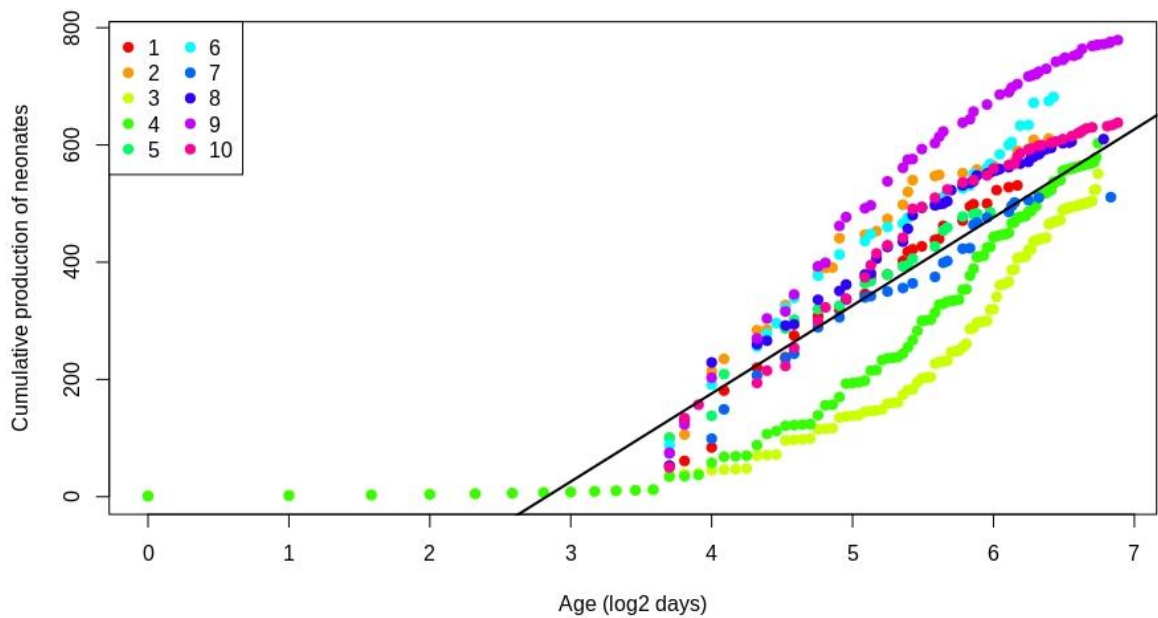
Figure 3.7 Neonate production decreases logarithmically with age in female *D. magna* Bham2. Fecundity declines with age in *D. magna* Bham2. Cumulative neonate production significantly declines with age ($\log_2$ transformed age; n=25, linear regression model: R^2 = 0.77, *p*-value = 2.22 x 10^{-16}).

3.4.2 Deterioration of physiological functions in ageing female and male *D. magna*.

As shown in Figures 3.8 and 3.9, although the average heart rate per minute (BPM) for males is consistently higher than the female *D. magna* Bham2, both sexes show a significant reduction (as percentage of lifespan: $p= 9.6 \times 10^{-41}$, as age in days: p-value $= 2.7 \times 10^{-74}$) in heart rate as they age. In females, heart rate decreases by 1.6 fold in 100 days old *Daphnia* (100% of lifespan) compared to 10 days old *Daphnia* (10% of lifespan). In males, the same trend is observed with a significant 1.2 fold reduction in the heart rate of 50 days old *Daphnia* (100% of lifespan) compared to 10 days old *Daphnia* (20% of lifespan). Most importantly, the rate of decline is significantly different between the two sexes with a higher rate of decline in the short lived male *Daphnia* compared to females which is less prominent when comparing the heart rate of the two sexes as percentage of their lifespan rather than their chronological age. As percentage of lifespan the BPM declines 2.02 fold faster in male *Daphnia* compared to female *Daphnia* (slopes for male and female *D. magna*, respectively are -1.196 and -0.5916, $p= 1.4 \times 10^{-96}$). As age in days the BPM declines 4.04 fold faster in male *Daphnia* compared to female *Daphnia* (slopes for male and female *D. magna*, respectively are –2.391 and -0.5916, p-value $= 3.6 \times 10^{-57}$).

Figure 3.10 highlights the average speed of swimming, measured as the distance (cm) travelled per second, also declines progressively with age in both female and male *D. magna* (combined data analysis normalised to body size: $R^2 = 0.86$, $p= 2.95 \times 10^{-4}$). The average swimming speed for 80 days old female *D. magna* (80% of lifespan, 0.87±0.56cm/s) significantly reduced by 3 fold compared to 10 days old female *D. magna* (10% of lifespan, 2.63±1.35 cm/s). A similar trend was observed for male *D.*

magna where 40 days old males (80% of lifespan, 0.89±0.23 cm/s) showed a 1.5 fold reduction in their average swimming speed compared to 10 days old males (20% of lifespan, 1.34±0.38cm/s). Furthermore, no movement was detected within 3 minutes of exposure to the stimulus light for both female and male *D. magna* at 100% of their lifespan (100% of lifespan equals to 100 days old and 50 days old female and male *D. magna*, respectively).
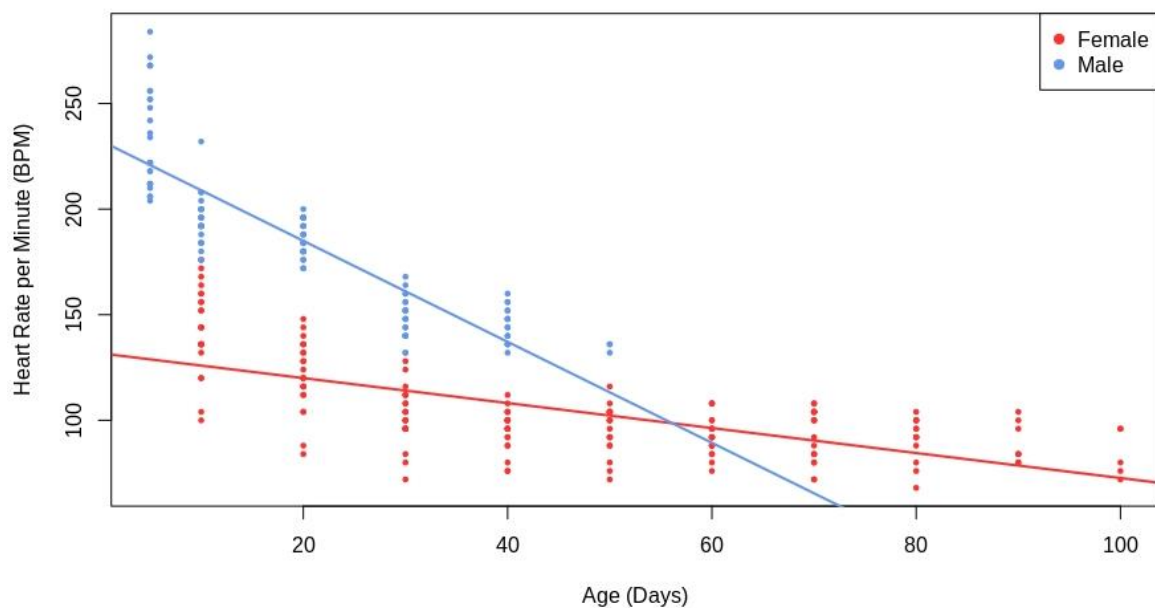
Figure 3.8: Heart rate declines at a faster rate in males than females as age in days in *Daphnia magna* Bham2. Heart rate per minutes (bpm) versus age (day) in female and male *Daphnia magna*. Heart rate decline (bpm) is occurring much earlier in males (blue, n= 5 biological replicates, each biological replicate containing 5 number of *Daphnia*) than females (red, n= 5 biological replicates, each biological replicate containing 5 number of *Daphnia*) in real time. The blue (male) and red (female) lines represent the mean linear regression (in combined analysis R^2= 0.81, *p*-value = $1.81x10^{-94}$). Heart rate decline is significant with age (*p*-value = $2.7x10^{-74}$) and between the two sexes (*p*-value = $3.6 x10^{-57}$). Both sexes show a significant decrease in heart rate with age (female only R^2 = 0.46, *p*-value = $14.84 x 10^{-24}$. Male only R^2 = 0.75, *p*-value = $1.12 x 10^{-28}$).
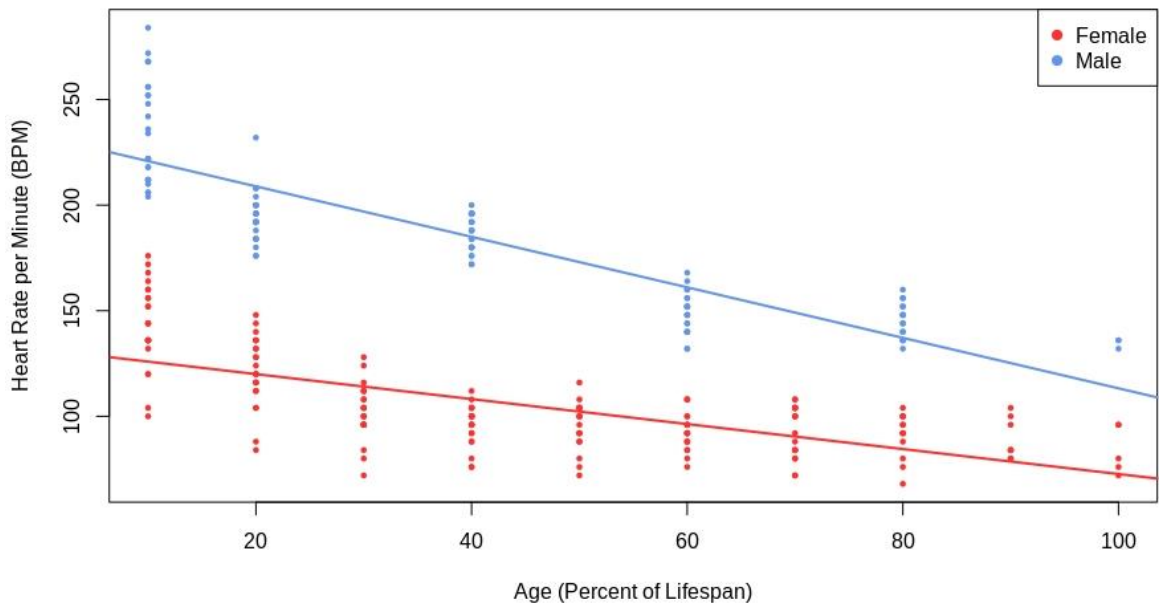
Figure 3.9: Heart rate declines at a similar rate in females and males as percentage of lifespan in D. magna Bham2. Heart rate per minutes (bpm) versus percentage of lifespan in female and male *Daphnia magna*. The blue (male, n= 5 biological replicates, each biological replicate containing 5 number of *Daphnia*) and the red (females, n= 5 biological replicates, each biological replicate containing 5 number of *Daphnia*) lines represent the mean linear regression (R^2 = 0.84, *p*-value = 6.32x10^{-105}). Heart rate decline is significant as a percentage of life (*p*-value = 9.6x10^{-41}) and between the two sexes (*p*-value = 1.4 x10^{-96}). Both sexes show a significant decline in heart rate as percent of lifespan (female only R^2 = 0.46, *p*-value = 1.84 x 10^{-24}, males only R^2 = 0.75, *p*-value = 6.32 x 10^{-105}).
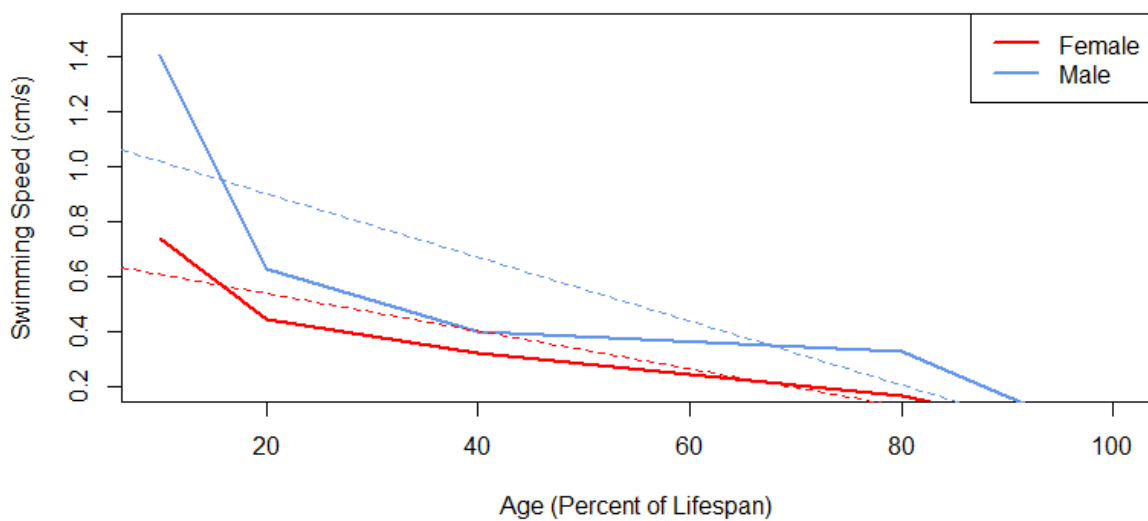
Figure 3.10: Swimming speed significantly declines with age in *Daphnia magna* Bham2. Swimming speed normalised to body size versus percentage of lifespan for female (red, n= 3 biological replicates, each biological replicate containing 5 number of *Daphnia*) and male (blue, n= 3 biological replicates, each biological replicate containing 5 number of *Daphnia*) *Daphnia magna*. Swimming speed (cm/s) declines with age in both sexes with age (R^2 for combined analysis = 0.86, *p*= 2.95 x 10^{-04}). Decline in swimming speed is significant in females and males (female only R^2 = 0.89, *p*-value = 0.015, males only R^2 = 0.72, *p*-value = 0.035).

3.4.3 Increased lipid peroxidation and decline in antioxidant protection in ageing female and male *D. magna*.

A significant increase in the lipid peroxidation product free malondialdehyde (FrMDA) was identified as a function of age in both females and male *D. magna* (Figure 3.11, combined analysis for both sexes: *p*-value = 4.98 x 10^{-10}; female: *p*-value = 3.10 x 10^{-06}; male: *p*-value = 4.97 x 10^{-09}). For female *D. magna* aged 20 days (20% of lifespan) the average FrMDA content (103.85±37.11 nMoles MDA/mg protein) increased 4.98 fold compared to aged 100 days (100% of lifespan, 517.48±39.50 nMoles MDA/mg protein). A similar trend is observed in male *D. magna* where the average FrMDA content increased 8.77 fold in 50 days (100% of lifespan, 57.37±3.79 nMoles MDA/mg protein) old male *D. magna* compared to 10 days old (20% of lifespan, 6.54±1.58 nMoles MDA/mg protein).

For the same samples, levels of the antioxidant glutathionine (GSH) were measured and showed to be significantly declining with age in female and male *D. magna* (Figure 3.12, *p*-value = 0.009). Females observed an average decline of 3.25 fold between aged 20 days (20% of lifespan, 446.5±53.25 nMoles GSH/mg protein) and aged 100 days (100% of lifespan, 137.26±17.17 nMoles GSH/mg protein). Males also showed an average decline of 3.18 fold between aged 10 days (20% of lifespan, 622.31±50.89

nMoles GSH/mg protein) and aged 50 days (100% of lifespan, 195.48±109.05 nMoles GSH/mg protein). The observed increase in peroxidation product FrMDA and decline in the protective antioxidant GSH suggests a more vulnerable environment to oxidative stress.
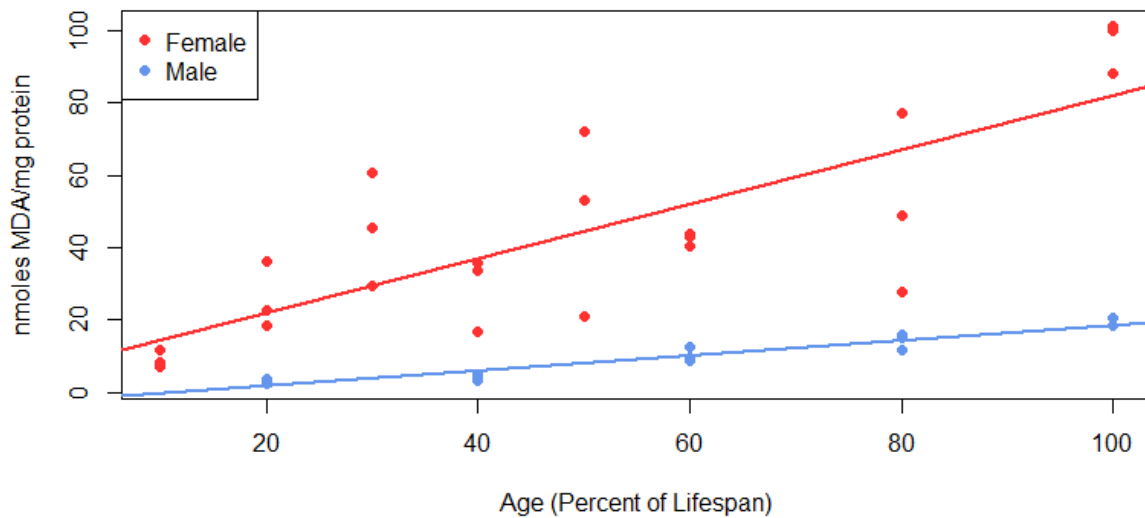
Figure 3.11: Lipid peroxidation product accumulates with age in female and male D. magna. An increase in the lipid peroxidation product free malondialdehyde (FrMDA) is observed with age in female (red) and male (blue) *D. magna* when normalised to protein content and adjusted for body size. The rate of FrMDA accumulation with age is significantly different between sexes (p-value = 5.24 x 10^{-09}) but a significant increasing trend is apparent in both sexes (combined linear regression model: as percent of lifespan + sex R^2 = 0.69, p= 4.98 x 10^{-10}, percent of lifespan only p-value = 1.82 x 10^{-05}). Lipid peroxidation product accumulation with age is significant in both female and male individuals (female only R^2 = 0.64, p-value = 3.10 x 10^{-06}; male only R^2 = 0.93, p-value = 4.97 x 10^{-09}).
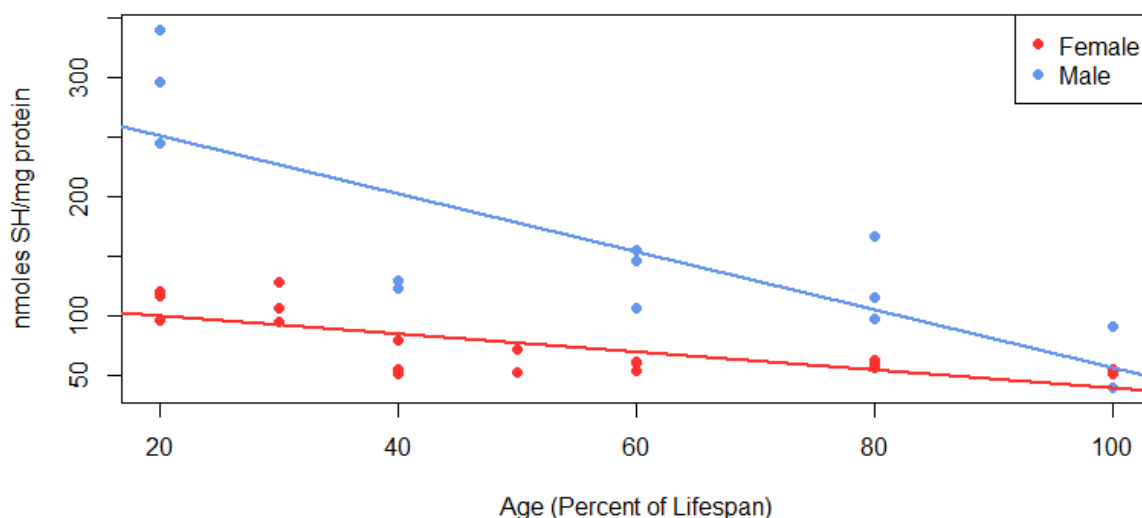
Figure 3.12: Thiol content declines with age in female and male D. magna. A decline in thiol content is evident in female (red) and male (blue) *D. magna* when normalised to protein and adjusted for body size (combined linear regression model: as percent of lifespan + sex $R^2 = 0.67$, $p= 1.09 \times 10^{-07}$, percent of lifespan only p-value $= 6.10 \times 10^{-05}$, sex only p-value $= 1.35 \times 10^{-06}$). Decline in reduced thiols is significant in both sexes separately (female only $R^2 = 0.54$, p-value $= 3.34 \times 10^{-04}$; males only $R^2 = 0.67$, p-value $= 6.41 \times 10^{-04}$).

3.4.4 DNA damage accumulation and reduced repair capacity with age in female and male *Daphnia*.

Comet assay was used to calculate DNA damage by measuring tail intensity (%). The more damaged and fragmented the DNA the larger the percentage of DNA found in the comet tail. A clear accumulation of DNA damage can be seen with age in both female and male *D. magna*. When presented as percent of lifespan damage appears to accumulate at a similar rate in both sexes initially before diverging to show higher damage in males from 60% lifespan compared to females (Figure 3.13, significance between sexes p-value $= 3.80 \times 10^{-20}$) but when presented in real time (chronological age) it is clear that DNA damage is accumulating significantly faster in males from

much earlier (Figure 3.14, significance between sexes p-value = 5.20 x 10^{-72}, 1.49 fold higher rate of DNA damage accumulation in male *D. magna* than female *D. magna*). When investigating sexes individually it is clear that DNA damage accumulates significantly with age in both females and males (female R^2 = 0.48, p-value = 3.30 x 10^{-87}; male R^2 = 0.35, p-value = 1.40 x 10^{-35}).

To investigate the efficiency of DNA damage repair throughout age, female and male *D. magna* were exposed to 0.1µg/ml cisplatin and RAD51, a marker of homologous repair was monitored at specified recovery stages (0, 1.5, 3 and 6 hrs of recovery) for the exposure groups and compared to control groups. Western blot analysis of the RAD51 confirmed specificity of the antibody used (Figure 3.17). As seen in Figure 3.15, repair foci also show a distinct difference between young and old females whereby at 6 hours of recovery RAD51 foci count for aged 10 days has 1.43 fold higher count compared to aged 80 days (7.41 and 5.17 respectively, p-value = 0.046). Also of note is the little variation between control RAD51 foci count and all recovery stages in females aged 80 days showing a lack of repair response to cisplatin exposure (multi-comparison post-hoc test resulted in a range of p-values between age groups ranging between 0.319 and 0.999, no significant difference between control and all recovery groups for females aged 80 days; see A2.T1, Appendix 2A). In male samples, RAD51 expression increases in all age groups following cisplatin exposure however younger males appear to respond better with a maximum RAD51 foci count for aged 10 days of 8.21 whilst maximum foci count for aged 40 day males is 7.04 (Figure 3.16). The clear decline in damage in younger *D. magna* in addition to high repair foci count compared to the continually high damage foci and unresponsive repair foci in older *D. magna* suggests repair efficiency is diminished with age.
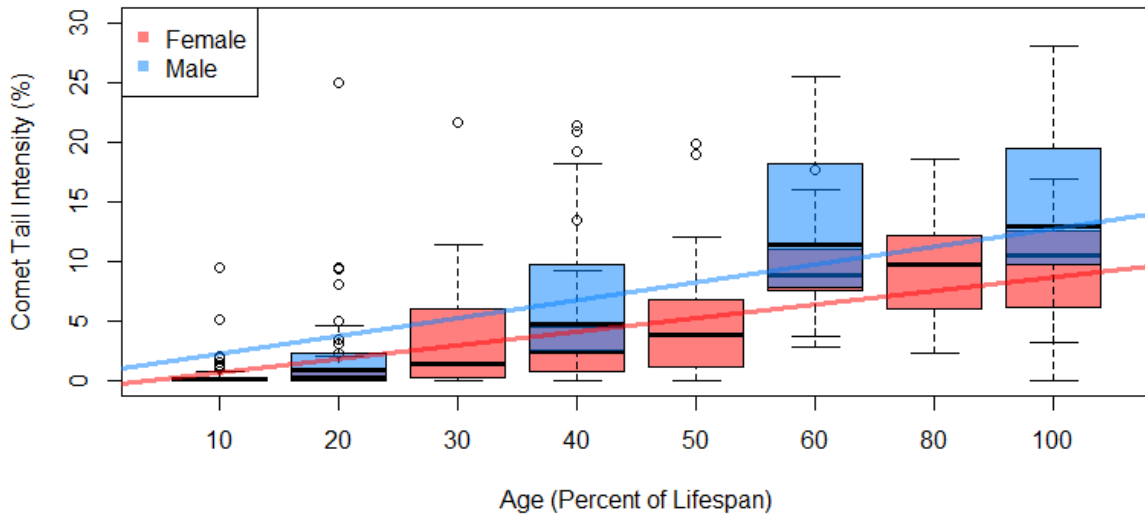
Figure 3.13: Accumulation of DNA damage with age as percentage of lifespan in female and male D. magna. Comet assay identifies accumulated damage in female and male *D. magna* as a percent of lifespan normalised to number of fields and comets counted then adjusted for body size (combined linear regression model: as percent of lifespan and sex: R^2 = 0.42, *p*-value = 7.29 x 10^{-115}, percent of lifespan only *p*-value = 9.10 x 10^{-105}, sex only *p*-value = 3.80 x 10^{-20}; females: n= 3 biological replicates, each replicate containing haemolymph from 5 *Daphnia*, total number of 75 nuclei scored; males: n= 3 biological replicates, each replicate containing haemolymph from 5 *Daphnia*, total number of 75 nuclei scored).
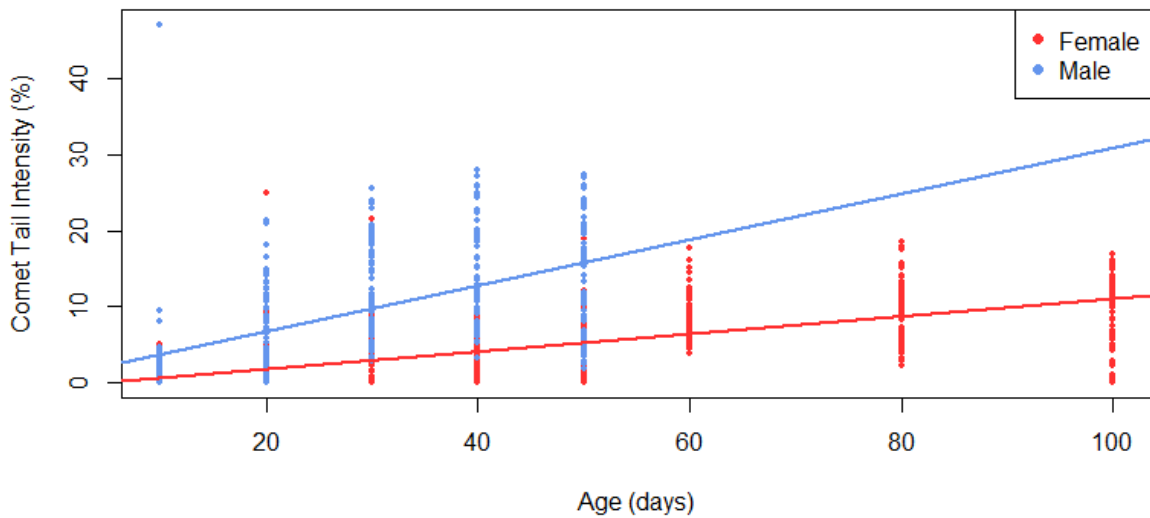
Figure 3.14: Accumulation of DNA damage by age in days in female and male D. magna. Comet assay analysis after adjustment for body size and presented as age in days shows higher rate of accumulation of damage in male *D. magna* compared to females (combined linear regression model: age in days $p = 1.20 \times 10^{-39}$, sex $p = 5.20 \times 10^{-72}$).
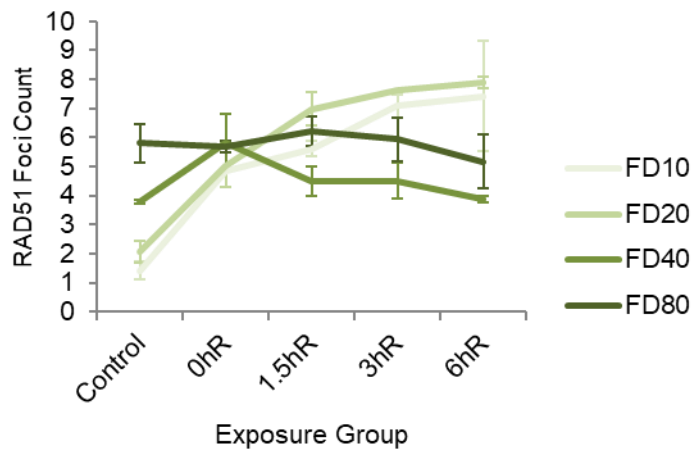
Figure 3.15: RAD51 foci count in female D. magna following cisplatin exposure. Quantification of RAD51 foci in female *D. magna* for control and cisplatin exposed haemolymph show an increased response to damage in younger individuals (light green) compared to older individuals (dark green). Error bars: SD. females: n= 3 biological replicates, each replicate containing haemolymph from 10 female *Daphnia*, 75 number of foci scored.
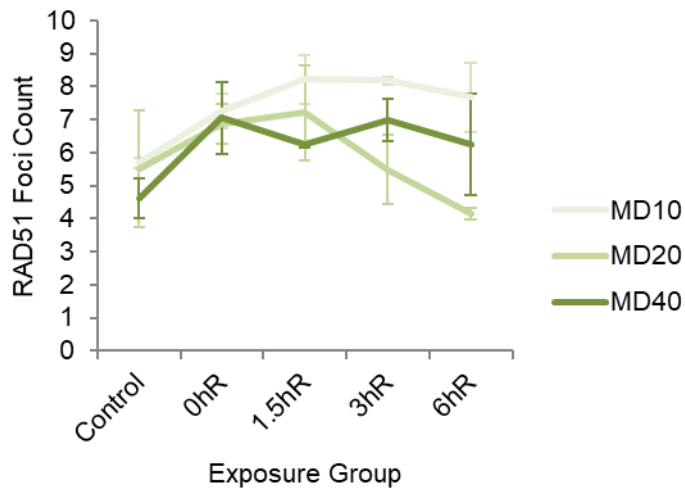
Figure 3.16: RAD51 foci count in male D. magna following cisplatin exposure.
Quantification of RAD51 foci in male *D. magna* for control and cisplatin exposed
haemolymph show an increased response to damage in younger individuals (light
green) compared to older individuals (dark green). Error bars: SD. males: n= 3
biological replicates, each replicate containing haemolymph from 10 male *Daphnia*, 75
number of foci scored.

Figure 3.17: Western blot of RAD51. Three replicates of female *D. magna* Bham2
protein extractions show specificity of RAD51 antibody at 37kDa as expected. Due to
testing only for antibody specificity and not quantification, not loading control was
necessary.
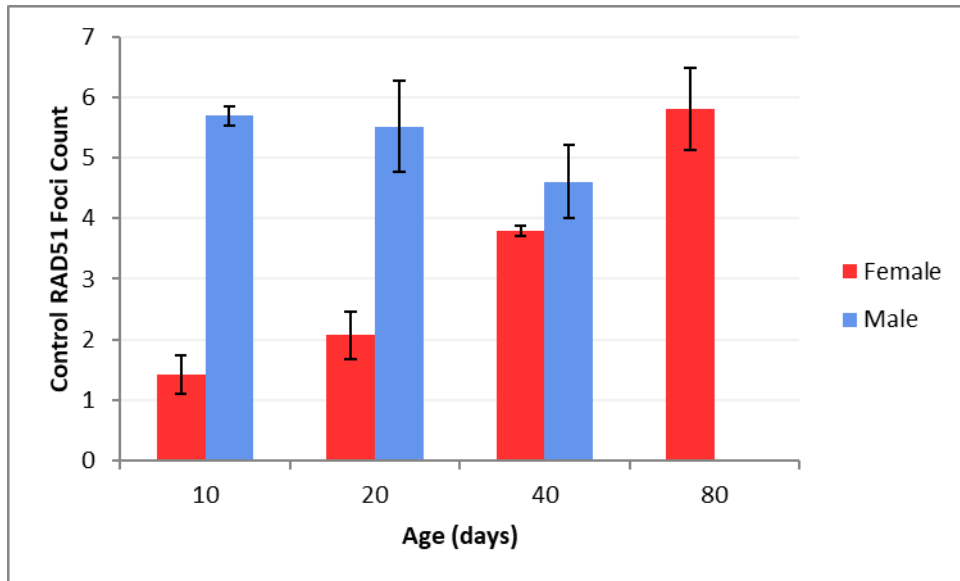
Female					Male			
Control	FD10	FD20	FD40	FD80	Control	MD10	MD20	MD40
FD10	x	0.314	0.001	0.000	MD10	x	0.978	0.488
FD20	0.314	x	0.004	0.000	MD20	0.978	X	0.596
FD40	0.001	0.004	x	0.002	MD40	0.488	0.596	x
FD80	0.000	0.000	0.002	x				

Figure 3.18: RAD51 foci count for control groups of female and male D. magna Bham2. Female *D. magna* at experimental age groups unexposed to cisplatin show a naturally occurring increase in RAD51 expression. Data based on quantification of RAD51 foci as included in Figures 3.13 and 3.14. Post-hoc Tukey results for comparisons between control groups of each age class for each sex are reported separately in the table above. Green highlights significant values (*p*-value <0.05).
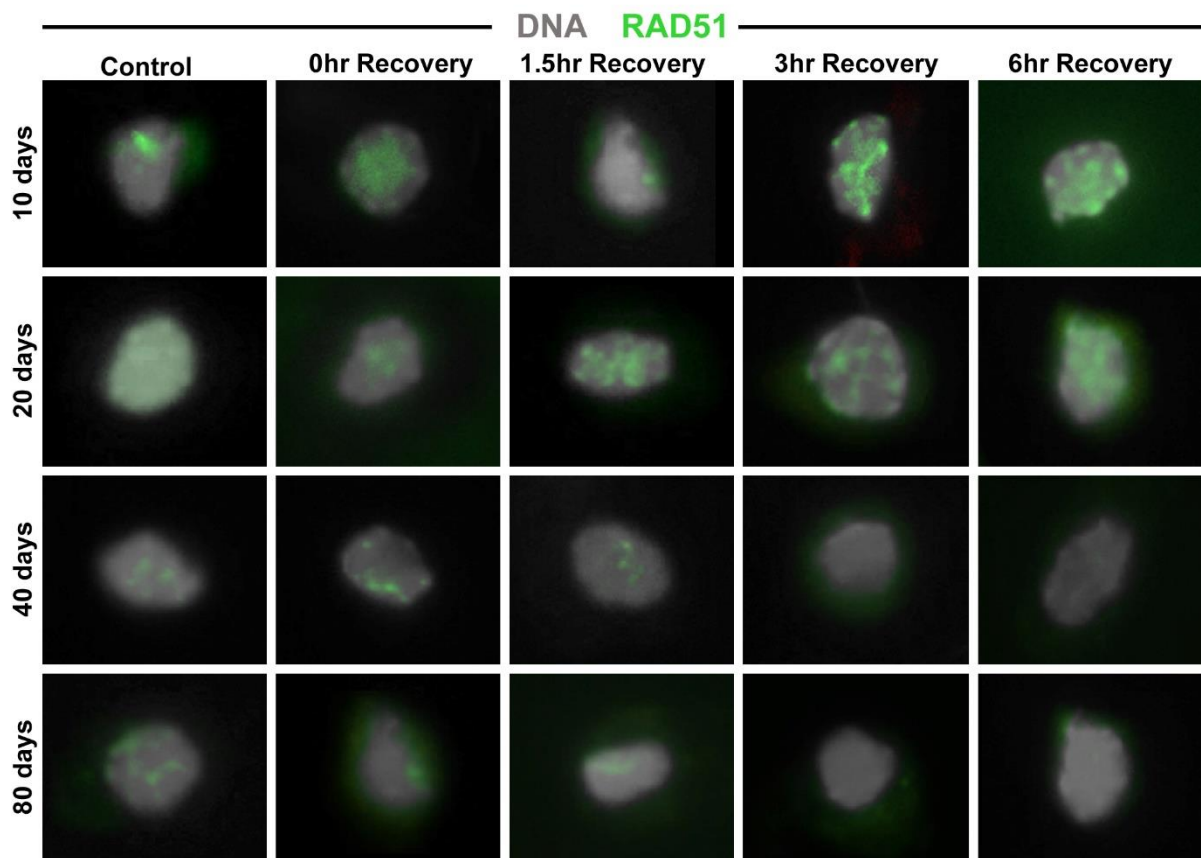
Figure 3.19: Representative images of RAD51 foci in female D. magna. Panel images representative of RAD51 (green) and Hoechst (blue) staining in female *D. magna* for untreated control groups, and at recovery time points following 6h cisplatin exposure for age groups 10, 20, 40 and 80 days.

3.5 Discussion

In this chapter biomarkers of ageing were investigated in genetically identical female and male *Daphnia magna* with diverse lifespans to support their establishment as a unique and valuable model for investigating sex difference in longevity. Such work is necessary to elucidate principal mechanisms of ageing and lifespan regulation.

3.5.1 Sex differences in physiological markers of health and ageing in *D. magna*

Physiological markers were observed in the form of life history studies. Life history studies form an analytical platform to investigate strategies adopted by an organism via natural selection covering traits such as lifespan, growth, age of sexual maturity and fecundity. Monitoring the age and stage-specific patterns of an organisms' life offer insight into physical and ecological dependencies of the organism. Given the predominant existence of female *D. magna* during non-stressed conditions, life history data for females provide baseline data which offer a reference to compare other conditions against. When establishing an ageing model this baseline data is essential for identifying key variations in modified conditions and in this instance highlight key differences between female and male *D. magna* in real-time, most importantly a significant difference in lifespan, but show as a percent of lifespan both are experiencing comparable life history traits.

A widely observed sex difference aside from lifespan is body size. Commonly referred to as sexual size dimorphism, the observed difference in size between adult females and males of a population (in both animals and plants) is often related to separate roles in reproduction (Fairbairn et al., 2007). As shown in Figure 3.4, female *D. magna* are approximately twice as large as their male counterparts. As naturally occurring populations of *D. magna* consist of females that reproduce via cyclical parthenogenesis to produce clonal daughters, it is suggested that females have adopted faster growth rate and larger body size to maximise energy availability for reproduction of multiple broods. Such adoptions maximise the number of produced offspring and promotes population survival (Pietrzak et al., 2010a). Furthermore, male

D. magna become established under non-favourable conditions which force the female *D. magna* to switch reproductive strategy to become sexually receptive to males. It is under stressed conditions that males are required for the production of 'resting eggs'. Resting eggs are encased in a hard outer capsule known as ephippia which allows the eggs to lay dormant in sediment until more favourable conditions return (Hebert, 1987). Given the biological role of males is for sexual reproduction in unfavourable conditions, different mechanisms have evolved to maximise male fitness. For example, here the males are much smaller and do not exert excess energy in a fast growth rate and large body size as seen in females, but instead may direct energy in to maximising egg fertilisation which would require contact with as many females as possible (Pietrzak et al., 2010a). Also notable is the similarity of age at sexual maturation in females and males, aged 9 days and 8 days respectively. It is possible that the shorter lifespan, smaller size and age at maturation of male *D. magna* is due to the biological role males play in reproduction.

In cases of sexual size dimorphism a divergence of life history and ecological variables is often observed (Fairbairn et al., 2007). Although body size differs between sexes, it is observed that both females and males reach maximum growth at approximately 40% of their lifespan. In a similar fashion, relative to body size both sexes lose their tail at a similar rate as percent of lifespan (Figure 3.6) however when considering respective lifespans this means both maximised growth and rate of tail loss is occurring twice as fast in real time in males compared to females. Across many species that undergo appendage loss and regeneration it is often observed that the regenerated appendage is smaller in comparison to non-regenerated appendages. Notably these smaller appendages can result in a negative impact on foraging, reproduction and/or

survivorship. Furthermore, regeneration capacity declines with each instar therefore as the animal ages regenerative ability is reduced (Maginnis, 2006).

As shown in Figure 3.10, females appear to swim faster than males which may be an evolutionary divergence necessary for maximal survival. In nature, females are likely to frequent closer to the surface of the waterbody where food is more plentiful to aid maximal reproduction and growth. However, higher risk of predation is also present closer to the surface therefore a faster swimming speed may be essential for survival. Additionally, males are often situated further away from the surface in cooler conditions with less risk of predation (Pietrzak et al., 2010a). It is believed the response of *Daphnia* to swim vertically away from light (deil vertical migration) has evolved for two reasons; firstly, to minimise mortality via predation by descending to darker depths of the waterbody, and secondly, to maximise development and reproductive rates by locating near the warmer surface of the waterbody throughout the night (Dodson et al., 1997). Irrespective of speed, both sexes express a significant consistent decline in swimming ability with age. *Daphnia* swim using the second set of antennae which are controlled by large muscles. The reduction in swimming speed may be potentially linked to age-dependent loss of strength and mass in this muscle however very little more is known about this mechanism. Furthermore, an age-dependent decline in heart rate in both sexes of *D. magna* was observed (Figure 3.8 and 3.9) which may be linked to reduced swimming speed. Similar observations have been recorded in *Drosophila melanogaster* where heart rate decline and reduced climbing ability have been linked to the observation in humans where a reduced resting heart rate is observed with age in addition to a more pronounced decline in maximum heart rate during exercise (Paternostro et al., 2001). It is possible that *Daphnia* experience an age-dependent

increase in muscle frailty as seen in other species which is linked to a time-dependent loss of muscle mass, integrity and function (Demontis et al., 2013), which if to be true, is occurring at different rates here between female and male *D. magna*. Additionally, *Daphnia* unlike most other invertebrates have a myogenic heart (R. Baylor, 1942) which may be utilised to investigate cardiac muscle degeneration and heart rate decline with age in addition to sex differences. These prospects should be investigated further.

Additionally, the inverse relationship between heart rate and lifespan presented here has also been identified across many species including humans (Gent et al., 2015) which has been linked to multiple factors including protein oxidation, free radical production, inflammation and telomere shortening (Zhang and Zhang, 2009). Interventions used to slow heart rate have resulted in extended lifespan (Singh, 2001, Cook et al., 2006, Gent et al., 2015) further supporting the role of heart rate on maximum lifespan. Effect of heart rate on longevity is also observed within species, evidenced by comparing lifespan of hibernating and non-hibernating bats. During hibernation heart rate is significantly slowed and it is observed that these hibernating bats live 70% longer than their non-hibernating counterparts (Cook et al., 2006). Additionally, body mass has been associated with heart rate and longevity in mammals, notably smaller mammals tend to show higher heart rate and shorter lifespan (Zhang and Zhang, 2009). Male *Daphnia magna* exhibit a much higher heart rate and a much smaller body mass therefore it is possible that this contributes to the observed lifespan of male *Daphnia magna* being approximately half that of their female counterparts. Due to the higher heart rate and shorter lifespan observed in males it is

possible that the age-dependent decline in heart rate is occurring at a much faster rate in males compared to females.

As previously described, there is a decline in overall swimming speed with age, however, also of note is the observed 'dip' in swimming speed at 20% of lifespan for females and 40% of lifespan for males, both of which equate to aged 20 days in real time (Figure 3.10). This decline in swimming speed in both sexes at the day 20 time point may be linked to the observed decline in reproductive capacity expressed by females at the same age (A2.F4, Appendix 2A). Initial reproduction between aged 11 and 20 days shows a steep increase however from aged 20 days reproduction begins to decline. The decline in female swimming speed may be attributed to the lesser demand for feeding to produce large broods whilst the males may be linked to age-dependent changes in mating behaviour and the potentially reduced fertility of the females after this time. It has been recorded in humans that both female and male fertility declines with age. Males can experience what is termed as 'male factor infertility' which encompasses various conditions related to sperm count, mobility and morphology (Harris et al., 2011). The observation of female and male fertility decline with age may be applied to *D. magna* and the observed decline in swimming speed may be as a result of reduced mating potential.

The gradual decline in reproduction with age seen in female *D. magna* (Figure 3.7) is a trait often observed in humans whilst a complete stop in reproduction after a certain age is observed in *C. elegans* and *Drosphila* (Grotewiel et al., 2005, Kenyon, 2010). It is widely known that as *Daphnia* grow they have a higher demand for food. Feeding a fixed volume throughout lifespan could therefore lead to limitation of growth if not

enough food is present, which in turn would result in modified resource allocation and thus lead to decline in reproduction. However, in a controlled laboratory environment it was clear that algae was present in the media at the time of media change suggesting an excess of algae was present therefore food is unlikely to have been a limiting factor. Female *D. magna* produce eggs from nurse cells in the ovary continuously throughout their lifecycle but the number of offspring per brood declines and time between broods increases with age. The observed decline in reproduction may be in part due to the impaired stem-cell function with age as observed in both vertebrates and invertebrates. One such contributing factor to this impairment is DNA damage indicated by comet analysis and impaired DNA repair identified in aging mice hematopoietic stem cells (Ahmed et al., 2017). The ability of *D. magna* to utilise nurse cells throughout life makes them a potentially interesting tool for stem cell research.

3.5.2 Sex differences in molecular markers of health and ageing in *D.magna*

Ageing is not only observed through physiological decline but also encompasses molecular and cellular changes. A decline in reduced glutathione (GSH) in addition to increased lipid peroxidation product malodialdehdye (MDA) with age is demonstrated here (Figures 3.11 and 3.12). One of the most well supported theories of ageing is the DNA damage theory (Gensler and Bernstein, 1981). This theory suggests the observed age-associated functional decline is largely caused by DNA damage accumulation over time which leads to cellular alterations and tissue homeostasis disruption (Freitas and de Magalhaes, 2011). However, the mechanisms driving genomic instability are only recently starting to be uncovered. One such mechanism suggested is an increase in macromolecule peroxidation which may be driven by depletion of antioxidant defence mechanisms such as thiol-containing glutathione.

GSH works as a protective barrier against oxidative damage by acting as a substrate for glutathione peroxidases including hydrogen peroxide and lipid peroxide. When oxidised, GSH takes on a disulphide form (GSSH). The age-related shift observed between GSH/GSSH redox couples has been identified in clinical studies in humans and is thought to contribute to ageing diseases such as cardiovascular disease, diabetes, rheumatoid arthritis and neurological disorders (Giustarini et al., 2006), similar to observations in *Drosophila* where GSH/GSSG ratios significantly decrease as the flies age (Rebrin et al., 2004). It has been suggested that the age-related decline in GSH is partly driven by an increased oxidative load over time (Giustarini et al., 2006). The results support the current understanding of GSH depletion and increased oxidative insult with age which suggests lesser protection and higher damaging load may be contributing to increased DNA damage with age. Notably, male *D. magna* appear to have consistently lower amounts of MDA compared to females when normalised to protein content. Lipid peroxidase preferentially oxidises poly-unsaturated fatty acids (Gaschler and Stockwell, 2017) therefore it is possible this difference between sexes is linked to differences in lipid composition which may exist due to variable reproductive demands.

Consistent with the DNA damage theory of ageing, both female and male *D. magna* experience DNA damage accumulation with age at comparative rates as a percentage of their lifespan (Figure 3.13). However, in real time DNA damage is accumulating at a much faster rate in males compared to females (Figure 3.14). The reported DNA damage accumulation may be in part due to the previously described decline in antioxidant protection from increasing peroxidation, but may also in part be a result of age-related decline in DNA damage repair efficiency. To monitor change in repair

efficiency with age both female and male *D. magna* were exposed to cisplatin. Cisplatin is a DNA damaging agent that works by 3 different mechanisms; A) addition of alkyl groups to DNA bases which leads to repair enzymes fragmenting the DNA when trying to substitute the alkylated base, B) by forming cross-links which inhibits synthesis or transcription and C) inducing mutations by mispairing nucleotides (Dasari and Tchounwou, 2014). Findings observed in *Drosophila melanogaster* show ɣH2AX foci persist for longer in older spermatagonia (Delabaere et al., 2017) and here, in older *D. magna* RAD51 expression becomes more pronounced with age and appears to become unresponsive to cisplatin exposure in the eldest age groups (Figure 3.15). This gradual reduction in recovery may be in part due to the decline in efficiency of repair via homologous recombination, a preferred repair pathway for double stand breaks. RAD51 plays an essential role in homologous recombination by driving recognition of homology and strand exchange between homologous templates. Following cisplatin exposure, younger female *D. magna* show an increase in RAD51 foci count and at ages 10 and 20 days levels of RAD51 remain high. By aged 80 days there is no significant difference between control levels of RAD51 compared to all recovery stages. This may suggest that repair via homologous recombination is at its maximum capacity in older animals due to the higher naturally occurring damage present with old age. Another possibility is shared by Delabaere et al. (2017) which proposes that homologous recombination becomes defective with age by the inability of RAD51 to dissociate. If RAD51 does not dissociate it blocks the progression of effective repair resulting in persisting damage which may explain not only the accumulation of DNA damage seen with age and higher number of RAD51 foci in older

animals but would also inhibit recovery of older *D. magna* exposed to the DNA damaging agent cisplatin.

Male *D. magna* aged 10 days follow a similar trend to female *D. magna* in terms of high RAD51 expression for the duration of the recovery period (Figure 3.16). However, control unexposed males appear to express higher levels of RAD51 even at a younger age comparatively to females of the same age and similar percent of lifespan (Figure 3.16). Control males aged 10 days have an average RAD51 foci count of 5.68 which is much higher than females aged 10 days with 1.42, or an equivalent of 20% lifespan at females aged 20 days showing an average foci count of 2.07. Given the maximum recorded average of RAD51 foci count is approximately 9 foci it would appear that male individuals are closer to maximum damage and recovery capacity much earlier in their lifetime. As the males age the trend of RAD51 foci begins to differ to that seen in the females. RAD51 is not only integral to DNA repair, but also in cell cycle arrest at the G2/M checkpoint where DNA damage is repaired prior to mitosis. A defective G2/M checkpoint results in death after cell division (Kostyrko et al., 2015). Given the dysregulation of RAD51 in DNA repair with age (Delabaere et al., 2017) it is possible that the G2/M checkpoint is also compromised given the importance of RAD51 signalling in the progression in to the G2 phase (Kostyrko et al., 2015).

Overall, the data clearly shows that lifespan and ageing rate can vary in genetically identical sexes of one specie. Physiological and molecular markers of ageing measured in this paper demonstrate that age-associated changes are occurring at the same rate as percentage of lifespan. However, considering that males have half the lifespan of females this indicates that the age-associated changes are occurring approximately twice as fast in male *D.magna* compared to females. The data

presented in this paper supports the use of this unique model organism for research into sex differences in longevity and aging. They provide a suitable platform for investigating the contribution of non-genetic factors and mechanisms, such as epigenetic factors, hormones, environmental factors, energy allocation and trait offs in determining lifespan and ageing rate.

CHAPTER 4

Characterisation of the dynamic nature of lipids throughout the lifespan of *Daphnia magna* Bham2 by UHPLC/MS analysis

This chapter has been published in (Constantinou et al., 2020)

4.1 Introduction

Lipids are essential for normal cellular functions including intracellular and extracellular signalling pathways, providing membrane fluidity and facilitating energy storage (Schroeder and Brunet, 2015, Kyle et al., 2016). The importance of lipid molecules in cellular processes is reflected in the vast diversity of their structures and functions and thus they are involved in many homeostatic processes but also play a role in disease and long-term health (Kyle et al., 2016).

Model organisms have been crucial in enhancing our understanding of the role of different lipid classes in regulation of ageing rate, lifespan and prevention or acceleration of age-related diseases (Mitrofanova et al., 2018). The first association between lipid composition and ageing rate was demonstrated in *Caenorhabditis elegans* (Wang et al., 2008), *Drosophila melanogaster* (Stark et al., 1993), laboratory *Mus musculus* (Hawcroft and Martin, 1974) and the budding yeast *Saccharomyces cerevisiae*. In *Saccharomyces cerevisiae* (Rattray. JB et al., 1975), mutations in insulin growth factor-2 pathway and the mechanistic target of rapamycin complex 1 (mTORC1) signalling pathway increased lipid storage and the elevated lipid storage is associated with increased lifespan and reduced reproduction (Mitrofanova et al., 2018). Therefore, there is a trade-off relationship between longevity, reproductive capacity and lipid storage. During reproduction, lipid reserves are used and depleted, while during low-reproductive periods lipid is accumulated, a phenomenon known as the *cost of reproduction*. Notably, animals with reduced reproduction often survive better, as energy from lipid reserves are invested into somatic maintenance and survival rather than reproduction (Hansen et al., 2013). In addition, in multiple species, including worms, flies, mice, rats, primates and spider mites, dietary restriction and

change in concentration of lipid molecules (either as recorded blood levels or controlled dietary input), such as oleic acid can impact longevity (Goodrick et al., 1990, Weindruch, 1996, Lakowski and Hekimi, 1998, Masoro, 2005, Skorupa et al., 2008, Mitrofanova et al., 2018, Li and Zhang, 2019). Using the yeast model organism *Saccharomyces cerevisiae*, it has been demonstrated that genetic and pharmacological interventions that can weaken but not completely inhibit metabolite flow through the pathway of *de novo* sphingolipid synthesis, can cause reduction in sphingolipid concentrations. The reduction in sphingolipid concentration can subsequently lead to increased replication and lifespan (Mitrofanova et al., 2018). For example, deletion of Lag1 (homolog to human CERS2,) extends *S. cerevisiae* replication lifespan without altering the chronological lifespan. Whereas deletion of lsc1 (homolog to human nSMase 2) has been shown to shorten *S. cerevisiae* chronological lifespan (Mitrofanova et al., 2018). This indicates a clear role for sphingolipids in regulation of replication and lifespan in yeast. Other lipids can regulate lifespan in *S. cerevisiae*, including triacylglycerides (TG). Excessive TG content is converted to ethanol which shortens chronological lifespan in yeast via an undetermined mechanism (Mitrofanova et al., 2018). Therefore, caloric restriction (CR) can extend yeast lifespan by reducing the amount of excessive TG. Additionally, changes to the composition of mitochondrial membrane phospholipids has been linked to altered lifespan in yeast (Mitrofanova et al., 2018). The changes in concentration of lipids and their impact on lifespan regulation and ageing process is a clear evidence of their significant role in regulation of health and disease. However, the relationship between lipids and longevity is complex and not all lipids within a class will have the same impact on lifespan (Bustos and Partridge, 2017). The complex nature of this relationship can

be demonstrated by the lipid class phosphatidylcholine (PC), where PC lipid species PC (O-34:1) and PC (O-34:3) have a negative association with diabetes and hypertension and a positive association with longevity (Gonzalez-Covarrubias et al., 2013). Conversely, other PC species show either no effect or a negative effect with longevity (Gonzalez-Covarrubias, 2013). This demonstrates the complex relationship between lipids, lifespan and healthspan.

In addition to lifespan, lipids can influence healthspan as the lipid composition and concentration directly affects cellular metabolism and function of a cell (Gonzalez-Covarrubias, 2013). For example, lipids in membrane can influence many diverse biological functions, such as membrane fluidity and influence signalling capacity (Egawa et al., 2016). Membranes are also responsible for protecting enzymes and genes from external environments. However, with age the composition of lipids within a cell alters, including the membrane lipids (Egawa et al., 2016). This subsequently results in structural, functional and behavioural changes within a cell (Egawa et al., 2016), which can increase the development of age-associated diseases. As a result, certain lipid profiles can predict the risk of age-associated diseases, such as type 2 diabetes (T2D), cancer, and coronary heart disease (Murphy and Nicolaou, 2013, Kyle et al., 2016). In T2D - a common age-associated disease - a relationship has been established between increased risk of T2D and lower carbon number and double bond content of TG (Rhee et al., 2011). This relationship stands true for other lipids, including ceramides (Cer), phosphatidylcholines (PC) and sphingomyelins (SM) (Rhee et al., 2011). Such findings begin to answer the question as to why dyslipidemia (the presence of an abnormal amount of lipids) is an independent risk factor of T2D (Rhee et al., 2011). Furthermore, TG and cholesterol are used to determine risk of

cardiovascular diseases (Gonzalez-Covarrubias, 2013) while TGs and lipoprotein levels have been linked with increased risk of obesity and hence can negatively impact health and longevity (Schroeder and Brunet, 2015). Altered lipid metabolism is also a prominent feature of cancer due to increased demand to support accelerated proliferation (Dutta and Sharma-Walia, 2019) with altered levels of TG specifically associated with many types of cancer (Lofterød et al., 2018, Anand et al., 2018, Bosco et al., 2018). These data provide clear support for role lipids in regulating healthspan in many species.

Most interestingly, it is well-established that females and males of various species have different average lifespan, healthspan and ageing rate (Austad and Fischer, 2016). However, the molecular pathways that contribute to these observed differences between male and females are not fully understood. As lipids clearly play a vital role in regulation of ageing rate, healthspan and lifespan (Hulbert et al., 2014), it is plausible that they may also contribute to the differences observed in ageing rate between the two sexes. Indeed, the lipid composition of male and females are different (Parisi et al., 2011, Wang et al., 2011, Mauvais-Jarvis, 2015, Sales et al., 2016). This is partly, due to different reproduction, hormonal and growth needs of both sexes. Furthermore, several studies have demonstrated that there are clear sex associated differences in lipid profile with age (Tognini et al., 2012, Auro et al., 2014, Anagnostis et al., 2016, Díaz et al., 2018, Gu et al., 2018). However, further detailed studies are required to enhance our understanding of the role of lipids in regulation of lifespan between sexes. Short-lived model organisms with different average lifespan between females and males can help to elucidate the molecular mechanisms of lifespan and healthspan regulation between sexes.

Daphnia magna are a recognised model organism by the U.S. National Institute of Health (Colbourne et al., 2011). They have been extensively used across a variety of research fields including ecotoxicology, ecology and population genetics and is ever-growing in importance for molecular studies of neurobiology and the biology of ageing (Constantinou et al., 2019). Importantly, *D. magna* reproduce via cyclical parthenogenesis whereby mothers produce genetically identical daughters. During unfavourable conditions or through hormonal stimulation, male *Daphnia* are produced for sexual reproduction. Both females and males are genetically identical yet demonstrate different average lifespans, body size, swimming speed and ageing rate (Constantinou et al., 2019). These observations bring *D. magna* to the forefront of alternative models for research into ageing. Therefore, in this study we used genetically identical female and male *D. magna* to gain a comprehensive understanding of how their lipid composition alters as function of age and sex. To capture the dynamics nature of lipids as a function of age and sex, we conducted a detailed time course lipidomics study with 90 samples covering 15 female age groups and 12 male age groups. The information can reveal how alteration to lipid profiles or lipid signalling influence longevity overall and provide greater insight into sex differences in longevity. It will also improve our understanding of inherited pro-longevity lipid profiles and help elucidate mechanisms behind lipid metabolism and it's interaction with lifespan extension (Schroeder and Brunet, 2015). Overall, the magnitude of this study, alongside using genetically identical female and male species that have evolved different average lifespan and ageing rate (Constantinou et al., 2019), makes this study unique and extremely powerful in regards to advancing our understanding of the molecular regulation of lifespan between sexes.

4.2 Experimental Design

Samples for UHPLC/MS analysis were collected as described in section 2.11.1. Samples were prepared as described in section 2.11.2 and LC/MS was run under conditions described in section 2.11.3 and 2.11.4. Data analysis was performed as described below. See Figure 4.1 for an overview of the experimental design.
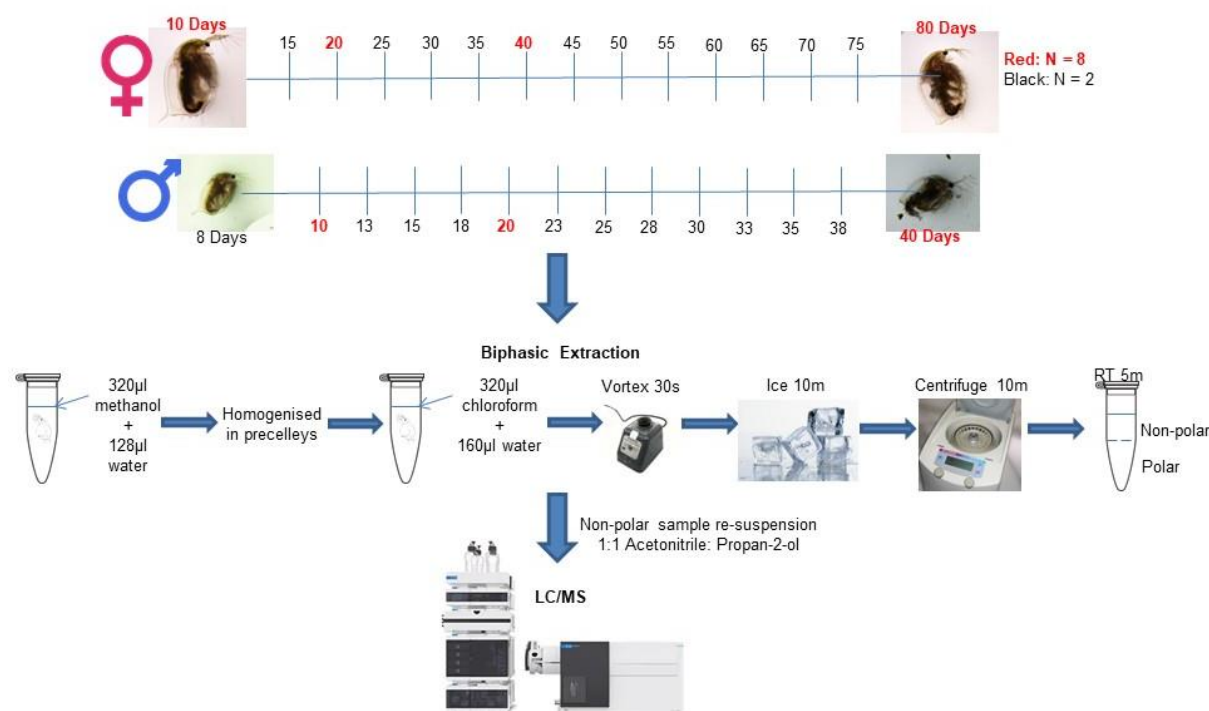
Figure 4.1: Lipidomics experimental design. Samples were collected at regular intervals for both female and male *Daphnia*. Once all samples were collected, samples were allocated in to batches and underwent biphasic extraction. The non-polar sample was taken forward for mass spectrometry analysis. More details can be found in section 2.11.

Briefly, six cultures of 100 female Daphnia and 14 cultures of 100 male Daphnia were maintained under normal conditions as described in section 2.3. Each replicate contained individuals from across multiple cultures. The number of individuals per replicate was determined and collected as described in section 2.11.1. The aim of

manipulating the number of individuals per sample to dry mass of the largest sample group was to normalise to body mass, thus accounting for differences in body size seen across difference age groups and between sexes.

4.3 Data Analysis

4.3.1 Lipidomics data analysis

LipidSearch (version 4.2, Thermo Fisher Scientific) was used to de-convolute and integrate peaks in the data, and annotate peaks based on their MS/MS fragmentation patterns. In terms of deconvolution, this software generated two data intensity matrices – one for positive and one for negative ionisation modes – containing samples as rows and annotated lipids as columns. Only lipids that were annotated from their MS/MS spectrum were retained in the datasets. For lipid annotation, all experimental LC-MS/MS spectra data were searched against a MS/MS lipid library in the LipidSearch software database. The generated MS/MS fragmentation spectrum can be used to identify the class and fatty chain composition of lipid species (some examples of MS/MS spectra from lipid species measured in this study are shown in Appendix 2B: Section B.). Experimental MS/MS spectra were searched against all lipid classes in the LipidSearch database using the following potential ion forms: positive ion = $[M+H]^+$, $[M+NH_4]^+$, $[M+Na]^+$, $[M+K]^+$, $[M+2H]^{2+}$; negative ion = $[M-H]^-$, $[M+HCOO]^-$, $[M+CH_3COO]^-$, $[M+Cl]^-$, $[M-2H]^{2-}$. The quality of the annotation was graded as A-C. This is defined as: Grade A = all fatty acyl chains and class were completely identified; Grade B = some fatty acyl chains and the class were identified; Grade C = either the lipid class or some fatty acyls were identified. Only peaks that had an annotation grade of A-C were retained in the dataset. Peaks in the data matrices were then filtered as follows: (i) peaks that were present in both the QCs and the extract blank with a extract

blank:QC intensity ratio of >10% were removed; (ii) samples with >20% missing values were removed; (iii) peaks with a median QC intensity RSD>30% were removed; (iv) matrix was normalised by PQN (Dieterle et al., 2006) and (v) missing values were filled by KNN (Fukunaga and Hostetler, 1975). R (R Project for Statistical Computing, http://www.r-project.org/, Version 3.5.2) was used for all statistical analyses and data visualisation. First, positive and negative data matrices were checked to ensure no overlapping ion forms were detected. The datasets were concatenated and treated as a single dataset for the remainder of the analysis. Principal component analysis (PCA) was applied and visualised using package ggplot2 (Wickham, 2016). Data was analysed by the R package 'Limma' (Ritchie et al., 2015) with the core capability of log2 transforming data then using linear models to assess differential expression in the context of multifactorial experiments (Phipson et al., 2016). Empirical Bayesian methods were then applied to smooth standard error to provide stable results for lipids in conditions age only (irrespective of sex), sex only (irrespective of age) and sex:age interaction. A further two results files were subsequently generated for the condition of age in females only and another for males only.

Venn diagrams, barplots and heat map were produced using R package 'ggplot2' and the results tables produced via Limma. For the barplots, significantly changing lipids showing an increasing trend or decreasing trend were selected by adjusted *p*-value <0.001 with a log fold change of <0 and >0, respectively. The method of adjustment applied was BH as described by Benjamini and Hochberg (1995). For heatmaps analysis, the results datasets (sex, ageF, ageM, sex:age interaction) were ordered by

adjusted *p*-value and the top 50 most significantly changing lipids from each ion mode were selected for heatmap visualisation.

4.4 Results

4.4.1 Age and sex influences lipid profile in *D. magna*

PCA was conducted on the normalised combined negative and positive ion mode lipidomics dataset. As demonstrated in Figure 4.2, *D. magna* samples were separated along the principal component 1 (PC1) according to sex (with no overlap between male and female groups). Samples were further separated along the PC2 axis according to age, from young (orange) to old (blue).
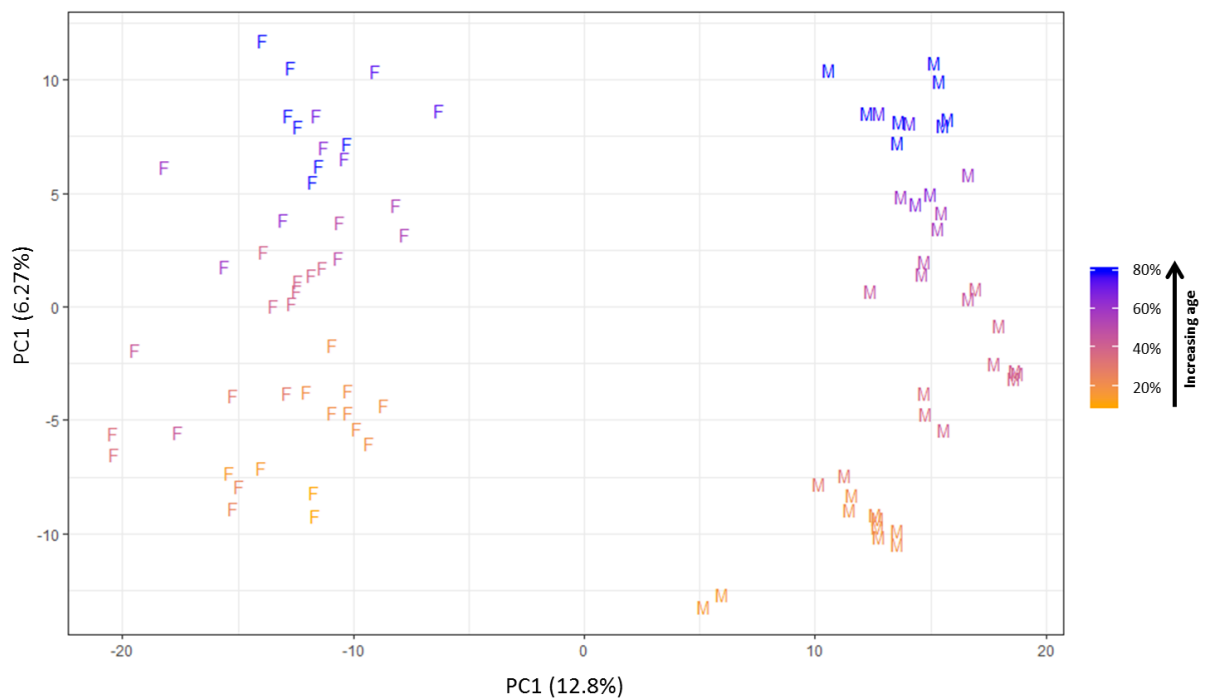
Figure 4.2: Principal component analysis of normalised positive and negative ionisation mode lipidomics data for male and female *Daphnia magna* demonstrated as percentage of lifespan. Principal component 1 shows clear separation based on sex (F = female, M = male) with females grouped to the left and males to the right. Principal component 2 shows separation by age depicted by colour ranging from orange (young) to blue (old). Female *D. magna* age range is 10 days to

80 days (maximum sampled age = 80 days). For female age groups 20, 40 and 80 days, eight technical replicates were used and for intermediate ages two technical replicates were used. Male *D. magna* age groups ranging from 8 days to 40 days were used (maximum sampled age = 40 days). For male *D. magna* age groups 10, 20 and 40 days, eight technical replicates were used and for intermediate age groups two technical replicates were used. For detailed information regarding biological replicate numbers see Tables 2.7 and 2.8 (section 2.11). Supplementary Figures S5 and S6 show PCA plots for positive and negative ion mode separately and highlight the grouping of the intrastudy QC sample.

Based on the PCA results, it was prudent to analyse the data in terms of sex, female ageing, male ageing and sex:age interaction. Throughout the analysis, it became apparent that not all lipid sub-species within a single class behave in the same way. Table 4.1 highlights 10 lipid sub-species and their associated class, ordered by most to least significantly changing relative intensity in the condition of sex:age interaction, with the response of the same lipid sub-species for the conditions of sex, female ageing and male ageing. Table 4.2 shows some reported biological functions related to the classes of the 10 lipids included in Table 4.1. The details for all annotated lipids are reported in 2B.T2 (Appendix 2B).

DESCRIPTION		SEX:AGE INTERACTION			SEX ONLY			FEMALE AGE ONLY			MALE AGE ONLY		
LipidIon	Class	logFC	AveExpr	adj.P.Val	logFC	AveExpr	adj.P.Val	logFC	AveExpr	adj.P.Val	logFC	AveExpr	adj.P.Val
SM(t40:2)+HCOO	SM	-0.1068	-1.6318	3.24E-21	1.9720	-1.6318	1.96E-13	0.0025	-1.3352	0.36712	-0.1042	-1.9647	7.53E-15
ChE(16:1)+NH4	ChE	0.1241	3.8752	1.55E-20	-3.4721	3.8752	1.67E-18	-0.0423	3.7010	2.19E-11	0.0825	4.0706	5.74E-15
SM(t40:2)+H	SM	-0.0675	2.4276	1.83E-20	1.2463	2.4276	1.08E-11	-0.0032	2.5644	0.09941	-0.0707	2.2741	1.29E-15
TG(2:0_14:0_16:3)+NH4	TG	0.0583	3.6851	1.89E-20	-1.0510	3.6851	4.47E-10	0.0166	3.6932	2.72E-09	0.0752	3.6759	8.65E-25
SM(d34:3)+H	SM	-0.0710	3.7734	3.59E-20	1.5936	3.7734	1.07E-14	-0.0027	3.7889	0.23171	-0.0733	3.7560	5.39E-16
TG(2:0_16:0_16:3)+NH4	TG	0.0459	6.3280	8.82E-20	-0.6185	6.3280	2.08E-06	0.0171	6.2759	1.51E-11	0.0633	6.3864	9.17E-26
ChE(18:1)+NH4	ChE	0.0945	6.3903	1.50E-19	-4.5301	6.3903	1.71E-31	-0.0356	7.1095	7.51E-14	0.0597	5.5834	1.38E-12
ChE(17:1)+NH4	ChE	0.1042	1.0156	1.66E-19	-3.8441	1.0156	5.71E-24	-0.0410	1.2567	1.23E-14	0.0632	0.7451	1.34E-10
TG(16:0_16:0_18:3)+NH4	TG	0.0165	12.7314	2.84E-19	-0.1669	12.7314	0.00035	0.0040	12.6646	9.19E-12	0.0205	12.8064	4.94E-16
TG(36:4)+NH4	TG	0.0491	7.880	6.88E-19	-0.6493	7.8801	4.74E-06	0.0158	7.7948	2.64E-09	0.0647	7.9759	5.30E-24

Table 4.1: Top 10 lipids with most significantly changing relative intensity in sex:age interaction plus response of the same lipids in sex, ageing in females only and ageing in males only. Lipids were ordered by adjusted *p*-value from most

significant to least for the condition of sex:age interaction. For the conditions of sex only, ageing in females only (female age only) and ageing in males only (male age only), lipids were ordered to match that of sex:age interaction. Log fold-change (logFC), average expression (AveExpr) and adjusted *p*-value (adj.P.Val) were recorded for each condition. Where average expression is positive: for sex:age interaction this is changing at a faster rate in females; for sex only this is higher in females; in female ageing only this is increasing with age; in male ageing only this is increasing with age. The MS/MS fragmentation spectra of all lipids listed in Table 4.1 have been manually reviewed (Appendix 2B: Section B).

Class	Biological Function	Reference
SM	SM facilitates formation of lateral membrane domains and has a strong interaction with cholesterol. SM has a varied and vast biological influence including but not limited to; regulation of endocytosis and receptor-mediated ligand uptake, ion channel and G-protein coupled receptor function, protein sorting, and functioning as receptor molecules for various bacterial toxins, and for non-bacterial pore-forming toxins.	(Slotte, 2013)
ChE	ChE is the inactive form of cholesterol and it is primarily used for transport of cholesterol to organs or to act as a biologically inert storage of excess cholesterol by the addition of fatty acids to the hydroxyl group results in less polarity making the lipid 'inert'	(Christie, 2019)
TG	TGs are the main form of fat recorded in humans and are present across many species. They are found in the blood and act as an energy supply for the body in addition to being stored as body fat when excess is present.	(Lampe et al., 1983, Flier, 1995)

Table 4.2: Biological function of lipid classes included in Table 4.1. The top 10 lipids with most significantly changing relative intensity in sex:age interaction were lipid sub-species of three lipid classes; SM (sphingomyelin, ChE (cholesterol ester) and TG (triglyceride).

4.4.2 Overview of changes in lipidomics of male and female *D. magna* as a function of age and sex

Of the total 2,556 annotated lipids (based on their MS/MS fragmentation pattern) used for the subsequent analysis, 2,051 lipids showed significantly altered relative intensity (FDR adjusted *p*-value <0.001) as a function of sex (1,413), age (1,169) or sex:age

interaction (1,011) (Figure 4.3A, 2B.T2 Appendix 2B). The significantly altered lipids are referred to as 'significant annotated lipids' for the remainder of the paper.

Roughly an equal number of significant annotated lipids are changing as a function of age (1,169) and are different between the sexes (1,413). Interestingly approximately half (1,011) of all significant annotated lipids are interacting between age and sex. A fraction of lipids (345) are changing as a function both sex and age (reported to change significantly as a function of sex and age), and also have significant interactions between age and sex (have different age-related changes in the two sexes). Lipids that are significant for only one variable are rare, especially for sex:age interactions. Only 27.67% (391/1,413) of sex-dependent changes show no age-related changes or sex:age interactions, meaning these lipids do not change during ageing, but are different between male and female *Daphnia*. A similar number of lipids (28.49%; 333/1,169) with age-related changes were equal in both sexes. While only 12.86% of sex:age interaction significant lipids had no significant changes for age or sex, meaning there are fewer lipids where the independent effects of sex and age is cancelled out. For example, when the lipid amount increases in one sex during ageing and at the same time decreases with age in the other sex with equal magnitude, the overall effect is cancelled out in an interaction setting. The identity of the lipids that alter as a function of age or sex can provide valuable information regarding the role of lipids that drive the differences observed in ageing rate between the two sexes.

As shown in Figure 4.3A, 16.82% of the significant annotated lipids are shared between all three categories (sex, age or sex:age interaction), meaning these lipids have age-related changes in both sexes, but also the rate of change is different between the sexes. Interestingly, 15.41% of the significant annotated lipids are shared between age

and sex groups and not present in sex:age interaction group. These lipids are changing the same way in both sexes during ageing, but there is also a basal difference in the lipid levels between the sexes.
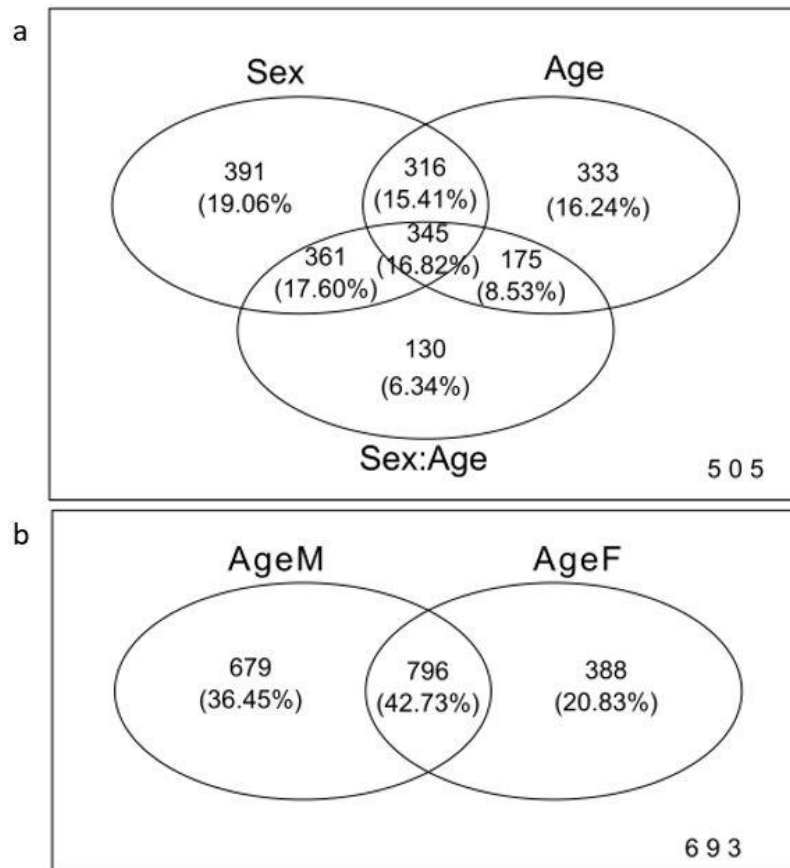
Figure 4.3: The Venn diagram represents an overview of the number of lipids with significant change in their relative intensity between categories of sex, age and sex:age interaction, and ageing in males and females in D. magna. A) The number of annotated lipids found to have a statistically-significant change in relative intensity (adjusted p-value <0.001) across the factors sex, age, and sex:age interaction are represented by numbers and the respective percentage within each grouping. The 505 lipids outside of the groupings do not show significantly (adjusted p-value <0.001) changing relative intensities in any of the conditions presented. B) The number of lipids identified as showing a significant change in relative intensity (adjusted p-value <0.001) observed within the conditions of ageF (female ageing data only) and ageM (male ageing data only) are represented by numbers and percentages within each grouping.

4.4.3 Age-dependent changes in lipid profile of female and male *D. magna*

When analysing age-associated changes in relative intensity of lipids in the context of ageing in female only (AgeF) and ageing in male only (AgeM), a total of 2,556 lipids were identified, of which 1,863 were expressing significantly altered lipid relative intensity (<0.001 adjusted p-value), see 2B.T2 (Appendix 2B). The lipids found to have statistically significant changes in relative intensity with ageing are referred to as 'age-related annotated lipids'.

As shown in Figure 4.3B, a high percentage of annotated lipids (42.73%) alter as function of age and independent of sex in *D. magna.* Interestingly, there are more unique age-related annotated lipids changing in male only samples (36.45%) compared to female only samples (20.83%).

LipidSearch 4.2 was used, as described in section 2.13, to identify the categories of significantly altering lipids as a function of sex. The identified lipids are categorised into five over-arching class groups as shown in Figure 4.4 and listed in 2B.T1 (Appendix 2B).

Within these six over-arching groups, certain sub-classes of lipids are more common in the overall dataset. For example, triglycerides (TG) and diglycerides (DG) account for 82.26% and 13.45% of the total neutral lipids and sterols. Phosphatidylethanolamine (PE) and phosphatidylcholines (PC) account for 34.47% and 29.92% of glycerophospholipids, respectively. Within sphingolipids, ceramides (Cer) and sphingomyelin (SM) account for 46.01% 42.97% of the lipids, respectively. Some MS/MS fragmentation spectra for species within each of the 6 over-arching classes (plus some other examples) were manually checked to confirm that the

identifications generated by the automated annotation software were correct (Appendix 2B: Section B).

Most interestingly, the sub-classes behave differently between sexes as seen in Figure 4.4 and 2B.T3 (Appendix 2B). For example, the level of TG (34% lower) and DG (70.70% lower) neutral lipids are generally lower in males compared to females. Likewise, the level of lipids categorised as sphingolipids are largely lower in males, as shown by 51.24% of ceramides demonstrating a lower amount in males and only 9.09% are higher in males compared to females. In contrast, the level of certain lipid sub-classes are generally higher in males than females, including SM, with 31.86% of SM demonstrating a higher amount in males than in females. Finally, there are lipid categories that display no significant difference between sexes, such as GD1a and Hex2Cer. The total number of lipids classified as within these groups occur at much lower frequencies compared to other classes (Figure 4.4).
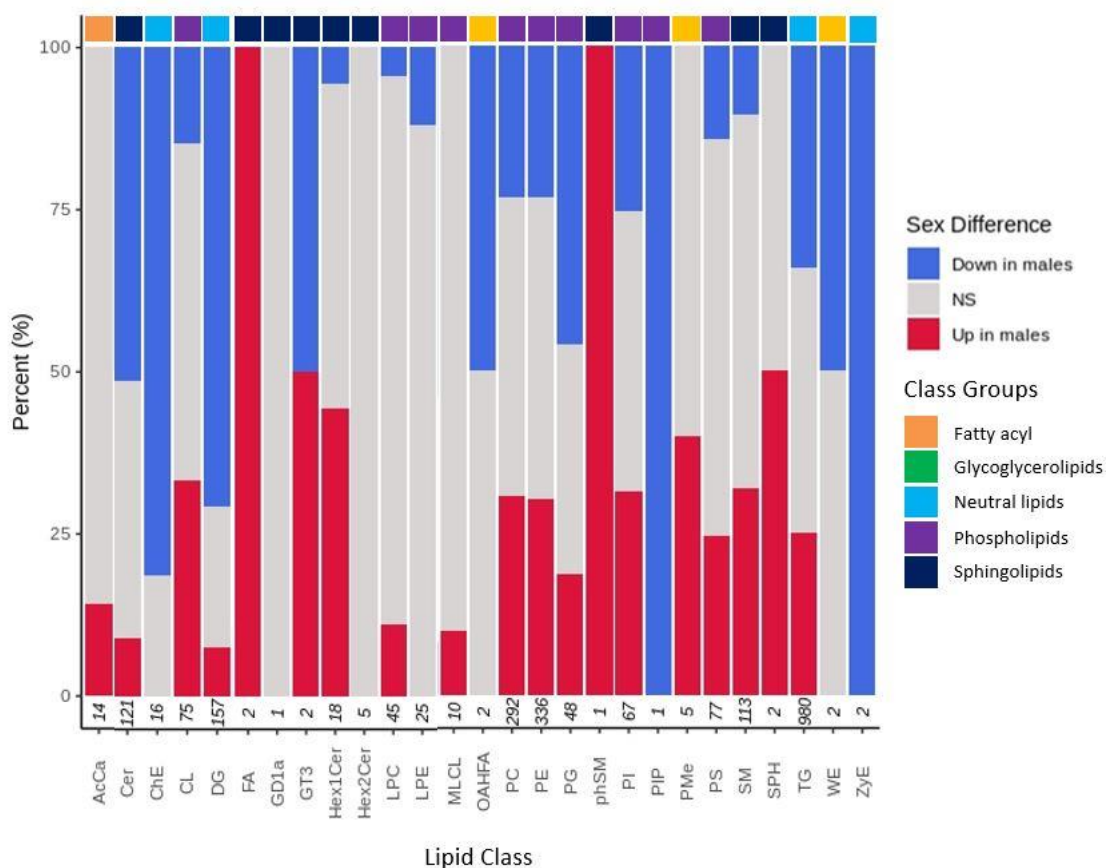
Figure 4.4: Differences in lipid class between male and female D. magna. Stacked normalised bar chart shows percentage of lipid classes with statistically-significant changes between sexes. Lipids lower in males are shown in blue whilst lipids higher in males are shown in red. Grey represents no significant difference between sexes (adjusted *p*-value <0.001). For female age groups 20, 40 and 80 days eight technical replicates were used and for intermediate age groups two technical replicates were used. For male *D. magna* age groups 10, 20 and 40 days eight technical replicates were used and for intermediate age groups two technical replicates were used. For detailed information regarding biological replicate numbers see Tables 2.7 and 2.8 (section 2.11). Numbers on the x-axis represent the total number of lipids identified in each class. Numbers on the x-axis represent the total number of lipids identified in each class, for lipid class abbreviation descriptions and classification see 2B.T1 (Appendix 2B).

4.4.4 Accumulative change in the levels of lipids in female and male *D. magna* with age

Figure 4.5A highlights the statistically-significant changes in lipid intensities across the main age groups of female *D. magna*; ages 20, 40 and 80 days compared to the youngest age group of 10 days old. When using age 10 days as the reference group for statistical comparisons, a clear statistically significant trend of change in intensities of lipids is observed between young (10 days old) and older (20, 40 and 80 days old) female *Daphnia*. Only 87 lipids are unique to aged 10 days compared to aged 20 days (age 10 vs 20), indicating relatively few differences between the lipidomes of these two age groups. By contrast, 340 lipids were found to have statistically-significant intensity differences when age groups 10 and 80 days were compared (age 10 vs 80) highlighting greater disparity between the lipidomes of these two age groups than between the 10 and 20 day groups. This clearly demonstrated that there is a gradual divergence of the lipidome over time leading to larger difference between the oldest age group of 80 days compared to aged 10 days. A similar trend can be observed when using females aged 20 days as the reference group (Table 4.3). Interestingly, at age 40 days old (approximately 40% of lifespan for female *D. magna*) there is 118 (4.62%) and 242 (9.47%) lipids with significantly altered lipid intensities compared to age 10 days and 80 days, respectively (Table 4.3). This data also provide evidence that the changes in lipid profile of *D. magna* as a function of age are accumulative and occur gradually throughout the lifespan of *Daphnia* rather than rapidly occurring at a specific time in the lifespan of *Daphnia.*

Finally, when using females aged 80 days as the reference group (Table 4.4), a similar trend to when using age 10 days old *Daphnia* was observed, supporting a continuous divergence of the lipidome with age.

The same trend observed in females is also observed in male *D. magna* whereby there is less difference between young age groups (e.g 8 and 10 days) and a larger difference between young and old age groups (e.g 8 and 40 days; see Figure 5B and Table 4.4). The main difference between sexes is that when 40% of lifespan in males (aged 20 days) is used as the reference, the range of results are much wider with 89 (3.48%) lipids comprising the smallest group (comparing 20 days v 8 days and 20 days v 40 days) and 428 (16.74%) lipids representing the largest group (20 days v 40 days). The 3.48% lipids uniquely altered in intensity in aged 20 days v 8 days, compared to aged 20 days v 40 days shows that the majority of lipids changing between 8 and 20 days are the same lipids continuing to significantly change between aged 20 days and 40 days, with only 3.48% difference. Overall the lipidome in ageing males appears to follow the same trend as seen in females with a gradual divergence over time.
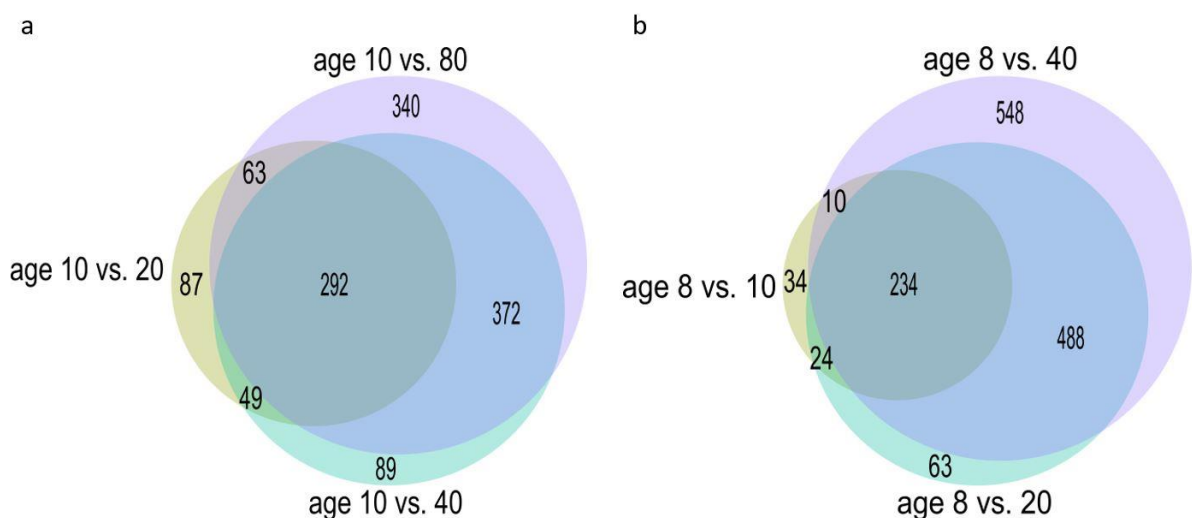
Figure 4.5: Venn diagram of lipids statistically-significantly changing lipid intensity with age between increment age groups compared to youngest age group for each sex. A) Comparison of lipids in female *D. magna* showing statistically-significant changes in lipid intensity (*p*-adjusted <0.001) from age groups 20, 40 and 80 days compared to youngest female group aged 10 days shows larger difference with increased age (e.g. between 10 and 20 days only 87 unique lipids identified showing similarity between age groups compared to 340 unique lipids between aged 10 days and 80 days). The size of the circle is proportionally relative to number of lipids. B) Comparison of significant lipids in male *D. magna* (*p*-adjusted <0.001) from age groups 10, 20 and 40 days compared to youngest male group aged 8 days shows larger difference with increased age (e.g. between 8 and 10 days only 34 unique lipids identified showing similarity between age groups compared to 548 unique lipids between aged 8 days and 40 days).

Certain lipid sub-classes behave differently (i.e. change in their relative intensity level) with age between female and male *D. magna* samples, leading to a different lipid profile between male and females as function of age (Figures 4.6A and 4.6B). For example, while the relative intensity (i.e. level) of equal number of lipids in the PE, PC and DG sub-categories decreases with age in both females and males, higher percentage of lipids in these sub-categories show an increase relative intensity as a function of age in males (PE: 26.79%, PC: 14.73%, DG: 75.80%) than females (PE: 2.38%, PC: 3.08%; DG: 47.77%). Other clear differences between females and males is detected in the Cer and SM sub-categories. Higher percentage of lipids in these sub-categories show a decrease in their relative intensity as a function of age in males (Cer: 40.50%, SM: 41.59%) than females (Cer: 30.58%, SM: 28.32%). While the opposite trend is observed for the TG sub-category with higher percentage of lipids in this sub-category demonstrating a decrease in their relative intensity as a function of age in females (TG: 23.16%) than in males (TG: 17.4%). Most interestingly, there are sub-categories that only alter in their relative intensity as a function of age in one of the sexes while remaining unchanged in the other sex. For examples, within the 16 ChE lipids, 93.75%

decline with age in females yet 0% decline with age in males. For the same lipids, 75.00% increase with age in males and 0% increase in females.

a
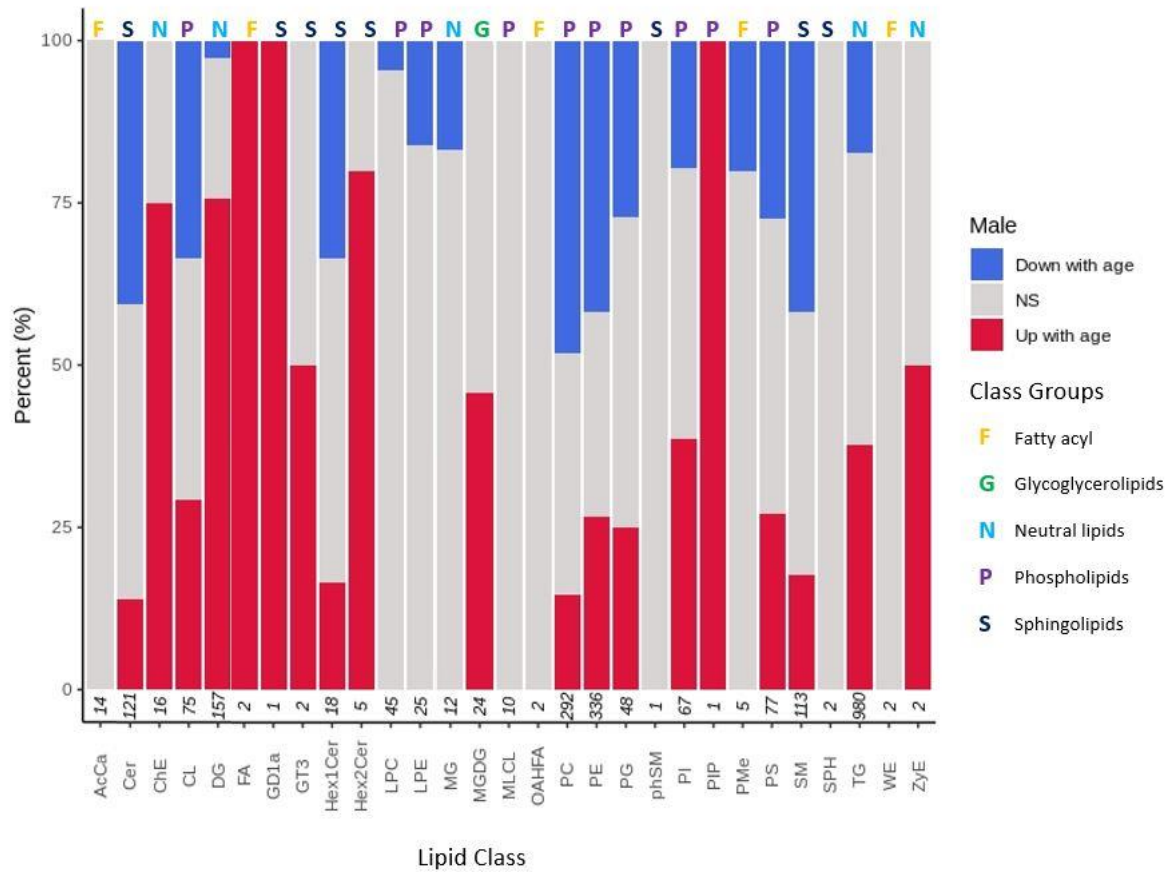
b
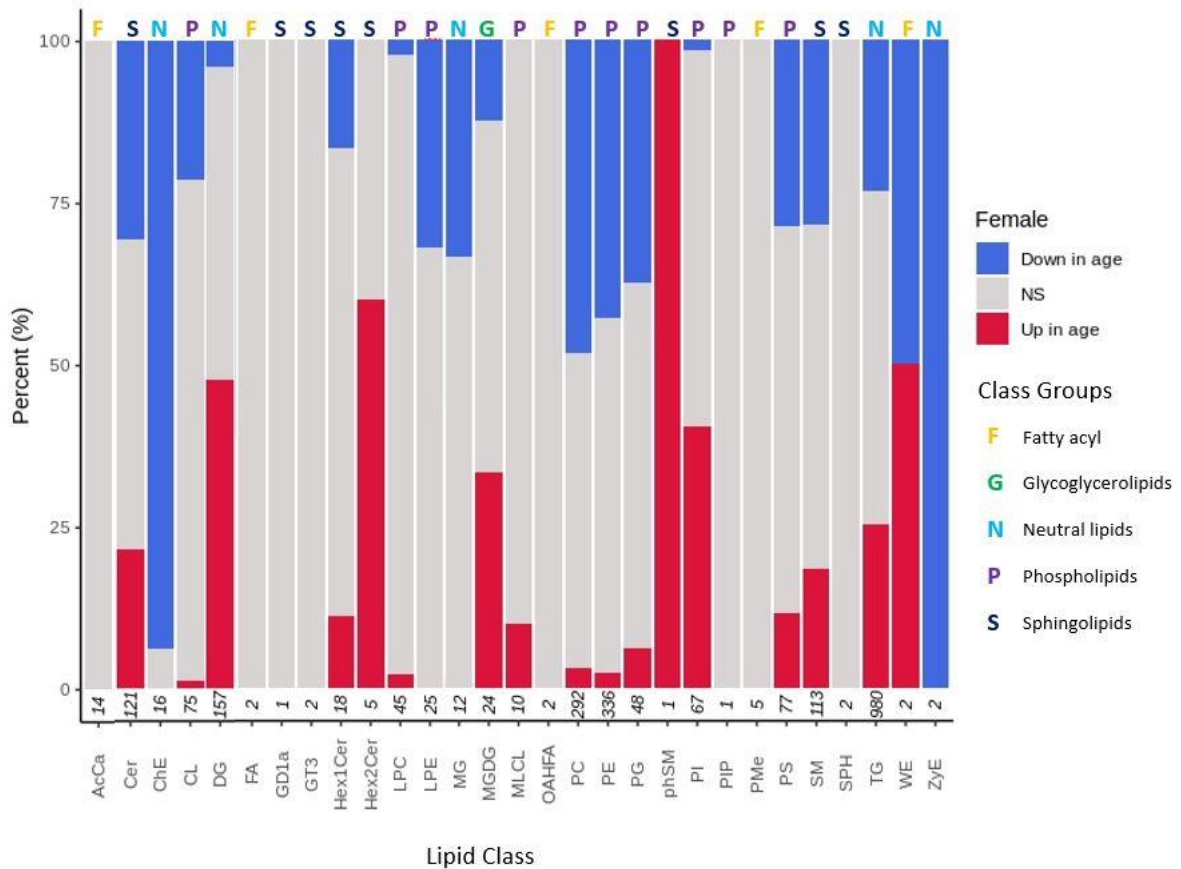
Figure 4.6: Directional change of lipid levels significantly changing in A) female and B) male D. magna. Stacked normalised bar chart shows percentage of lipid classes that are changing with age in *D. magna*. Lipids showing overall decline with age are shown in blue whilst lipids showing overall increase with age are shown in red. Grey represents no significant change with age (adjusted *p*-value <0.001). Numbers on the x-axis represent the total number of lipids identified in each class, for lipid class abbreviation descriptions and classification see 2B.T1 (Appendix 2B). For female age groups 20, 40 and 80 days eight technical replicates were used and for intermediate age groups two technical replicates were used. For detailed information regarding biological replicate numbers see Table 2.7. For male age groups 10, 20 and 40 days eight technical replicates were used and for intermediate age groups two technical replicates were used. For detailed information regarding biological replicate numbers see Table 2.8.

FEMALE					
Aged 10 days as reference					
	10:20	10:40	10:80	Significant across all group comparisons	292
10:20	87	49	63	Non-significant	1264
10:40	49	89	372	Total significant lipids shown in table	1000
10:80	63	372	340	Total lipids	2556
Aged 20 days as reference					
	20:10	20:40	20:80	Significant across all group comparisons	161
20:10	174	44	112	Non-significant	1000
20:40	44	67	532	Total significant lipids shown in table	1395
20:80	112	532	466	Total lipids	2556
Aged 40 days as reference					
	40:10	40:20	40:80	Significant across all group comparisons	235
40:10	223	226	118	Non-significant	1169
40:20	226	213	130	Total significant lipids shown in table	1152
40:80	118	130	242	Total lipids	2556
Aged 80 days as reference					
	80:10	80:20	80:40	Significant across all group comparisons	463
80:10	206	350	48	Non-significant	964
80:20	350	311	147	Total significant lipids shown in table	1129
80:40	48	147	67	Total lipids	2556

Table 4.3: Comparison of lipids showing significant change in levels between female D. magna age groups. Significance determined by adjusted *p*-value <0.001. Reference age group set at 10 20, 40 and 80 days respectively. Lipids highlighted within the table represent those present in the reference group but not in the comparison group (e.g. 10:20 shows 87 significantly changing lipids present in aged 10 days but not aged 20 days, 10:20 verses 10:40 shows 49 lipids unique to aged 10 days not shared with aged 20 or 40 days). 'Significant across all group comparisons' represents lipids significantly changing levels in the reference group only, not shared with any other age. 'Non-significant' represent lipids identified in lipidomics analysis not shown to change in level >0.001 adjusted *p*-value. 'Total significant lipids' shown in table represent the total number of lipids significantly changing level highlighted in the cross comparison table. 'Total lipids' represent the total number of lipids identified during analysis and is always equal to 2556.

MALE					
Aged 8 days as reference					
	8:10	8:20	8:40	Significant across all group comparisons	234
8:10	34	24	10	Non-significant	1155
8:20	24	63	488	Total significant lipids shown in table	1167
8:40	10	488	548	Total lipids	2556
Aged 10 days as reference					
	10:8	10:20	10:40	Significant across all group comparisons	187
10:8	47	23	45	Non-significant	865
10:20	23	119	631	Total significant lipids shown in table	1504
10:40	45	631	639	Total lipids	2556
Aged 20 days as reference					
	20:8	20:10	20:40	Significant across all group comparisons	201
20:8	113	406	89	Non-significant	966
20:10	406	219	134	Total significant lipids shown in table	1389
20:40	89	134	428	Total lipids	2556
Aged 40 days as reference					
	40:8	40:10	40:20	Significant across all group comparisons	579
40:8	119	553	29	Non-significant	809
40:10	553	223	147	Total significant lipids shown in table	1168
40:20	29	147	97	Total lipids	2556

Table 4.4: Comparison of lipids showing significant change in levels between male D. magna age groups. A Significance determined by adjusted *p*-value <0.001. Reference age group set at 8, 10 20 and 40 days respectively. Lipids highlighted within the table represent those present in the reference group but not in the comparison group (e.g. 8:10 shows 34 significantly changing lipids present in aged 8 days but not aged 10 days, 8:10 verses 8:20 shows 24 lipids unique to aged 8 days not shared with aged 10 or 20 days). 'Significant across all group comparisons' represents lipids significantly changing levels in the reference group only, not shared with any other age. 'Non-significant' represent lipids identified in lipidomics analysis not shown to change in level >0.001 adjusted *p*-value. 'Total significant lipids shown in table' represent the total number of lipids significantly changing level highlighted in the cross comparison table. 'Total lipids' represent the total number of lipids identified during analysis and is always equal to 2556.

4.4.5 Sex:age interaction

Sex:age interaction group represents differential rate of change during ageing in the

two sexes in the relative intensity of the lipids. The concentrations of different lipids in

different sub-classes alter at different rates as a function of age between females and males (Figure 4.7). For example, the concentrations of 26.94% and 61.15% of the lipids in the sub-classes of TG and DG, respectively, alter at a higher rate in males compared to females. On the other hand, the concentration of 30.58% and 21.14% of lipids in the ceramides and sphingomyelin sub-classes, respectively, alter at a much slower rate in males compared to females with age.

The differential rate of change of some lipid intensities with age appear to show significance in one sex, for example either reportedly changing at a faster rate in males or no significant change (no lipid sub-species are seemingly changing at a faster rate in females). Of the 34 lipids that change in a single direction only, 29.41% express a faster rate of change in males. Contrastingly, only 5.88% are changing at a slower rate in males (faster rate in females) and 14.70% have no significant change in either direction.
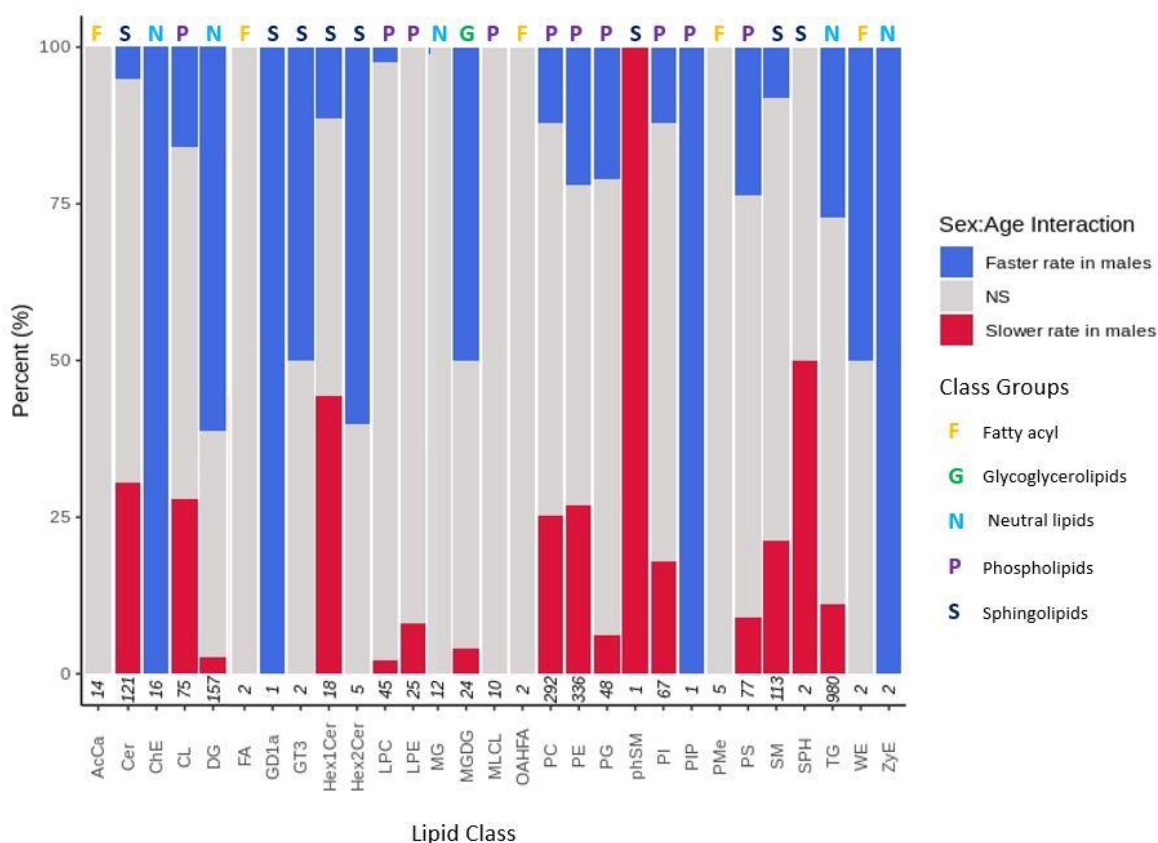
Figure 4.7: Lipid class changes in sex:age interaction in male and female D. magna. Stacked normalised bar chart shows percentage of lipid classes that are changing with sex:age interaction. A faster rate of change in males with age is shown in blue whilst slower rate in males with age (faster rate in females) is shown in red. Grey represents no significant change with interaction between sex and age (adjusted *p*-value <0.001)). For female age groups 20, 40 and 80 days eight technical replicates were used and for intermediate age groups two technical replicates were. For male *D. magna* age groups 10, 20 and 40 days eight technical replicates were used and for intermediate age groups two technical replicates were used. For detailed information regarding biological replicate numbers see Table 2.7 and 2.8 (section 2.11). Numbers on the x-axis represent the total number of lipids identified in each class. Numbers on the x-axis represent the total number of lipids identified in each class, for lipid class abbreviation descriptions and classification see 2B.T1 (Appendix 2B).

Figure 4.8 is the heatmap representation of the intensity levels of the top 50 lipids, in both negative and positive ion modes, with the most significant adjusted *p*-value in their intensity as a function of interaction between age and sex. As shown in this figure, the intensity of the lipids (i.e. lipid profile) changes as a function of both sex (red =

female, blue = male) and age (young = yellow, old = blue). Furthermore, within each class of lipids, subcategories of lipids are identified that demonstrate increased intensity and decreased intensity as function of age in both sexes. For example, in each row a change of colour from blue in females to red in males along the age axis indicates a faster rate of change with age in males. Similar trends are observed in sex only and age only analysis of the lipids data, see Figures 4.9 and 4.10.
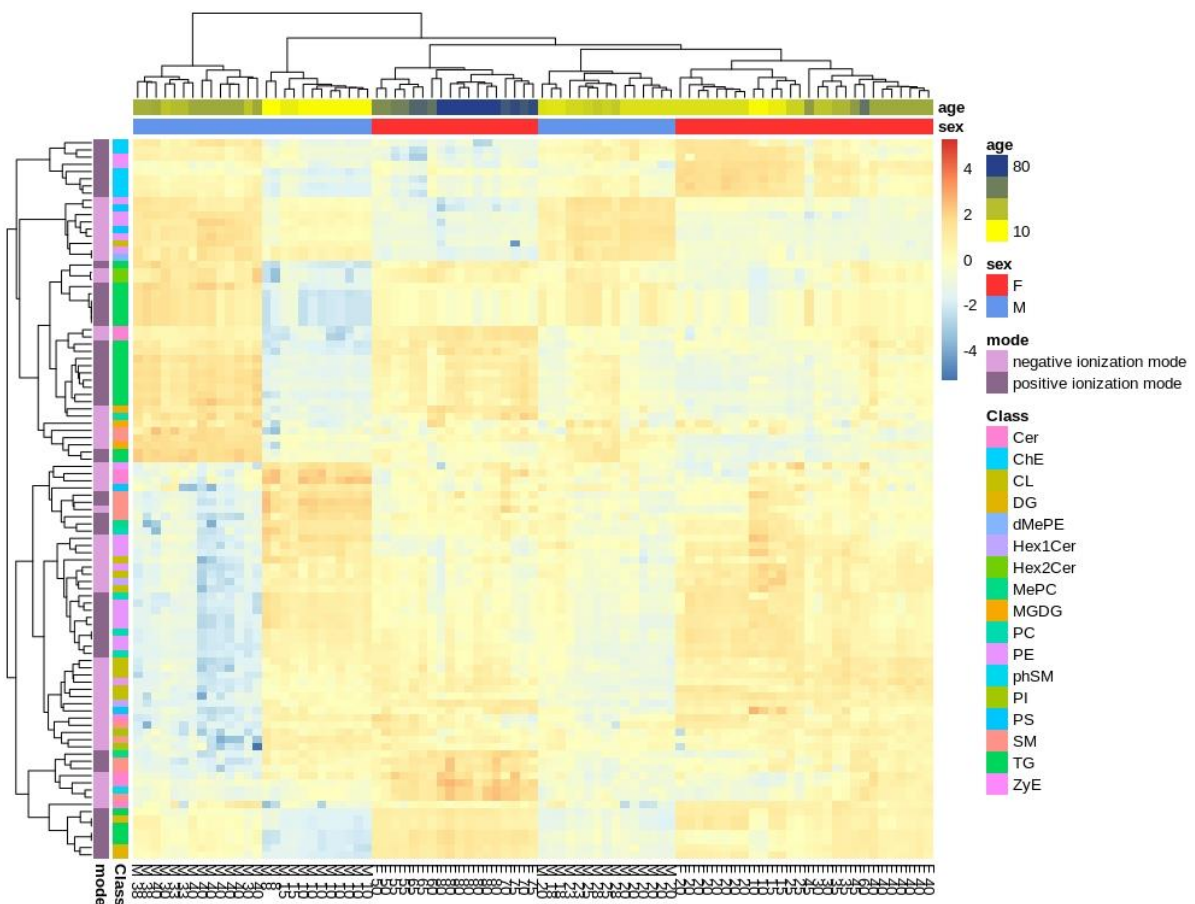
Figure 4.8: Heatmap of lipid changes with sex:age interaction. Heatmap of lipidomics analysis for top 50 lipids significantly-changing concentrations in positive ion mode (dark purple) and top 50 lipids significantly changing levels in negative ion mode (light purple, adjusted *p*-value <0.001) in *D. magna*. The heat map shows 100 selected lipids indicated by class colours (rows) and 29 samples (columns). Colours correspond to per-lipid z-score that is computed from area under the curve. Lipids and samples were hierarchically clustered based on Euclidean cluster extraction and average linkage. Numbers on the x-axis represent the total number of lipids identified in each

class, for lipid class abbreviation descriptions and classification see 2B.T1 (Appendix 2B).
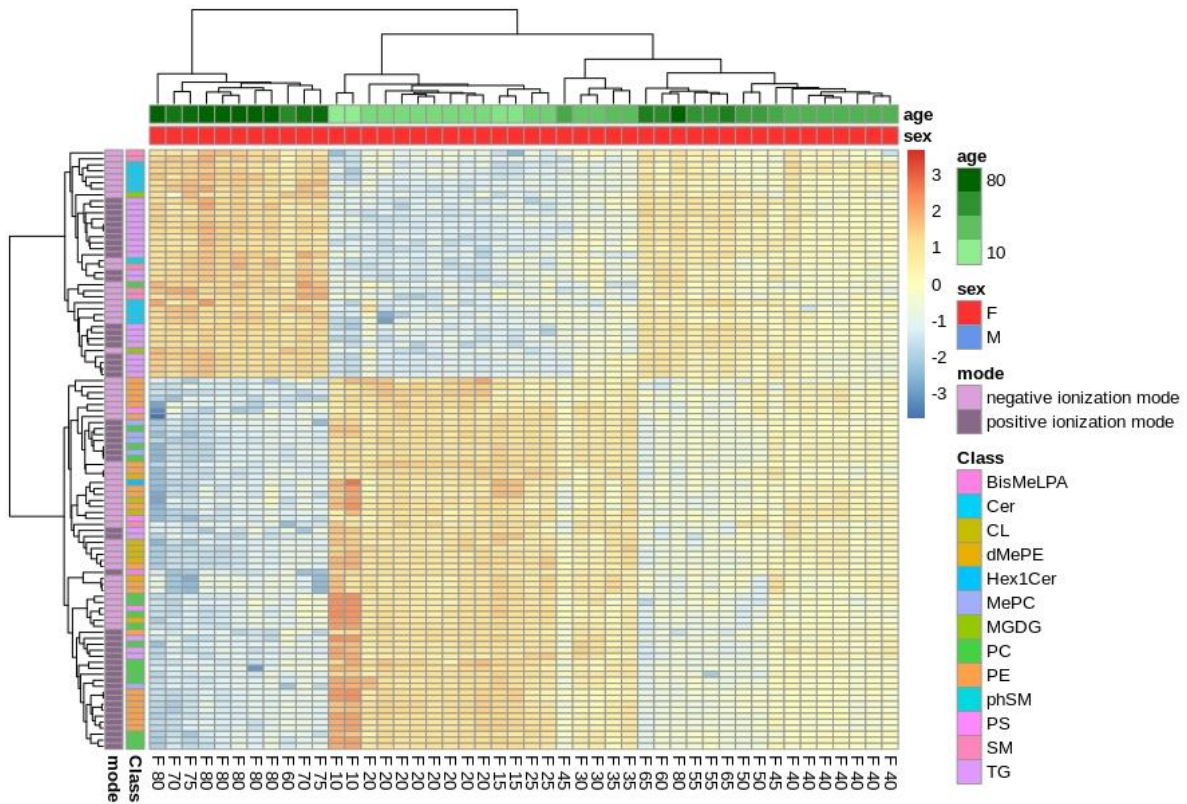
Figure 4.9: Heatmap of lipid changes with age in female D. magna only. Heatmap of lipidomics analysis for top 50 lipids significantly-changing lipid intensities in positive ion mode (dark purple) and top 50 lipids significantly changing levels in negative ion mode (light purple, adjusted *p*-value <0.001) in female *D. magna* with age. The heat map shows 100 selected lipids indicated by class colours (rows) and 29 samples (columns). Colours correspond to per-lipid z-score that is computed from area under the curve. Lipids and samples were hierarchically clustered based on Euclidean cluster extraction and average linkage.
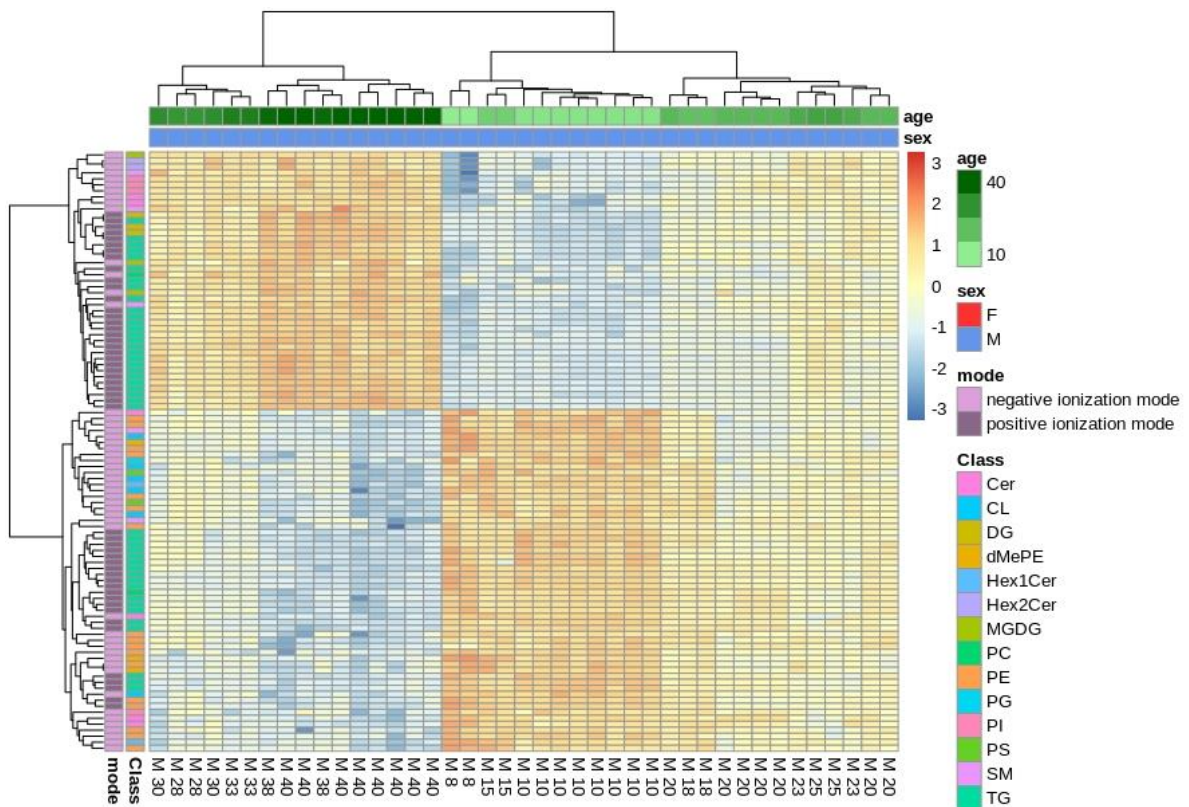
Figure 4.10: Heatmap of lipid changes with age in male D. magna only. Heatmap of lipidomics analysis for top 50 lipids significantly-changing lipid intensities in positive ion mode (dark purple) and top 50 lipids significantly changing levels in negative ion mode (light purple, adjusted *p*-value <0.001) in male *D. magna* with age. The heat map shows 100 selected lipids indicated by class colours (rows) and 29 samples (columns). Colours correspond to per-lipid z-score that is computed from area under the curve. Lipids and samples were hierarchically clustered based on Euclidean cluster extraction and average linkage.

4.5 Discussion

Female and male *Daphnia magna* are genetically identical and yet show considerable differences in ageing rate and their overall lifespans (Constantinou et al., 2019). Earlier studies using a variety of model organisms have revealed lipids as important contributors to both ageing and lifespan. In this study, we provide the first evidence of the contribution of lipids to ageing in both male and female *Daphnia magna*, finding

that more than half of all lipids measured are statistically different between female and male *D. magna* with age.

4.5.1 Genetically identical female and male D. magna show distinct lipid profiles based on sex.

The present study clearly demonstrates that sex is the main factor that influences lipid composition in *D. magna* (Figure 4.2). Previous studies across a wide range of species have identified similar trends whereby the composition and level of lipids differ between sexes (Parisi et al., 2011, Baars et al., 2018, Palmisano et al., 2018, Zore et al., 2018), with the primary cause linked to differences in reproductive needs and hormone levels between the sexes (Palmisano et al., 2018). Currently, our knowledge regarding molecular mechanisms of hormone regulation in *Daphnia* is limited. However, it has been shown that male *Daphnia* are induced by the juvenile hormone (JH) or a JH pathway-related molecules emitted by the mother in response to environmental conditions, known as environmental sex determination (Kashian and Dodson, 2004, Oda et al., 2005, Toyota et al., 2014, Toyota et al., 2015, Miyakawa et al., 2018). Therefore, the reproductive demands placed on female and male daphnids are extremely different. *Daphnia* reproduce by cyclical parthenogenesis. Under normal conditions with low levels of stress factors, *Daphnia* reproduces asexually and the mother clonally produces daughters. Under stressed conditions, male *Daphnia* are produced for sexual reproduction, leading to production of diapause eggs that remain in arrested development until more favourable reproductive conditions return (Ebert, 2005). As the purpose of male production is for sexual reproduction and sexual reproduction in *Daphnia* is limited to a narrow window of time, males characteristically have much shorter lifespans and smaller body size than females. Therefore, males

usually invest less energy into growth and instead the majority of their energy is directed towards maximising egg fertilisation (Constantinou et al., 2019). Therefore, it is possible that the lipidome of *D. magna* separate strongly by sex due in part to the energy demands related to the different reproductive roles.

It is important to highlight that lipids are diverse and play a multitude of roles within biological systems. Therefore, by investigating changes in different classes of lipids between sexes it may provide clues with regards to differences in regulation of biological pathways and needs of both sexes. For example, triglycerides (TG) and diglycerides (DG) are more frequently, but not exclusively, lower in male compared to female *D. magna* (Figure 4.4). TGs are the main form of fat recorded in humans and are present across many species. They are found in the blood and act as an energy supply for the body in addition to being stored as body fat when excess is present. The role of TG as the most abundant and accessible energy supply supports the idea that female *D. magna* would require higher concentrations due to the energy demand placed on cyclical parthenogenetic reproduction, growth rate, body size and swimming speed.

Glycerophospholipids appear to show the opposite trend to neutral lipids with phosphatidylethanolamine (PE) and phosphatidylcholine (PC) both observed to be predominantly, but not exclusively, higher in male compared to female *D. magna* (Figure 4.4); however overall across both sexes PE and PC largely decline with age (Figure 4.6A and 4.6B). PEs are an essential component of biological membranes and play a key role in cell and organelle membrane fusion, trafficking and curvature, oxidative phosphorylation, mitochondrial biogenesis and autophagy (Calzada et al., 2016). In total, PEs account for approximately 25% of all mammalian

glycerophospholipids and are particularly enriched in the brain where they account for 45% of total glycerophospholipids and reportedly act as a precursor to the ligand for cannabinoid receptors (Vance and Tasseva, 2013). In recent years the role of PE in mammalian health has begun to be established, following the discovery of a relationship with Alzheimer's disease, Parkinson's disease, non-alcoholic liver disease and virulence of some pathogenic organisms (Calzada et al., 2016). PE and PC are directly linked as in mammalian liver the enzyme phosphatidylethanolamine *N*-methyltransferase (PEMT) catalyses the conversion of PE to PC by the transfer of three methyl groups from *S*-adenosylmethionine to PE. PC is also a major component of biological membranes and is a pulmonary surfactant whilst also acting as an important membrane cell-signalling molecule (Vance, 2013). Previous research has reported the decline of PE and PC with age in mouse liver and brain. The impact of this is altered membrane fluidity as membranes become more fluid when containing a low PC: PE ratio, or low cholesterol content. Membrane fluidity has shown the decline with age in rat brain, liver and heart, whilst in the long-lived naked mole rat maintains membrane fluidity through a specific glycerophospholipid/fatty acid saturation profile (Papsdorf and Brunet, 2019). The loss of membrane fluidity with age may be in-part due to dyslipidemia observed with age. Investigation in a Japanese population highlighted a link between increased total ester-linked PE and PC species with age, but a decline in specific ether-linked PE and PC species with age (Kawanishi et al., 2018). The different behaviour of specific lipid species with age may be linked to the role of each lipid species. In hEP-2 cells, ether-linked PE has an alkenyl group and represents 70-80% of the inner leaflet of the plasma membrane, where-as ether-linked PC species tend to have an alkyl group and represent 70-80% of the outer leaflet of

the plasma membrane (Bergan et al., 2013). The abundance of ether-linked glycerophospholipids indicates their biological importance; however the specific role remains unclear. Possible suggestions include that alkenyl-PE species are the main source of polyunsaturated fatty acids for prostanoid production and cell signalling. Alkenyl-linked glycerophospholipids (plasmalogens) are reportedly active in protection from oxidative damage and alkenyl-PE is essential for cholesterol transport from the cell surface and endocytic compartments to the endoplasmic reticulum (Bergan et al., 2013). The overall higher relative lipid intensity of PE and PC in males to females (Figure 4.6) could possibly be linked to the anti-oxidant role as male *D. magna* show a faster accumulation of DNA damage in real-time (Constantinou et al., 2019) and thus when not considering age may show a higher demand for oxidative protection measures.

In *D. magna*, we observed that sphingomyelin (SM) levels are higher in males. The same trend has been observed with humans whereby females have lower recorded SM (Rauschert et al., 2017). This has been linked to the different distribution of each lipid species and the metabolic consequences associated with that (Rauschert et al., 2017). SM is a major component of the lipid bilayer of cell membranes and so mirrors the observations seen for PE and PC which are also both major lipids present in the membrane lipid bilayer. Interestingly, the more predominant sphingolipid, ceramide (Cer), is largely lower in male *D. magna*. Cer is considered a centre for sphingolipid metabolism which has been linked to regulation of antiproliferative responses such as growth inhibition, apoptosis, differentiation and senescence (Hannun and Obeid, 2008, Trayssac et al., 2018). Often changes with Cer and SM are linked with ageing, discussed later in this article. Thus it is possible that when investigating sex differences

without considering the age of the females and males, we are measuring the overall difference in the level of Cer and SM with age encapsulated by each sex (Trayssac et al., 2018).

4.5.2 Genetically identical female and male D. magna show divergence of lipidome as a function of age.

To elucidate age related changes within each sex, changes in the lipid composition of male and female *Daphnia* as a function of age was investigated (Table 4.3, Table 4.4, Figure 4.6A and Figure 4.6B). Although female *Daphnia magna* reproduce via cyclical parthenogenesis throughout the duration of their lifespan, their reproductive capacity and clutch size declines as they age when they reach 20% of their lifespan (Constantinou et al., 2019). Furthermore, the swimming speed also declines continuously with age in female *Daphnia* (Constantinou et al., 2019). The reduced energy demand for reproduction and movement is reflected in the changes observed in the lipid composition of females as a function of age (Table 4.3). A similar trend was also observed among male *D. magna,* whereby the lipid composition and concentrations changed linearly with age (Table 4.3). This could also be linked to decline in swimming speed as a function of age in males. Furthermore, fertilisation success is reduced in both females and males as they age and thus males may demand less energy for reproduction (Constantinou et al., 2019).

As demonstrated in Table 4.3, the lipid composition of 40 days old females (40% of their lifespan) is equally as diverged and distinct from a young sexually mature *Daphnia* (10% of lifespan) as it is from an old *Daphnia* (80% of lifespan). This indicates that lipid composition is continuously altering and evolving with age, reflective of the different needs of an individual as they age. Figure 4.6B and Table 4.4 demonstrates that males

follow the same trend; however, the changes in lipid composition are much more pronounced in the second half of their life. The more pronounced changes in the lipidome of male *Daphnia* at later stages of their life compared to their midlife point could be partly due to the time points that were used for the male samples. In this analysis, we used samples that represent 16%, 20%, 40% and 80% of the lifespan of the male *Daphnia*. Males are not sexually mature until 8 days therefore it was not possible to use a representative sample of 10% of lifespan (5 days) to match the youngest age group for females where aged 10 days is representative of 10% of lifespan.

When considering age for both sexes separately in the analysis (Figure 4.6A and 4.6B), we identified a higher proportion of TG and DG lipid classes changing with age of which the majority are increasing. Notably, DG shows the bigger gap between those decreasing and increasing in relative intensity in addition to male DG relative intensity increasing with age 1.59-fold more than those seen increasing in females. DG can be metabolised by bacteria, yeast, plants and animals. It is crucial for cell growth and development as it acts as a basis to which components can be added to synthesise complex lipids whilst also acting as a source of free fatty acids (Carrasco and Mérida, 2007). DG acts as a direct precursor for PC, PE, phosphatidic acid (PA) and TG and in doing so has a downstream effect on the production of phosphatidylinositol (PI) and cardiolipins (Carrasco and Mérida, 2007). Given the crucial role of DG, regulation is essential to maintain a permanent reservoir. During the ageing process, lipid dysregulation can occur, often exemplified by humans with the age-associated link to type 2 diabetes, dyslipidemia and altered lipid profiles seen in many cancers. It is possible that age-related dysregulation is occurring in *D. magna* resulting in the

reservoir of DG not being utilised efficiently. If true, this may contribute to the majority of PE and PC lipids showing a decline in relative intensity with age across both sexes separately (Figure 4.6A and 4.6B).

Cholestrol ester (ChE) is a neutral lipid that appears to decline in relative intensity with age in females yet increases in intensity with age in males. ChE is the inactive form of cholesterol and it is primarily used for transport of cholesterol to organs or to act as a biologically inert storage of excess cholesterol by the addition of fatty acids to the hydroxyl group results in less polarity making the lipid 'inert' (Christie, 2019). In humans, free cholesterol is esterified by lecithin:cholesterol acyltransferase (LCAT) to form high-density lipoprotein (HDL) particles. In turn, HDL particles can bind to hepatocytes to uptake ChE from HDL in to the liver where it can be hydrolysed by cholesterol ester hydrolase to either be converted back to free cholesterol or turned into bile acids. Alternatively, ChE can be exchanged from HDL for TG which can influence composition, size and ultimately function of lipoproteins (Talbot et al., 2018). Currently there is limited information available about how cholesterol esters levels change during ageing or between sexes. However, the altered activity of LCAT and HDL levels have been widely investigated in association with age-related diseases (Talbot et al., 2018, Tanaka et al., 2018, Gerl et al., 2018, Button et al., 2019). Furthermore, it has been demonstrated that high levels of SM inhibit the activity of LCAT. In humans, SM level is reportedly lower in males compared to females, exposing females to greater risk of LCAT suppression which could explain differences in the rate of age-associated diseases between sexes (Rauschert et al., 2017). HDL particles have many positive effects such as anti-inflammatory, anti-oxidant, anti-apoptotic, anti-thrombotic and vasodilation (Talbot et al., 2018). If conversion of

cholesterol to ChE is limited with ageing in female *D. magna* by altered HDL efficacy, it is possible that reduced HDL efficacy contributes to the observed increase in oxidative damage observed in female *D. magna* with age (Constantinou et al., 2019). Given that some lipids are more prone to oxidative damage it is likely that the difference in lipid composition between male and female *D. magna* contributes to observed differences in age-related DNA damage. Lower HDL-Cholesterol in males has been reported to associate with lower SM concentrations compared to females, resulting in males having an increased cardiovascular risk (Rauschert et al., 2017).

4.5.3 Genetically identical female and male D. magna show different rates of change in relative lipid intensities with age between sexes

Changes in lipid composition as a function of sex and age interaction was also investigated (Figure 4.7). The neutral lipids TG and DG both show a stronger relationship with age in males compared to females. Given that the lifespan of a male *Daphnia* is half the lifespan of a female *Daphnia* (Constantinou et al., 2019), it is plausible that the faster rate of change in certain lipids is to account for/contributes to the observed shorter lifespan in males. However, this idea does not hold true for glycerophospholipids PE and PC as they demonstrate a more balanced relationship between faster and slower rates of change in males compared to females, moderately biased towards slower rate. A slower rate of change in males based on age in days indicates a dramatically slower rate as a factor of proportional longevity. As previously discussed, the relative intensity of PE and PC largely decline with age. A slower rate of change in males indicates that this loss is occurring at a slower pace compared to females. Given that DG, a precursor to PE and PC, shows a much higher increase in relative intensity with age in males (1.59-fold more than females), it bodes well for the

continued production of PE and PC from the DG reserve through-out the lifespan of a male *Daphnia*.

Sphingolipids SM and Cer show the opposite trend to neutral lipids, displaying a greater bias towards changing lipid intensity at a much slower rate in males compared to females. Sphingolipids have been linked to many functions and diseases influenced by the ageing process, including immune response, inflammation, cancer, metabolic and cardiovascular diseases and neurodegeneration. Ceramide induces cellular senescence, a mode of suspended cell division which has positive tumour suppressor effects as well as negative impacts on cardiovascular system, metabolic and immune systems (Trayssac et al., 2018). Senescence has been shown to contribute to ageing and may partially explain the association of sphingolipids with age-associated conditions. In humans, SM can be degraded to produce Cer and PC and reversely, PC and Cer can be utilised to produce SM and DG (Trayssac et al., 2018). These interactions between various lipid groups create a complex and sensitive feedback loop constantly shifting and moderating in response to lipid alterations. The interaction effect in male *D. magna* of SM and Cer is likely linked to alterations observed in DG and PC.

Finally, Figure 4.8 highlights clustering of lipids altered in sex:age interaction is based largely on sex followed closely by age. The interaction of sex and age encapsulates approximately half of changes to lipid intensity observed in sex and age (Figure 4.3A). To conclude, in this study we have demonstrated, for the first time, profound differences in the lipid composition of male and female *Daphnia magna*. We have also demonstrated marked shifts in lipid composition with age, indicating a possible relationship between *Daphnia* lipid composition and age-related processes.

CHAPTER 5

Gene expression changes with sex, age and sex:age interaction

5.1 Introduction

Early studies have reported that females and males show differentially expressed genes across a number of taxa. For example, studies of *D. melanogaster* and *D. simulans* gene expression profiles found that ~50% of the genes were differentially expressed and that sex-dependent selection may promote differential expression of many of the most rapidly evolving genes in the *Drosophila* transcriptome (Ranz et al., 2003) whilst studies in mouse brain found sex differences in X-Y gene expression suggesting that many mechanisms influenced sex differences in brain development and function (Xu et al., 2002). Interestingly in humans, obvious phenotypic differences such as muscle mass have been linked to higher expression of mitochondrial and ribosomal proteins in male skeletal muscle compared to higher expression of muscle regulators such as growth factor receptor-bound 10 (GRB10) and activin A receptor IIB in female skeletal muscle (Welle et al., 2008). Notably, GRB10 encodes a protein that inhibits IGF-1 (Welle et al., 2008). As previously discussed is section 1.4, it is now known that IGF-1 plays a key role in regulation of lifespan and if more highly inhibited in females compared to males, it may go some way to explaining the sex difference in lifespan observed in humans.

Largely, sex differences in gene expression have been investigated in a disease setting. Some age-related diseases appear to be influenced by sex, for example, females have a longer average lifespan compared to males but higher incidence of Alzheimer's disease and osteoporosis whilst males have higher incidence of cancer and Parkinson's disease (Tower, 2017). Although a hugely complex question, understanding sex difference in disease susceptibility and progression is an important task. Sex differences in gene expression may go some way to elucidating these

differences. For example, expression of three genes important in the circadian rhythm of human cerebral cortex, *PER2, PER3* and *ARNTL1*, show timing differences where all three are expressed earlier in women compared to men. This is of significance as neurological processes such as cognition, epilepsy, and in the interest of Alzheimer's disease, soluble amyloid beta levels, show time of day variation (Lim et al., 2013). Such research highlights the importance of investigating sex difference in ageing.

Little has been investigated in the role of gene expression changes with age and between sexes to elucidate this relationship. Difficulties in investigating gene expression changes with age and between sexes arise in many forms such as the uncontrolled environment and long lifespan of humans, long lifespan of mammalian model organisms and the absence of male and female counterparts such as in model species *C. elegans*. As discussed in previous chapters, unique characteristics such as the short lifespan of *D. magna*, easy generation of large clonal populations and production of female and male individuals lend themselves to the use of *Daphnia* as a high throughput model organism for early stage investigation of sex differences in ageing.

5.2 Experimental Design

Detailed description for RNA sequencing methodology is included in section 2.12. Samples were collected as described in section 2.12.1. RNA extraction and quantification are detailed in sections 2.12.2 and 2.12.3. RNA library preparation and sequencing methodology is described in section 2.12.5. Data analysis was performed as described below. See Figure 5.1 for an overview of the experimental design.
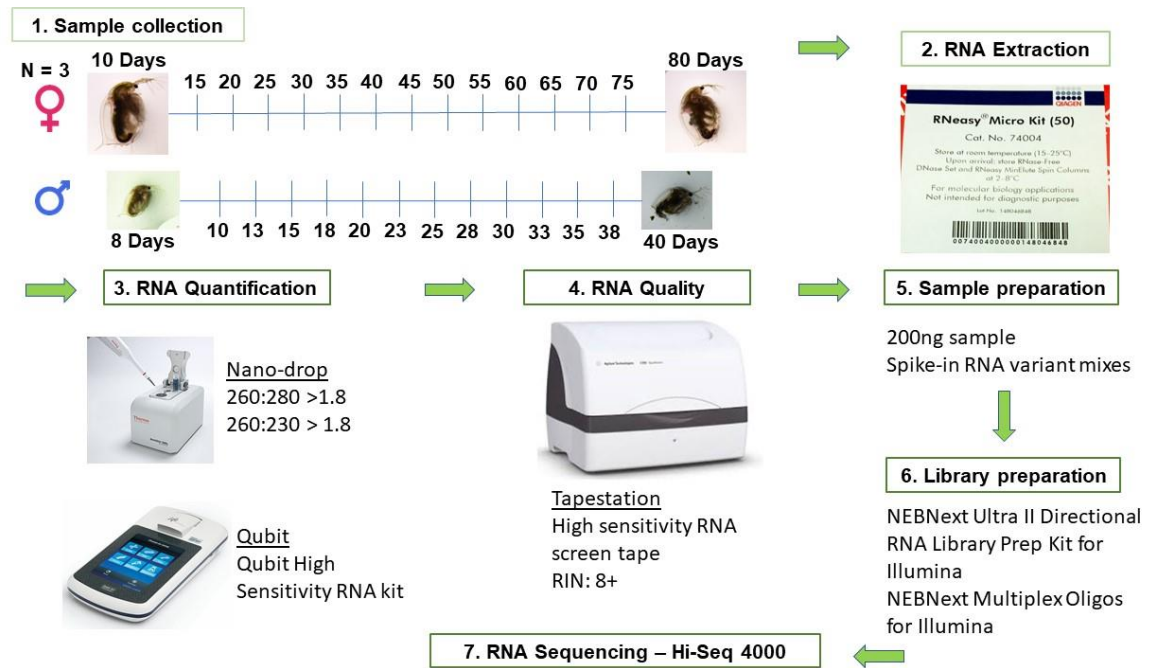
Figure 5.1: RNA sequencing experimental design. Samples were collected at regular intervals for both female and male *Daphnia*. Once all samples were collected, samples were allocated into batches and underwent RNA extraction and quantification. Good quality RNA was taken forward for sequencing. More details can be found in section 2.12.

Briefly, four cultures containing 100 female Daphnia and 12 cultures containing 100 male Daphnia were maintained under normal conditions as described in section 2.3. The number of individuals per replicate was determined and collected as described in section 2.12.1. The aim of manipulating the number of individuals per sample to dry mass of the largest sample group was to normalise to body mass, thus accounting for differences in body size seen across difference age groups and between sexes.

5.3 Data Analysis

5.3.1 RNA-sequencing data analysis

FastQC was used to check the quality of the raw sequencing data before use. Then, Tophat v2.1.1 was used for sequence alignment using the short-read aligner Bowtie v2.2.3, to map the RNA-sequencing reads to *Daphnia* genome

GCA_001632505.1_daphmag2.4 (wfleabase.com). Once mapped, further bioinformatic investigation was performed using R (R Project for Statistical Computing, http://www.r-project.org/, Version 3.5.2). Using the 'featureCounts' library in the 'RSubreads' package, paired-end data was mapped to genomic features such as genes, exons and promoters. Once the count data matrix had been prepared, DESeq analysis was performed using R package 'DESeq2' (Love et al., 2014).

DESeq2 estimates variance-mean distribution in count data from high-throughput sequencing assays and tests for differential expression based on a model using the negative binomial distribution (Love et al., 2014). The analysis pipeline begins by generating a DESeqDataSet (dds) which contains the count details and associated genomic ranges details and a design formula to include conditions of 'sex' and 'age'. This design formula is used to estimate dispersions and log2 fold changes of the model. DESeq2 allows the standard differential expression analysis to be collapsed into a single function, for which a detailed description can be found in Love et al. (2014). Using the 'results' function, results tables containing log2 fold change, p-values and adjusted p-values were generated for the conditions of sex, age and sex:age interaction.

The results files were taken forward for further visualisation and interrogation. For the condition of sex only, a total of 11,391 genes have an adjusted p-value < 0.01. Of these, 103 (0.90%) were outliers and 4,746 (41.66%) had low counts. Similarly, with age only, a total of 10,767 genes reported an adjusted p-value <0.01. Of these, 103 (0.95%) were outliers and 4,277 (37.72%) had low counts. In the condition of sex:age interaction only 8,329 genes in total were below the significance cut-off (adjusted p-value <0.01). Of these, 103 (1.24%) are recognised as outliers and the majority, 6,651

(79.85%), were considered low count. All outliers and low count data was removed. PCA analysis, venn diagrams and volcano plots were applied and visualised using package ggplot2 (Wickham, 2016). Enrichment analysis was performed using both Reactome and KEGG. Reactome uses a single column of identifiers, in this instance the equivalent human Gene ID, to map to pathways and run over-representation and pathway topology analysis. Over-representation analysis is a statistical analysis based on hypergeometric distribution to determine if pathways are enriched in the dataset which produces a probability score, corrected for false discovery rate using Benjamini-Hochberg method. Pathway topology analysis considers the connectivity between reactions in the pathway and looks for the proportion of the pathway that is matched. This has no probability score. Expression data overlay is also performed where the count data is used to generate scaled coloured overlays to visualise relative expression levels (Reactome, 2020). Both dotplots for Reactome and KEGG analysis show GeneRatio. GeneRatio is defined as k/n where k is the size of the overlap of 'a vector of gene ID' that is input with a specific gene set and refers to only unique genes within that set that are annotated to the node. 'n' refers to the size of the overlap of 'a vector of gene ID' that is input with all the members of the collection of gene sets (e.g. Reactome). Count refer to the number of genes in the test data (differentially regulated genes) belonging to the category of interest (for example TCA).

D. magna results for each condition were compared against findings for comparative conditions in flies, worms and mice. For the condition of sex, age and sex:age interaction in *Caenorhaditis elegans*, the NCBI GEO dataset GSE124994 was used in addition to genome annotation GCF_000002985.6_WBcel235_genomic.gff.gz. For the condition of age in *Drosophila melanogaster*, the NCBI GEO dataset GES24324 was

used in addition to genome annotation GCF_000001215.4_Release_6_plus_ISO1_MT_genomic.gff.gz. For the condition of sex across multiple *Drosophila* genotypes (*D. ananassae, D. mojavensis, D. persimilis, D. pseudoobscura, D. virilise, D. willistoni, D. yakuba* and a synthetic construct orgR), NCBI GEO dataset GSE99574 was used. Finally, for conditions of sex, age and sex:age interaction in *Mus musculus*, the NCBI GEO dataset GSE58733 and genome annotation GCF_000001635.26_GRCm38.p6_genomic.gff.gz were used.

5.4 Results

5.4.1 Gene expression profile in *D. magna* is influenced by age and sex

The effect of sex and age on gene expression variation was analysed with PCA. The sexes separated by the first component (PC1, which accounted for 68% of variation) and age by the second component (PC2 9%), as demonstrated in Figure 5.2.
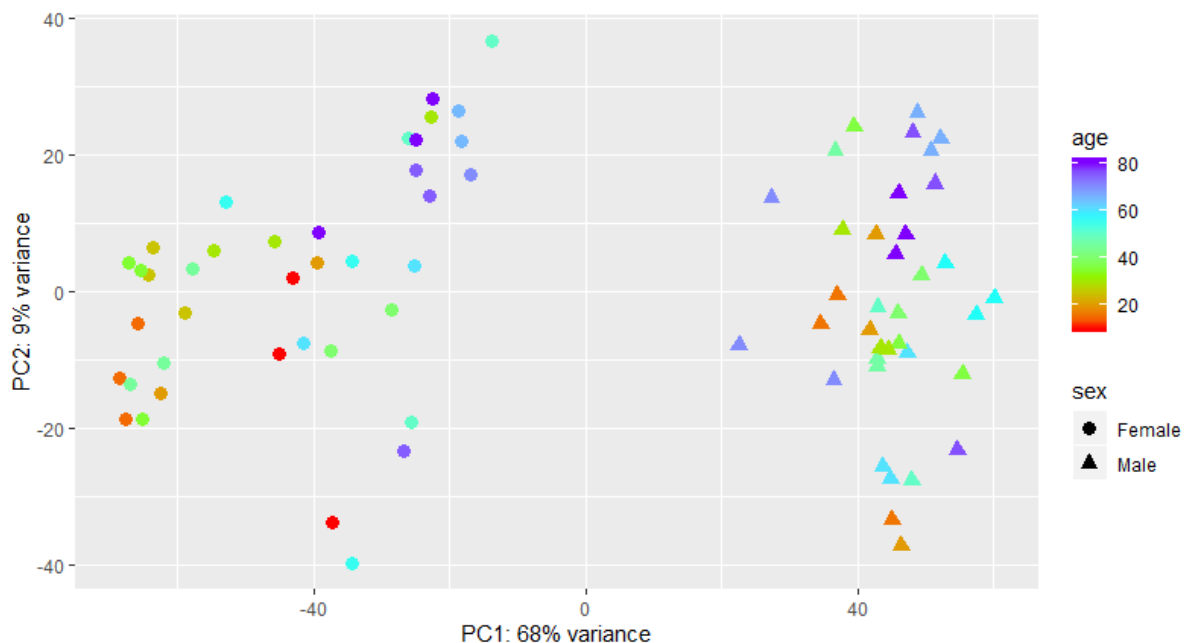
Figure 5.2: Principal component analysis of RNA-sequencing count matrix data for male and female *Daphnia magna* demonstrated as percentage of lifespan. Principal component 1 shows clear separation based on sex (● = female, ▲ = male) with females grouped to the left and males to the right. Combination of principal

components 1 and 2 show separation by age depicted by colour ranging from red (young) to blue (old). Female *D. magna* age range is 10 days to 80 days (maximum sampled age and average life expectancy = 80 days). For all female age groups, three technical replicates were used. Male *D. magna* age groups ranging from 8 days to 40 days were used (maximum sampled age and average life expectancy = 40 days). For all male *D. magna* age groups, three technical replicates were used. For detailed information regarding biological replicate numbers refer to Tables 2.7 and 2.8 (section 2.11).

5.4.2 Impact of sex and age on the expression of genes

Change in the expression of genes were analysed for sex, age and sex by age interaction. Sex by age interaction is the differential rate of change in gene expression between sexes with age.

After removing outliers and genes with low count reads (see section 2.13.3), a total of 6,542 genes were identified with a statistically significant (adjusted *p*-value < 0.01) change in their expression as a function of sex (Figure 5.4A). Of these, 2,735 (41.80%) were expressed at a higher level in females compared to males and 3,807 (58.19%) had a higher expression level in males compared to females. Similarly, 6,383 genes (Figure 5.4B) were identified with statistically significant (adjusted *p*-value < 0.01) change in their expression levels as a function of age. Of these, 3,499 (54.82%) showed increased expression with age and 2,884 (45.18%) showed decreased expression level with age. When considered in an interaction setting (Figure 5.4C) which assesses the rate of change in gene expression level between sexes with age, the results are considerably lower with only 1,575 genes in total meeting the significance cut-off (adjusted *p*-value <0.01). Of these, only 594 (37.71%) showed increased expression level at a faster rate in females compared to males with age. While 981 (62.29%) genes showed increased expression levels at a faster rate in males compared to females with age.
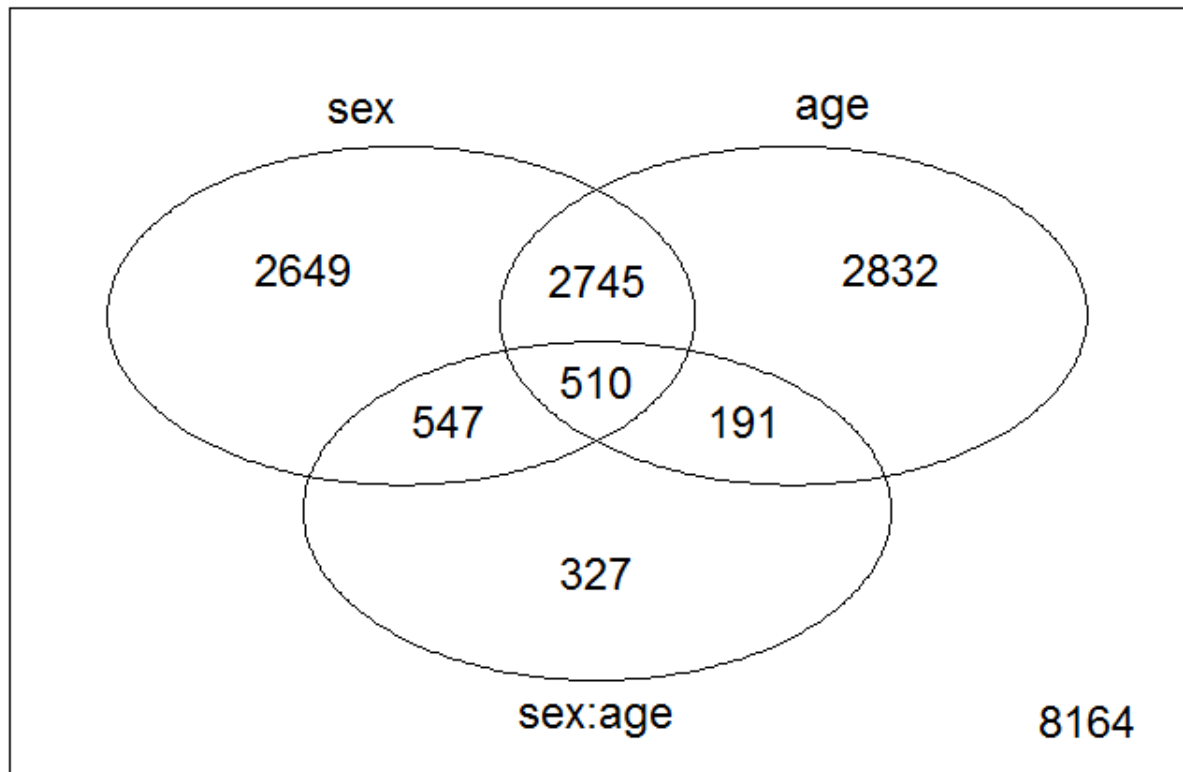
Figure 5.3: Overlap of genes showing relative expression changes in conditions of sex, age and sex:age interaction for female and male *D. magna*. Venn diagram representing an overview of the number of genes with statistically significant change in their relative gene expression (adjusted *p*-value <0.01) across the conditions of sex, age and sex:age interaction. The 7,570 genes accounted for outside of the groupings do not show significantly (adjusted *p*-value <0.001) changing relative intensities in any of the conditions investigated.

Significant gene expression changes with age
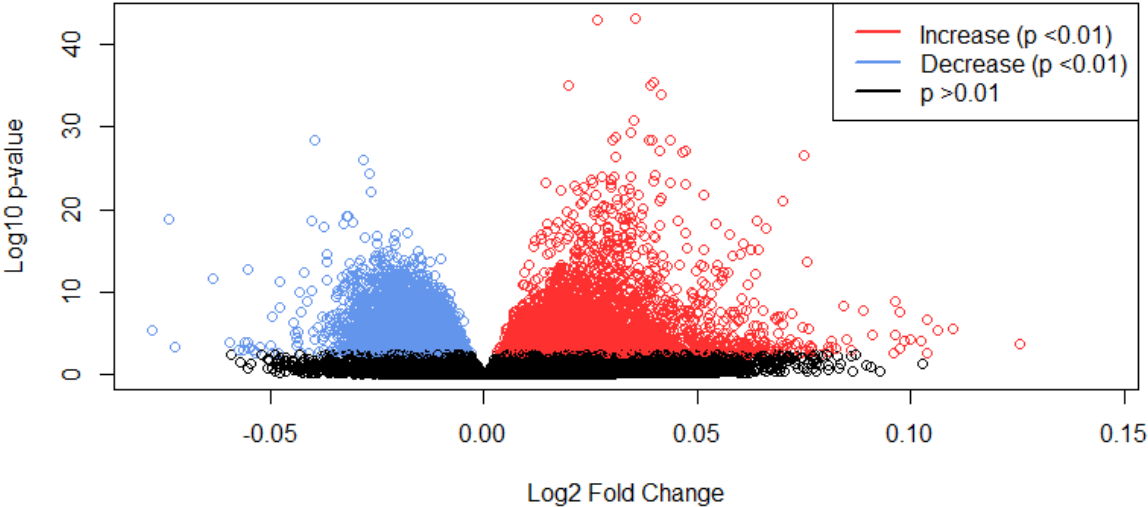
Significant gene expression changes between genders

Significant gene expression changes with sex:age interaction
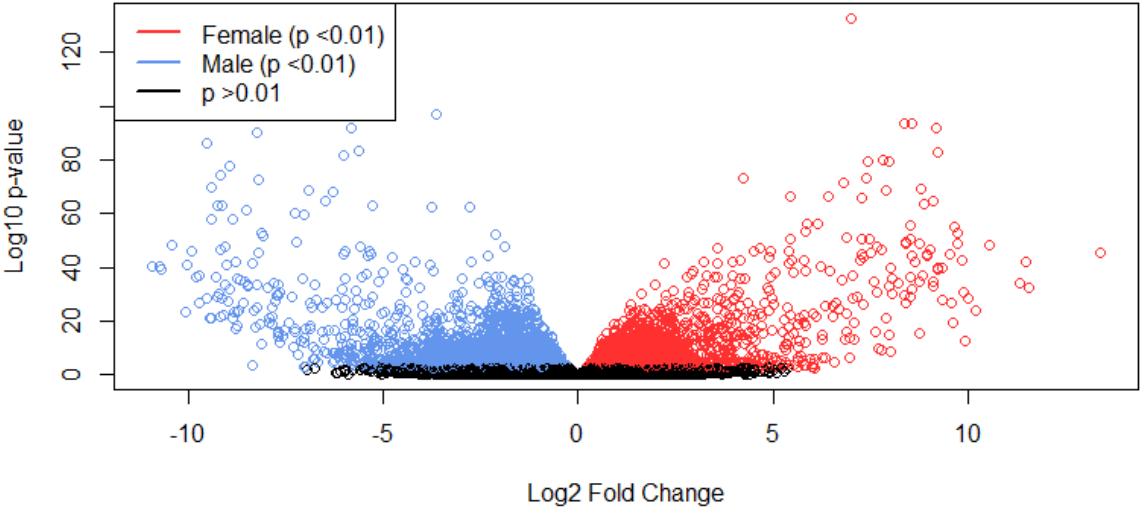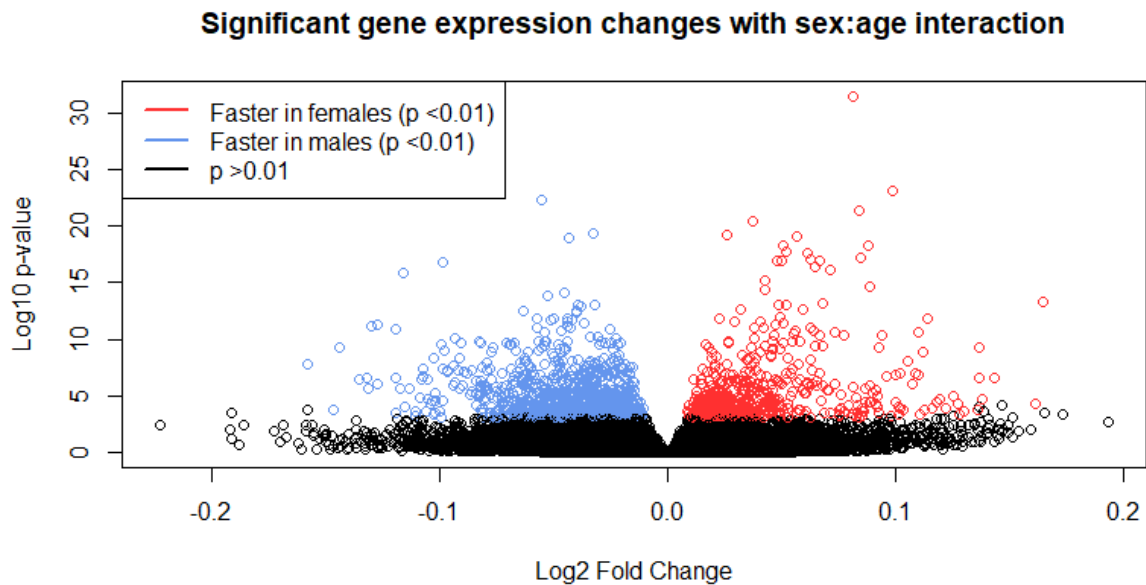
Figure 5.4: Distribution of genes showing relative expression changes in conditions of sex, age and sex:age interaction for female and male D. magna. A) Volcano plot for the condition of age only showing log2 fold change on the x-axis and negative log10 *p*-value on the y-axis (red = significant increased expression with age with adjusted *p*-value <0.01, blue = significant decreased expression with age with adjusted *p*-value <0.01, black = non-significant with adjusted *p*-value >0.01). B) Volcano plot for the condition of sex only showing log2 fold change on the x-axis and -log10 *p*-value on the y-axis (red = significantly higher in females with adjusted *p*-value <0.01, blue = significantly higher in males with adjusted *p*-value <0.01, black = non-significant change with adjusted *p*-value >0.01). C) Volcano plot for the condition of sex:age interaction showing log2 fold change on the x-axis and log10 *p*-value on the y-axis (red = significant with adjusted *p*-value <0.01, black = non-significant with adjusted *p*-value >0.01).

5.4.3 Pathway analysis of sex, age and sex:age interaction

To investigate which pathways were enriched in each of the three conditions of sex, age, sex:age interaction, Reactome and KEGG pathway analysis were performed on the differentially expressed genes (see section 2.13.3). A Reactome pathway enrichment analysis is shown in Figure 5.5. The pathway analysis yields general pathways largely incorporating RNA processing and the tricarboxylic acid (TCA) cycle for the condition of sex only, the cell cycle for the condition of age only, and the TCA

cycle and gluconeogenesis for the condition of sex:age interaction. For the condition of sex, 'rRNA processing', 'rRNA processing in the nucleus and cytosol' and 'major pathway of rRNA processing in the nucleolus and cytosol' make up the three largest groups with highest GeneRatio (~0.05), highest gene count (~100-120) and most significant adjusted p-values (adjusted p-value <0.02). The TCA cycle takes up the second largest proportion of pathways containing genes which their expression levels are significantly altered as a result of age. The 'TCA cycle and respiratory electron transport' and 'Pyruvate metabolism and TCA cycle' are both highly significant (adjusted p-value <0.02) with GeneRatio of 0.035 and 0.014 and counts of ~80 and 40 respectively, see 2C.F1 (Appendix 2C).

In total 1,736 genes were identified with statistically significant altered expression level as a function of age. Majority of these genes showed a decreased expression (65.4%) and smaller fraction (34.6%) showed an expressed expression level with age. KEGG pathway enrichment analysis identified several pathways enriched for the genes with decreased expression as a function of age, such as cell cycle, RNA transport, ribosome biogenesis and DNA replication. For example, the expression level of the genes in the enriched cell cycle pathway are mainly statistically significantly (adjusted p-value $<2 \times 10^{-05}$) decreasing with age as shown in Figure 5.5 (see 2C.F2, Appendix 2C). While pathways, such as bile secretion, retinol and xenobiotic metabolism and mineral absorption were enriched for the genes with increased expression as a function of age (2C.F2, Appendix 2C).

The total number of genes showing a significant change in relative expression level as a function of sex and a function of age, that also have a significant interaction between sex and age (sex:age interaction) are much smaller. Genes where expression level is

significantly increasing (adjusted *p*-value <0.005) at a higher rate in males compared to females in the sex:age interaction category are mainly enriched for the TCA cycle as shown in 2C.F3 (Appendix 2C). While genes that their expression level is significantly increasing at a higher rate in females compared to males in the sex:age interaction category are mainly enriched for membrane trafficking, metabolism of lipids and fatty acid metabolism pathways (2C.F3, Appendix 2C).

A KEGG pathway enrichment analysis is shown in Figure 5.6 for sex, age and sex:age interaction. The highly significant sex-related differences in gene expression level associated with Parkinson disease, Alzheimer disease and thermogenesis (adjusted *p*-value <0.001) are more highly expressed in males compared to females as shown in 2C.F1 (Appendix 2C). Gene expression changes associated with oxidative phosphorylation and Huntingdon disease are also observed to be higher in males (2C.F1, Appendix 2C). Gene expression changes linked to RNA transport and ribosome biogenesis in eukaryotes are more highly expressed in females compared to males. Interestingly, in the condition of age only in KEGG analysis, changes associated with RNA transport and ribosome biogenesis are increasing in relative expression with age, in addition to cell cycle and DNA replication (2C.F2, Appendix 2C). In an interaction setting, most gene expression changes are highly significant with a reported adjusted *p*-value <0.01. Carbon metabolism, gluconeogenesis and TCA cycle related changes are reportedly changing at a faster rate in males compared to females (2C.F3, Appendix 2C).
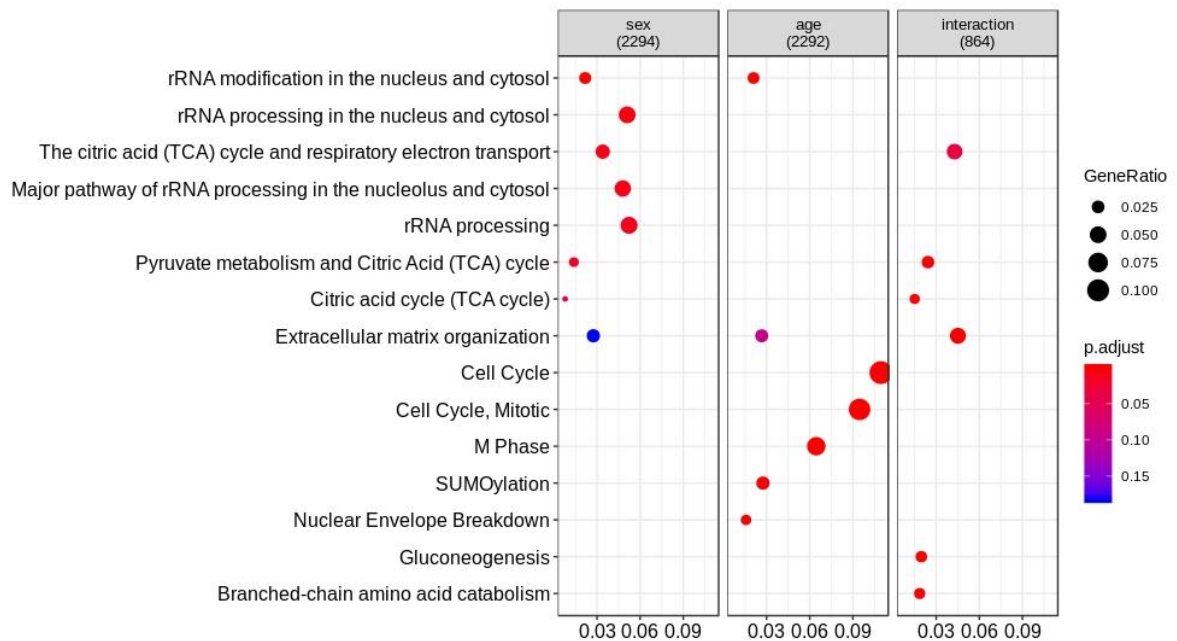
Figure 5.5: Reactome pathway enrichment analysis for conditions of sex, age and sex:age interaction in female and male *D. magna*. Reactome pathway enrichment analysis highlights gene expression changes in RNA processing and TCA cycle as pathways as a function of age, and the cell cycle in the condition of age. Interaction refers to sex:age interaction and highlights TCA cycle, gluconeogenesis and amino acid catabolism as pathways showing enrichment. Circle size represents GeneRatio (see section 2.13.3) where smaller size represents a lower GeneRatio and bigger size represents a higher GeneRatio. The colour of the circle represents statistical significance of the enrichment where red represents high statistical significance (adjusted *p*-value <0.05) and blue which represents low statistical significance (adjusted *p*-value >0.15).
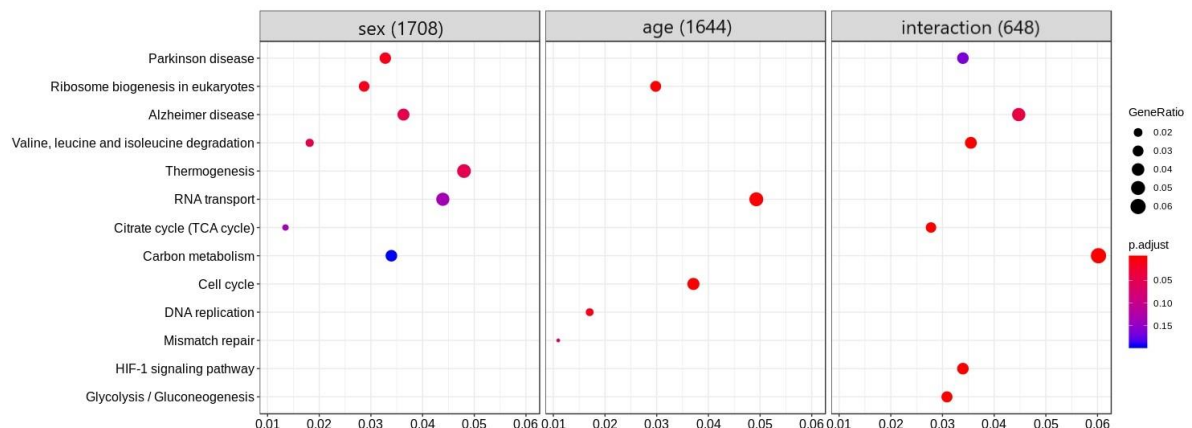
Figure 5.6: KEGG pathway enrichment analysis for conditions of sex, age and sex:age interaction in female and male *D. magna*. KEGG pathway enrichment analysis highlights gene expression changes that are associated with Parkinson and Alzheimer disease whilst age shows changes associated with the RNA transport and the cell cycle. Interaction represents the condition of sex:age interaction and shows HIF-1 signalling and gluconeogenesis are enriched in an interaction setting. Circle size represents GeneRatio (see section 2.13.3) where smaller size represents a lower GeneRatio and bigger size represents a higher GeneRatio. The colour of the circle represents statistical significance of the enrichment where red represents high statistical significance (adjusted *p*-value <0.05) and blue which represents low statistical significance (adjusted *p*-value >0.15).

5.4.4 Sex, age and sex:age interaction are enriched for different pathways

From the total number of genes (2,312 genes) identified with a statistically different expression level between sexes, 44% (1,016 genes) are included in the top 10 enriched pathways, as shown in Figure 5.7. The most enriched pathway is rRNA processing, accounting for 177 genes, of which 66.67% are higher in females compared to males. The enriched pathways linked to rRNA processing consistently show higher relative expression level in females compared to males. Host interactions of HIV factors also show the same profile whereby 65.71% of genes significantly associated with this pathway are higher expressed in females compared to males, see 2C.T5. In contrast, enriched pathways linked to the TCA cycle are largely more highly expressed in males. In total the expression level of 104 genes were significantly altered in the TCA pathway which accounts for the majority of the genes that comprise the citric acid cycle (TCA) and the respiratory electron transport. Of these, 72.12% show higher relative expression in males compared to females. Furthermore, 61.11% of the genes linked to mitochondrial calcium ion transport are more highly expressed in males, see Appendix 2C, Table 5 (2C.T5). A list of all genes and associated enriched pathways are provided in Appendix 2C, Table 6 (2C.T6). As an example, the CSN1KE

gene, linked to DNA repair and replication, and the ME1 gene, linked to TCA cycle and

fatty acid biosynthesis, are a couple of examples of genes with high read count in the

enriched pathways for the condition of sex. Interestingly, CSN1KE is also enriched in

age only and sex:age interaction categories.
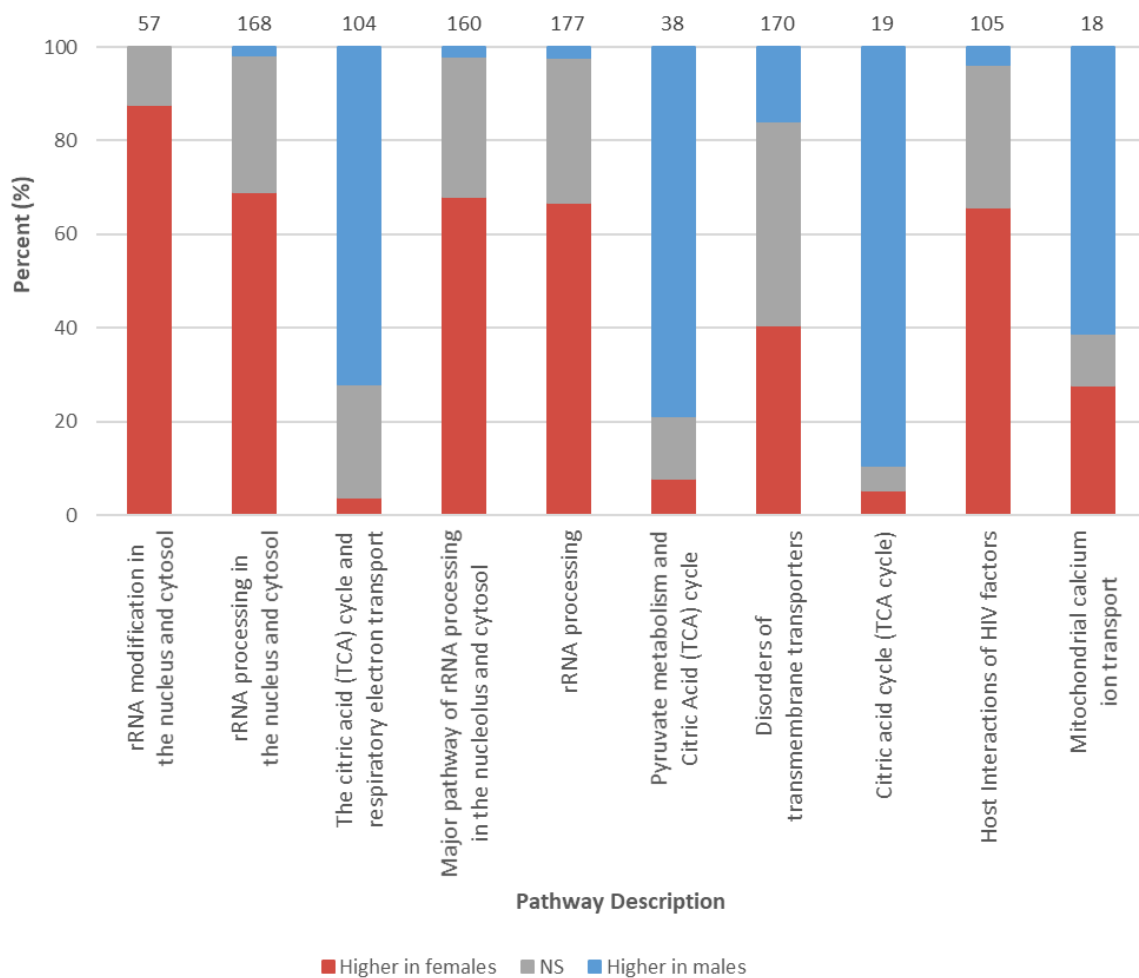
Figure 5.7: Percentage split of top 10 enriched pathways in *D. magna* by Reactome pathway enrichment analysis for the condition of sex. Stacked normalised bar chart shows percentage of top 10 enriched pathways that are showing differences between sexes. Genes showing higher relative expression in females are shown in red and genes showing higher relative expression in males (lower in females) are shown in blue. Grey represents no significant difference in relative expression level

between females and males. Three technical replicates were used for each age group for both females and males. Age groups are detailed in section 2.11.2. For detailed information regarding biological replicate numbers see Tables 2.7 and 2.8 (section 2.11). Numbers above the stacked bars represent the total number of genes identified in each pathway.

Of the 2,310 genes reported to show a change in relative expression level with age, 69% (1,594 genes) are included in the top 10 enriched pathways, as shown in Figure 5.8. Consistently across all 10 enriched pathways, the majority of genes are showing a decrease in relative expression level with age. Of the 413 genes linked to the cell cycle pathway, 60.77% decrease with age. Similarly, for 'cell cycle, mitotic' and 'M phase', the next two largest groups, 61.54% and 59.45% of genes are declining in relative expression level with age, respectively. Interestingly, for three of the top 10 enriched pathways, the expression levels of all genes either decrease or show no significant change with age (rRNA modification in the nucleus and the cytosol, nuclear envelope breakdown and interactions of Rev with host cellular proteins), see Appendix 2C, Table 7 (2C.T7).

The gene TPR is identified across the majority of enriched pathways in age-related analysis (52/156), see Appendix 2C, Table 8 (2C.T8). LMNA (10/156) and CCNB1 (19/156) are also implicated in multiple enriched pathways with sex as the condition.
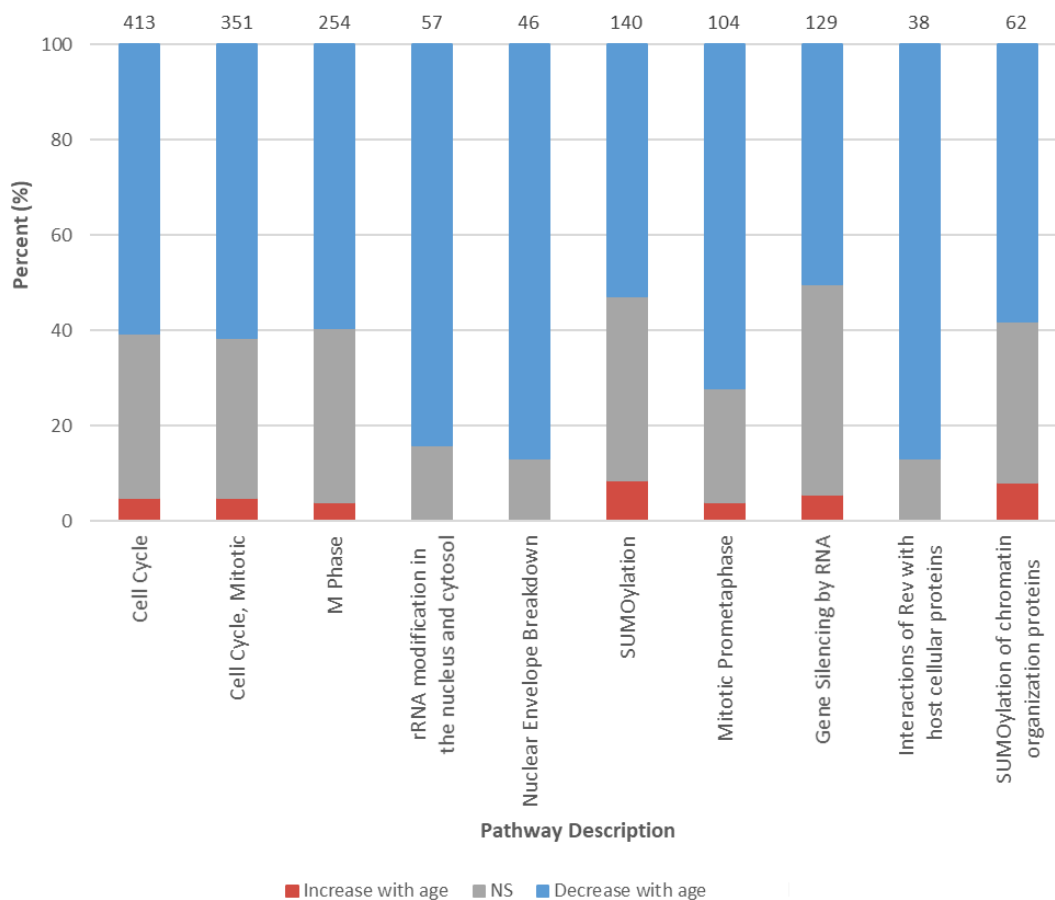
Figure 5.8: Percentage split of top 10 enriched pathways in *D. magna* by Reactome pathway enrichment analysis for the condition of age. Stacked normalised bar chart shows percentage of top 10 enriched pathways that are showing changes in relative expression with age. Genes showing increase in relative expression level with age are shown in red and genes showing decrease in relative expression level with age are shown in blue. Grey represents no significant difference in relative expression level throughout age. Three technical replicates were used for each age group for both females and males. Age groups are detailed in section 2.11.3. For detailed information regarding biological replicate numbers see Tables 2.7 and 2.8 (section 2.11). Numbers above the stacked bars represent the total number of genes identified in each pathway.

In total 80% (697 genes out of 873 genes) of the genes that demonstrate a significant change in relative expression level with age are included in the top 10 enriched pathways, represented in Figure 5.9. A general trend across the top 10 enriched pathways highlights a faster rate of change in relative gene expression level in males compared to females. The largest represented pathway is extracellular matrix

organisation, incorporating 201 genes. Of these, 76.12% show no significant difference in rate of change in expression level between sexes with age, 16.42% of the genes show a faster rate of change in their expression levels in males and 7.46% are showing a significant faster rate of change in relative expression level in females. The next two largest enriched pathways are muscle contraction and the TCA cycle and respiratory electron transport, accounting for 113 and 104 genes, respectively. Similar trends is observed for TCA cycle and respiratory electron transport pathways. Briefly, the expression levels of 34.51% and 34.61% of the genes are changing at a faster rate in males, for the mentioned two pathway, respectively while 63.72% and 64.42% of the genes show no significant difference in their expression levels, for both pathways respectively. Finally, the expression levels of 1.76% and 0.96% of the genes are changing at a faster rate in females, for the two pathways respectively. A list of all genes and their expression level for the enriched pathways is provided in Appendix 2C, Table 9 (2C.T9). As an example, the highest count comes from the pathway 'Transport of small molecules' (84/873) which includes the gene CALM1, also found in many of the other enriched pathways (16/43). Another gene associated with multiple pathways for sex:age interaction is ARRB1, present in 10/43 enriched pathways 2C.T9 (Appendix 2C).
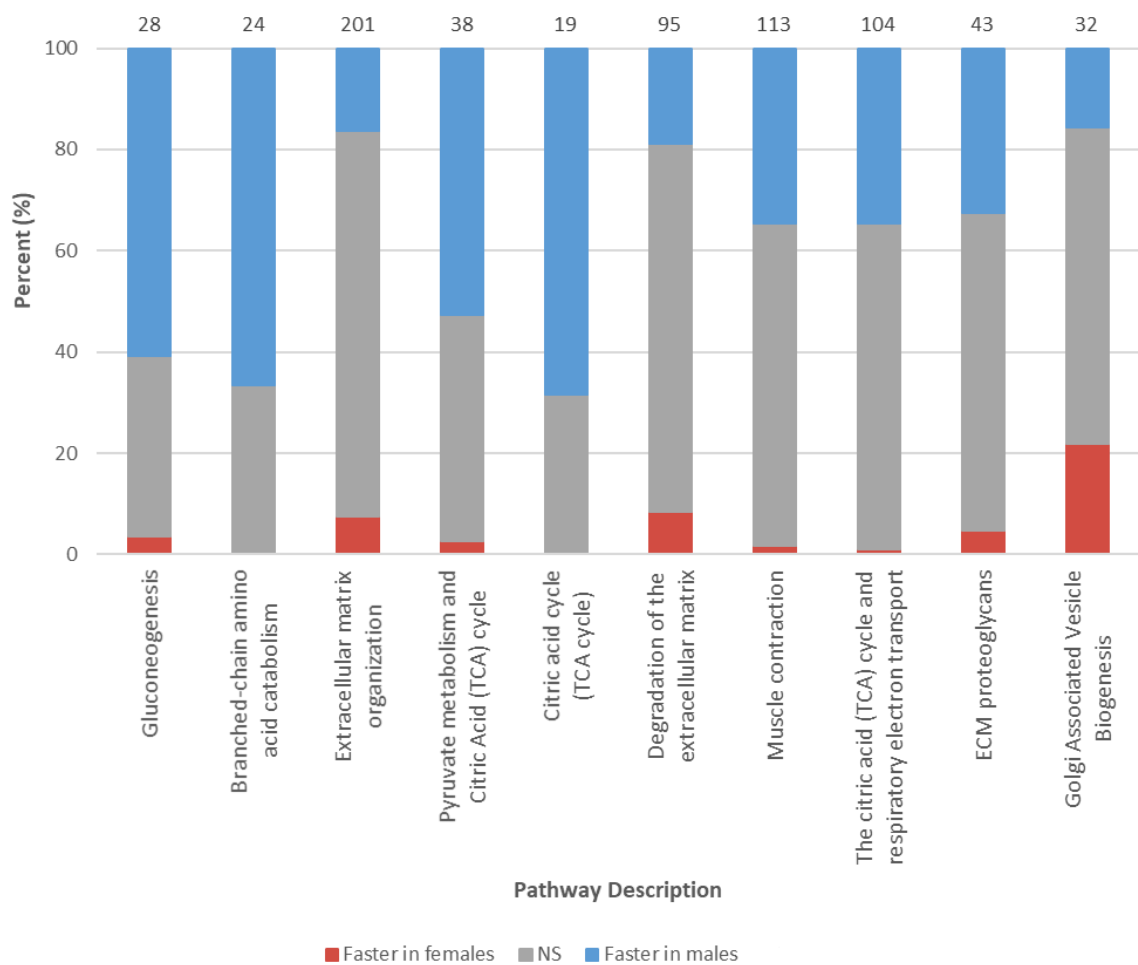
Figure 5.9: Percentage split of top 10 enriched pathways in *D. magna* by Reactome pathway enrichment analysis for the condition of sex:age interaction. Stacked normalised bar chart shows percentage of top 10 enriched pathways that are showing changes in relative expression level with sex:age interaction. Genes showing a faster rate of change in relative expression level with age in females are shown in red and genes showing a faster rate of change in relative expression level with age in males (slower rate in females) are shown in blue. Grey represents no significant difference in relative expression in sex:age interaction. Three technical replicates were used for each age group for both females and males. Age groups are detailed in sections 2.11 and 2.13. For detailed information regarding biological replicate numbers see Tables 2.1 and 2.2. Numbers above the stacked bars represent the total number of genes identified in each pathway.

5.4.5 Comparison of *D. magna* to other species for conditions of sex, age and sex:age interaction

A shared set of orthologous genes in *D. melanogaster*, *C. elegans*, *M. musculus, D. magna* and human was identified (2C.T1, Appendix 2C). As described in section 2.13.3, genes that are differentially expressed as a function of age only, sex only, or sex:age interaction were identified for each specie (see 2C.T1, 2C.T2, 2C.T3, Appendix 2C). Of the differentially expressed genes for age in mice, 92.9% have a *D. magna* homolog (6,641 genes in the DESeq2 analysis output were present out of 7,151 homologs between *M. musculus* and *D. magna*). Of all genes present in the DeSeq2 analysis output for age in *C. elegans*, 97.5% of genes are also present in the master file (5,014 genes in DeSeq2 analysis output were present out of 5,143 homologs *C. elegans* and *D. magna*). For the condition of age, *D. melanogaster* DeSeq2 analysis output contained 99.5% of genes (6,524 genes from the DeSeq2 analysis output were present out of 6,555 homologs between *D. melanogaster* and *D. magna*). The results for the various *Drosophila* genotypes used in the sex difference analysis can be found in Table 5.1 below. For further analysis, the genotype *D. ananassae* was used for the condition of sex. Although synthetic construct orgR retuned overall highest results (Table 5.1), *D. ananassae* is the natural ecotype with the highest results returned.

Table 5.1: Percentage of genes present in DeSeq2 analysis output for the condition of sex that have a *D. magna* homolog

Genotype	Total number of genes from DeSeq2 analysis output that have homologs with *D. melanogaster* and *D. magna*	Total number of homologs between *D. melanogaster* and *D. magna*	Percentage (%)
D. ananassae	6,264	6,555	95.56

D. mojavensis	6,198	6,555	94.55
D. persimilis	5,938	6,555	90.59
D. pseudoobscura	6,069	6,555	92.59
D. virilise	6,222	6,555	94.92
D. willistoni	6,157	6,555	93.93
D. yakuba	6,063	6,555	92.49
Synthetic construct orgR	6,396	6,555	97.16

Of the genes from the DeSeq2 analysis output files (listed in 2C.T2, 2C.T3 and 2C.T4, Appendix 2C) that had a *D. magna* and *H. sapiens* homolog, those with an adjusted *p*-value <0.05 were selected for Reactome pathway enrichment analysis.

5.4.6 Comparison of sex-related enriched pathways between species

The Reactome enrichment analysis output for the condition of sex only for *D. magna* (male and female), *D. ananassae* (male and female), *C. elegans* (male and hermaphrodite) and *M. musculus* (male and female) is shown in Figure 5.20. As described in section 2.13.3, the 2,312 genes with altered expression level as a function of sex in *D. magna* are largely enriched for pathways associated with rRNA processing. In *D. ananassae,* not only the same pathways identified for *D.magna* are enriched but additional pathways, such as metabolism of amino acids and GTP hydrolysis are also enriched for the 961 genes with altered expression level as a function of sex. In addition, KEGG pathway enrichment analysis was conducted for genes with differential expression level between females and males in *D. ananassae*. Majority of the 756 genes identified are expressed at a higher level in males compared to females (440/756) and are mainly enriched for pathways associated with ribosomes, RNA transport and protein export, see Appendix 2C, Figure 4 (2C.F4). The remaining 316 genes are higher in females and are enriched for pathways linked to proteasome, lysosome and EB virus infection. Reactome pathway enrichment analysis of *D.*

mojavensis produces similar results to *D. magna* with a large proportion of highlighted pathways relating to rRNA processing in addition to pathways enriched in *D. ananassae* (2C.F5, Appendix 2C). Whereas for *D. persimilis* majority of the enriched pathways for the genes that are differentially expressed between sexes, relate to elongation and translation (2C.F6, Appendix 2C). The pathways enriched for the 1,369 *C. elegans* genes that are differentially expressed between sexes, do not overlap with those seen in *D. magna* and *D. ananassae*, as they relate to mRNA metabolism and splicing. Between sexes, pathways related to Wnt signalling and amino acid metabolism are higher in hermaphrodites (based on 177/1,016 genes) but spliceosome and RNA transport are higher in males (based on 839/1,016 genes) see 2C.F7 (Appendix 2C). Finally, only 18 genes are identified to be differentially expressed between sexes in mice and have *D. magna* homolog. These are enriched for pathways related to phase I functionalisation of compounds, biological oxidations and cytochrome P450. There is no overlap between pathways highlighted for sex difference in mice and those highlighted for the other species.
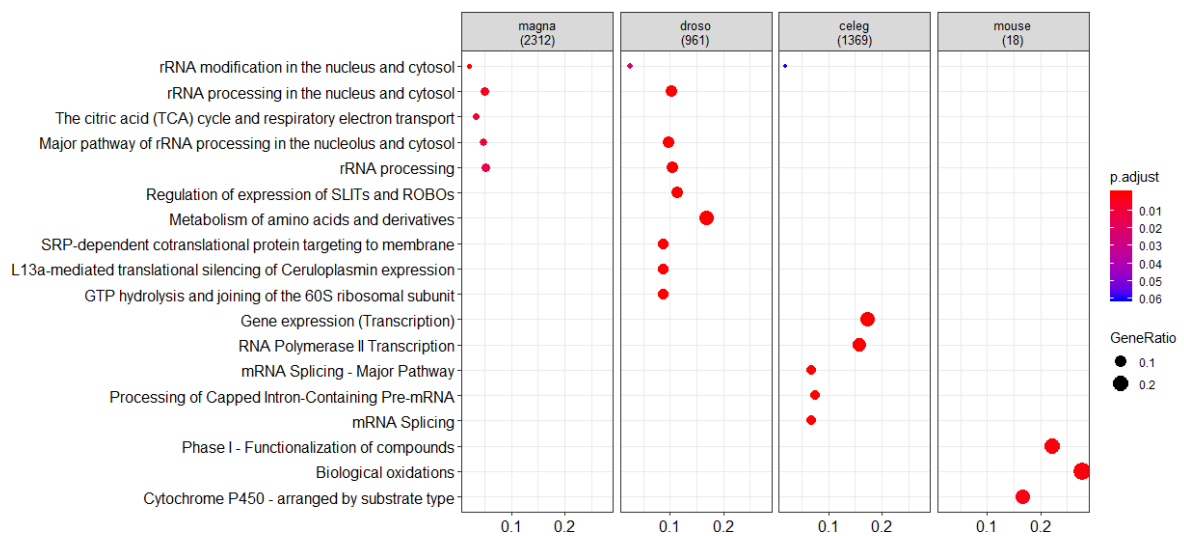
Figure 5.20: Reactome pathway enrichment analysis for conditions of sex in _D. magna_, _D. ananassae_, _C. elegans_ and _M. musculus_. Reactome pathway enrichment analysis highlights gene expression changes in the condition of sex across _D. magna_ (magna), _D. ananassae_ (droso), _C. elegans_ (celeg) and _M. musculus_ (mouse). Circle size represents GeneRatio (see section 2.13.3) where smaller size represents a lower GeneRatio and bigger size represents a higher GeneRatio. The colour of the circle represents statistical significance of the enrichment where red represents lower statistical significance (adjusted _p_-value <0.01) to blue which represents higher statistical significance (adjusted _p_-value <0.05).

5.4.7 Comparison of age-related enriched pathways between species

The most significantly enriched pathways via Reactome pathway enrichment analysis in ageing _D. magna_ relate to cell cycle and cell cycle regulation, as discussed previously and shown in Figure 5.21. Of 671 _C. elegans_ genes, the enriched pathways relate to the TCA cycle and respiratory electron transport which do not overlap with _D. magna_ results (Figure 5.21). KEGG pathway analysis of _C. elegans_ demonstrates that the majority of genes show an increase in relative expression with age (2C.F9, Appendix 2C), and that these relate to pathways linked to oxidative phosphorylation, carbon metabolism, Parkinson disease, Alzheimer's disease and amino acid degradation, similar to KEGG enrichment analysis of _D. magna_.

M. musculus display much overlap of age-related enriched pathways as reported for _C. elegans_ with the addition of rRNA processing and lipid metabolism pathways also enriched (Figure 5.21 and 2C.F10, Appendix 2C). KEGG pathway enrichment for ageing in mice only highlights 888 genes decreasing in relative expression level with age which are enriched for pathways linked to RNA transport, DNA replication and ribosomes. Opposing, 987 genes demonstrate increased relative expression with age and are enriched for pathways linked to amino acid degradation, non-alcoholic fatty liver disease, Alzheimer disease and tryptophan and propanoate metabolism (2C.F10,

Appendix 2C). *D. melanogaster* did not produce significant results for the condition of age and thus could not be included in the age comparison.
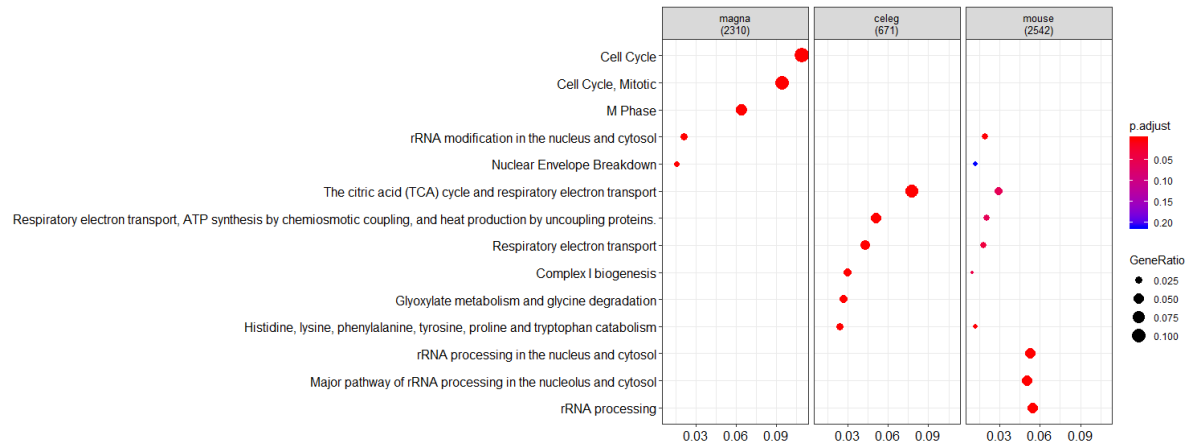
Figure 5.21: Reactome pathway enrichment analysis for conditions of age in *D. magna*, *C. elegans* and *M. musculus*. Reactome pathway enrichment analysis highlights gene expression changes in the condition of age across *D. magna* (magna), *C. elegans* (celeg) and *M. musculus* (mouse). Circle size represents GeneRatio (see section 2.13.3) where smaller size represents a lower GeneRatio and bigger size represents a higher GeneRatio. The colour of the circle represents statistical significance of the enrichment where red represents high (adjusted *p*-value <0.01) to blue which represents low (adjusted *p*-value <0.05).

5.4.8 Comparison of sex:age interaction-related enriched pathways between species

Of the 873 *D. magna* genes, 1,842 *C. elegans* genes and 30 *M. musculus* genes significantly changing in relative expression level in the condition of sex:age interaction, there is no shared enriched pathways (Figure 5.22). *D. magna* pathways relate largely to TCA cycle, *C. elegans* to mRNA splicing and *M. musculus* cover pathways related to a range of processes from GCPR ligand binding to biological oxidants.
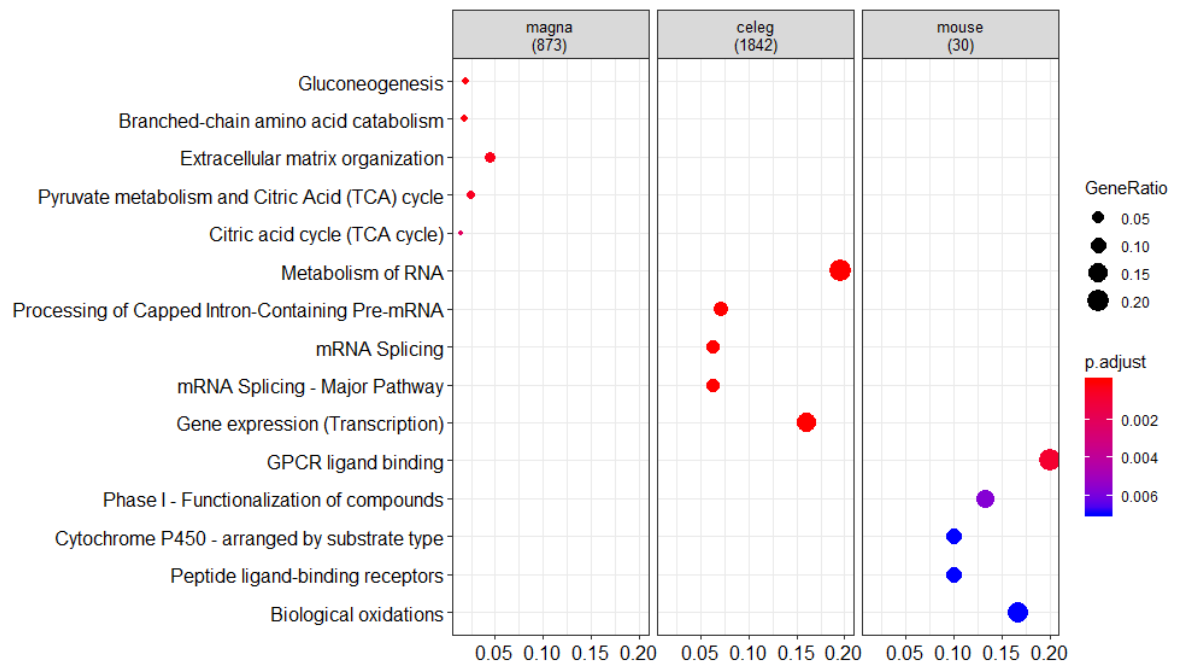
Figure 5.22: Reactome pathway enrichment analysis for conditions of sex:age interaction in *D. magna*, *C. elegans* and *M. musculus*. Reactome pathway enrichment analysis highlights gene expression changes in the condition of age across *D. magna* (magna), *C. elegans* (celeg) and *M. musculus* (mouse). Circle size represents GeneRatio (see section 2.13.3) where smaller size represents a lower GeneRatio and bigger size represents a higher GeneRatio. The colour of the circle represents statistical significance of the enrichment where red represents low (adjusted *p*-value <0.01) to blue which represents higher (adjusted *p*-value <0.05).

5.5 Discussion

Genetically identical female and male *Daphnia magna* show substantial differences in both lifespan and ageing rate (Constantinou et al., 2019). Gene expression changes with age have been observed across multiple species and have been linked to many age-related diseases. In this study, we provide the first evidence of gene expression changes with age in both male and female *Daphnia magna*, finding that age and sex have separate effects on overall gene expression trends.

Figure 5.2 clearly highlights the main factor differentiating gene expression groups is sex, followed secondly by age. The conditions of both sex and age significantly

influence a relatively balanced number of genes; 6,451 and 6,278, respectively. Interestingly, only half (a total of 3,255) are shared between sex and age, and thus the remaining are influenced by sex and age in manners distinctive of each other.

5.5.1 Sex differences in gene expression of female and male *Daphnia magna*

In species absent of genetic sex determination, opposite sexes are genetically identical yet often express wide-ranging phenotypic differences (Ellegren and Parsch, 2007). Furthermore, even those with genetic sex determination, the sexes differ only by a few genes located on sex-specific chromosomes. This leads to the conclusion that phenotypic sex differences must arise from differential expression of genes present in both sexes that are subject to differing and possibly conflicting selection pressures (Ellegren and Parsch, 2007). Differential expression arising from conflicting selection pressures are referred to as 'sexual antagonism' whereby expression of a gene is beneficial to one sex and detrimental to the other (Ellegren and Parsch, 2007). Sexual antagonism has been described in many species including mouse, wasps and flies (Wu and Yujun Xu, 2003, Beukeboom et al., 2009, Innocenti and Morrow, 2010). *D. magna* are genetically identical, yet females and males show significant phenotypic differences in terms of body size and growth rate as well as in ageing rate (Constantinou et al., 2019). Given the natural cycle of female *D. magna* producing clonal daughters unless environmental stressors or hormonal cues cause the production of males, the pressures on females and males are exceptionally different and thus it is no stretch to believe sexual antagonism is occurring. For example, females need a bigger body size for successful production of large, healthy broods whereas males instead require smaller body size and faster movement for successful copulation for production of resting eggs in unfavourable conditions to facilitate long-

term survival of the population (Constantinou et al., 2019). These differing pressures on female and male *D. magna* and their role in population survival may have led to evolutionary differences in gene expression.

Differences in gene expression between sexes in *D. magna* are enriched for pathways related to rRNA processing (Reactome), and Alzheimers' and Parkinsons disease (KEGG), see Figures 5.4 and 5.5. The outcome of such general pathways is common for pathway enrichment analysis with large hits as this often results in unspecific but significant outcomes (Amberkar and Kaderali, 2015). rRNA processing involves modifications to pre-RNA transcripts to produce functional rRNA and thus fundamental differences in expression between sexes will have a large impact on protein production within each sex, likely to affect all biological processes in some manner. Interestingly, males show higher enrichment for pathways associated with Alzheimers' and Parkinsons disease compared to females (2C.F1, Appendix 2C). Alzheimers' and Parkinsons disease are both considered 'age-related' as incidence increases significantly in people aged over 60 years. Notably, previous research has suggested male *D. magna* age at a faster rate than female *D. magna* (Constantinou et al., 2019) and thus it is possible that the changes in gene expression that are typically seen in Alzheirmers and Parkinson disease are in fact age-related changes that are more rapidly occurring in male *D. magna*.

Figure 5.7 highlights that pathways related to rRNA processing are largely higher in females compared to males. The relative expression of CSNK1E is reported to significantly differ between sexes and is relevant to all rRNA process-linked pathways listed. CSNK1E encodes a member of the casein kinase I protein family, serine/threonine protein kinase also known as casein kinase Iε or more colloquially

referred to as the circadian rhythm gene. CSNK1E is located in the cytoplasm and is responsible for phosphorylating a number of proteins and known to play a role in the circadian timing system by phosphorylating a circadian rhythm protein (Innominato et al., 2010). The control of rhythmic events across a 24-hour period such as the cell cycle, DNA repair, apoptosis and angiogenesis in normal and cancerous tissue is driven by the circadian timing system (Innominato et al., 2010). It is possible that the sex differences seen in expression of CSNK1E can be linked to the observed differences in DNA damage accumulation and repair between female and male *D. magna* (Constantinou et al., 2019).

5.5.2 Age related changes in gene expression in *Daphnia magna*

Gene expression changes with age have been reported, yet these changes are unknown whether to be a cause of ageing or simply a response to the age effect (de Magalhães et al., 2009). Irrespective of the role of gene expression changes with age (cause or response), the differentially expressed genes and associated pathways provide possible targets for investigation as biomarkers and for intervention of the ageing process and thus as interventions of age-associated health issues (de Magalhães et al., 2009).

Here, we have identified 3,499 genes becoming more highly expressed with age, whilst 2,884 are expressed at a lower level in older *D. magna* compared to young. Although a higher number of genes overall show higher expression with age, across the top 10 most enriched pathways, the involved genes show an age-associated reduction in gene expression (Figure 5.8). The cell cycle is the most enriched pathway and 60.77% of associated genes show a decrease in expression level with age. One such gene is TPR. This encodes a protein that is necessary for trafficking across the nuclear

envelope, plays a role in checkpoint signalling during mitosis and exports mRNAs transcribed from chromatin in the HSP70 promoter, and from mRNAs transcribed from the HSP70 promoter under stressed conditions (NIH, 2020). HSP70 gene expression declines with age in *Daphnia* (Schumpert et al., 2014). It plays an active role in stress protection and thus a decline with age allows susceptibility to stress-induced DNA damage (Schumpert et al., 2014). This idea is supported by accumulation of DNA damage with age in *D. magna* , exacerbated by reduced effectiveness of DNA damage repair with age (Constantinou et al., 2019). Furthermore, unrepaired DNA damage can lead to premature onset of mitosis, resulting in mitotic catastrophe (failure to proceed with prometaphase or metaphase) and is associated with a defective G2/M checkpoint (Hayashi and Karlseder, 2013). Additional to TPR influencing the G2/M checkpoint, CCNB1 is also shown to have lower relative expression in older animals compared to young and is essential for proper control of the G2/M transition phase of the cell cycle (NIH, 2020). It is possible that the versatile role of TPR and the essential role of CCNB1 combined with reduced expression with age is linked to observed DNA damage accumulation.

5.5.3 Sex:Age interaction related changes in gene expression in *Daphnia magna*

Across the top 10 most highly enriched pathways in sex:age interaction, there is an apparent trend of gene expression changing at a faster rate in males compared to females. Previous research has supported the idea that during the lifespan of male *Daphnia*; which is approximately half that of female counterparts, males accumulate ageing phenotypes at a faster rate (Constantinou et al., 2019). With this in mind, it is unsurprising to observe a faster rate of change in gene expression levels in males compared to females. Across many of the top 10 enriched pathways, the gene *CALM1*

is identified as significantly changing expression level in the setting of sex:age interaction. *CALM1* is a primary sensor of intracellular concentration shifts and is required for correct neural development (Gruner et al., 2019, Nyegaard and Overgaard, 2019). The decreased expression of *CALM1* with age, in addition to sex differences, has also been observed in *D. melanogaster* which was investigated for its role in degeneration of dopamine neurons, a common feature of Parkinsons' disease (Howell et al., 2019). Interestingly, the largest risk factors for Parkinson's Disease are age and sex; most cases occur after age 60 and males have nearly twice the incidence of Parkinson's as females (Howell et al., 2019).

5.5.4 Pathway enrichment shows little overlap between species

For the conditions of sex, age and sex:age interaction, there is little overlap between enriched pathways in *D. magna*, *D. ananassae*, *C. elegans* and *M. musculus* (Figures 5.9, 5.10 and 5.11). Sex differences are not biologically conserved traits and thus although it would be reasonable to expect certain genes to be shared, it is unlikely to be significant at the pathway level. This would influence not only the sex difference enrichment analysis but also sex:age interaction and so may go someway to explain the limited overlap in enriched pathways between *D. magna* and other species in these conditons.

It is clear that there are signifcant differences in gene expression changes with age between sexes in *D. magna*. By combining the data generated here with the lipidomics data from Chapter 4 and DNA methylation data (future area for research) it would be possible to explore a more wholesome picture through multiomics analysis.

CHAPTER 6

Cumulative effects of maternal age on fitness of offspring: evidence from multigenerational studies in *Daphnia magna*

6.1 Introduction

Ageing is defined as the gradual decline in normal physiological functions in a time-dependent manner that ultimately results in death (Plaistow et al., 2015, Constantinou et al., 2019). Many theories of ageing have been developed over time, most of which focus on explaining inter-individual differences in ageing rate caused as a result of genetic variation or differences in environmental conditions. However, since 1918 it has been suggested that parental age can influence and alter the phenotype of subsequent generations by non-genetic inheritance (Bell, 1918, Priest et al., 2002). One such non-genetic inherited trait is the observed shorter lifespan of populations derived from older mothers compared to younger mothers, referred to as Lansing effect. The Lansing effect was first observed by Albert Lansing in rotifers (Lansing, 1947)which have since been recorded in a diverse range of species, such as duckweed, houseflies, stink bugs, fruit flies, flour beetles, mealworms, nematodes, yeast and humans (Priest et al., 2002, Plaistow et al., 2015). Currently there is no consensus on the molecular mechanism that cause or contribute to the Lansing effect (Plaistow et al., 2015). However, two main theories have been proposed, the senescent parent hypothesis (SPH) and the offspring response hypothesis (ORH) (Plaistow et al., 2015).

The SPH describes recorded parental age-effects such as; overall shorter lifespan, reduced reproductive capacity and lower fitness, altered timings of offspring life history milestones and greater variation in offspring morphology of offspring from older parents compared to counterparts from younger parents, as a consequence of parental senescence (Ankutowicz and Laird, 2018). This theory proposes these effects are due to inheritance of the age-related physiological deterioration by the offspring (Kong et

al., 2012). The transmission of the deteriorated state is proposed to occur through three possible mechanisms; i) reduced offspring provisioning, ii) a decline in development environment, or iii) transmission of higher mutation load (Plaistow et al., 2015). This is evidenced by multiple studies (Gillespie et al., 2013, Plaistow et al., 2015, Barks and Laird, 2016, Ankutowicz and Laird, 2018, Eisenberg Dan and Kuzawa Christopher, 2018, Bock et al., 2019) which highlight reduced fitness and predict elevated biological age in offspring from older mothers.

The ORH (also referred to as the developmental constraints hypothesis) has some overlap with the senescent parent hypothesis. The ORH assumes that reduced maternal investment of energy into offspring leads to offspring demonstrating a negative compensatory response, such as developmental constrain on offspring growth and reduced fitness (Plaistow et al., 2015, Berghänel et al., 2017). This response can also manifest in the form of early on-set senescence and shortened lifespan or increased early-life reproductive effort and reproductive energy. These changes can subsequently shorten the lifespan of young parents and can result in altered timings of offspring life history milestones and greater variation in offspring morphology (Ankutowicz and Laird, 2018).

Plaistow et al. (2015) found that in *Daphnia pulex* the Lansing effect was present and concludes that this is likely explained by offspring response hypothesis in the form of offspring response to increased egg provisioning by older mothers leading to higher offspring growth rates. The results suggest that older mothers place more energy into offspring to compensate for their aged condition resulting in larger offspring with faster growth rate, were larger at age of maturation and demonstrated increased fecundity in early broods (Plaistow et al., 2015). Higher growth rate has been reported to influence

age-related processes such as antioxidant defence (Blount et al., 2003), telomere dynamics (Hall et al., 2004) and stress response (McEwen, 2007) which could explain the lifespan effect of older mothers (Plaistow et al., 2015).

Here, the waterflea *Daphnia magna* (*D. magna*) is used to further investigate advanced maternal age effects. *D. magna* reproduces through cyclical parthenogenesis to produce large numbers of genetically clonal daughters that have a relatively short lifespan of maximum 120 days (Constantinou et al., 2019). Biomarkers of ageing have previously been described (Constantinou et al., 2019) which can be utilised to monitor and compare age-related decline in offspring produced from young and old mothers. The aim of this study was to elucidate the impact of advanced maternal age effects on *D. magna* populations and to determine if ageing phenotypes are inherited across multiple generations, and if maternal age-effects can be reversed. Here it is shown that show that successive generations of older mothers result in significantly increased ageing phenotype in later life. This is evidenced by offspring from these successive generations of older mothers at aged 80 days showing ageing biomarkers that align more closely with offspring aged 100 days from successive generations of younger mothers. Concomitantly, young offspring from successive generations of older mothers have significantly higher DNA damage, reduced fitness and shorter lifespan compared to comparative populations from younger mothers which supports both the Lansing effect and SPH. Although body size at maturation is significantly different between populations of young and old mothers, analysis does not identify body size as significantly influential in predicting the aged phenotype and there was no significant difference between early-age brood sizes thus our findings do not align with ORH.

Notably, the maternal age effects transmitted from a single generation can be partially undone through subsequent generations produced from younger mothers.

6.2 Experimental Design

The experimental design for this study is demonstrated in detail in Figure 6.1. All experimental groups were generated originally from a single daphnid. F1-YA, F2-YA and F3-YA are generated from consistent 3rd broods (mothers aged 12 days) and represent the normal culturing conditions of *D. magna*. F1-GB is generated from the same maternal culture as F1-YA but is the 10th brood (mothers aged 40 days). F1-YA (mothers aged 12 days) and F1-GB (mothers aged 40 days) represent age effects in offspring from the same mothers. F2-GA is the 3rd brood of the offspring generated from older mothers (F1-GB) and F3-GA is the 3rd brood from F2-GA. F2-GA and F3-GA represent the recovery of age-effects inherited from older mothers in F1-GB across subsequent generations generated from younger mothers. F3-GB are the offspring of three generations produced from aged mothers.
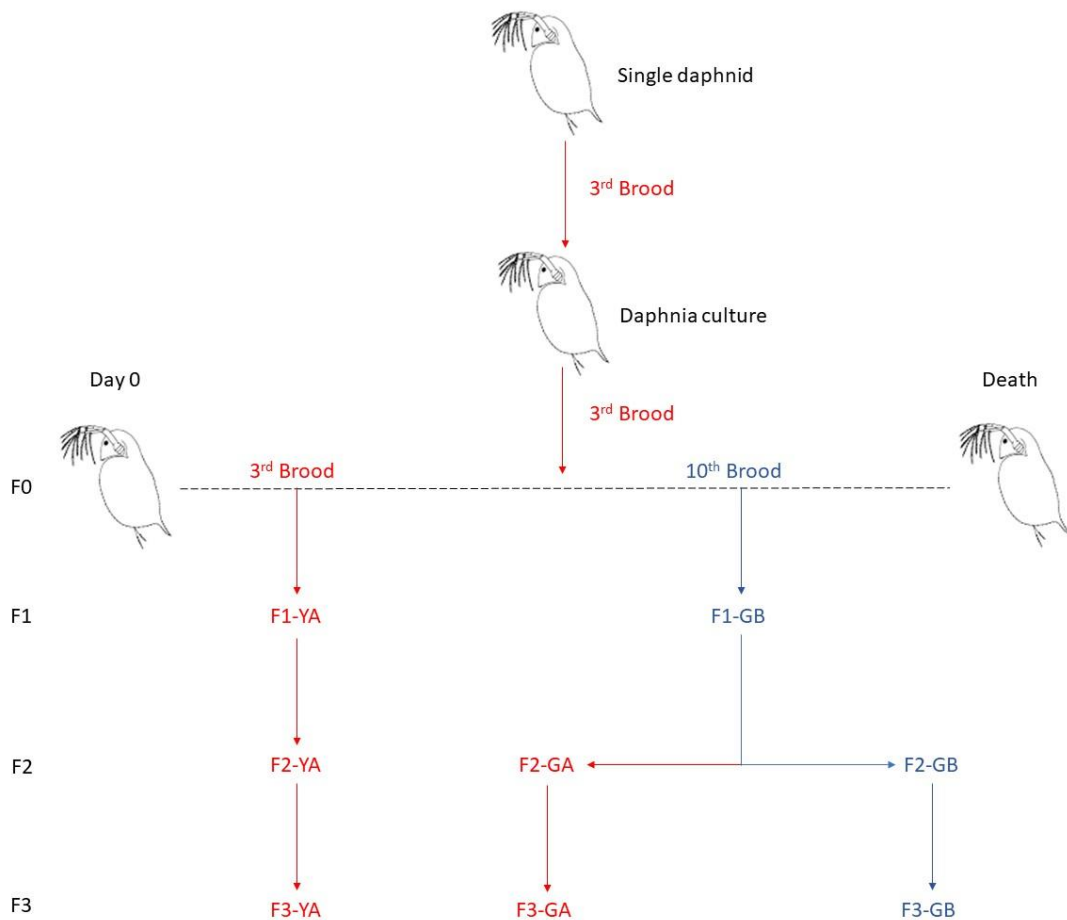
Figure 6.1: Experimental design for across generation inheritance of ageing phenotypes. Young (F1-YA; 3rd brood at approximately 12 days old) and geriatric (F1-GB; from adults aged 40 days, approximately 10th brood) lines of *D. magna* parents were generated by randomly selecting neonates from young mothers originating from a single daphnid. Subsequent generations were created by randomly selecting neonates from broods produced once mothers had reached the appropriate age (3rd brood for young mothers and brood released at 40 days of age for older mothers). Y = culture produced from young mother in F1 generation, G – culture produced from geriatric mother in F1 generation, A = culture selected from 3rd brood, B = culture selected from 10th brood.

Briefly, for lifespan studies, 5 cultures containing 5 female Daphnia were maintained under normal conditions as described in section 2.3. Fecundity was determined by counting the number of neonates produced every other day. The volume of media and amount of algae was adjusted accordingly as the number of individuals declined across

the duration of the lifespan study. The average lifespan and neonate production per culture was calculated followed by the average across the replicate cultures.

For body size studies, 5 cultures containing 5 Daphnids were maintained under normal conditions as described in section 2.3. For the duration of their lifespan, the individuals from each culture were measured at 10-day intervals for body measurements as previously described. The average body measurements per culture for each age were then taken and an average across the 5 cultures calculated. Throughout the study, where individual daphnids died, the volume of media and amount of algae per culture was reduced to maintain a consistent environment.

For the remaining experiments, three larger cultures were maintained for each experimental generation, ensuring the 50ml media per daphnid and algae ratio was maintained. Comet analysis was performed on multiple individuals across three replicates as described in sections 2.5-2.10. A single replicate (containing multiple individuals) was taken from each of the larger cultures and individual daphnids selected from throughout the 1L beaker so as not to select only those from a single area (e.g. not to select only those at the top of the beaker). For swimming speed, 5 individuals were selected from across the three larger cultures, again making sure to select individuals from throughout the culture.

The effect of advancing maternal age on life history, lifespan, reproductive capacity, swimming speed and DNA damage accumulation was assessed for F1-YA, F3-YA, F1-GB, F2-GA, F3-GA and F3-GB as described by Constantinou et al. (2019) and detailed in Chapter 2. F2-YA and F2-GB were not measured as the interest of the study was

persistent potentially inherited long-term effects and thus intermediate stages were not deemed relevant.

6.3 Data Analysis

R (R Project for Statistical Computing, http://www.r-project.org/, Version 3.5.2) was used for all statistical analyses and data visualisation. Firstly, analysis of the F0 generation was performed between adults at the ages of 3rd brood release and 10th brood release. Shapiro-Wilk analysis was performed to determine normality followed be either Kruskal-Wallis test for non-normally distributed data or t-test for normally distributed data. Secondly, comparisons between F3-YA and F1-GB were performed, similar to the F0 analysis, Shapiro-Wilk analysis was followed appropriately by either Kruskal-Wallis test or t-test analysis. Finally, F3-YA to F3-GB were analysed using multivariate analysis techniques. No significant difference was observed between F1-YA and F3-YA therefore only F3-YA was included in further analysis, see Appendix 2D for comparison of F1-YA to F3-YA. Comet tail intensity and swimming speed were normalised to body size by dividing by average body length. R packages 'ggplot2' (Wickham, 2016) and 'factoextra' (Kassambara and Mundt, 2017) were used to visualise the data by variables PCA plot. Stepwise regression was applied to determine the best model and highlight factors affecting ageing rate. R packages 'Leaps' (Lumley and Lumley, 2013) and 'FactoMineR' (Lê et al., 2008) were applied as a second method to select the best model and highlight factors affecting ageing rate. R package survival was applied for proportional survivorship (Therneau and Grambsch, 2013). Cox proportional-hazard model and log-rank analysis was applied to survivorship and ANOVA was applied to fecundity analysis.

6.4 Results

Monitoring of the population used to generate F1-YA and F1-GB showed that at the older age of 40 days when producing population F1-GB, they were showing significant increased biomarkers of ageing compared to the same population at the age of 10 days closer to producing population F1-YA, as shown in Figure 6.2.

6.4.1 Ageing biomarkers are apparent by 40 days of age in female *Daphnia magna*
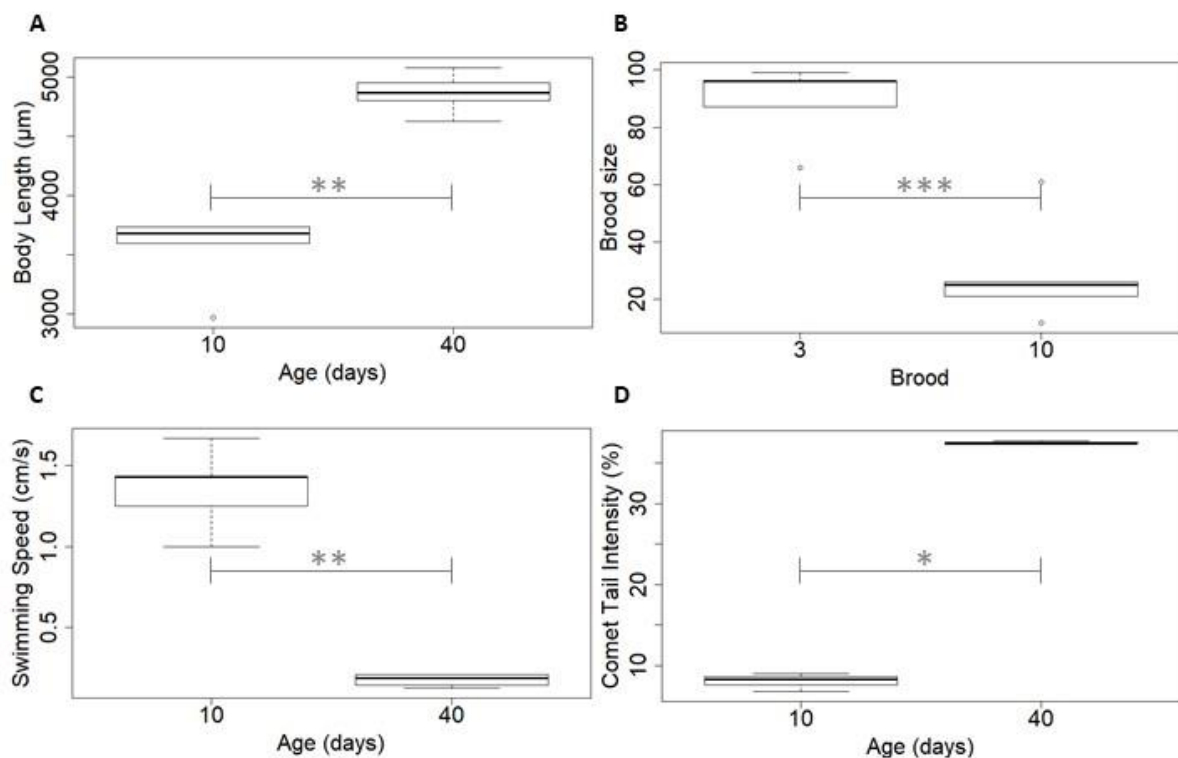
Figure 6.2: Biomarkers of ageing in female *Daphnia magna* comparing females from F0 at aged 10 days (mothers of F1-YA) and 40 days (mothers of F1-GB). A) Female *D. magna* aged 40 days have a significantly larger body size than female *D. magna* aged 10 days (n = 25, *p*-value = 7.413e-08; Kruskal-Wallis: *p*-value = 0.009023). B) The brood size of female *D. magna* aged 40 days (approximately 10th brood) is significantly smaller than the 3rd brood (released at approximately ages 16 days) (n = 25, Shapiro-Wilk: *p*-value = 0.07313; t-test: *p*-value = 0.0005807). C) Swimming speed of female *D. magna* at age 40 days is statistically significantly reduced compared to aged 10 days (n = 5, Shapiro-Wilk: *p*-value = 0.001374; Kruskal-Wallis: *p*-value = 0.008611). D) DNA damage is statistically significantly increased at female *D. magna* aged 40 days compared to female *D. magna* aged 10 days (biological

replicate: n = 3 [average of 3 x 25 comets], biological replicate: n = 5, *p*-value = 0.008931; Kruskal-Wallis: *p*-value = 0.04953). Significance markers: ***= *p*-value < 0.001, **= *p*-value < 0.01, *= *p*-value < 0.05, ns = *p*-value > 0.05.

Normal ageing was monitored by investigating biomarkers of ageing in the same individuals at aged 10 days (mothers to F1-YA) and aged 40 days (mothers of F1-GB). Figure 6.2A shows females aged 40 days (average length 4865µm) are significantly (*p*-value = 7.41 x 10-08) larger than those at aged 10 days (average length 3546µm), yet brood size is significantly *p*-reduced between the same age groups (*p*-value =5.81 x 10^{-04}) whereby 3rd brood per daphnid is 89 neonates on average and 10th brood produced from the same individuals is 29 neonates per daphnid on average (Figure 6.2B). At 10 days of age, female *Daphnia* swim at an average speed of 1.35cm/s which is significantly different from females at aged 40 days with an average swimming speed of 0.18cm/s (Figure 6.2C). Finally, Figure 6.2D shows significant increase in accumulated DNA damage as indicated by comet tail intensity (CTI%). At aged 10 days CTI% is very low at an average of 8.03% but by aged 40 days is significantly *p*-higher at 37.52% (*p*-value = 8.93 x 10^{-03}).

6.4.2 The survival rate and body size of the offspring are influenced by the age of the mother at the time of brood release.

It is apparent that the age of the mother at time of brood release has a negative impact on the survival and body size of offspring, as well as influence over DNA damage accumulation as evidenced below in Figure 6.3.
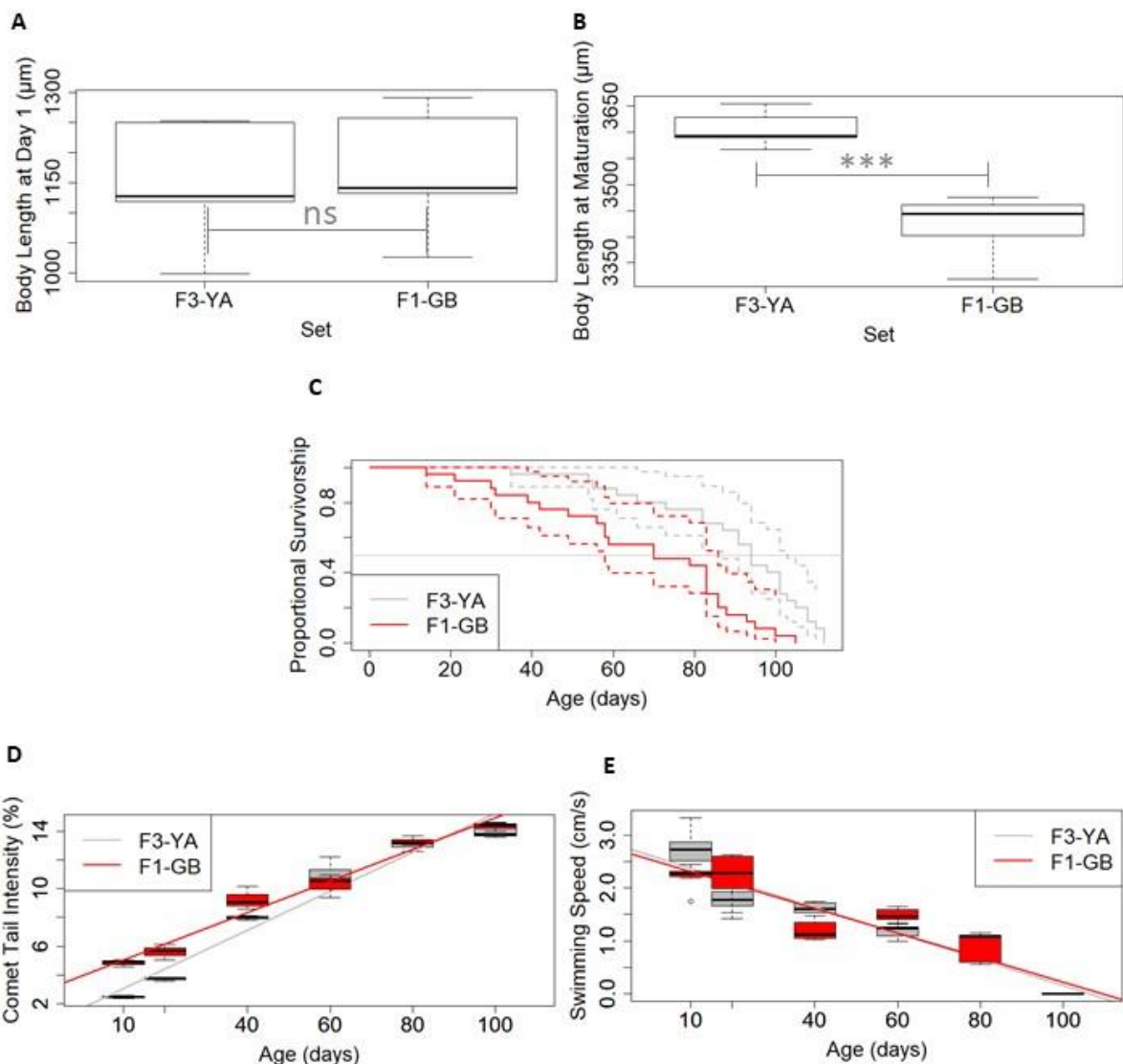
Figure 6.3: Differences in ageing biomarkers between 3rd brood (F3-YA, mothers aged 12 days) and 10th brood (F1-GB, mothers aged 40 days). A) No significant difference in body size at birth was observed between 3rd and 10th brood neonates (n = 25, t-test: *p*-value = 0.7702). B) By maturation age (age 9-10 days), there is statistically significant difference in body size between 3rd brood (F3-YA) and 10th brood (F1-GB) individuals (n = 25, t-test: *p*-value = 0.0009854). C) Survival rate of 10th brood (F1-GB) is significantly reduced compared to F3-YA (3rd brood) (n = 25, Log-rank test: *p*-value = 3 x 10^{-4}). D) Comet assay identifies accumulated DNA damage with age in both offspring derived from young (F3-YA) and offspring derived from old (F1-GB) mothers (biological replicate: n = 3 [average of 3 x 25 comets], biological replicate: n = 5, combined linear regression model: comet tail intensity (%) by age and brood: R^2 = 0.94, *p*-value = 2.75 x 10^{-21}, effect of age: *p*-value = 3.90 x 10^{-22}, slope F3-YA: 0.7124, slope F1-GB: 0.6873). E) Swimming speed statistically significantly declines with age in both offspring derived from young (F3-YA) and offspring derived from old (F1-GB)

mothers (n = 5, combined linear regression model: swimming speed by age and brood: R^2 = 0.85, *p*-value = 1.86 x 10^{-24}, effect of brood: *p*-value = 0.95, effect of age: *p*-value = 2.10 x 10^{-25}, slope F3-YA: -0.006910, slope F1-GB: -0.006719). Significance markers: ***= *p*-value < 0.001, **= *p*-value < 0.01, *= *p*-value < 0.05, ns = *p*-value > 0.05.

Neonates produced from young mothers (3rd brood, F3-YA) and old mothers (10th brood, F1-GB) show no significant difference in body length at birth with F3-YA showing an average size of 1149mm at aged 1 day and F1-GB recording an average size of 1169mm at aged 1 day (Figure 6.3A). By age of maturation (~aged 10 days old), F1-GB have ~5% reduction in size (F1-GB length: 3420mm) in comparison to F3-YA (F3-YA length: 3607mm), see Figure 6.3B. Proportional survivorship between offspring derived from young parents (F3-YA; 112 days) and offspring derived from old parents (F1-GB; 105 days) are also statistically significantly different (log-rank: *p*-value = 3.0 x 10^{-4}, coxph: *p*-value = 5.75 x 10^{-4}; Figure 6.3C). Figure 6.3D shows that offspring derived from both young and old parents display accumulated DNA damage with age at a similar rate (linear regression for age only; *p*-value = 1.0). However, interestingly offspring derived from old parents (F1-GB) display a significant consistently higher amount of damage compared to offspring derived from young parents (F3-YA) (linear regression for difference between broods; *p*-value = 0.005). Finally, swimming speed declines at a similar rate with age in both offspring groups.

6.4.3 Ageing rate in the offspring is influenced by the age of the mother at the time of brood release.
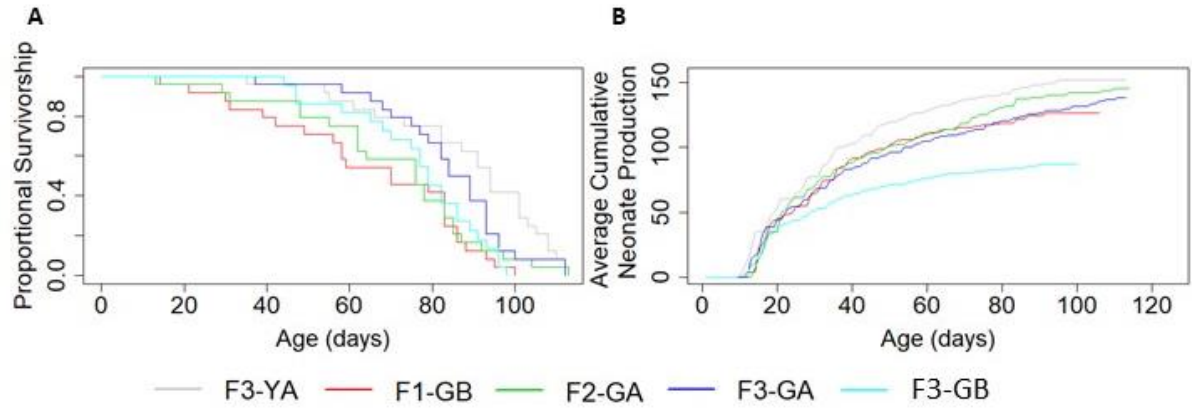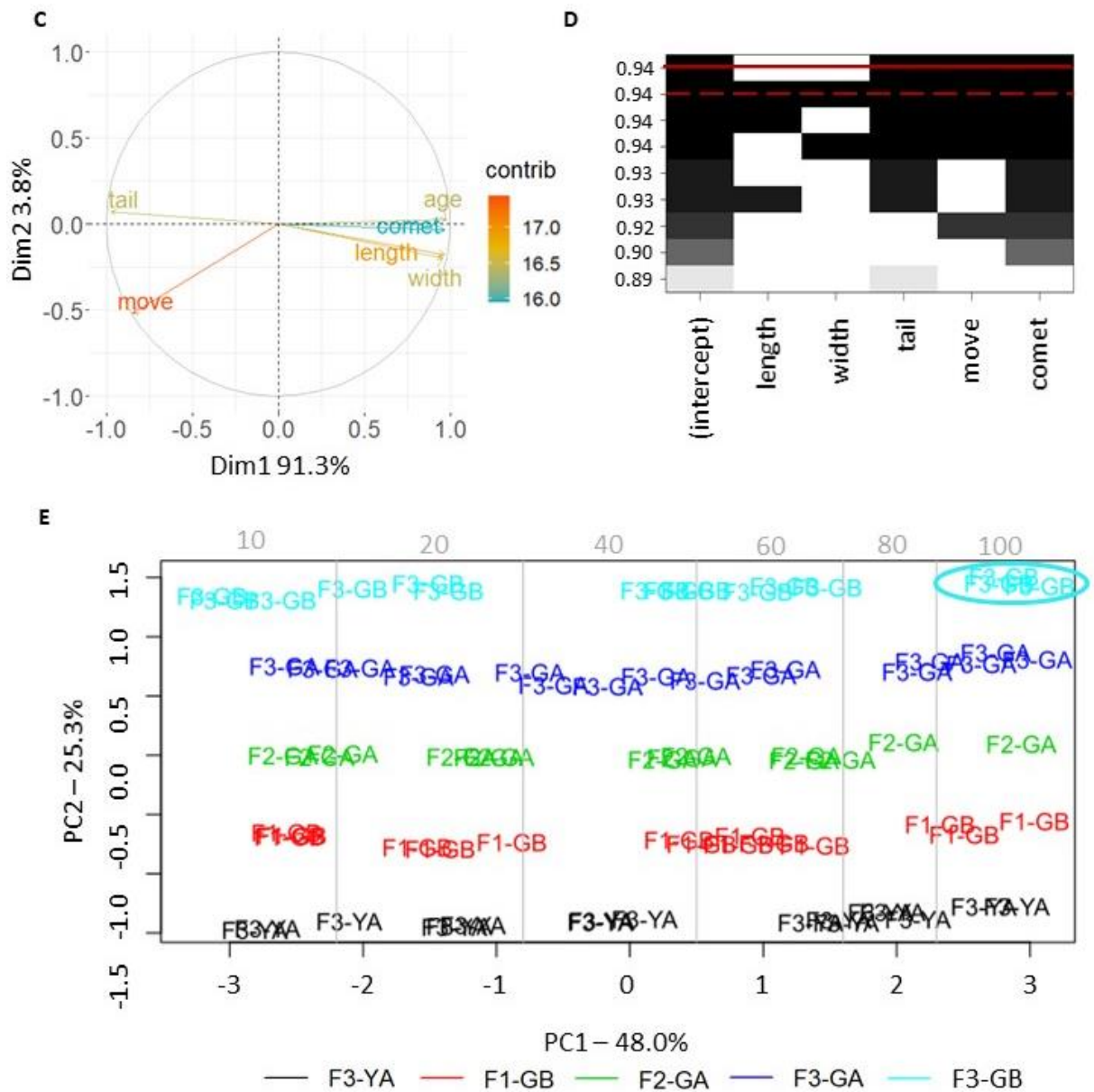
Figure 6.4: Multivariate analysis shows ageing rate in offspring is influenced by the age of the mother. A) Proportional survivorship of offspring between F3-YA – F3-GB (Key: F3-YA: offspring derived from young mother and young grandmother; F1-GB: offspring derived from geriatric mother; F2-GA: offspring derived from young mother but geriatric grandmother; F3-GA: offspring derived from young mother, young grandmother but geriatric great-grandmother; F3-GB: offspring derived from a geriatric mother, geriatric grandmother and geriatric great-grandmother (see Figure 1 for detailed description of how each line was generated) has an overall significant difference between sets (Log-rank: p-value = 0.001). B) Fecundity declines with age across all sets, however brood size is overall significantly different between sets (ANOVA: p-value = 4.59 x 10^{-13}). C) Variable PCA analysis separate factors by those

that increase (right) or decrease (left) as a result of age. Positive correlations are represented by vectors close in space whilst negative correlations are represented by vectors in opposite directions. Perpendicular vectors are not correlated, and the length of the vector represents the amount of variation associated with that phenotype. Colours represent the contribution of that variable to the principal axes (red = higher contribution, blue = lower contribution). D) Regression subsets plot visualises that all factors add to the ageing profile, however length and width can be removed with no change to the adjusted R^2 value. Tail length (tail), swimming speed (move) and comet tail intensity (%, comet) contribute to the ageing model. Dashed red line marks adjusted R^2 value of 0.95 with length and width included in the model. Solid red line marks fewest variables that describe the ageing phenotype with the highest adjusted R^2 value of 0.95 (does not include length and width in the model). Black box represents inclusion in the model, white represents excluded from the model. E) PCA analysis shows separation on PC1 by age labelled in grey and PC2 by set. Notably, F3-GB aged 80 days aligns with aged 100 days from all other sets. Key: F3-YA: offspring derived from young mother and young grandmother; F1-GB: offspring derived from geriatric mother; F2-GA: offspring derived from young mother but geriatric grandmother; F3-GA: offspring derived from young mother, young grandmother but geriatric great-grandmother; F3-GB: offspring derived from a geriatric mother, grandmother and great-grandmother (see Figure 6.1 for detailed description of how each line was generated).

Proportional survivorship (Figure 6.4A) is variable across all sets, but the effect of set overall significantly impacts survival (log-rank: p=.0.001). Cox proportional hazard highlights F1-GB, F2-GA and F3-GB as having significantly different proportional survival compared against F3-YA (*p*-value = 0.00140, *p*-value = 0.00544 and *p*-value = 0.02147, respectively). F3-GA is not significantly different in survival to F3-YA (*p*-value = 0.36423). Similarly, fecundity is variable across sets (Figure 4B), but the overall effect of set on fecundity is significant (ANOVA: *p*-value = 4.59 x 10^{-13}). Tukey HSD post-hoc analysis records a significant difference in fecundity between both F3-YA and F3-GB with all other sets (Table 6.1).

Table 6.1: Significance values for difference in fecundity between all investigative sets

	F3-YA	F1-GB	F2-GA	F3-GA	F3-GB
F3-YA	-				
F1-GB	0.0000000***	-			
F2-GA	0.0000005***	0.5748531	-		
F3-GA	0.0000000***	0.8847114	0.1027505	-	
F3-GB	0.0000000***	0.0000000***	0.0000000***	0.0000000***	-

Tukey HSD Post-Hoc *p*-values; *Significant below 0.05, ***Significant below 0.001

Key: F3-YA: offspring derived from young mother; F3-YA: offspring derived from young mother and young grandmother; F1-GB: offspring derived from old mother; F2-GA: offspring derived from young mother but old grandmother; F3-GA: offspring derived from young mother, young grandmother but old great-grandmother; F3-GB: offspring derived from an old mother, grandmother and great-grandmother (see Figure 6.1 for detailed description of how each line was generated).

Utilising multivariate analysis, when testing for residuals the overall effect of set is significant (ANOVA; *p*-value = 0.006858). Considering variables length, width, comet tail intensity (%), swimming speed and tail length, all sets are significantly different to F3-YA with the exception of F3-GA (F1-GB: *p*-value = 0.032607; F2-GA: *p*-value = 0.005829, F3-GA: *p*-value = 0.737485 and F3-GB: *p*-value = 0.000617). Figure 6.4C shows 91.3% of total offspring phenotypic variation is explained by PC1 which separates factors that increase or decrease with age. Stepwise regression was applied to determine which factors influence the difference between sets (Figure 6.4D) which determines that length and width are of no consequence, but that tail length (*p*-value = 0.00168), comet tail intensity (%) (*p*-value = 9.79×10^{-08}) and swimming speed (*p*-value = 0.002648) significantly contribute to the ageing profiles observed across the

sets (Adjusted R^2: 0.9374, *p*-value = 2.20 x 10^{-16}). Confirmation of these three contributing factors comes from analysis completed using another method, using R packages 'Leaps' and 'FactoMineR', which also selects the same factors as significantly contributing to the ageing profiles.

6.4.4 Phenotypes inherited from offspring from older mothers can be partially recovered through subsequent generations from younger mothers

The ageing profile of *D. magna* offspring from young mothers who had been preceded by a generation of young mothers (mothers were produced from a generation of young mothers aged 16 days) and old grandmothers (grandmothers were produced from a generation of old mothers aged 40 days) was generated by monitoring F3-GA. The ageing profile of offspring that were the product of three generations of older mothers (aged 40 days at brood release) was generated by monitoring F3-GB.

The effect of an aged mother is evidenced by F1-GB compared to F3-YA as described above, however, this effect can be recovered following subsequent generations produced from younger mother (F3-GA). Notably, the impact of consecutive generations produced from older mothers has a clear inherited and progressively detrimental impact on the health of subsequent generations (F3-GB), see Figure 6.5.
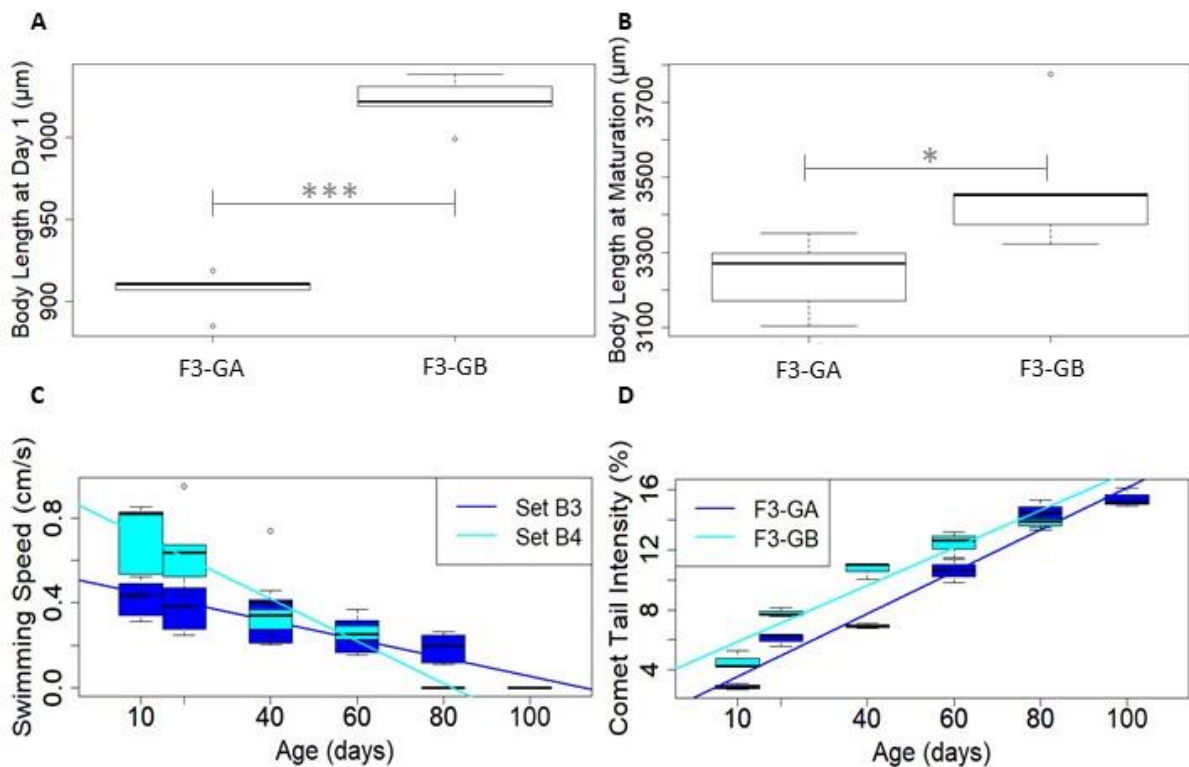
Figure 6.5: Differences in ageing biomarkers between offspring of young mothers preceded by young mothers and old grandmothers (F3-GA) and offspring from subsequent generations of older mothers (F3-GB). A) Statistically significant difference in size at birth was recorded between F3-GA and F3-GB (n = 25, wilcox.test: *p*-value = 1.247 x 10^{-06}). B) At age of maturation (age 9-10 days), there is statistically significant difference in body size between F3-GA and F3-GB individuals (n = 25, t-test: *p*-value = 0.03758). C) Swimming speed statistically significantly declines with age in both F3-GA and F3-GB (n = 5, combined linear regression model: swimming speed by age and set: R^2 = 0.66, *p*-value = 5.75 x 10^{-13}, effect of brood: *p*-value = 0.0012, effect of age: *p*-value = 6.30 x 10^{-13}, slope F3-GA: -0.004304, slope F3-GB: -0.009923). D) Comet assay identifies accumulated DNA damage with age in both offspring derived from F3-GA and F3-GB (biological replicate: n = 3 [average of 3 x 25 comets], biological replicate: n = 5, combined linear regression model: comet tail intensity (%) by age and set: R^2 = 0.94, *p*-value = 5.83 x 10^{-19}, effect of brood: *p*-value = 1.30 x 10^{-05}, effect of age: *p*-value = 1.10 x 10^{-24}, slope F3-GA: 0.1399, slope F3-GB: 0.1252). Significance markers: ***= *p*-value < 0.001, **= *p*-value < 0.01, *= *p*-value < 0.05, ns = *p*-value > 0.05.

Figure 6.5A shows females from F3-GA (average 907µm) are significantly smaller than

those from F3-GB (average 1022µm), yet by age of maturation the difference between

the two groups is significant but reduced with average body lengths of 3239µm and

3476μm for F3-GA and F3-GB, respectively (Figure 6.5B). Figure 6.5C shows that offspring generated from successive generations of older parents (F3-GB) lose swimming speed significantly faster than offspring produced from old great grandmothers and young grandmothers and mothers (F3-GA), as by 80 days of age F3-GB do not swim away from the light source but this does not occur in F3-GA until aged 100 days. Finally, Figure 5D shows significant increase in accumulated DNA damage with age in both sets by increased comet tail intensity, but F3-GB has consistent and significantly higher amounts of DNA damage compared to F3-GA.

6.5 Discussion

6.5.1 Ageing biomarkers are apparent by 40 days of age in female *Daphnia magna*

Biomarkers of ageing in *Daphnia magna* (*D. magna*) include change in body size, decline in reproductive capacity, decline in swimming speed and DNA damage accumulation (Constantinou et al., 2019). When monitoring female *Daphnia magna* throughout normal ageing, it is apparent that as body size increases, fecundity declines (Figure 6.2A and 6.2B). This relationship is linked to the trade-off of energy utilisation for growth against reproduction (Lemaître et al., 2015). *D. magna* reach maximum body size by 40 days of age, yet reproduction continues through-out the duration of lifespan at an ever-declining rate (Constantinou et al., 2019) which suggests this energy trade-off cannot be the only contributing factor to the observed age-related loss of reproduction. A possible explanation is the decline in fitness associated with DNA damage accumulation. DNA damage is associated with an increase in reactive oxygen species (ROS) and reduced repair capacity (Chen et al., 2007). In *D. magna* it has been shown that DNA damage and lipid peroxidation product accumulate with age, but

that thiol content (a form of protection against ROS) and RAD51 expression (required for successful homologous recombinant repair of DNA double strand breaks) are reduced with age (Constantinou et al., 2019). Here, we show that at aged 40 days, at the time of the 10th brood release, DNA damage recorded by comet assay is significantly higher than that of aged 10 days females (Figure 6.2D). DNA damage is a moderator of replicative and premature cellular senescence (Chen et al., 2007) and thus it is possible reduced reproductive capacity is associated with the age-related increase in reproductive senescence (Karniski et al., 2018, Jarak et al., 2018, Sepil et al., 2019).

6.5.2 Ageing rate in offspring is influenced by the age of the mother at the time of brood release

The negative impact of maternal age on offspring lifespan and ageing has been reported across many taxa (Plaistow et al., 2015, Bock et al., 2019). In *D. magna* we demonstrate that average body size at birth is unaffected by maternal age, however by age of maturation average body size is significantly reduced in offspring from older mothers (Figure 6.3A and 6.3B). Interestingly, age of maturation is not altered as both offspring derived from young mothers (F3-YA) and old mothers (F1-GB) reach sexual maturation by aged 10 days. However, reproductive capacity represented by brood size is significantly reduced in offspring from older mothers (F1-GB) compared to offspring from younger mothers (F3-YA), see Table 6.1 and Figure 6.4B. Bock et al. (2019) found that in rotifer (*Brachionus manjavacas)*, the impact of maternal age did not appear to impact offspring development rate as age of maturation remained the same between offspring derived from young and old mother. However interestingly reproductive senescence onset occurred significantly earlier in offspring from older

parents than offspring from younger parents. Earlier onset of reproductive senescence in offspring derived from older mother may explain the observed reduced reproductive capacity of *D. magna* offspring, F1-GB (derived from old mothers) compared to F3-YA (young mothers). Given the observed increase in DNA damage with age in both sets, but the significantly higher amount of accumulated damage in F1-GB compared to F3-YA (Figure 6.3D), it is possible that DNA damage is contributing to earlier onset of reproductive senescence in offspring from older mothers.

Figure 6.3D highlights that at age of sexual maturation (10 days), F1-GB (offspring from old mothers aged 40 days) has twice as much DNA damage than F3-YA (offspring from the same mothers as F1-GB but at aged 12 days), suggesting offspring from older mothers inherit a higher amount of DNA damage. This may contribute to the significantly reduced lifespan and proportional survivorship of F1-GB compared to F3-YA (Figure 6.3C). Across a diverse range of species, it has been observed that lifespan and fitness of offspring derived from older parents is significantly reduced exemplified by rotifer populations *Philodina citrina* (Lansing, 1954) and *Euclanis triquetra* (Lansing, 1947) as reported by Plaistow et al. (2015), the seed beetle *Callosobruchus maculatus* (Fox et al., 2003) and in wild populations of red-billed choughs (Reid et al., 2010). Such maternal age effects have also been reported in humans (Wilding et al., 2014, Schroeder et al., 2015). This reduced lifespan is termed the 'Lansing effect'. As a means to explain these observations, the senescent parent hypothesis (SPH) proposes that offspring from older parents have shorter lifespan due to inheritance of the parents age-related physiological deterioration by the offspring through three possible mechanisms; i) direct reduction in offspring provisions, ii) decline in the development environment of the offspring or iii) transmission of higher mutation load

(Plaistow et al., 2015). The hypothesis is supported by observations of reduced fitness in offspring from older parents (Fox et al., 2003, Reid et al., 2010, Plaistow et al., 2015) which may in part explain the greater variation observed in swimming speed in F1-GB compared to F3-YA (Figure 3E). Swimming speed can be considered a measurement of fitness as it requires substantial energy and it is important for *D. magna* to be able to move for food availability and risk of predation (Pietrzak et al., 2010a). The age-related decline in swimming speed in both sets is significant but in F1-GB at each age there is greater variability in response to light when compared to F3-YA.

The senescent parent hypothesis predicts that offspring from older mothers are born with an elevated biological age which is presented as higher age-independent mortality rates, lower age-independent reproductive potential and lower growth rate (Kong et al., 2012). This is evident in *D. magna* from the differences observed between offspring from young mothers (F3-YA) and offspring from older mothers (F1-GB). This becomes even more pronounced through subsequent generations of older mothers, depicted by F3-GB (offspring derived from a line of old mothers, old grandmothers and old great-grandmothers, see Figure 6.1). Notably, overall lifespan of F3-GB is significantly lower than all other investigative sets, supporting previous observations of the Lansing effect shown across many other species (Figure 6.4A). Significantly reduced lifespan following successive generations of older parents has also been demonstrated in rotifer populations *Philodina citrina* and *Euclanis triquetra* (Lansing, 1947, Lansing, 1954) and highlights that across multiple generations the Lansing effect becomes more pronounced. Interestingly, here we show by F3-GA that it is possible to un-do some of the detrimental inherited effect on lifespan of one generation in subsequent generations produced from younger mothers, that is to say the damage is not

permanently submitted to subsequent generations. This is exemplified by F3-GA lifespan being most significantly different to F3-GB (p-value = 0.00002), and moderately different to F3-YA (p-value = 0.03). In addition, F3-GB presents significantly reduced reproductive capacity throughout lifespan compared to all other investigative sets (Figure 6.4B). When considering the biomarkers of swimming speed and DNA damage, the significantly difference between F3-GA and F3-GB presents data suggestive of a more healthy ageing profile in F3-GA (maintains swimming speed for longer and has overall less DNA damage throughout ageing compared to F3-GB, Figure 6.5C and 6.5D). Plaistow et al. (2015) report that as a response to the aged phenotype of older mothers, offspring from older mothers are often larger in size as a compensatory mechanism from the mother, producing fewer but larger offspring to increase survival. Although not seen within offspring from a single population that produces offspring from young (F3-YA) and old (F1-GB) mothers, it becomes apparent after successive generations of older mothers. When comparing size at brood release of F3-GA and F3-GB, F3-GB neonates were on average significantly larger. This is in-line with the theory that the Lansing effect becomes more pronounced over successive generations produced from older mothers, but that it can be partially recovered by subsequent generations produced by younger mothers as F3-GA aligns more closely with the reproductive profile of all sets except F3-GB.

To explain the phenotypic variation across sets, multivariate analysis was performed taking in to account factors including age, body length (length), body width (width), tail spine length (tail), DNA damage by comet tail intensity (comet) and swimming speed (move). As shown in Figure 4D, the adjusted R^2 value remains at 0.95 whether body length and body width are included or not and so have a lesser impact on the variation

across sets, and thus the ageing rate and phenotypic differences significantly separating the sets with age are tail length, DNA damage and swimming speed. As previously described, *D. magna* lose their tail spine with age (Constantinou et al., 2019). In a controlled laboratory environment, tail spine loss occurs naturally with age, however it has been described that tail spine loss is accelerated when daphnids are exposed to fish kairomones and food shortages (Carter et al., 2013). This tail spine loss under stressed conditions is hypothesised to be a consequence of energetic allocation to maximising growth, development and earlier reproduction when at risk of predation or shortage of food supply (Carter et al., 2013). This can also be applied to ageing whereby as damage increases and reproductive capacity is lost, energy is diverted from other mechanisms such as tail spine growth and allocated towards reproductive capacity instead. As we demonstrate an accumulative Lansing effect across successive generations produced from older mothers, it is possible that the inherited ageing phenotype causes energetic allocation in to reproductive capacity leading to a faster tail loss in F3-GB compared to other groups. If happening, even with this energetic re-allocation, reproductive capacity is reduced (Figure 6.4B). The DNA damage profile across ageing is also different between sets and attributes to the overall significantly different ageing phenotypes between sets (Figure 6.4D). The reproductive capacity may be hindered by the inherited DNA damage possibly leading to early onset reproductive senescence as described in the fruit fly *Drosophila melanogaster* (Bloch Qazi et al., 2017) and the rotifer *Brachionus manjavacas* (Bock et al., 2019). Importantly, the inherited phenotype combined with natural age effects results in the clustering of aged 80 day females from F3-GB with the ageing phenotype of aged 100 day females from all other sets (Figure 6.4E). This exemplifies clearly the increased

ageing phenotype in *D. magna* populations derived from successive generations of older parents.

In conclusion, this research has demonstrated in *D. magna* that non-genetic factors influence the ageing phenotype of subsequent generations, and that these factors are accumulative across successive generations of older parents. The ageing phenotype is influenced by DNA damage, swimming speed and tail length and observes reduced reproductive capacity likely due to earlier onset of reproductive senescence and overall reduced lifespan in populations from older parents. However, this inherited ageing phenotype can be partially recovered if subsequent generations are produced from younger mothers.

CHAPTER 7:

General Discussion

7.1 Challenges for ageing research

Global average life expectancy at birth has increased by 5.5 years between 2000 and 2016 to 72.0 years (WHO 2020), which partly can be attributed to advances in the field of medical sciences. However, as life expectancy has increased the prevalence of age-related diseases has also increased. Significant research into age-related diseases has resulted in greater understanding of the molecular mechanism of individual diseases. In some cases, this has led to identification of new therapeutic targets and development of novel treatment strategies. However, the realisation that the risk of certain diseases (referred to as age-associated diseases) usually increases as individuals age, has highlighted the importance of researching the ageing process as the common factor between all these diseases. By understanding and subsequently targeting and slowing down the adverse effects of ageing process, it may be possible to target most age-related diseases. It may be possible to delay the onset of age-associated diseases and/or slow their progression and limit their impact on quality of life to a shorter percentage of human lifespan. This approach will lead to promoting and increasing the health-span. Health-span describes both the length of healthy life and the fraction of total lifespan spent free of disease (Campisi et al., 2019). To achieve this, it is first essential to understand the molecular mechanism of ageing and the physiological changes associated with the ageing process.

The complexity and plasticity of ageing process, in addition to the genetic diversity observed in human populations, makes it an extremely complex process to elucidate. To aid the investigations into the molecular mechanism of ageing, conventional and non-conventional model organisms have been used.

The use of model organisms has been fundamental in illuminating molecular regulation of ageing. One of the most important revelations was the discovery of the role IGF-1 receptor pathway in ageing. Inhibition of insulin/IGF-1 signalling leads to lifespan extension and delay in onset of age-related diseases (Kenyon, 2011). This life-extension pathway was initially discovered in *C. elegans* (Kenyon et al., 1993), and since then has been found to be conserved from yeast to humans (Longo et al., 2005). The use of model organisms also highlighted the positive effect of caloric restriction without malnutrition on extending lifespan and promoting healthy ageing. The idea was first presented by McCay et al in 1935 where data showed restrictive caloric intake in both female and male mice resulted in extended lifespan (McCay et al., 1935). Since this discovery, similar results have been observed across many species including rats, hamsters, dogs, fish, flies, worms, yeast and primates (Heilbronn and Ravussin, 2003, Masoro, 2005). These discoveries have helped to enhanced our understanding of the molecular basis of the ageing process and have evolved the field of ageing research away from simply identifying ageing phenotypes to investigating the relationship between genetic/epigenetic pathways of ageing and ageing phenotypes (Campisi et al., 2019). This shift, which has been greatly facilitated by the use of model organisms, has revealed that ageing is regulated by a complex network of interacting intracellular signalling pathways (Campisi et al., 2019).

7.2 *Daphnia magna* as a model for ageing research

The overall aim of this thesis was to characterise *Daphnia magna* as a model for ageing research. To achieve this, several specific aims were outlined (section 1.6). Initially, phenotypic and molecular biomarkers of ageing were described (Chapter 3, Constantinou et al, 2019). Following the observation of accumulated lipid droplets with

age, and the sex differences observed in ageing phenotypes and molecular markers, an in-depth lipidomics analysis was undertaken which described differences in the lipidome with age, between sexes and with sex:age interaction (Chapter 4, Constantinou et al, 2020). For the same conditions, RNA-sequencing was performed, and gene expression profiles analysed (Chapter 5). Finally, the influence of maternal age-effect was investigated (Chapter 6).

As discussed throughout this thesis *Daphnia spp.* posses many unique and useful characteristics for ageing research, see section 1.8. These characteristics have been harnessed in recent years giving rise to increased utilisation of *Daphnia spp.* for ageing research (Pietrzak et al., 2010b, Latta et al., 2012, Dudycha and Hassel, 2013, Lohr and Haag, 2015, Schumpert et al., 2015a, Asselman et al., 2016).

7.3 *Daphnia magna* as a model for investigating sex differences in ageing process

The research presented in this thesis further supports the use of *Daphnia spp*; specifically, *Daphnia magna* (*D. magna*), as a model for ageing research. Importantly, the results highlight the ability to investigate sex-difference in ageing – a long known and little understood phenomena across many species, including humans.

The data clearly shows that lifespan and ageing rate can vary in genetically identical sexes of one specie. Using *D. magna* strain Bham 2 whose female population has a lifespan double that of their genetically identical male counterpart, it is clearly evidenced in this thesis that as a percentage of lifespan, these populations are showing heart rate and swimming speed decline, as well as DNA damage accumulation at a similar rate. Notably, this suggests the novel finding that male *D. magna* are presenting

ageing markers approximately two-times faster than their clonal female counterparts (Chapter 3).

It has been observed in many species that males have a shorter lifespan than females, with a widely perceived explanation for this that higher selection pressure promotes female longevity in comparison to males (Clutton-Brock and Isvaran, 2007).

In birds and mammals there is a high degree of parental care in rearing offspring (Stockley and Hobson, 2016). However, this is most commonly performed by either the female alone, or in monogamous species by both sexes (Stockley and Hobson, 2016). Possible explanations include the gestation and lactation capabilities of the mother in most species placing higher demand on the female (Smith, 1977, Clutton-Brock, 2019). The investment of the male in caring for offspring is traded-off against engaging in further mating opportunities and so the cost must outweigh the benefit (Smith, 1977, Wade and Shuster, 2002).

The differentiation of reproductive strategies between the sexes is thought to achieve sex-specific optimum characteristics (Bonduriansky et al., 2008). Ultimately, the effect of these optimum characteristics on longevity and ageing often results in increased ageing rate and shorter lifespan of males compared to females (Bonduriansky et al., 2008).

As *Daphnia* males are produced in response to stressed conditions to allow for resting egg production via sexual reproduction, the sexual strategy of males is significantly different to females and there is no requirement for parental care, therefore following the selection pressure theory described above, it is sensical that male ageing rate is much faster and lifespan much shorter in comparison to females. Thus the results

presented here are consistent with sex difference as a consequence of selection pressure. The useful traits of *Daphnia spp.* as a model organism can be harvested to test linkages between sex, ageing rate and longevity which currently remain poorly understood.

Furthermore, it is presented here that *D. magna* can be used for advanced techniques such as lipidomics which has been utilised to uncover statistically significant age-related changes in triglycerides, diglycerides, phosphatidylcholine, phosphatidylethanolamine, ceramide and sphingomyelin lipid groups. Most interestingly, the rate and direction of change can differ between genetically identical female and male *D. magna*, which could be the cause and/or the consequence of the different average lifespans between the two genetically identical sexes.

Chapter 4 provides a benchmark dataset to understand how lipids alter as a function of age in genetically identical female and male species with different average lifespan and ageing rate.

A review by Johnson and Stolzing (2019) compiled an array of findings that exemplify the importance of lipid metabolism in the ageing process. For example, impairment of genes involved in ceramide and sphingolipid synthesis extends lifespan in worms and flies (Guillas et al., 2001, Aerts et al., 2006, Cutler et al., 2014). This thesis presents data that sphingolipid and ceramide relative intensity decrease at a faster rate in males with age when compared to females with a higher relative intensity present in female *D. magna*. This is consistent with findings reported by Gonzalez-Covarrubias (2013) where sex-specific age differences in lipid content were identified with sphingomyelin, a sphingolipid, higher in females than males.

Levels of triglycerides in blood increase with age (Greenfield et al., 1980). In this study, frequently but not exclusively, triglyceride relative intensity is lower is males compared to females. The role of triglyceride as the most abundant and accessible energy supply supports the idea that female *D. magna* would require higher concentrations due to the energy demand placed on cyclical parthenogenetic reproduction, growth rate, body size and swimming speed. These findings suggest that perhaps these lipid profiles are a consequence of selection pressures driven by sex-specific optimum characteristics.

Notably, evidence from extremely long-lived species have identified resistance to lipid peroxidation as a possible protective mechanism that allows extended life (Munro and Blier, 2012). In both female and male *D. magna* lipid peroxidation product increases with age whilst thiol content decreases. Thiols are one of the main protective mechanisms against lipid peroxidation and so the decrease in this protection is likely adding to the observed increase in damage (see Chapter 3). Notably, the decrease in thiol content is more severe in males compared to female *D. magna* and so may be a contributing factor in the shorter lifespan of males.

The collation of many findings in the Johnson and Stolzing (2019) review highlight clearly the potential of lipids in relation to interventions for improving longevity as well as a mechanism for monitoring human ageing, i.e. as a biomarker. Given the complications associated with investigating lipids in humans (genetic, epigenetic and environmental influences as well as time and cost implications), the use of model organisms is essential for understanding underlying processes to create a foundation of knowledge on which to build and to screen for potential targets that require further investigation in more complex models. The findings within this thesis exemplify the potential that *Daphnia* hold in respect of this.

Moreover, it is apparent that these ageing biomarkers can be inherited by subsequent generations produced from older mothers, with significant difference between populations produced from third generation of young mothers compared to third generation of older mothers in swimming speed, tail loss and DNA damage accumulation. Reassuringly, the damage inherited from a single generation of older mothers was recovered through subsequent generations produced by younger mothers suggesting the impact is plastic and reversible (Chapter 6).

The significance of such findings is that as *D. magna* are genetically identical and produce clonal daughters, thus indicating that the traits are potentially epigenetically inherited. The identification of epigenetics as a possible mechanism for transgenerational inheritance is a relatively new concept being investigated, with genetics and environmental factors historically considered the driving influences (Lacal and Ventura, 2018). The most widely studied form of epigenetics in ageing are those that occur throughout life, known as epigenetic drift (Issa, 2014). However, there are other modes of epigenetic influence; factors that affect the womb during gestation events and factors that affect predecessors long before conception that are inherited through epigenetics, referred to as transgenerational inheritance (Lacal and Ventura, 2018). As this field of research is relatively emergent, there is much to be unwrapped and investigated and the use of model organisms to do so will be fundamental.

Given the growing importance of this field of research, it was important to investigate the suitability of *Daphnia* for studying molecular mechanism of ageing. This thesis clearly presents research that identifies similarities in the ageing process between *Daphnia* and other models, with the added advantages that *Daphnia* have genetically

identical males and females. This thesis provides a foundation from which to build the next stage.

The results of this thesis show *D. magna* provide a suitable platform for investigating the contribution of non-genetic factors and mechanisms, such as epigenetic factors, hormones, environmental factors, energy allocation and trait trade-offs in determining lifespan and ageing rate.

7.4 Future Research

7.4.1 *Daphnia magna* and epigenetic research

Epigenetics is an ever-growing branch of ageing research and has largely focussed on DNA methylation. Extensive studies have identified DNA methylation to be biologically relevant in the ageing process (Catania and Fairweather, 1991, Jin et al., 2014, Marttila et al., 2015, Spiers et al., 2016, Stubbs et al., 2017)

A common trait in vertebrates is the overall highly methylated genome with high and low methylation in the promoter region associated with gene silencing or gene expression, respectively. Regulation via DNA methylation is essential for correct spatial and temporal gene expression which ultimately influences normal function and correct development. The ageing process sees a de-regulation of this tightly controlled process. Commonly, hypomethylation at repetitive DNA sequences leading to heterochromatin loss is observed in mammalian ageing. Hypomethylation at repetitive sequences can promote genomic instability (Pal and Tyler, 2016).

The capability of *Daphnia* to methylate DNA was first described in 2009 with the discovery of homologs of the three main DNA methyltransferases (Vandegehuchte et

al., 2009). The study confirmed that DNA methylation was occurring by exposure to various chemicals known to affect DNA methylation.

DNA methylation in *Daphnia* is largely enriched within coding regions of genes, with the highest levels observed at exons 2-4 (Kvist et al., 2018). Although this differs to the global methylation of vertebrates as described above, the highest methylation levels are observed at exon 2 and then maintained across the gene body (Kvist et al., 2018). Both vertebrate and invertebrate methylation profiles share a bimodal distribution and genes linked to highly methylated CpG sites are highly transcribed and conserved across the experimental species (*D. magna* (strains Bham 2 and Xinb3)*, N. vitripennis, A. mellifera, M. musculus and H. sapiens*). It is proposed by Kvist et al. (2018) that the positive correlation between internal exons and gene expression and the negative regulation of gene expression via methylation and promoters and exon 1 seen in vertebrates is a secondary mechanism evolved as species became more complex.

As previously mentioned, *Daphnia* reproduce through cyclical parthenogenesis. This is not only beneficial for cultivating large numbers of a clonal population for statistical relevance, but also allows investigation of epigenetic factors in the absence of confounding genetic differences (Harris et al., 2012). Epigenetic marks are the interface between the environment and the genome as they can be modified by external factors. This is obvious in survival mechanisms expressed by *Daphnia* such as the development of neck spines, helmets and production switch from females to males during stressful conditions and high predation (Harris et al., 2012). Additionally, epigenetic changes are adaptive and can be passed from one generation to another, in some cases passing on an advantageous phenotype but possibly also passing on negative traits such as in ageing.

Here, data presented shows a clear impact of aged mothers on the fitness and ageing profile of offspring (Chapter 6). With subsequent generations of older mothers, the inherited aged phenotype becomes accumulative and more pronounced, however the healthier phenotype can be recovered by subsequent generations of younger mothers. The transmission of phenotypic traits, either positive or negative, is important to understand. A future are of research includes investigating the epigenetic basis of this transmission to discover possible key differences that promote either a healthy or unhealthy offspring which will have life-long influence and consequence.

7.4.2 Gene knockout and impact on lifespan regulation

Additionally, a genetically static population allows for phenotypic characterisation of single gene knock outs for statistically relevant sample sizes. The latter is easily achievable due to the availability of various genetic manipulation tools such as CRISPR, TALEN and RNAi for *Daphnia* (Schumpert et al., 2016, Nakanishi et al., 2016, Kumagai et al., 2017). Furthermore, *Daphnia* shares the most genes in common with humans among any other arthropod and other established invertebrate model organisms of ageing (Colbourne et al., 2011). Most interestingly, genetically identical female and male *Daphnia* have evolved different average lifespans (Schwarzenberger et al., 2014), providing a unique opportunity for understanding the underlying mechanisms of ageing and regulation of lifespan.

Notably, the RNAi feeding technique has been optimised for *Daphnia* which allows the knockdown of genes in adults (Schumpert et al., 2015b) and was successfully implemented for the knockdown of Sir2 (Schumpert et al., 2016). This technique further expands the practicality of *Daphnia* as a model for ageing research. It would be of interest to knockdown genes known to influence lifespan and evaluate the ageing

phenotypic and molecular markers described here, as well as add to the developing pool of knowledge of the role of epigenetics in ageing. *Daphnia* is an ecologically and evolutionary important organism which has much to offer to the understanding of epigenetics (Harris et al., 2012).

With advancements in technologies and big data it is now possible to perform multi-omics studies. In this thesis, lipidomics and RNA-sequencing data were generated which individually show differences with sex, age and sex:age interaction, discussed in depth in Chapters 4 and 5. The combination of these data with DNA methylation could provide insights into the regulation of gene expression and impact of this on regulatory pathways which influence the difference in ageing between sexes observed in *D. magna* shown here.

The future of ageing research holds much promise for increasing health-span with the possibility of extending maximum lifespan. The use of model organisms has so far been fundamental in progressing the field and *Daphnia* has potential to be an invaluable asset in future advancements.

References

AERTS, A. M., FRANÇOIS, I. E. J. A., BAMMENS, L., CAMMUE, B. P. A., SMETS, B., WINDERICKX, J., ACCARDO, S., DE VOS, D. E. & THEVISSEN, K. 2006. Level of M(IP)2C sphingolipid affects plant defensin sensitivity, oxidative stress resistance and chronological life-span in yeast. *FEBS Letters,* 580**,** 1903-1907.

AFAR. 2011. *Animal models for ageing research* [Online]. American Federation of Aging Research. Available: https://www.afar.org/docs/migrated/111114_ANIMAL_MODELSFR.pdf [Accessed June 2017 2017].

AHMED, A. S. I., SHENG, M. H. C., WASNIK, S., BAYLINK, D. J. & LAU, K.-H. W. 2017. Effect of aging on stem cells. *World Journal of Experimental Medicine,* 7**,** 1-10.

ALLMAN, J., ROSIN, A., KUMAR, R. & HASENSTAUB, A. 1998. Parenting and survival in anthropoid primates: Caretakers live longer. *Proceedings of the National Academy of Sciences,* 95**,** 6866.

AMBERKAR, S. S. & KADERALI, L. 2015. An integrative approach for a network based meta-analysis of viral RNAi screens. *Algorithms for Molecular Biology,* 10**,** 6.

AMIN, S. 2018. *The Life Extension Revolution: Theories of Ageing* [Online]. Available: https://medium.com/predict/the-life-extension-revolution-theories-of-aging-5929345a94c3 [Accessed 26/05/2020 2020].

ANAGNOSTIS, P., STEVENSON, J. C., CROOK, D., JOHNSTON, D. G. & GODSLAND, I. F. 2016. Effects of gender, age and menopausal status on serum apolipoprotein concentrations. *Clinical Endocrinology,* 85**,** 733-740.

ANAND, K., SUDHEER, A. & CHATTERJEE, K. 2018. Alteration in serum lipid profile pattern in oral cancer and oral submucous fibrosis patients. *Journal of Indian Academy of Oral Medicine and Radiology,* 30**,** 38-40.

ANDERSON, R. M., BITTERMAN, K. J., WOOD, J. G., MEDVEDIK, O. & SINCLAIR, D. A. 2003. Nicotinamide and PNC1 govern lifespan extension by calorie restriction in Saccharomyces cerevisiae. *Nature,* 423**,** 181-185.

ANDZIAK, B., O'CONNOR TIMOTHY, P., QI, W., DEWAAL ERIC, M., PIERCE, A., CHAUDHURI ASISH, R., VAN REMMEN, H. & BUFFENSTEIN, R. 2006. High oxidative damage levels in the longest-living rodent, the naked mole-rat. *Aging Cell,* 5**,** 463-471.

ANKUTOWICZ, E. J. & LAIRD, R. A. 2018. Offspring of older parents are smaller—but no less bilaterally symmetrical—than offspring of younger parents in the aquatic plant Lemna turionifera. *Ecology and Evolution,* 8**,** 679-687.

ARANDA-ANZALDO, A. & DENT, M. A. R. 2007. Reassessing the role of p53 in cancer and ageing from an evolutionary perspective. *Mechanisms of Ageing and Development,* 128**,** 293-302.

ASSELMAN, J., DE CONINCK, D. I., PFRENDER, M. E. & DE SCHAMPHELAERE, K. A. 2016. Gene Body Methylation Patterns in Daphnia Are Associated with Gene Family Size. *Genome Biol Evol,* 8**,** 1185-96.

ATHANASIO, C. G., CHIPMAN, J. K., VIANT, M. R. & MIRBAHAI, L. 2016. Optimisation of DNA extraction from the crustacean Daphnia. *PeerJ,* 4**,** e2004.

ATHANASIO, C. G., SOMMER, U., VIANT, M. R., CHIPMAN, J. K. & MIRBAHAI, L. 2018. Use of 5-azacytidine in a proof-of-concept study to evaluate the impact of pre-natal and post-natal exposures, as well as within generation persistent DNA methylation changes in Daphnia. *Ecotoxicology*.

AURO, K., JOENSUU, A., FISCHER, K., KETTUNEN, J., SALO, P., MATTSSON, H., NIIRONEN, M., KAPRIO, J., ERIKSSON, J. G., LEHTIMÄKI, T., RAITAKARI, O., JULA, A., TIITINEN, A., JAUHIAINEN, M., SOININEN, P., KANGAS, A. J., KÄHÖNEN, M., HAVULINNA, A. S., ALA-KORPELA, M., SALOMAA, V., METSPALU, A. & PEROLA, M. 2014. A metabolic view on menopause and ageing. *Nature Communications,* 5**,** 4708.

AUSTAD, S. N. & FISCHER, K. E. 2016. Sex Differences in Lifespan. *Cell Metab,* 23**,** 1022-1033.

BAARS, A., OOSTING, A., LOHUIS, M., KOEHORST, M., EL AIDY, S., HUGENHOLTZ, F., SMIDT, H., MISCHKE, M., BOEKSCHOTEN, M. V., VERKADE, H. J., GARSSEN, J., VAN DER BEEK, E. M., KNOL, J., DE VOS, P., VAN BERGENHENEGOUWEN, J. & FRANSEN, F. 2018. Sex differences in lipid metabolism are affected by presence of the gut microbiota. *Scientific Reports,* 8**,** 13426.

BARATA, C., CARLOS NAVARRO, J., VARO, I., CARMEN RIVA, M., ARUN, S. & PORTE, C. 2005a. Changes in antioxidant enzyme activities, fatty acid composition and lipid peroxidation in Daphnia magna during the aging process. *Comparative Biochemistry and Physiology Part B: Biochemistry and Molecular Biology,* 140**,** 81-90.

BARATA, C., VARO, I., NAVARRO, J. C., ARUN, S. & PORTE, C. 2005b. Antioxidant enzyme activities and lipid peroxidation in the freshwater cladoceran Daphnia magna exposed to redox cycling compounds. *Comparative Biochemistry and Physiology Part C: Toxicology & Pharmacology,* 140**,** 175-186.

BARBIERI, M., BONAFÈ, M., FRANCESCHI, C. & PAOLISSO, G. 2003. Insulin/IGF-I-signaling pathway: an evolutionarily conserved mechanism of longevity from yeast to humans. *American Journal of Physiology-Endocrinology and Metabolism,* 285**,** E1064-E1071.

BARKS, P. M. & LAIRD, R. A. 2016. A multigenerational effect of parental age on offspring size but not fitness in common duckweed (Lemna minor). *Journal of Evolutionary Biology,* 29**,** 748-756.

BELL, A. G. 1918. *The duration of life and conditions associated with longevity: a study of the Hyde genealogy*, Genealogical Record Office.

BENEDETTO, A., BAMBADE, T., AU, C., TULLET, J. M., MONKHOUSE, J., DANG, H., CETNAR, K., CHAN, B., CABREIRO, F. & GEMS, D. 2019. New label-free automated survival assays reveal unexpected stress resistance patterns during C. elegans aging. *Aging cell,* 18**,** e12998.

BENJAMINI, Y. & HOCHBERG, Y. 1995. Controlling the False Discovery Rate: A Practical and Powerful Approach to Multiple Testing. *Journal of the Royal Statistical Society: Series B (Methodological),* 57**,** 289-300.

BENZIE, J. A. 2005. *The Genus Daphnia (including Daphniopsis):(Anomopoda, Daphniidae)*, Kenobi Productions.

BERGAN, J., SKOTLAND, T., SYLVÄNNE, T., SIMOLIN, H., EKROOS, K. & SANDVIG, K. 2013. The ether lipid precursor hexadecylglycerol causes major changes in the lipidome of HEp-2 cells. *PloS one,* 8**,** e75904-e75904.

BERGHÄNEL, A., HEISTERMANN, M., SCHÜLKE, O. & OSTNER, J. 2017. Prenatal stress accelerates offspring growth to compensate for reduced maternal investment across mammals. *Proceedings of the National Academy of Sciences,* 114**,** E10658.

BEUKEBOOM, L., PANNEBAKKER, B., GERRITSMA, S. & GEUVERINK, E. 2009. A role for sexual conflict in the evolution of reproductive traits in Nasonia wasps? *Animal Biology,* 59**,** 417-434.

BLOCH QAZI, M. C., MILLER, P. B., POESCHEL, P. M., PHAN, M. H., THAYER, J. L. & MEDRANO, C. L. 2017. Transgenerational effects of maternal and grandmaternal age on offspring viability and performance in Drosophila melanogaster. *Journal of Insect Physiology,* 100**,** 43-52.

BLOUNT, J. D., METCALFE, N. B., ARNOLD, K. E., SURAI, P. F., DEVEVEY, G. L. & MONAGHAN, P. 2003. Neonatal nutrition, adult antioxidant defences and sexual attractiveness in the zebra finch. *Proceedings of the Royal Society of London. Series B: Biological Sciences,* 270**,** 1691-1696.

BOCK, M. J., JARVIS, G. C., COREY, E. L., STONE, E. E. & GRIBBLE, K. E. 2019. Maternal age alters offspring lifespan, fitness, and lifespan extension under caloric restriction. *Scientific Reports,* 9**,** 3138.

BONDURIANSKY, R., MAKLAKOV, A., ZAJITSCHEK, F. & BROOKS, R. 2008. Sexual selection, sexual conflict and the evolution of ageing and life span. *Functional Ecology,* 22**,** 443-453.

BOSCO, C., GARMO, H., HAMMAR, N., WALLDIUS, G., JUNGNER, I., MALMSTRÖM, H., HOLMBERG, L. & VAN HEMELRIJCK, M. 2018. Glucose, lipids and gamma-glutamyl transferase measured before prostate cancer diagnosis and secondly diagnosed primary tumours: a prospective study in the Swedish AMORIS cohort. *BMC Cancer,* 18**,** 205.

BUFFENSTEIN, R. 2005. The Naked Mole-Rat: A New Long-Living Model for Human Aging Research. *The Journals of Gerontology: Series A,* 60**,** 1369-1377.

BUFFENSTEIN, R. 2008. Negligible senescence in the longest living rodent, the naked mole-rat: insights from a successfully aging species. *Journal of Comparative Physiology B,* 178**,** 439-445.

BUFFENSTEIN, R., EDREY, Y. H. & LARSEN, P. L. 2008. Animal Models in Aging Research. *In:* CONN, P. M. (ed.) *Sourcebook of Models for Biomedical Research.* Totowa, NJ: Humana Press.

BUSTOS, V. & PARTRIDGE, L. 2017. Good Ol' Fat: Links between Lipid Signaling and Longevity. *Trends in biochemical sciences,* 42**,** 812-823.

BUTTON, E. B., ROBERT, J., CAFFREY, T. M., FAN, J., ZHAO, W. & WELLINGTON, C. L. 2019. HDL from an Alzheimer's disease perspective. *Current Opinion in Lipidology,* 30.

CALZADA, E., ONGUKA, O. & CLAYPOOL, S. M. 2016. Phosphatidylethanolamine Metabolism in Health and Disease. *International review of cell and molecular biology,* 321**,** 29-88.

CAMPISI, J., KAPAHI, P., LITHGOW, G. J., MELOV, S., NEWMAN, J. C. & VERDIN, E. 2019. From discoveries in ageing research to therapeutics for healthy ageing. *Nature,* 571**,** 183-192.

CARRASCO, S. & MÉRIDA, I. 2007. Diacylglycerol, when simplicity becomes complex. *Trends in Biochemical Sciences,* 32**,** 27-36.

CARTER, M. J., SILVA-FLORES, P., OYANEDEL, J. P. & RAMOS-JILIBERTO, R. 2013. Morphological and life-history shifts of the exotic cladoceran Daphnia exilis in response to predation risk and food availability. *Limnologica,* 43**,** 203-209.

CATANIA, J. & FAIRWEATHER, D. S. 1991. DNA methylation and cellular ageing. *Mutation Research/DNAging,* 256**,** 283-293.

CHEN, J.-H., HALES, C. N. & OZANNE, S. E. 2007. DNA damage, cellular senescence and organismal ageing: causal or correlative? *Nucleic Acids Research,* 35**,** 7417-7428.

CHRISTIE, W. W. 2019. *Sterols: 1. Cholesterol and Cholesterol Esters* [Online]. The Lipid Web. Available: http://lipidhome.co.uk/lipids/simple/cholest/index.htm [Accessed 14.05.19 2019].

CLUTTON-BROCK, T. H. 2019. *The evolution of parental care*, Princeton University Press.

CLUTTON-BROCK, T. H. & ISVARAN, K. 2007. Sex differences in ageing in natural populations of vertebrates. *Proc. R. Soc. B.,* 274**,** 8.

COLBOURNE, J. K., PFRENDER, M. E., GILBERT, D., THOMAS, W. K., TUCKER, A., OAKLEY, T. H., TOKISHITA, S., AERTS, A., ARNOLD, G. J., BASU, M. K., BAUER, D. J., CÁCERES, C. E., CARMEL, L., CASOLA, C., CHOI, J.-H., DETTER, J. C., DONG, Q., DUSHEYKO, S., EADS, B. D., FRÖHLICH, T., GEILER-SAMEROTTE, K. A., GERLACH, D., HATCHER, P., JOGDEO, S., KRIJGSVELD, J., KRIVENTSEVA, E. V., KÜLTZ, D., LAFORSCH, C., LINDQUIST, E., LOPEZ, J., MANAK, J. R., MULLER, J., PANGILINAN, J., PATWARDHAN, R. P., PITLUCK, S., PRITHAM, E. J., RECHTSTEINER, A., RHO, M., ROGOZIN, I. B., SAKARYA, O., SALAMOV, A., SCHAACK, S., SHAPIRO, H., SHIGA, Y., SKALITZKY, C., SMITH, Z., SOUVOROV, A., SUNG, W., TANG, Z., TSUCHIYA, D., TU, H., VOS, H., WANG, M., WOLF, Y. I., YAMAGATA, H., YAMADA, T., YE, Y., SHAW, J. R., ANDREWS, J., CREASE, T. J., TANG, H., LUCAS, S. M., ROBERTSON, H. M., BORK, P., KOONIN, E. V., ZDOBNOV, E. M., GRIGORIEV, I. V., LYNCH, M. & BOORE, J. L. 2011. The Ecoresponsive Genome of Daphnia pulex. *Science,* 331**,** 555.

CONSTANTINOU, J., SULLIVAN, J. & MIRBAHAI, L. 2019. Ageing differently: Sex-dependent ageing rates in Daphnia magna. *Experimental Gerontology,* 121**,** 33-45.

CONSTANTINOU, J. K., SOUTHAM, A. D., KVIST, J., JONES, M. R., VIANT, M. R. & MIRBAHAI, L. 2020. characterisation of the dynamic nature of lipids throughout the lifespan of genetically identical female and male Daphnia magna. *Scientific reports,* 10**,** 1-15.

COOK, S., TOGNI, M., SCHAUB, M. C., WENAWESER, P. & HESS, O. M. 2006. High heart rate: a cardiovascular risk factor? *European heart journal,* 27**,** 2387-2393.

CUTLER, R. G., THOMPSON, K. W., CAMANDOLA, S., MACK, K. T. & MATTSON, M. P. 2014. Sphingolipid metabolism regulates development and lifespan in Caenorhabditis elegans. *Mechanisms of ageing and development,* 143**,** 9-18.

D'AQUILA, P., ROSE, G., BELLIZZI, D. & PASSARINO, G. 2013. Epigenetics and aging. *Maturitas,* 74**,** 130-136.

DASARI, S. & TCHOUNWOU, P. B. 2014. Cisplatin in cancer therapy: molecular mechanisms of action. *European journal of pharmacology,* 0**,** 364-378.

DASHEIFF, B. D. & DASHEIFF, R. M. 2002. Photonegative Response in Brown Planaria (Dugesia tigrina) Following Regeneration. *Ecotoxicology and Environmental Safety,* 53**,** 196-199.

DAVINELLI, S. & DE VIVO, I. 2019. Lifestyle Choices, Psychological Stress and Their Impact on Ageing: The Role of Telomeres. *Centenarians.* Springer.

DE MAGALHÃES, J. P., CURADO, J. & CHURCH, G. M. 2009. Meta-analysis of age-related gene expression profiles identifies common signatures of aging. *Bioinformatics,* 25**,** 875-881.

DE MAGALHÃES, J. P. & PASSOS, J. F. 2018. Stress, cell senescence and organismal ageing. *Mechanisms of Ageing and Development,* 170**,** 2-9.

DE MAGALHAES, J. P., STEVENS, M. & THORNTON, D. 2017. The Business of Anti-Aging Science. *Trends Biotechnol,* 35**,** 1062-1073.

DELABAERE, L., ERTL, H., MASSEY, D., HOFLEY, C., SOHAIL, F., BIENENSTOCK, E., SEBASTIAN, H., CHIOLO, I. & LAROCQUE, J. 2017. Aging impairs DSBs repair by homologous recombination in *Drosophila* germ cells. *Aging Cell***,** 9.

DEMONTIS, F., PICCIRILLO, R., GOLDBERG, A. L. & PERRIMON, N. 2013. Mechanisms of skeletal muscle aging: insights from Drosophila and mammalian models. *Disease Models &amp; Mechanisms*.

DÍAZ, M., FABELO, N., FERRER, I. & MARÍN, R. 2018. "Lipid raft aging" in the human frontal cortex during nonpathological aging: gender influences and potential implications in Alzheimer's disease. *Neurobiology of Aging,* 67**,** 42-52.

DICKINSON, D. A. & FORMAN, H. J. 2002. Cellular glutathione and thiols metabolism. *Biochemical Pharmacology,* 64**,** 1019-1026.

DIETERLE, F., ROSS, A., SCHLOTTERBECK, G. & SENN, H. 2006. Probabilistic Quotient Normalization as Robust Method to Account for Dilution of Complex Biological Mixtures. Application in 1H NMR Metabonomics. *Analytical Chemistry,* 78**,** 4281-4290.

DODSON, S. I., TOLLRIAN, R. & LAMPERT, W. 1997. Daphnia swimming behavior during vertical migration. *Journal of Plankton Research,* 19**,** 969-978.

ĐỨC, N. T., CHI, V., DAO, C.-T., NGO XUAN, Q. & DAO, S. 2016. *CHRONIC EFFECTS OF INDUSTRIAL WASTEWATER ON LIFE HISTORY TRAITS OF Daphnia magna UNDER THE LABORATORY CONDITIONS*.

DUDYCHA, J. L. & HASSEL, C. 2013. Aging in sexual and obligately asexual clones of Daphnia from temporary ponds. *Journal of Plankton Research,* 35**,** 253-259.

DUTTA, A. & SHARMA-WALIA, N. 2019. Curbing Lipids: Impacts ON Cancer and Viral Infection. *International Journal of Molecular Sciences,* 20.

EBERT, D. 2005. *Ecology, Epidemiology and Evolution of Parasitism in Daphnia*.

EDREY, Y. H., HANES, M., PINTO, M., MELE, J. & BUFFENSTEIN, R. 2011. Successful Aging and Sustained Good Health in the Naked Mole Rat: A Long-Lived Mammalian Model for Biogerontology and Biomedical Research. *ILAR Journal,* 52**,** 41-53.

EGAWA, J., PEARN, M. L., LEMKUIL, B. P., PATEL, P. M. & HEAD, B. P. 2016. Membrane lipid rafts and neurobiology: age-related changes in membrane lipids and loss of neuronal function. *The Journal of Physiology,* 594**,** 4565-4579.

EISENBERG DAN, T. A. & KUZAWA CHRISTOPHER, W. 2018. The paternal age at conception effect on offspring telomere length: mechanistic, comparative and adaptive perspectives. *Philosophical Transactions of the Royal Society B: Biological Sciences,* 373**,** 20160442.

ELLEGREN, H. & PARSCH, J. 2007. The evolution of sex-biased genes and sex-biased gene expression. *Nature Reviews Genetics,* 8**,** 689-698.

ERMOLAEVA, M., NERI, F., ORI, A. & RUDOLPH, K. L. 2018. Cellular and epigenetic drivers of stem cell ageing. *Nature Reviews Molecular Cell Biology,* 19**,** 594-610.

EVANS, E. A., CHEN, W. C. & TAN, M. W. 2008. The DAF-2 insulin-like signaling pathway independently regulates aging and immunity in C. elegans. *Aging Cell,* 7**,** 879-93.

EYER, M., DAINAT, B., NEUMANN, P. & DIETEMANN, V. 2017. Social regulation of ageing by young workers in the honey bee, Apis mellifera. *Experimental Gerontology,* 87**,** 84-91.

FAIRBAIRN, D. J., BLANCKENHORN, W. U. & SZÉKELY, T. 2007. *Sex, Size and Gender Roles: Evolutionary Studies of Sexual Dimorphism*, Oxford University Press.

FAKOURI, N. B., HOU, Y., DEMAREST, T. G., CHRISTIANSEN, L. S., OKUR, M. N., MOHANTY, J. G., CROTEAU, D. L. & BOHR, V. A. 2019. Toward understanding genomic instability, mitochondrial dysfunction and aging. *The FEBS Journal,* 286**,** 1058-1073.

FLIER, J. S. 1995. The adipocyte: storage depot or node on the energy information superhighway? *Cell,* 80**,** 15-18.

FOX, C. W., BUSH, M. L. & WALLIN, W. G. 2003. Maternal age affects offspring lifespan of the seed beetle, Callosobruchus maculatus. *Functional Ecology,* 17**,** 811-820.

FREITAS, A. A. & DE MAGALHAES, J. P. 2011. A review and appraisal of the DNA damage theory of ageing. *Mutat Res,* 728**,** 12-22.

FUKUNAGA, K. & HOSTETLER, L. 1975. The estimation of the gradient of a density function, with applications in pattern recognition. *IEEE Transactions on Information Theory,* 21**,** 32-40.

GARSIN, D. A., VILLANUEVA, J. M., BEGUN, J., KIM, D. H., SIFRI, C. D., CALDERWOOD, S. B., RUVKUN, G. & AUSUBEL, F. M. 2003. Long-lived C. elegans daf-2 mutants are resistant to bacterial pathogens. *Science,* 300**,** 1921-1921.

GASCHLER, M. M. & STOCKWELL, B. R. 2017. Lipid peroxidation in cell death. *Biochemical and Biophysical Research Communications,* 482**,** 419-425.

GENSLER, H. L. & BERNSTEIN, H. 1981. DNA Damage as the Primary Cause of Aging. *The Quarterly Review of Biology,* 56**,** 279-303.

GENT, S., KLEINBONGARD, P., DAMMANN, P., NEUHÄUSER, M. & HEUSCH, G. 2015. Heart rate reduction and longevity in mice. *Basic research in cardiology,* 110**,** 2.

GERL, M. J., VAZ, W. L. C., DOMINGUES, N., KLOSE, C., SURMA, M. A., SAMPAIO, J. L., ALMEIDA, M. S., RODRIGUES, G., ARAÚJO-GONÇALVES, P., FERREIRA, J., BORBINHA, C., MARTO, J. P., VIANA-BAPTISTA,

M., SIMONS, K. & VIEIRA, O. V. 2018. Cholesterol is Inefficiently Converted to Cholesteryl Esters in the Blood of Cardiovascular Disease Patients. *Scientific Reports,* 8**,** 14764.

GILLESPIE, D. O. S., RUSSELL, A. F. & LUMMAA, V. 2013. THE EFFECT OF MATERNAL AGE AND REPRODUCTIVE HISTORY ON OFFSPRING SURVIVAL AND LIFETIME REPRODUCTION IN PREINDUSTRIAL HUMANS. *Evolution,* 67**,** 1964-1974.

GIUSTARINI, D., DALLE-DONNE, I., LORENZINI, S., MILZANI, A. & ROSSI, R. 2006. Age-Related Influence of Thiols, Disulfide, and Protein-Mixed Disulfide Levels in Human Plasma. *Journal of Gerontology,* 61A**,** 9.

GÓMEZ, R., VAN DAMME, K., GOSÁLVEZ, J., MORÁN, E. S. & COLBOURNE, J. K. 2016. Male meiosis in Crustacea: synapsis, recombination, epigenetics and fertility in Daphnia magna. *Chromosoma,* 125**,** 769-787.

GONZALEZ-COVARRUBIAS, V. 2013. Lipidomics in longevity and healthy aging. *Biogerontology,* 14**,** 663-672.

GONZALEZ-COVARRUBIAS, V., BEEKMAN, M., UH, H.-W., DANE, A., TROOST, J., PALIUKHOVICH, I., VAN DER KLOET, F. M., HOUWING-DUISTERMAAT, J., VREEKEN, R. J., HANKEMEIER, T. & SLAGBOOM, E. P. 2013. Lipidomics of familial longevity. *Aging Cell,* 12**,** 426-434.

GOODRICK, C. L., INGRAM, D. K., REYNOLDS, M. A., FREEMAN, J. R. & CIDER, N. 1990. Effects of intermittent feeding upon body weight and lifespan in inbred mice: interaction of genotype and age. *Mechanisms of Ageing and Development,* 55**,** 69-87.

GOPALAKRISHNAN, S., CHEUNG, N. K. M., YIP, B. W. P. & AU, D. W. T. 2013. Medaka fish exhibits longevity gender gap, a natural drop in estrogen and telomere shortening during aging: a unique model for studying sex-dependent longevity. *Frontiers in Zoology,* 10**,** 78.

GREENFIELD, M. S., KRAEMER, F., TOBEY, T. & REAVEN, G. 1980. Effect of age on plasma triglyceride concentrations in man. *Metabolism,* 29**,** 1095-9.

GRIBBLE, K. E. 2018. MATERNAL EFFECTS ON OFFSPRING AGING: ROTIFERS AS A MODEL SYSTEM FOR AGING. *Innovation in Aging,* 2**,** 625-625.

GRINTZALIS, K., GEORGIOU, C. D. & SCHNEIDER, Y. J. 2015. An accurate and sensitive Coomassie Brilliant Blue G-250-based assay for protein determination. *Anal Biochem,* 480**,** 28-30.

GRINTZALIS, K., PAPAPOSTOLOU, I., ZISIMOPOULOS, D., STAMATIOU, I. & GEORGIOU, C. D. 2014. Multiparametric protocol for the determination of thiol redox state in living matter. *Free Radic Biol Med,* 74**,** 85-98.

GRINTZALIS, K., ZISIMOPOULOS, D., GRUNE, T., WEBER, D. & GEORGIOU, C. D. 2013. Method for the simultaneous determination of free/protein malondialdehyde and lipid/protein hydroperoxides. *Free Radic Biol Med,* 59**,** 27-35.

GROTEWIEL, M. S., MARTIN, I., BHANDARI, P. & COOK-WIENS, E. 2005. Functional senescence in Drosophila melanogaster. *Ageing Research Reviews,* 4**,** 372-397.

GRUNER, H. N., BAE, B., LYNCH, M., OLIVER, D., SO, K., MASTICK, G. S., YAN, W. & MIURA, P. 2019. Precise removal of Calm1 long 3' UTR isoform by CRISPR-Cas9 genome editing impairs dorsal root ganglion development in mice. *bioRxiv,* 553990.

GRUNTENKO, N. E., WEN, D., KARPOVA, E. K., ADONYEVA, N. V., LIU, Y., HE, Q., FADDEEVA, N. V., FOMIN, A. S., LI, S. & RAUSCHENBACH, I. Y. 2010. Altered juvenile hormone metabolism, reproduction and stress response in Drosophila adults with genetic ablation of the corpus allatum cells. *Insect Biochem Mol Biol,* 40**,** 891-7.

GU, T., ZHOU, W., SUN, J., WANG, J., ZHU, D. & BI, Y. 2018. Gender and Age Differences in Lipid Profile Among Chinese Adults in Nanjing: a Retrospective Study of Over 230,000 Individuals from 2009 to 2015. *Exp Clin Endocrinol Diabetes,* 126.

GUILLAS, I., KIRCHMAN, P. A., CHUARD, R., PFEFFERLI, M., JIANG, J. C., JAZWINSKI, S. M. & CONZELMANN, A. 2001. C26-CoA-dependent ceramide synthesis of Saccharomyces cerevisiae is operated by Lag1p and Lac1p. *The EMBO journal,* 20**,** 2655-2665.

HALL, M. E., NASIR, L., DAUNT, F., GAULT, E. A., CROXALL, J. P., WANLESS, S. & MONAGHAN, P. 2004. Telomere loss in relation to age and early environment in long-lived birds. *Proceedings of the Royal Society of London. Series B: Biological Sciences,* 271**,** 1571-1576.

HANNUN, Y. A. & OBEID, L. M. 2008. Principles of bioactive lipid signalling: lessons from sphingolipids. *Nature Reviews Molecular Cell Biology,* 9**,** 139.

HANSEN, M., FLATT, T. & AGUILANIU, H. 2013. Reproduction, fat metabolism, and life span: what is the connection? *Cell metabolism,* 17**,** 10-19.

HAREL, I., BENAYOUN, BÉRÉNICE A., MACHADO, B., SINGH, PARAM P., HU, C.-K., PECH, MATTHEW F., VALENZANO, DARIO R., ZHANG, E., SHARP, SABRINA C., ARTANDI, STEVEN E. & BRUNET, A. 2015. A

Platform for Rapid Exploration of Aging and Diseases in a Naturally Short-Lived Vertebrate. *Cell,* 160**,** 1013-1026.

HAREL, I. & BRUNET, A. 2015. The African Turquoise Killifish: A Model for Exploring Vertebrate Aging and Diseases in the Fast Lane. *Cold Spring Harb Symp Quant Biol,* 80**,** 275-9.

HARMAN, D. 1956. Aging: A Theory Based on Free Radical and Radiation Chemistry. *Journal of Gerontology,* 11**,** 298-300.

HARRIS, I. D., FRONCZAK, C., ROTH, L. & MEACHAM, R. B. 2011. Fertility and the Aging Male. *Reviews in Urology,* 13**,** e184-e190.

HARRIS, K. D., BARTLETT, N. J. & LLOYD, V. K. 2012. Daphnia as an emerging epigenetic model organism. *Genet Res Int,* 2012**,** 147892.

HAWCROFT, D. M. & MARTIN, P. A. 1974. Studies on age related changes in the lipids of mouse liver microsomes. *Mechanisms of Ageing and Development,* 3**,** 121-130.

HAYASHI, M. T. & KARLSEDER, J. 2013. DNA damage associated with mitosis and cytokinesis failure. *Oncogene,* 32**,** 4593-4601.

HE, Y. & JASPER, H. 2014. Studying aging in Drosophila. *Methods,* 68**,** 129-33.

HEARN, J., CHOW FRANKLIN, W.-N., BARTON, H., TUNG, M., WILSON PHILIP, J., BLAXTER, M., BUCK, A. & LITTLE TOM, J. 2018a. Daphnia magna microRNAs respond to nutritional stress and ageing but are not transgenerational. *Molecular Ecology,* 27**,** 1402-1412.

HEARN, J., PEARSON, M., BLAXTER, M., WILSON, P. J. & LITTLE, T. J. 2018b. Genome-wide Methylation Patterns Under Caloric Restriction in Daphnia magna. *bioRxiv*.

HEBERT, P. 1987. Genetics of Daphnia. *Daphnia. Mem Inst Ital Idrobiol,* 45**,** 439-460.

HECKMANN, L. H., CONNON, R., HUTCHINSON, T. H., MAUND, S. J., SIBLY, R. M. & CALLAGHAN, A. 2006. Expression of target and reference genes in Daphnia magna exposed to ibuprofen. *BMC Genomics,* 7**,** 175.

HEID, J., CENCIONI, C., RIPA, R., BAUMGART, M., ATLANTE, S., MILANO, G., SCOPECE, A., KUENNE, C., GUENTHER, S. & AZZIMATO, V. 2017. Age-dependent increase of oxidative stress regulates microRNA-29 family preserving cardiac health. *Scientific reports,* 7**,** 1-15.

HEILBRONN, L. K. & RAVUSSIN, E. 2003. Calorie restriction and aging: review of the literature and implications for studies in humans. *The American Journal of Clinical Nutrition,* 78**,** 361-369.

HEWITT, J. 2017. *How to grow old like an athlete* [Online]. World Economic Forum. Available: https://www.weforum.org/agenda/2017/02/healthspan-vs-lifespan/ [Accessed June 2017 2017].

HIPP, M. S., KASTURI, P. & HARTL, F. U. 2019. The proteostasis network and its decline in ageing. *Nature Reviews Molecular Cell Biology,* 20**,** 421-435.

HORVATH, S. 2013. DNA methylation age of human tissues and cell types. *Genome Biology,* 14**,** 3156.

HORVATH, S., GURVEN, M., LEVINE, M. E., TRUMBLE, B. C., KAPLAN, H., ALLAYEE, H., RITZ, B. R., CHEN, B., LU, A. T., RICKABAUGH, T. M., JAMIESON, B. D., SUN, D., LI, S., CHEN, W., QUINTANA-MURCI, L., FAGNY, M., KOBOR, M. S., TSAO, P. S., REINER, A. P., EDLEFSEN, K. L., ABSHER, D. & ASSIMES, T. L. 2016. An epigenetic clock analysis of race/ethnicity, sex, and coronary heart disease. *Genome Biology,* 17**,** 171.

HOWELL, R., DOMINGUEZ-LOPEZ, S., PARIKH, I., CHUCAIR-ELLIOTT, A. J., OCANAS, S., FREEMAN, W. M. & BECKSTEAD, M. J. 2019. Female mice are resilient to age-related decline of substantia nigra dopamine neuron firing parameters. *bioRxiv***,** 621680.

HULBERT, A. J., KELLY, M. A. & ABBOTT, S. K. 2014. Polyunsaturated fats, membrane lipids and animal longevity. *Journal of Comparative Physiology B,* 184**,** 149-166.

IAMPOLSKIĬ, L. I. & GALIMOV, I. 2005. Evolutionary genetics of aging in Daphnia. *Zhurnal obshchei biologii,* 66**,** 416-424.

INNOCENTI, P. & MORROW, E. H. 2010. The sexually antagonistic genes of Drosophila melanogaster. *PLoS biology,* 8**,** e1000335.

INNOMINATO, P. F., LÉVI, F. A. & BJARNASON, G. A. 2010. Chronotherapy and the molecular clock: Clinical implications in oncology. *Advanced Drug Delivery Reviews,* 62**,** 979-1001.

ISSA, J.-P. 2014. Aging and epigenetic drift: a vicious cycle. *The Journal of Clinical Investigation,* 124**,** 24-29.

JARAK, I., ALMEIDA, S., CARVALHO, R. A., SOUSA, M., BARROS, A., ALVES, M. G. & OLIVEIRA, P. F. 2018. Senescence and declining reproductive potential: Insight into molecular mechanisms through testicular metabolomics. *Biochimica et Biophysica Acta (BBA) - Molecular Basis of Disease,* 1864**,** 3388-3396.

JEFFERY, W. R. 2018. Regeneration and Aging in the Tunicate Ciona intestinalis. *Conn's Handbook of Models for Human Aging.* Elsevier.

JIN, L., JIANG, Z., XIA, Y., LOU, P. E., CHEN, L., WANG, H., BAI, L., XIE, Y., LIU, Y., LI, W., ZHONG, B., SHEN, J., JIANG, A. A., ZHU, L., WANG, J., LI, X. & LI, M. 2014. Genome-wide DNA methylation changes in skeletal muscle between young and middle-aged pigs. *BMC Genomics,* 15**,** 653.

JOHNSON, A. A. & STOLZING, A. 2019. The role of lipid metabolism in aging, lifespan regulation, and age-related disease. *Aging cell,* 18**,** e13048-e13048.

KALBEN, B. B. 2000. Why Men Die Younger. *North American Actuarial Journal,* 4**,** 83-111.

KAPAHI, P., KAEBERLEIN, M. & HANSEN, M. 2017. Dietary restriction and lifespan: Lessons from invertebrate models. *Ageing Res Rev,* 39**,** 3-14.

KARNISKI, C., KRZYSZCZYK, E. & MANN, J. 2018. Senescence impacts reproduction and maternal investment in bottlenose dolphins. *Proc Biol Sci,* 285.

KASHIAN, D. R. & DODSON, S. I. 2004. Effects of vertebrate hormones on development and sex determination in Daphnia magna. *Environmental Toxicology and Chemistry,* 23**,** 1282-1288.

KASSAMBARA, A. & MUNDT, F. 2017. Package 'factoextra'. *Extract and visualize the results of multivariate data analyses,* 76.

KAWANISHI, N., KATO, Y., YOKOZEKI, K., SAWADA, S., SAKURAI, R., FUJIWARA, Y., SHINKAI, S., GODA, N. & SUZUKI, K. 2018. Effects of aging on serum levels of lipid molecular species as determined by lipidomics analysis in Japanese men and women. *Lipids in Health and Disease,* 17**,** 135.

KENYON, C. 2011. The first long-lived mutants: discovery of the insulin/IGF-1 pathway for ageing. *Philosophical Transactions of the Royal Society B: Biological Sciences,* 366**,** 9-16.

KENYON, C., CHANG, J., GENSCH, E., RUDNER, A. & TABTIANG, R. 1993. A C. elegans mutant that lives twice as long as wild type. *Nature,* 366**,** 461-464.

KENYON, C. J. 2010. The genetics of ageing. *Nature,* 464**,** 504.

KILHAM, S. S., KREEGER, D. A., SCOTT, S. G., GOULDEN, C. E. & HERRERA, L. 1998. COMBO: A defined freshwater culture medium for algae and zooplankton. *Hydrobiologia***,** 13.

KIM, E., ANSELL CHRISTINE, M. & DUDYCHA JEFFRY, L. 2013. Resveratrol and food effects on lifespan and reproduction in the model crustacean Daphnia. *Journal of Experimental Zoology Part A: Ecological Genetics and Physiology,* 321**,** 48-56.

KIM, R.-O., JO, M.-A., SONG, J., KIM, I.-C., YOON, S. & KIM, W.-K. 2018. Novel approach for evaluating pharmaceuticals toxicity using Daphnia model: analysis of the mode of cytochrome P450-generated metabolite action after acetaminophen exposure. *Aquatic Toxicology,* 196**,** 35-42.

KONG, A., FRIGGE, M. L., MASSON, G., BESENBACHER, S., SULEM, P., MAGNUSSON, G., GUDJONSSON, S. A., SIGURDSSON, A., JONASDOTTIR, A. & JONASDOTTIR, A. 2012. Rate of de novo mutations and the importance of father's age to disease risk. *Nature,* 488**,** 471-475.

KOSTYRKO, K., BOSSHARD, S., URBAN, Z. & MERMOD, N. 2015. A role for homologous recombination proteins in cell cycle regulation. *Cell Cycle,* 14**,** 2853-2861.

KUMAGAI, H., NAKANISHI, T., MATSUURA, T., KATO, Y. & WATANABE, H. 2017. CRISPR/Cas-mediated knock-in via non-homologous end-joining in the crustacean Daphnia magna. *PloS one,* 12**,** e0186112.

KVIST, J., GONÇALVES ATHANÀSIO, C., SHAMS SOLARI, O., BROWN, J. B., COLBOURNE, J. K., PFRENDER, M. E. & MIRBAHAI, L. 2018. Pattern of DNA Methylation in Daphnia: Evolutionary Perspective. *Genome Biology and Evolution,* 10**,** 1988-2007.

KYLE, J. E., ZHANG, X., WEITZ, K. K., MONROE, M. E., IBRAHIM, Y. M., MOORE, R. J., CHA, J., SUN, X., LOVELACE, E. S., WAGONER, J., POLYAK, S. J., METZ, T. O., DEY, S. K., SMITH, R. D., BURNUM-JOHNSON, K. E. & BAKER, E. S. 2016. Uncovering biologically significant lipid isomers with liquid chromatography, ion mobility spectrometry and mass spectrometry. *The Analyst,* 141**,** 1649-1659.

LACAL, I. & VENTURA, R. 2018. Epigenetic inheritance: concepts, mechanisms and perspectives. *Frontiers in molecular neuroscience,* 11**,** 292.

LAKOWSKI, B. & HEKIMI, S. 1996. Determination of life-span in Caenorhabditis elegans by four clock genes. *science,* 272**,** 1010-1013.

LAKOWSKI, B. & HEKIMI, S. 1998. The genetics of caloric restriction in Caenorhabditis elegans. *Proceedings of the National Academy of Sciences,* 95**,** 13091.

LAMPE, M. A., BURLINGAME, A., WHITNEY, J., WILLIAMS, M. L., BROWN, B. E., ROITMAN, E. & ELIAS, P. M. 1983. Human stratum corneum lipids: characterization and regional variations. *Journal of lipid research,* 24**,** 120-130.

LANSING, A. I. 1947. A transmissible, cumulative, and reversible factor in aging. *Journal of Gerontology, 2*, 228-239.

LANSING, A. I. 1954. A nongenic factor in the longevity of rotifers. *Annals of the New York Academy of Sciences, 57*, 455-464.

LATTA, L. C., WEIDER, L. J., COLBOURNE, J. K. & PFRENDER, M. E. 2012. The evolution of salinity tolerance in Daphnia: a functional genomics approach. *Ecology Letters, 15*, 794-802.

LÊ, S., JOSSE, J. & HUSSON, F. 2008. FactoMineR: an R package for multivariate analysis. *Journal of statistical software, 25*, 1-18.

LEMAÎTRE, J.-F., BERGER, V., BONENFANT, C., DOUHARD, M., GAMELON, M., PLARD, F. & GAILLARD, J.-M. 2015. Early-late life trade-offs and the evolution of ageing in the wild. *Proceedings of the Royal Society B: Biological Sciences, 282*, 20150209.

LEUPOLD, S., HUBMANN, G., LITSIOS, A., MEINEMA, A. C., TAKHAVEEV, V., PAPAGIANNAKIS, A., NIEBEL, B., JANSSENS, G., SIEGEL, D. & HEINEMANN, M. 2019. Saccharomyces cerevisiae goes through distinct metabolic phases during its replicative lifespan. *Elife, 8*, e41046.

LI, G.-Y. & ZHANG, Z.-Q. 2019. The sex- and duration-dependent effects of intermittent fasting on lifespan and reproduction of spider mite Tetranychus urticae. *Frontiers in zoology, 16*, 10-10.

LIM, A. S., MYERS, A. J., YU, L., BUCHMAN, A. S., DUFFY, J. F., DE JAGER, P. L. & BENNETT, D. A. 2013. Sex difference in daily rhythms of clock gene expression in the aged human cerebral cortex. *Journal of biological rhythms, 28*, 117-129.

LIU, J., WANG, L., WANG, Z. & LIU, J.-P. 2019. Roles of telomere biology in cell senescence, replicative and chronological ageing. *Cells, 8*, 54.

LOFTERØD, T., MORTENSEN, E. S., NALWOGA, H., WILSGAARD, T., FRYDENBERG, H., RISBERG, T., EGGEN, A. E., MCTIERNAN, A., AZIZ, S., WIST, E. A., STENSVOLD, A., REITAN, J. B., AKSLEN, L. A. & THUNE, I. 2018. Impact of pre-diagnostic triglycerides and HDL-cholesterol on breast cancer recurrence and survival by breast cancer subtypes. *BMC Cancer, 18*, 654.

LOHR, J. N. & HAAG, C. R. 2015. Genetic load, inbreeding depression, and hybrid vigor covary with population size: an empirical evaluation of theoretical predictions. *Evolution, 69*, 3109-3122.

LONGO, V. D., MITTELDORF, J. & SKULACHEV, V. P. 2005. Programmed and altruistic ageing. *Nature Reviews Genetics, 6*, 866.

LOPEZ-OTIN, C., BLASCO, M. A., PARTRIDGE, L., SERRANO, M. & KROEMER, G. 2013. The hallmarks of aging. *Cell, 153*, 1194-217.

LOVE, M. I., HUBER, W. & ANDERS, S. 2014. Moderated estimation of fold change and dispersion for RNA-seq data with DESeq2. *Genome Biology, 15*, 550.

LUMLEY, T. & LUMLEY, M. T. 2013. Package 'leaps'. *Regression Subset Selection. Thomas Lumley Based on Fortran Code by Alan Miller. Available online:* http://CRAN. *R-project. org/package= leaps (accessed on 18 March 2018).*

MAGINNIS, T. L. 2006. The costs of autotomy and regeneration in animals: a review and framework for future research. *Behavioral Ecology, 17*, 857-872.

MAGWERE, T., CHAPMAN, T. & PARTRIDGE, L. 2004. Sex Differences in the Effect of Dietary Restriction on Life Span and Mortality Rates in Female and Male Drosophila Melanogaster. *The Journals of Gerontology: Series A, 59*, B3-B9.

MAKLAKOV, A. A., HALL, M. D., SIMPSON, S. J., DESSMANN, J., CLISSOLD, F. J., ZAJITSCHEK, F., LAILVAUX, S. P., RAUBENHEIMER, D., BONDURIANSKY, R. & BROOKS, R. C. 2009. Sex differences in nutrient-dependent reproductive ageing. *Aging cell, 8*, 324-330.

MANINI, T. M. 2010. Energy Expenditure and Aging. *Ageing research reviews, 9*, 1.

MARTÍNEZ-JERÓNIMO, F. 2011. Description of the individual growth of Daphnia magna (Crustacea: Cladocera) through the von Bertalanffy growth equation. Effect of photoperiod and temperature. *Limnology, 13*, 65-71.

MARTTILA, S., KANANEN, L., HÄYRYNEN, S., JYLHÄVÄ, J., NEVALAINEN, T., HERVONEN, A., JYLHÄ, M., NYKTER, M. & HURME, M. 2015. Ageing-associated changes in the human DNA methylome: genomic locations and effects on gene expression. *BMC Genomics, 16*, 179.

MASORO, E. J. 2005. Overview of caloric restriction and ageing. *Mechanisms of Ageing and Development, 126*, 913-922.

MAUVAIS-JARVIS, F. 2015. Sex differences in metabolic homeostasis, diabetes, and obesity. *Biology of Sex Differences, 6*, 14.

MCCARTNEY, D. L., ZHANG, F., HILLARY, R. F., ZHANG, Q., STEVENSON, A. J., WALKER, R. M., BERMINGHAM, M. L., BOUTIN, T., MORRIS, S. W., CAMPBELL, A., MURRAY, A. D., WHALLEY, H. C., PORTEOUS, D. J., HAYWARD, C., EVANS, K. L., CHANDRA, T., DEARY, I. J., MCINTOSH, A. M., YANG, J., VISSCHER, P. M., MCRAE, A. F. & MARIONI, R. E. 2019. An epigenome-wide association study of sex-specific chronological ageing. *Genome Medicine,* 12**,** 1.

MCCAY, C. M., CROWELL, M. F. & MAYNARD, L. A. 1935. The Effect of Retarded Growth Upon the Length of Life Span and Upon the Ultimate Body Size: One Figure. *The Journal of Nutrition,* 10**,** 63-79.

MCEWEN, B. S. 2007. Physiology and neurobiology of stress and adaptation: central role of the brain. *Physiological reviews,* 87**,** 873-904.

MIRBAHAI, L., SOUTHAM, A. D., SOMMER, U., WILLIAMS, T. D., BIGNELL, J. P., LYONS, B. P., VIANT, M. R. & CHIPMAN, J. K. 2013. Disruption of DNA Methylation via S-Adenosylhomocysteine Is a Key Process in High Incidence Liver Carcinogenesis in Fish. *Journal of Proteome Research,* 12**,** 2895-2904.

MITROFANOVA, D., DAKIK, P., MCAULEY, M., MEDKOUR, Y., MOHAMMAD, K. & TITORENKO, V. I. 2018. Lipid metabolism and transport define longevity of the yeast Saccharomyces cerevisiae. *Frontiers in Bioscience,* 23**,** 1166-1194.

MIYAKAWA, H., SATO, T., SONG, Y., TOLLEFSEN, K. E. & IGUCHI, T. 2018. Ecdysteroid and juvenile hormone biosynthesis, receptors and their signaling in the freshwater microcrustacean Daphnia. *The Journal of Steroid Biochemistry and Molecular Biology,* 184**,** 62-68.

MUNRO, D. & BLIER, P. U. 2012. The extreme longevity of Arctica islandica is associated with increased peroxidation resistance in mitochondrial membranes. *Aging cell,* 11**,** 845-855.

MURPHY, S. A. & NICOLAOU, A. 2013. Lipidomics applications in health, disease and nutrition research. *Molecular Nutrition & Food Research,* 57**,** 1336-1346.

MURTHY, M. & RAM, J. L. 2015. Invertebrates as model organisms for research on aging biology. *Invertebrate Reproduction & Development,* 59**,** 1-4.

NAKANISHI, T., KATO, Y., MATSUURA, T. & WATANABE, H. 2016. TALEN-mediated knock-in via non-homologous end joining in the crustacean Daphnia magna. *Scientific reports,* 6**,** 36252.

NIEDERNHOFER, L. J., GURKAR, A. U., WANG, Y., VIJG, J., HOEIJMAKERS, J. H. J. & ROBBINS, P. D. 2018. Nuclear Genomic Instability and Aging. *Annual Review of Biochemistry,* 87**,** 295-322.

NIH. 2020. *TPR Gene* [Online]. National Institute of Health. Available: https://ghr.nlm.nih.gov/gene/TPR [Accessed 28 May 2020].

NOVARINA, D., JANSSENS, G. E., BOKERN, K., SCHUT, T., VAN OERLE, N. C., KAZEMIER, H. G., VEENHOFF, L. M. & CHANG, M. 2020. A genome-wide screen identifies genes that suppress the accumulation of spontaneous mutations in young and aged yeast cells. *Aging cell,* 19**,** e13084.

NYEGAARD, M. & OVERGAARD, M. T. 2019. The International Calmodulinopathy Registry: recording the diverse phenotypic spectrum of un-CALM hearts. *European heart journal,* 40**,** 2976.

ODA, S., TATARAZAKO, N., WATANABE, H., MORITA, M. & IGUCHI, T. 2005. Production of male neonates in Daphnia magna (Cladocera, Crustacea) exposed to juvenile hormones and their analogs. *Chemosphere,* 61**,** 1168-1174.

OFNS. 2020. *Population estimates for the UK, England and Wales, Scotland and Northern Ireland provision: mid-2019* [Online]. Office for National Statistics. Available: https://www.ons.gov.uk/peoplepopulationandcommunity/populationandmigration/populationestimates/bulletins/annualmidyearpopulationestimates/latest [Accessed May 2020 2020].

OLMSTEAD, A. W. & LEBLANC, G. A. 2002. Juvenoid hormone methyl farnesoate is a sex determinant in the crustacean Daphnia magna. *J Exp Zool,* 293**,** 736-9.

PAL, S. & TYLER, J. K. 2016. Epigenetics and aging. *Science Advances,* 2.

PALMISANO, B. T., ZHU, L., ECKEL, R. H. & STAFFORD, J. M. 2018. Sex differences in lipid and lipoprotein metabolism. *Molecular metabolism,* 15**,** 45-55.

PAPSDORF, K. & BRUNET, A. 2019. Linking Lipid Metabolism to Chromatin Regulation in Aging. *Trends in Cell Biology,* 29**,** 97-116.

PARISI, M., LI, R. & OLIVER, B. 2011. Lipid profiles of female and male Drosophila. *BMC Research Notes,* 4**,** 198.

PATERNOSTRO, G., VIGNOLA, C., BARTSCH, D. U., OMENS, J. H., MCCULLOCH, A. D. & REED, J. C. 2001. Age-Associated Cardiac Dysfunction in Drosophila melanogaster. *Circulation Research,* 88**,** 1053-1058.

PÉREZ, V. I., BUFFENSTEIN, R., MASAMSETTI, V., LEONARD, S., SALMON, A. B., MELE, J., ANDZIAK, B., YANG, T., EDREY, Y., FRIGUET, B., WARD, W., RICHARDSON, A. & CHAUDHURI, A. 2009. Protein stability and

resistance to oxidative stress are determinants of longevity in the longest-living rodent, the naked mole-rat. *Proceedings of the National Academy of Sciences*.

PHIPSON, B., LEE, S., MAJEWSKI, I. J., ALEXANDER, W. S. & SMYTH, G. K. 2016. ROBUST HYPERPARAMETER ESTIMATION PROTECTS AGAINST HYPERVARIABLE GENES AND IMPROVES POWER TO DETECT DIFFERENTIAL EXPRESSION. *The annals of applied statistics,* 10**,** 946-963.

PIETRZAK, B., BEDNARSKA, A. & GRZESIUK, M. 2010a. Longevity of Daphnia magna males and females. *Hydrobiologia,* 643**,** 71-75.

PIETRZAK, B., GRZESIUK, M. & BEDNARSKA, A. 2010b. Food quantity shapes life history and survival strategies in Daphnia magna (Cladocera). *Hydrobiologia,* 643**,** 51-54.

PIPER, M. D. W. & PARTRIDGE, L. 2018. Drosophila as a model for ageing. *Biochimica et Biophysica Acta (BBA) - Molecular Basis of Disease,* 1864**,** 2707-2717.

PLAISTOW, S. J., SHIRLEY, C., COLLIN, H., CORNELL, S. J. & HARNEY, E. D. 2015. Offspring Provisioning Explains Clone-Specific Maternal Age Effects on Life History and Life Span in the Water Flea, Daphnia pulex. *The American Naturalist,* 186**,** 376-389.

PRATICÒ, D. 2002. Lipid Peroxidation and the Aging Process. *Science of Aging Knowledge Environment,* 2002**,** re5.

PRIEST, N. K., MACKOWIAK, B. & PROMISLOW, D. E. L. 2002. THE ROLE OF PARENTAL AGE EFFECTS ON THE EVOLUTION OF AGING. *Evolution,* 56**,** 927-935.

PROMISLOW, D. E. L. 1992. Costs of sexual selection in natural populations of mammals. *Proceedings of the Royal Society of London. Series B: Biological Sciences,* 247**,** 203.

R. BAYLOR, E. 1942. *Cardiac pharmacology of the cladoceran, Daphnia*.

RAM, J. L. & COSTA II, A. J. 2018. *Invertebrates as Model Organisms for Research on Aging Biology*, Academic Press.

RANZ, J. M., CASTILLO-DAVIS, C. I., MEIKLEJOHN, C. D. & HARTL, D. L. 2003. Sex-Dependent Gene Expression and Evolution of the Drosophila Transcriptome. *Science,* 300**,** 1742.

RATTRAY. JB, SCHIBECI. A & DK, K. 1975. Lipids of yeasts. *Bacteriol Rev,* 39**,** 35.

RAUSCHERT, S., UHL, O., KOLETZKO, B., MORI, T. A., BEILIN, L. J., ODDY, W. H. & HELLMUTH, C. 2017. Sex differences in the association of phospholipids with components of the metabolic syndrome in young adults. *Biology of sex differences,* 8**,** 10-10.

REACTOME. 2020. *Analysis Tools* [Online]. Reactome. Available: https://reactome.org/userguide/analysis [Accessed May 2020 2020].

REBRIN, I., BAYNE, A.-CÉCILE V., MOCKETT, ROBIN J., ORR, WILLIAM C. & SOHAL, RAJINDAR S. 2004. Free aminothiols, glutathione redox state and protein mixed disulphides in aging Drosophila melanogaster. *Biochemical Journal,* 382**,** 131.

REID, J. M., BIGNAL, E. M., BIGNAL, S., MCCRACKEN, D. I., BOGDANOVA, M. I. & MONAGHAN, P. 2010. Parent age, lifespan and offspring survival: structured variation in life history in a wild population. *Journal of Animal Ecology,* 79**,** 851-862.

RHEE, E. P., CHENG, S., LARSON, M. G., WALFORD, G. A., LEWIS, G. D., MCCABE, E., YANG, E., FARRELL, L., FOX, C. S., O'DONNELL, C. J., CARR, S. A., VASAN, R. S., FLOREZ, J. C., CLISH, C. B., WANG, T. J. & GERSZTEN, R. E. 2011. Lipid profiling identifies a triacylglycerol signature of insulin resistance and improves diabetes prediction in humans. *The Journal of Clinical Investigation,* 121**,** 1402-1411.

RISTOW, M. & SCHMEISSER, K. 2014. Mitohormesis: Promoting Health and Lifespan by Increased Levels of Reactive Oxygen Species (ROS). *Dose-response : a publication of International Hormesis Society,* 12**,** 288-341.

RITCHIE, M. E., PHIPSON, B., WU, D., HU, Y., LAW, C. W., SHI, W. & SMYTH, G. K. 2015. limma powers differential expression analyses for RNA-sequencing and microarray studies. *Nucleic acids research,* 43**,** e47-e47.

ROGINA, B., REENAN, R. A., NILSEN, S. P. & HELFAND, S. L. 2000. Extended life-span conferred by cotransporter gene mutations in Drosophila. *Science,* 290**,** 2137-2140.

RUBY, J. G., SMITH, M. & BUFFENSTEIN, R. 2018. Naked mole-rat mortality rates defy Gompertzian laws by not increasing with age. *eLife,* 7**,** e31157.

RUEPPELL, O., AUMER, D. & MORITZ, R. F. A. 2016. Ties between ageing plasticity and reproductive physiology in honey bees (Apis mellifera) reveal a positive relation between fecundity and longevity as consequence of advanced social evolution. *Current Opinion in Insect Science,* 16**,** 64-68.

SAEBELFELD, M., MINGUEZ, L., GRIEBEL, J., GESSNER, M. O. & WOLINSKA, J. 2017. Humic dissolved organic carbon drives oxidative stress and severe fitness impairments in Daphnia. *Aquatic Toxicology,* 182**,** 31-38.

SALES, S., GRAESSLER, J., CIUCCI, S., AL-ATRIB, R., VIHERVAARA, T., SCHUHMANN, K., KAUHANEN, D., SYSI-AHO, M., BORNSTEIN, S. R., BICKLE, M., CANNISTRACI, C. V., EKROOS, K. & SHEVCHENKO, A. 2016. Gender, Contraceptives and Individual Metabolic Predisposition Shape a Healthy Plasma Lipidome. *Scientific Reports,* 6**,** 27710.

SALINERO, A. E., ANDERSON, B. M. & ZULOAGA, K. L. 2018. Sex differences in the metabolic effects of diet-induced obesity vary by age of onset. *International journal of obesity,* 42**,** 1088-1091.

SCHROEDER, E. A. & BRUNET, A. 2015. Lipid Profiles and Signals for Long Life. *Trends in endocrinology and metabolism: TEM,* 26**,** 589-592.

SCHROEDER, J., NAKAGAWA, S., REES, M., MANNARELLI, M.-E. & BURKE, T. 2015. Reduced fitness in progeny from old parents in a natural population. *Proceedings of the National Academy of Sciences,* 112**,** 4021.

SCHUMPERT, C., HANDY, I., DUDYCHA, J. L. & PATEL, R. C. 2014. Relationship between heat shock protein 70 expression and life span in Daphnia. *Mech Ageing Dev,* 139**,** 1-10.

SCHUMPERT, C., NELSON, J., KIM, E., DUDYCHA, J. L. & PATEL, R. C. 2015a. Telomerase Activity and Telomere Length in Daphnia. *PLOS ONE,* 10**,** e0127196.

SCHUMPERT, C. A., ANDERSON, C., DUDYCHA, J. L. & PATEL, R. C. 2016. Involvement of *Daphnia pulicaria* Sir2 in regulating stress response and lifespan. *Aging,* 8**,** 16.

SCHUMPERT, C. A., DUDYCHA, J. L. & PATEL, R. C. 2015b. Development of an efficient RNA interference method by feeding for the microcrustacean Daphnia. *BMC Biotechnology,* 15**,** 91.

SCHWARZENBERGER, A., CHRISTJANI, M. & WACKER, A. 2014. Longevity of Daphnia and the attenuation of stress responses by melatonin. *BMC Physiology,* 14**,** 8.

SEALS, D. R. & MELOV, S. 2014. Translational geroscience: emphasizing function to achieve optimal longevity. *Aging (Albany NY),* 6**,** 718.

SEPIL, I., HOPKINS, B. R., DEAN, R., BATH, E., FRIEDMAN, S., SWANSON, B., OSTRIDGE, H., BUEHNER, N., WOLFNER, M., KONIETZNY, R., THÉZÉNAS, M.-L., SANDHAM, E., CHARLES, P. D., FISCHER, R., STEINHAUER, J., KESSLER, B. M. & WIGBY, S. 2019. An exposition of ejaculate senescence and its inhibition in <em>Drosophila</em&gt. *bioRxiv***,** 624734.

SERGIEV, P. V., DONTSOVA, O. A. & BEREZKIN, G. V. 2015. Theories of Aging: An Ever-Evolving Field. *Acta Naturae,* 7**,** 9-18.

SINGH, B. N. 2001. Morbidity and mortality in cardiovascular disorders: impact of reduced heart rate. *Journal of cardiovascular pharmacology and therapeutics,* 6**,** 313-331.

SKORUPA, D. A., DERVISEFENDIC, A., ZWIENER, J. & PLETCHER, S. D. 2008. Dietary composition specifies consumption, obesity, and lifespan in Drosophila melanogaster. *Aging cell,* 7**,** 478-490.

SLOTTE, J. P. 2013. Biological functions of sphingomyelins. *Progress in Lipid Research,* 52**,** 424-437.

SMITH, J. M. 1977. Parental investment: A prospective analysis. *Animal Behaviour*.

SMITH, P., WILLEMSEN, D., POPKES, M., METGE, F., GANDIWA, E., REICHARD, M. & VALENZANO, D. R. 2017. Regulation of life span by the gut microbiota in the short-lived African turquoise killifish. *elife,* 6**,** e27014.

SNELL, T. W., JOHNSTON, R. K., GRIBBLE, K. E. & MARK WELCH, D. B. 2015. Rotifers as experimental tools for investigating aging. *Invertebrate reproduction & development,* 59**,** 5-10.

SOBOČANEC, S., BALOG, T., ŠVERKO, V. & MAROTTI, T. 2003. Sex-dependent Antioxidant Enzyme Activities and Lipid Peroxidation in Ageing Mouse Brain. *Free Radical Research,* 37**,** 743-748.

SPIERS, H., HANNON, E., WELLS, S., WILLIAMS, B., FERNANDES, C. & MILL, J. 2016. Age-associated changes in DNA methylation across multiple tissues in an inbred mouse model. *Mechanisms of Ageing and Development,* 154**,** 20-23.

STARK, W. S., LIN, T.-N., BRACKHAHN, D., CHRISTIANSON, J. S. & SUN, G. Y. 1993. Fatty acids in the lipids ofDrosophila heads: Effects of visual mutants, carotenoid deprivation and dietary fatty acids. *Lipids,* 28**,** 345-350.

STOCKLEY, P. & HOBSON, L. 2016. Paternal care and litter size coevolution in mammals. *Proceedings. Biological sciences,* 283**,** 20160140.

STOLLEWERK, A. 2010. The water flea Daphnia - a 'new' model system for ecology and evolution? *Journal of Biology,* 9**,** 21.

STUBBS, T. M., BONDER, M. J., STARK, A.-K., KRUEGER, F., BOLLAND, D., BUTCHER, G., CHANDRA, T., CLARK, S. J., CORCORAN, A., ECKERSLEY-MASLIN, M., FIELD, L., FRISING, U. C., GILBERT, C., GUEDES, J., HERNANDO-HERRAEZ, I., HOUSELEY, J., KEMP, F., MACQUEEN, A., VON MEYENN, F., OKKENHAUG, K., REIK, W., RHOADES, M., SANTBERGEN, M. J. C., STARK, A.-K., STEBEGG, M., STUBBS, T. M., VELDHOEN, M., VON MEYENN, F., STEGLE, O., REIK, W. & TEAM, B. I. A. C. 2017. Multi-tissue DNA methylation age predictor in mouse. *Genome Biology,* 18**,** 68.

TALBOT, C. P. J., PLAT, J., RITSCH, A. & MENSINK, R. P. 2018. Determinants of cholesterol efflux capacity in humans. *Progress in Lipid Research,* 69**,** 21-32.

TANAKA, S.-I., FUJIOKA, Y., TSUJINO, T., ISHIDA, T. & HIRATA, K.-I. 2018. Impact of serum cholesterol esterification rates on the development of diabetes mellitus in a general population. *Lipids in Health and Disease,* 17**,** 180.

TATAR, M., KOPELMAN, A., EPSTEIN, D., TU, M.-P., YIN, C.-M. & GAROFALO, R. 2001. A mutant Drosophila insulin receptor homolog that extends life-span and impairs neuroendocrine function. *Science,* 292**,** 107-110.

TESCHENDORFF, A. E., WEST, J. & BECK, S. 2013. Age-associated epigenetic drift: implications, and a case of epigenetic thrift? *Human Molecular Genetics,* 22**,** R7-R15.

THERNEAU, T. M. & GRAMBSCH, P. M. 2013. *Modeling survival data: extending the Cox model*, Springer Science & Business Media.

TISSENBAUM, H. A. 2015. Using C. elegans for aging research. *Invertebrate Reproduction & Development,* 59**,** 59-63.

TISSENBAUM, H. A. & GUARENTE, L. 2002. Model Organisms as a Guide to Mammalian Aging. *Developmental Cell,* 2**,** 9-19.

TOGNINI, S., POLINI, A., PASQUALETTI, G., URSINO, S., CARACCIO, N., FERDEGHINI, M. & MONZANI, F. 2012. Age and Gender Substantially Influence the Relationship Between Thyroid Status and the Lipoprotein Profile: Results from a Large Cross-Sectional Study. *Thyroid,* 22**,** 1096-1103.

TOWER, J. 2006. Sex-specific regulation of aging and apoptosis. *Mechanisms of Ageing and Development,* 127**,** 705-718.

TOWER, J. 2017. Sex-Specific Gene Expression and Life Span Regulation. *Trends in Endocrinology & Metabolism,* 28**,** 735-747.

TOYOTA, K., KATO, Y., MIYAKAWA, H., YATSU, R., MIZUTANI, T., OGINO, Y., MIYAGAWA, S., WATANABE, H., NISHIDE, H., UCHIYAMA, I., TATARAZAKO, N. & IGUCHI, T. 2014. Molecular impact of juvenile hormone agonists on neonatal Daphnia magna. *Journal of Applied Toxicology,* 34**,** 537-544.

TOYOTA, K., MIYAKAWA, H., HIRUTA, C., FURUTA, K., OGINO, Y., SHINODA, T., TATARAZAKO, N., MIYAGAWA, S., SHAW, J. R. & IGUCHI, T. 2015. Methyl farnesoate synthesis is necessary for the environmental sex determination in the water flea Daphnia pulex. *Journal of Insect Physiology,* 80**,** 22-30.

TRAYSSAC, M., HANNUN, Y. A. & OBEID, L. M. 2018. Role of sphingolipids in senescence: implication in aging and age-related diseases. *The Journal of Clinical Investigation,* 128**,** 2702-2712.

TRIVERS, R. 1985. *Social evolution*.

VALENZANO DARIO, R., ABOOBAKER, A., SELUANOV, A. & GORBUNOVA, V. 2017. Non-canonical aging model systems and why we need them. *The EMBO Journal,* 36**,** 959-963.

VALENZANO, DARIO R., BENAYOUN, BÉRÉNICE A., SINGH, PARAM P., ZHANG, E., ETTER, PAUL D., HU, C.-K., CLÉMENT-ZIZA, M., WILLEMSEN, D., CUI, R., HAREL, I., MACHADO, BEN E., YEE, M.-C., SHARP, SABRINA C., BUSTAMANTE, CARLOS D., BEYER, A., JOHNSON, ERIC A. & BRUNET, A. 2015. The African Turquoise Killifish Genome Provides Insights into Evolution and Genetic Architecture of Lifespan. *Cell,* 163**,** 1539-1554.

VALENZANO, D. R., SHARP, S. & BRUNET, A. 2011. Transposon-Mediated Transgenesis in the Short-Lived African Killifish Nothobranchius furzeri, a Vertebrate Model for Aging. *G3: Genes|Genomes|Genetics,* 1**,** 531.

VAN GINNEKEN, V. 2017. *Are there any Biomarkers of Aging? Biomarkers of the Brain*.

VANCE, D. E. 2013. Physiological roles of phosphatidylethanolamine N-methyltransferase. *Biochimica et Biophysica Acta (BBA) - Molecular and Cell Biology of Lipids,* 1831**,** 626-632.

VANCE, J. E. & TASSEVA, G. 2013. Formation and function of phosphatidylserine and phosphatidylethanolamine in mammalian cells. *Biochimica et Biophysica Acta (BBA) - Molecular and Cell Biology of Lipids,* 1831**,** 543-554.

VANDEGEHUCHTE, M., LEMIÈRE, F. & JANSSEN, C. 2009. Quantitative DNA-methylation in Daphnia magna and effects of multigeneration Zn exposure. *Comparative Biochemistry and Physiology Part C: Toxicology & Pharmacology,* 150**,** 343-348.

VINA, J., BORRAS, C. & MIQUEL, J. 2007. Theories of ageing. *IUBMB Life,* 59**,** 249-54.

VOJNOVIC, B., BARBER, P. R., JOHNSTONE, P., GREGORY, H. C., MARPLES, B., JOINER, M. C. & LOCKE, R. J. 2013. A High Sensitivity, High Throughput, Automated Single-Cell Gel Electrophoresis ('Comet') DNA Damage Assay. *Physics in Medicine and Biology***,** 15.

WADE, M. J. & SHUSTER, S. M. 2002. The evolution of parental care in the context of sexual selection: a critical reassessment of parental investment theory. *The American Naturalist,* 160**,** 285-292.

WANG, M. C., ROURKE, E. J. & RUVKUN, G. 2008. Fat Metabolism Links Germline Stem Cells and Longevity in <em>C. elegans</em&gt. *Science,* 322**,** 957.

WANG, X., MAGKOS, F. & MITTENDORFER, B. 2011. Sex differences in lipid and lipoprotein metabolism: it's not just about sex hormones. *The Journal of clinical endocrinology and metabolism,* 96**,** 885-893.

WANJALA, G. W., ONYANGO, A., ONYANGO, C. & MAKAYOTO, M. 2017. Reactive oxygen species (ROS) generation, impacts on tissue oxidation and dietary management of non-communicable diseases: A review. *African Journal of Biochemistry Research,* 11**,** 79-90.

WEINDRUCH, R. 1996. The Retardation of Aging by Caloric Restriction: Studies in Rodents and Primates. *Toxicologic Pathology,* 24**,** 742-745.

WEISMANN, A. 1882. *Ueber die Dauer des Lebens*, G. Fischer.

WELLE, S., TAWIL, R. & THORNTON, C. A. 2008. Sex-related differences in gene expression in human skeletal muscle. *PloS one,* 3**,** e1385-e1385.

WHITMAN, L. J. & MILLER, R. J. 1982. The Phototactic Behaviour of Daphnia magna as an Indicator of Chronic Toxicity. *Proceedings of the Oklahoma Academy Science***,** 11.

WHO 2015. *World report on ageing and health*, World Health Organization.

WICKHAM, H. 2016. *ggplot2: elegant graphics for data analysis*, Springer.

WILDING, M., COPPOLA, G., DE ICCO, F., ARENARE, L., DI MATTEO, L. & DALE, B. 2014. Maternal non-Mendelian inheritance of a reduced lifespan? A hypothesis. *Journal of Assisted Reproduction and Genetics,* 31**,** 637-643.

WILLIAMS GEORGE, C. 1957. PLEIOTROPY, NATURAL SELECTION, AND THE EVOLUTION OF SENESCENCE. *Evolution,* 11**,** 398-411.

WU, C.-I. & YUJUN XU, E. 2003. Sexual antagonism and X inactivation – the SAXI hypothesis. *Trends in Genetics,* 19**,** 243-247.

WU, H., SOUTHAM, A. D., HINES, A. & VIANT, M. R. 2008. High-throughput tissue extraction protocol for NMR- and MS-based metabolomics. *Analytical Biochemistry,* 372**,** 204-212.

WU, J. J., LIU, J., CHEN, EDMUND B., WANG, JENNIFER J., CAO, L., NARAYAN, N., FERGUSSON, MARIE M., ROVIRA, ILSA I., ALLEN, M., SPRINGER, DANIELLE A., LAGO, CORY U., ZHANG, S., DUBOIS, W., WARD, T., DECABO, R., GAVRILOVA, O., MOCK, B. & FINKEL, T. 2013. Increased Mammalian Lifespan and a Segmental and Tissue-Specific Slowing of Aging after Genetic Reduction of mTOR Expression. *Cell Reports,* 4**,** 913-920.

XU, J., BURGOYNE, P. S. & ARNOLD, A. P. 2002. Sex differences in sex chromosome gene expression in mouse brain. *Human Molecular Genetics,* 11**,** 1409-1419.

ZHANG, G. Q. & ZHANG, W. 2009. Heart rate, lifespan, and mortality risk. *Ageing research reviews,* 8**,** 52-60.

ZIEHM, M., KAUR, S., IVANOV, D. K., BALLESTER, P. J., MARCUS, D., PARTRIDGE, L. & THORNTON, J. M. 2017. Drug repruposing for ageing research using model organisms. *Aging Cell***,** 11.

ZORE, T., PALAFOX, M. & REUE, K. 2018. Sex differences in obesity, lipid metabolism, and inflammation—A role for the sex chromosomes? *Molecular Metabolism,* 15**,** 35-44.

ZUPKOVITZ, G., KABILJO, J., MARTIN, D., LAFFER, S., SCHÖFER, C. & PUSCH, O. 2018a. Phylogenetic analysis and expression profiling of the Klotho gene family in the short-lived African killifish Nothobranchius furzeri. *Development genes and evolution,* 228**,** 255-265.

ZUPKOVITZ, G., LAGGER, S., MARTIN, D., STEINER, M., HAGELKRUYS, A., SEISER, C., SCHÖFER, C. & PUSCH, O. 2018b. Histone deacetylase 1 expression is inversely correlated with age in the short-lived fish Nothobranchius furzeri. *Histochemistry and cell biology,* 150**,** 255-269.